Journal of Immunology Research

Immunotherapy and Vaccine Development

Lead Guest Editor: Carol Leung
Guest Editors: Christian Münz and Angelika Riemer

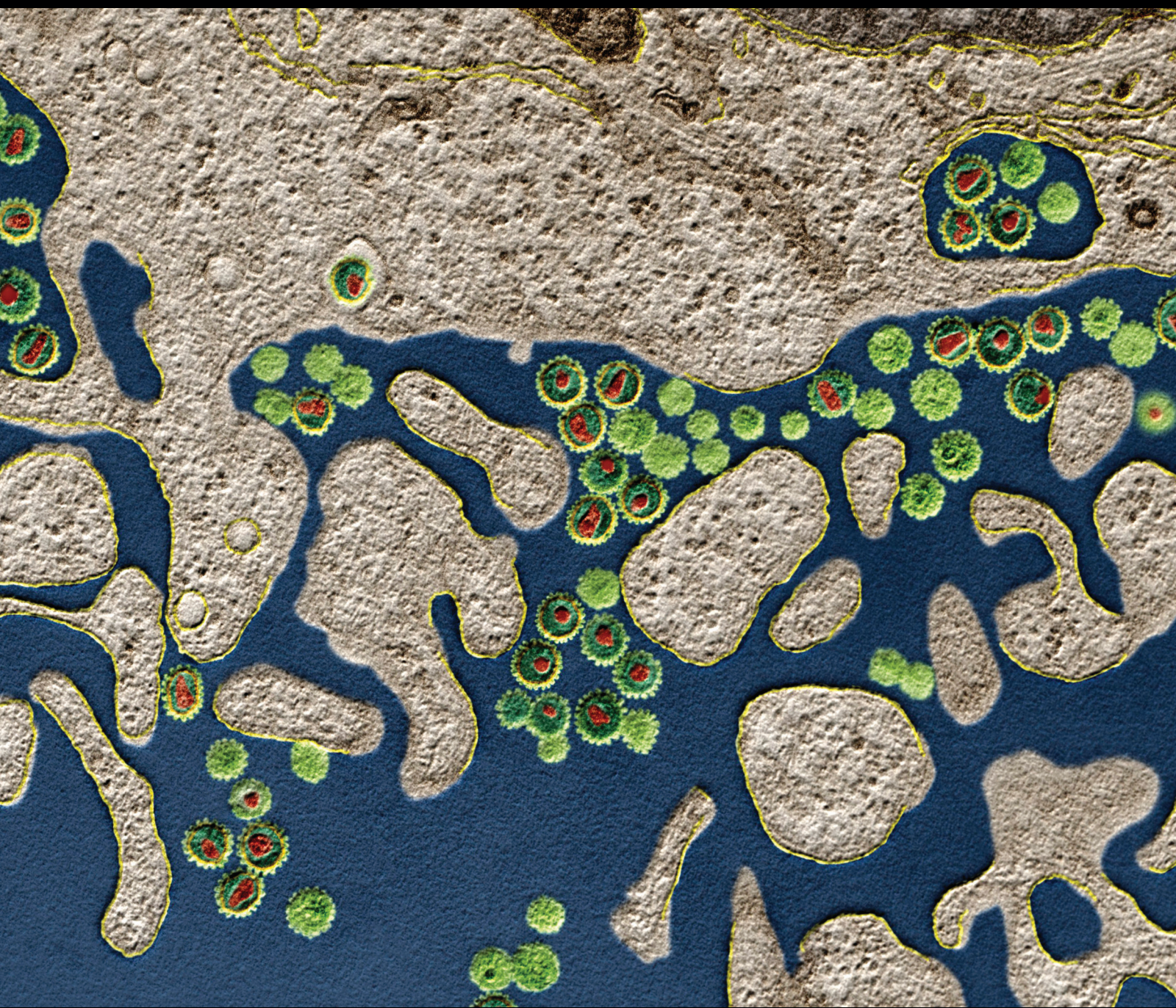

Immunotherapy and Vaccine Development

Journal of Immunology Research

Immunotherapy and Vaccine Development

Lead Guest Editor: Carol Leung
Guest Editors: Christian Münz and Angelika Riemer

Editorial Board

Contents

Hindawi
Journal of Immunology Research
Volume 2018, Article ID 8751027, 2 pages
https://doi.org/10.1155/2018/8751027

Editorial

Immunotherapy and Vaccine Development

Carol Leung,[1] **Christian Münz**,[2] **and Angelika Riemer**[3]

[1]*Ludwig Institute for Cancer Research, Nuffield Department of Medicine, University of Oxford, Oxford, UK*
[2]*Viral Immunobiology, Institute of Experimental Immunology, University of Zürich, Zürich, Switzerland*
[3]*Immunotherapy & Immunoprevention, German Cancer Research Center (DKFZ), Heidelberg, Germany*

Correspondence should be addressed to Carol Leung; carol.leung@ludwig.ox.ac.uk

Received 8 May 2018; Accepted 8 May 2018; Published 13 June 2018

Recent advances in immunotherapy have led to effective treatments for patients with different diseases including cancer. The use of immune checkpoint-blocking monoclonal antibodies (CPB) and adoptive cellular therapy induces long-term clinical benefits in a number of advanced cancer patients. However, CPB treatment benefits only a small fraction of patients and can be outweighed by autoimmune toxicity, while the adoptive cell therapy approach is complex and requires the culture and transduction of patient-specific immune cells, which can be time-consuming and costly. Cancer vaccines are considered to be a promising alternative, but most trials have failed miserably, apart from the ones targeting virus-associated cancers. A better understanding of the immunological mechanisms is thus crucial in advancing the development of immunotherapy.

In this special issue, seven original research studies and three review articles highlight some recent discoveries in immunotherapy and vaccine development. On vaccine design and development, S. Heinimäki et al. investigated the importance of delivering the VLP-based norovirus vaccine mucosally to induce not only systemic but also the desired mucosal antibody responses. Also, B. Behrouz et al. followed a mucosal vaccination approach and used bivalent flagellin as an immunogen, which induced humoral and cellular immune responses and protected mice from *Pseudomonas aeruginosa*-mediated acute pneumonia. S. Choi et al. assessed if the *Mycobacterium tuberculosis* (Mtb) protein Rv3841, which plays a crucial role in the growth of Mtb, can also serve as a vaccine target. They found that the protein activated dendritic cells (DCs) induced Th1 responses, which could inhibit mycobacterial growth. The topic of antigen production in plants is covered in the article by P.-F. Liu et al. They expressed staphylococcal enterotoxin B in radish leaves by agroinfiltration and showed antibody induction against the antigen after immunizing mice with homogenized leaves. In the area of immunotherapy for autoimmune diseases, J. Yang et al. showed that tolerogenic DCs could expand TGFβ-induced regulatory T cells (iTregmtDC), which reduced the severity of collagen-induced arthritis in mice. This implies that iTregmtDC might have a therapeutic potential in autoimmune arthritis. For adjuvant studies, J. Laiño et al. described that the dual TLR2/7 ligands, CL413, and CL53, could suppress allergic Th2 immune responses in mice and could act as potential adjuvants for allergy treatment. In the field of animal models for studying immunotherapies and vaccine strategy, C. Leung analyzed the oncofetal antigen ROR1 expression in humanized mice and suggested that humanized mice could be a useful tool to study B cell malignant diseases. In the first of the review articles, A. P. F. Costa et al. carried out a meta-analysis of studies on the safety of the recently introduced nonavalent prophylactic HPV vaccine, which they showed to be as safe as the quadrivalent one. On immunotherapy, S. Sun et al. reviewed the strategies to overcome the toxicities of chimeric antigen receptor (CAR) T cell therapy. In addition, F.-S. Hsu et al. gave a comprehensive review on the use of immune checkpoint inhibitors for treating urothelial carcinoma.

In conclusion, these articles have showcased some novel advances in multiple topics within the field of immunotherapy and vaccine development. We hope the readers will be stimulated by and find applications of the interesting findings.

Acknowledgments

We would like to thank the authors for submitting their manuscripts to this special issue and we are very grateful to the reviewers for their precious time and valuable insights.

Carol Leung
Christian Münz
Angelika Riemer

Hindawi
Journal of Immunology Research
Volume 2018, Article ID 2480931, 10 pages
https://doi.org/10.1155/2018/2480931

Research Article

Analysis of ROR1 Protein Expression in Mice with Reconstituted Human Immune System Components

Carol S. Leung [1,2]

[1]*Department of Hematology, University College London Cancer Institute, University College London, London, UK*
[2]*Ludwig Institute for Cancer Research, Nuffield Department of Medicine, University of Oxford, Oxford, UK*

Correspondence should be addressed to Carol S. Leung; carol.leung@ludwig.ox.ac.uk

Received 15 September 2017; Revised 1 February 2018; Accepted 11 March 2018; Published 18 April 2018

Academic Editor: Kurt Blaser

Receptor tyrosine kinase-like orphan receptor 1 (ROR1) is an oncofetal antigen expressed on multiple tumors and has no significant expression on normal human tissues. ROR1 is highly upregulated in chronic lymphocytic leukemia (CLL) B cells. NOD-scid IL2rg$^{-/-}$ (NSG) mice engrafted with human CD34^{+} hematopoietic progenitor cells (huNSG) achieved multilineage human immune cell reconstitution including B cells, T cells, NK cells, and DCs. Like the CLL patients, huNSG mice have abnormally high percentage of CD5-expressing B cells in the periphery. In light of this, we aim to determine whether ROR1 is expressed on huNSG B cells. Using flow cytometry analysis, we found that ROR1 was highly expressed in a proportion of bone marrow, spleen, and blood B cells, which were mostly immature B cells. Transplantation of the oncogene TCL-1-transduced CD34^{+} cells in neonatal NSG mice did not increase the frequency of ROR1-expressing B cells, but the mouse with the highest engraftment of transduced cells developed a tumor-like lump consisting of a high percentage of ROR1-expressing B cells. This study highlights the potential use of huNSG mice to study B cell malignant diseases and to evaluate immunotherapeutics targeting ROR1.

1. Introduction

Receptor tyrosine kinase-like orphan receptor 1 (ROR1) is an oncofetal antigen expressed in a number of malignancies. The overexpression of ROR1 in malignancy was first identified on chronic lymphocytic leukemia (CLL) B cells [1] and was subsequently found in many other hematological malignancies [2–4] and solid tumors [5]. It has been shown that ROR1 could play a crucial role in tumorigenesis [6] and cell migration [7]. As ROR1 has expression on tumor cells but not on normal human tissues except at low levels in adipose tissues, parathyroid, pancreatic islet cells, and some regions of the gastrointestinal tract [8], this makes it an attractive antigen target for cancer therapy. Indeed, a number of ROR1-specific monoclonal antibodies and chimeric antigen receptor (CAR) T cells have been developed and are under testing [9, 10]. However, a preclinical small animal model is currently lacking to evaluate ROR1-targeted immunotherapies.

Immunodeficient NOD-scid IL2rg$^{-/-}$ (NSG) mice engrafted with human fetal liver-derived CD34^{+} hematopoietic progenitor cells (huNSG) achieved multilineage human immune cell reconstitution including B cells, T cells, natural killer (NK) cells, and dendritic cells (DCs) [11]. These so called humanized mice are a powerful tool to study human infectious diseases, hematopoiesis, and model immune system tumor interaction and can be used to evaluate novel antitumor immunotherapies [12, 13]. However, incomplete B cell development in huNSG mice has been documented [14]. Like CLL patients, huNSG mice have abnormally high frequency of B cells in the periphery, and a subset of B cells expresses CD5. In light of these, we hypothesized that huNSG mice have a high proportion of ROR1^{+} B cells and could represent a ROR1^{+} tumor model *in vivo*.

Here, we evaluated ROR1 protein expression in engrafted human immune cells in 3 different cohorts of huNSG mice. We analyzed the phenotypes and characteristics of ROR1-expressing B cells. Moreover, CD34^{+} human hematopoietic progenitor cells transduced with the oncogene T cell leukemia/lymphoma 1 (TCL-1) were transplanted in neonatal NSG mice to study the effect of this oncogene on inducing ROR1-expressing tumors in huNSG mice.

2. Materials and Methods

2.1. Generation of huNSG Mice. NOD, Cg-*Prkdc*^{scid} *Il2rg*^{tm1Wjl}/SzJ (NSG), mice were obtained from The Jackson Laboratory and raised under specific pathogen-free conditions. Human fetal liver samples were obtained from Advanced Bioscience Resources; human CD34$^+$ hematopoietic progenitor cells were isolated using the human CD34 MicroBead kit (Miltenyi Biotec). HuNSG mice were generated as previously described [11]. Animal protocols were approved by the UK Home Office, and all animal experiments were performed in accordance with institutional guidelines under protocol number 70/7295. This study was also approved by the Research Ethics Committee with REC reference number 16/EE/0043.

2.2. Lentiviral Vector Construction and Human CD34$^+$ Cell Transduction. The coding sequence of the human TCL-1 gene was synthesized by Genscript and cloned into the lentiviral vector pCCL-GFP (Addgene) with the EF1α promoter. This created pCCL-EF1α-TCL1-GFP. Lentivirus expressing TCL-1 was then prepared by cotransfecting 293T cells with pCCL-EF1α-TCL1-GFP, lentiviral packaging and envelope plasmids. Lentivirus-containing supernatant was harvested after 48 hours and was used to transduce human CD34$^+$ cells. Frozen CD34$^+$ cells were thawed and cultured in StemPro-34 SFM complete medium (Gibco) with the cytokines SCF and IL-3, in combination with the lentiviral vectors. After 24 hours of transduction, culture media were changed and cells were cultured for another 72 hours. GFP expression was evaluated by flow cytometry before injecting these cells into NSG mice.

2.3. Flow Cytometry. Cells were washed in PBS and stained for 20 minutes with conjugated antibodies or isotype control obtained from BioLegend, eBioscience, or BD. The following purified mouse anti-human antibodies were used for staining: anti-CD45-Pacific Blue, anti-CD45-BV605, anti-CD19-PE-Cy7, anti-CD19-APC-Cy7, CD10-BV605, anti-CD27-PE-Cy7, anti-IgD-PE, anti-ROR1-APC (clone 2A2), anti-CD5-PerCP-Cy5.5, anti-CD38-BV711, anti-CD23-FITC, anti-NKp46-FITC, anti-CD3-Pacific Blue, anti-CD4-APC-Cy7, and anti-CD8-PE. Live and dead cell staining was performed with aqua fluorescent reactive dye from Invitrogen. Peripheral blood mononuclear cells (PBMCs) from heathy donors and CLL patients were kindly provided by Dr. Vania Coelho, University College London. Flow cytometry analysis was done using a BD LSRII Fortessa using FACSDiva software (BD Biosciences), and data were analyzed with FlowJo (Tree Star).

2.4. B Cell Proliferation Assay. Frozen splenocytes from huNSG mice in the same reconstitution cohort were thawed and stained with 5 μM CellTrace Violet (Invitrogen) and washed, and 200,000 live splenocytes were plated in 200 μl of culture medium in each well of 96-well flat-bottom plates. The cells were stimulated with 5 μg/ml CpG ODN 2006 (InvivoGen), 167 ng/ml pokeweed mitogen (PWM) extract (Sigma), and 1/2400 fixed *Staphylococcus aureus* cells (SAC) (Calbiochem) for 96 hours and analyzed by flow cytometry.

2.5. Western Blot. Untransduced or transduced CD34$^+$ hematopoietic progenitor cells by lentivirus expressing TCL-1 were lysed by RIPA buffer containing protease inhibitor (Sigma). Protein extracts were separated by Bis-Tris gels and transferred to the PVDF membrane by Western blotting and probed with TCL-1-specific monoclonal antibody clone 1-21 (Cell Signaling). Goat anti-mouse IgG coupled with HRP was used as a secondary antibody. Blots were developed using the ECL kit (GE Healthcare), and protein bands were detected on X-ray film.

3. Results

3.1. ROR1 Expression on B Cells in huNSG Mice. We first examined the ROR1 surface expression on reconstituted human immune cells in huNSG mice. These mice were generated by engrafting newborn immunodeficient NSG mice with human fetal liver-derived CD34$^+$ hematopoietic progenitor cells [11, 15]. We generated 3 cohorts of huNSG mice with human CD34$^+$ hematopoietic progenitor cells derived from 3 different fetal liver tissues. Most of the huNSG mice achieved a frequency of more than 50% of human CD45$^+$ cells in total leukocytes after 3 months of reconstitution, with engraftment of CD19$^+$ B cells, CD3$^+$ T cells, and NKp46$^+$ NK cells (Figure 1). Afterwards, we investigated the ROR1 surface expression on engrafted human immune cells in huNSG mice, comparing such expression with that in a human healthy donor and a CLL patient. PBMCs from the healthy donor did not express ROR1 while a high proportion of ROR1-expressing B cells was observed in the PBMCs of the CLL patient (Figure 2(a)). Interestingly, we found a high percentage of CD19$^+$ROR1$^+$ B cells in huNSG mice, especially in the bone marrow and spleen. This was observed in mice from all 3 cohorts, with a mean of 47.2% in the bone marrow, 13.7% in the spleen, and 2.0% in the blood (Figure 2(b)). On the other hand, only a negligible amount of CD45$^+$CD19$^-$ immune cells expressed ROR1.

3.2. Frequency of ROR1-Expressing B Cells Maintained in huNSG Mice. The abnormally high percentage of ROR1$^+$ B cells may have been caused by the incomplete B cell development in huNSG mice [14]. A previous study has suggested that human B cell maturity improves with time following the reconstitution [16], so we tested if the frequency of ROR1$^+$ B cells changes over time after the transplantation of human cells. In Figure 3(a), the percentage of ROR1$^+$CD19$^+$ B cells in the periphery remained largely unchanged between 3 and 8 months after human progenitor cell engraftment. This was observed in both individual cohorts and the pooled cohort. In addition, the frequency of this subset was also stable over time in the bone marrow and spleen of huNSG mice, although it should be noted that each cohort only contributed to one single time point (Figure 3(b)). Also, the reconstituted frequency of ROR1$^+$CD19$^+$ B cells correlated positively with CD19 reconstitution ($r = 0.53$) and negatively with CD3 reconstitution ($r = -0.74$), but to a lesser extent with NKp46$^+$ NK cell reconstitution ($r = -0.31$).

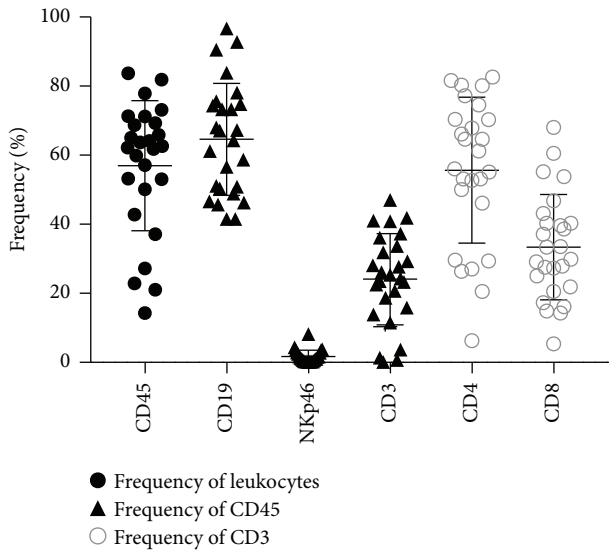

Figure 1: NOD-scid IL2rg$^{-/-}$ (NSG) mice injected with fetal liver-derived CD34$^+$ hematopoietic progenitor cells were reconstituted with human immune cells. Peripheral blood of reconstituted NSG mice was analyzed 3 months after injection of human hematopoietic progenitor cells. The frequencies of different immune cell compartments are indicated. Frequencies of human CD45$^+$ cells within the leukocyte gate, frequencies of CD19$^+$ B cells, NKp46$^+$ NK cells, and CD3$^+$ T cells within human CD45$^+$ cells, and frequencies of CD4$^+$ and CD8$^+$ T cells within CD3$^+$ cells are shown. Horizontal lines represent the mean and SD. Data are from 3 different reconstitution cohorts with CD34$^+$ cells derived from 3 different fetal liver tissues.

3.3. ROR1-Expressing B Cells Were Mostly Immature B Cells. We examined the phenotype of the ROR1$^+$CD19$^+$ B cells in huNSG mice. In the bone marrow, ROR1-expressing B cells were mainly CD27 and IgD double negative (99.2%), CD10$^+$, and CD38$^+$ but were CD5$^-$ (Figure 4(a)). The majority of the splenic ROR1-expressing B cells were also CD27$^-$IgD$^-$ and CD10$^+$CD38$^+$, with slightly larger CD27$^-$IgD$^+$, CD10$^-$CD5$^+$, and CD10$^-$CD38$^-$ populations than those of the bone marrow. The peripheral blood ROR1-expressing B cells had the relatively highest frequency of CD27$^-$IgD$^+$, CD10$^-$CD5$^+$, and CD10$^-$CD38$^-$ population compared to those of the spleen and bone marrow, but again the majority were mainly CD27$^-$IgD$^-$ and CD10$^+$CD38$^+$ cells. Although we observed a high percentage of CD5$^+$ B cells in huNSG mice, these cells rarely expressed ROR1 (data not shown). These results indicated that ROR1-expressing B cells in huNSG mice were mostly immature human B cells. We next tested if the ROR1$^+$ B cells can proliferate better than the ROR1$^-$ B cells. It has been shown that the combination of potent B cell stimulators, PWM, CpG, and SAC, could lead to B cell activation and proliferation [17, 18]. We then stimulated the splenocytes of the huNSG mice with PWM, CpG, and SAC for 4 days and measured the proliferation by fluorescence dye dilution. The unstimulated ROR1$^+$CD19$^+$ B cells had a slightly higher percentage of proliferating cells than the unstimulated ROR1$^-$CD19$^+$ B cells (18.3% versus 11.7%), while the stimulated cells had a comparable high proliferation (over 85%).

3.4. Engraftment of TCL-1-Transduced Human CD34$^+$ Cells in NSG Mice Could Induce ROR1-Expressing Tumors. The first transgenic mouse model of CLL was generated by overexpressing the TCL-1 gene under the control of the immunoglobulin heavy chain variable region promoter and immunoglobulin heavy chain enhancer [19]. We therefore introduced the human TCL-1 gene to human CD34$^+$ hematopoietic progenitor cells by lentiviral transduction. A viral 2A sequence was used for the simultaneous overexpression of both the TCL-1 gene and enhanced green fluorescent protein (GFP), so the TCL-1 transduction efficiency could be monitored by GFP expression. We achieved a transduction efficiency of around 40% (Figure 5(a)), and the expression of TCL-1 in the CD34$^+$ cells was confirmed by Western blotting (Figure 5(b)). The transduced cells were used to engraft newborn NSG mice. After 3 months of engraftment, most of the mice had achieved a comparable frequency of human CD45$^+$ cells in total leukocytes, with engraftment of CD19$^+$ B cells, CD3$^+$ T cells, and NKp46$^+$ NK cells. Four out of the five reconstituted mice had GFP-positive cells in the periphery, with the majority being CD3$^+$ T cells (Figure 5(c)). Two mice had a relatively higher proportion of GFP-positive B cells. However, the frequency of ROR1$^+$ B cells in these mice was similar to that in the huNSG mice reconstituted using untransduced CD34$^+$ cells (Figures 2(b) and 5(c)). Interestingly, the mouse with the highest engrafted GFP$^+$ cells in the periphery developed a tumor-like lump after 6 months of reconstitution. This has never been observed in other cohorts of huNSG mice engrafted with unmanipulated CD34$^+$ cells. Single suspension cells isolated from this lump had more than 90% CD45$^+$ human cells, without GFP expression. A high proportion of the CD45$^+$ cells was ROR1-expressing CD19$^+$ B cells, and more than 50% of the ROR1$^+$CD19$^+$ cells coexpressed CD5 and CD23 (Figure 5(d)).

4. Discussion

In line with other findings [15, 20], our huNSG mice were reconstituted with all major subsets of immune cells after neonatal hematopoietic progenitor cell transplantation. huNSG mice have a high frequency of CD19$^+$ B cells in the periphery, and over 50% of these B cells express the CD5 antigen [21] (data not shown). CLL patients also have a high frequency of CD5$^+$ B cells in the periphery [22], and most of the CLL cases are positive for ROR1 surface expression [23]. Our data show that a high percentage of B cells in huNSG mice expresses ROR1, especially in the bone marrow and spleen.

HuNSG mice can also be generated using CD34$^+$ hematopoietic progenitor cells isolated from umbilical cord blood or from GM-CSF-mobilized peripheral blood cells [24, 25], other than the human fetal liver. A number of studies have documented incomplete B cell development in different humanized mouse models, including the BLT mice [21, 26, 27]. If the ROR1$^+$ immature B cells are indeed the by-product of incomplete B cell development in huNSG mice, it is likely that these cells are also present in other humanized mouse models. In contrast, with recent advances

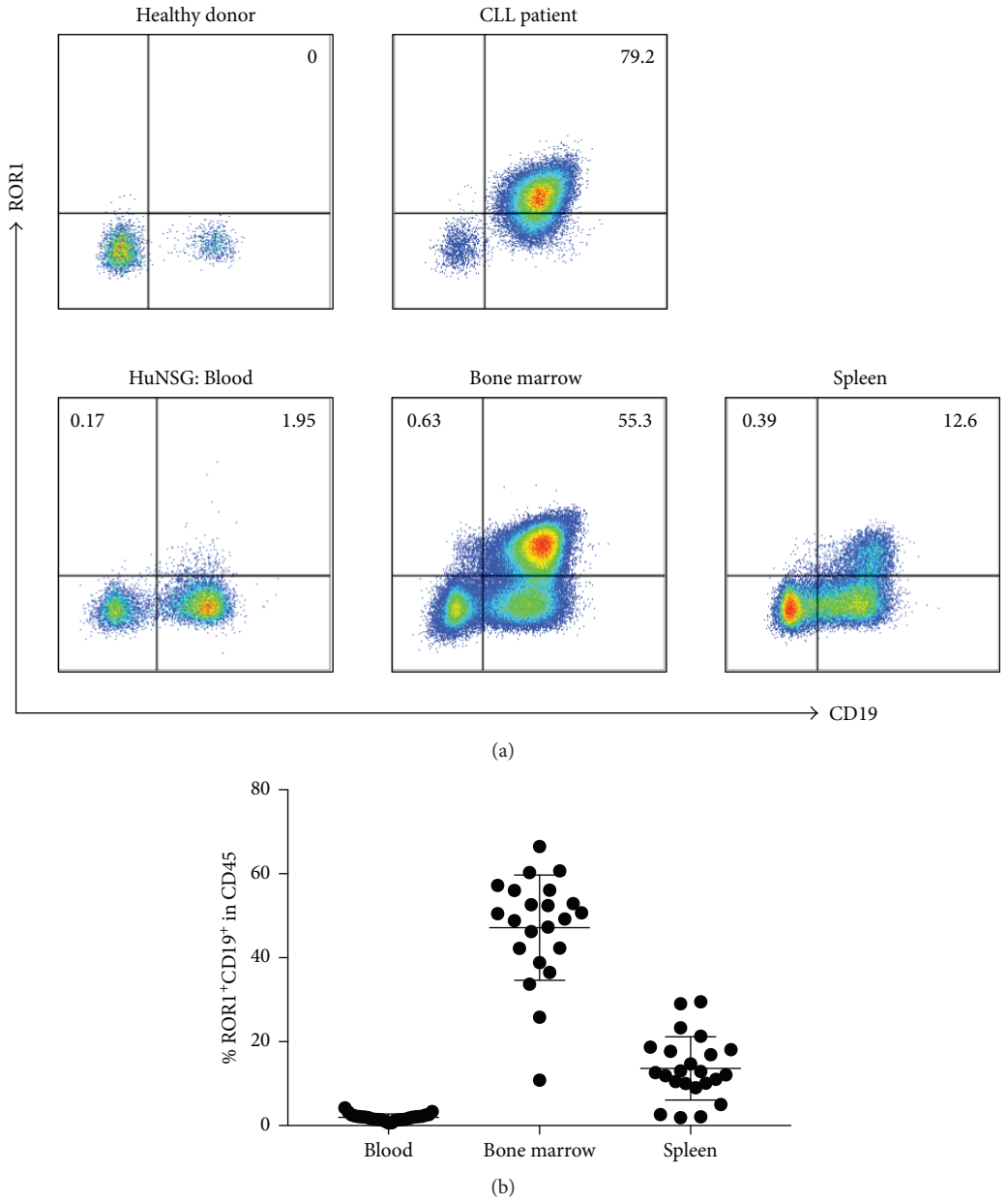

Figure 2: ROR1 expression on B cells in huNSG mice. (a) Flow cytometry staining of $CD19^+$ and $ROR1^+$ cells in PBMCs isolated from a healthy donor and a CLL patient (upper panel) and cells isolated from the blood, bone marrow, and spleen (lower panel) of huNSG mice. Samples were pregated as live cells, singlet cells positive for human CD45. The numbers indicate the frequency of $CD19^+$ and $ROR1^+$ cells within human $CD45^+$ cells. (b) Composite data from 3 independent experiments are shown. Each data point represents one individually analyzed mouse. Horizontal lines represent the mean and SD.

in using new mouse strain to generate better humanized mice with improved human B cell compartment [28, 29], we would expect to see less $ROR1^+$ immature B cells in these new models.

It has been reported that human T cells were required for B cell maturation in a humanized mouse model [16]. This might explain the significant inverse correlation of $ROR1^+$ B cells with T cells in our model. A higher number of reconstituted human T cells could aid B cell maturity and lead to a decrease in immature B cells. Since ROR1-expressing B cells were mostly immature B cells, the numbers decreased with increasing T cells. In the case of NK cells, we did not observe a significant inverse correlation with $ROR1^+$ B cells, suggesting that NK cells did not play a role in B cell maturation in huNSG mice.

ROR1 is a novel target for cancer immunotherapy as it is overexpressed in a number of malignancies without significant expression in normal adult tissues [30]. Different approaches including CAR T cells [10], monoclonal antibodies [9, 31], and bi-specific T cell engagers (BiTEs) [32] targeting ROR1 have been developed to treat tumors. All these immunotherapies require the help of other immune cells to

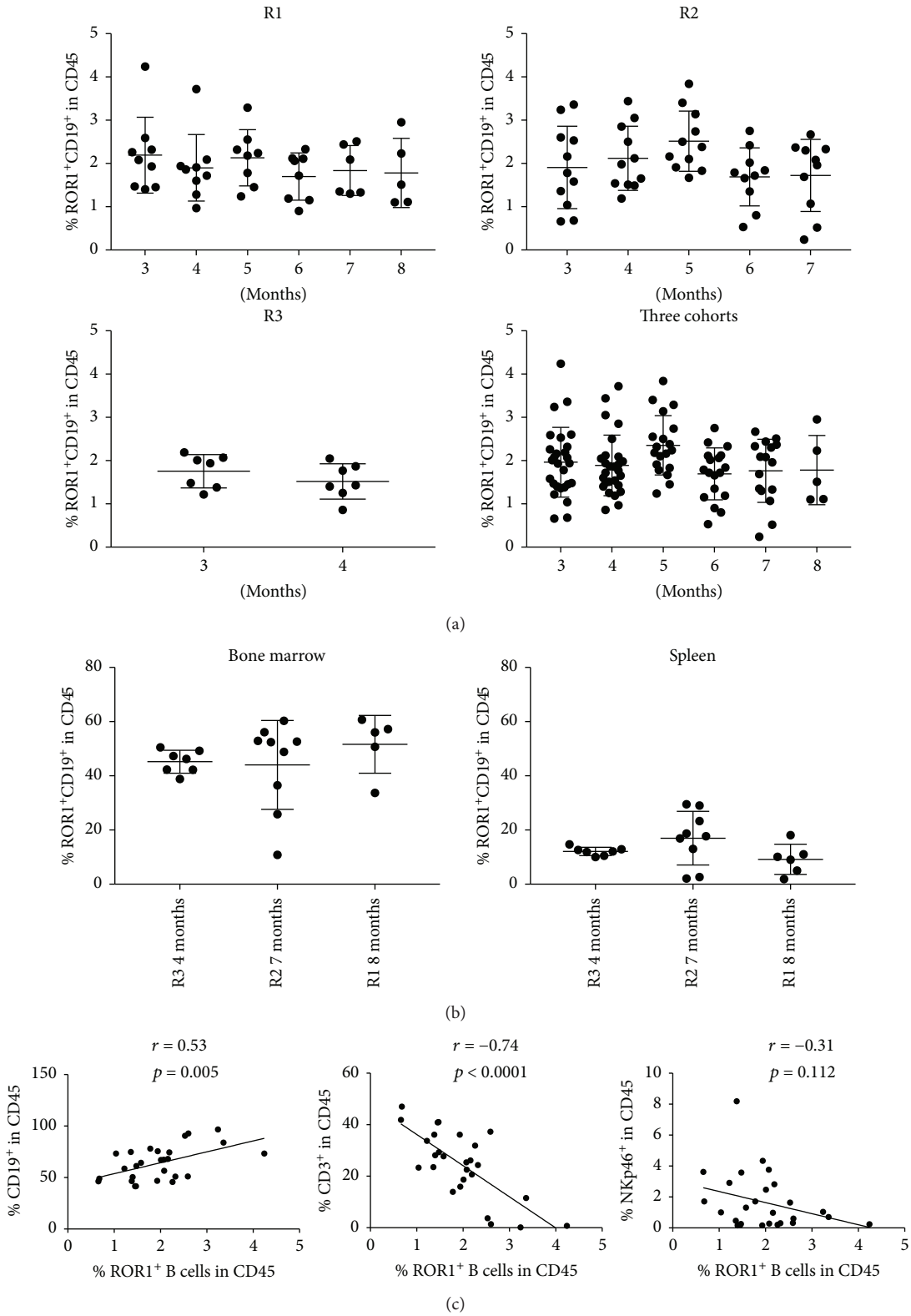

Figure 3: Frequency of ROR1-expressing B cells maintained in huNSG mice. (a) The frequency of ROR1$^+$ B cells within human CD45$^+$ cells in the blood of huNSG mice was analyzed in different time points after reconstitution. Data from 3 different cohorts of huNSG mice are shown individually (R1, R2, and R3) and as composite data (three cohorts). (b) Frequency of ROR1$^+$ B cells within human CD45$^+$ cells in the bone marrow (left) and spleen (right) of huNSG mice at different time points. Horizontal lines represent mean and SD. (c) Correlation of the frequencies of ROR1$^+$CD19$^+$ cells with the frequencies of human CD19$^+$ B cells, CD3$^+$ T cells, and NKp46$^+$ NK cells in huNSG mice. The Pearson coefficient r is shown, a two-tailed statistical analysis was performed, and the p value is shown.

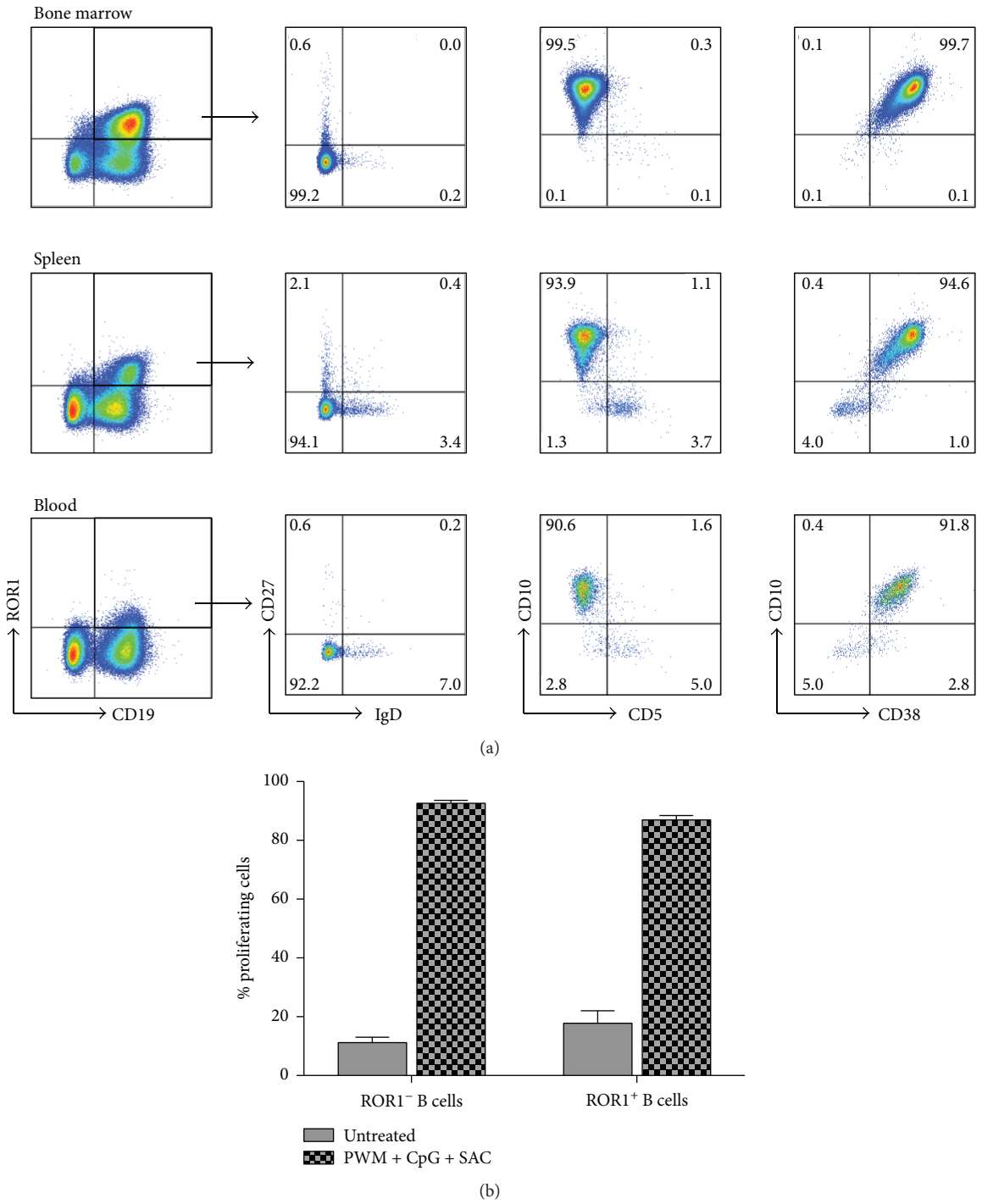

Figure 4: ROR1-expressing B cells were mostly immature B cells. (a) Flow cytometry staining of cells from the bone marrow, spleen, and blood of huNSG mice. Cells from the left panel were pregated as live cells, singlet cells positive for human CD45. ROR1$^+$CD19$^+$ cells were further analyzed for their expression of CD27, IgD, CD10, CD5, and CD38. Representative data from 3 different cohorts of huNSG mice are shown. (b) Splenocytes from huNSG mice were stained with CellTrace Violet and stimulated with PWM, CpG, and SAC or left unstimulated. After 4 days, cells were harvested and stained with CD19 and ROR1 antibodies, and percentage of proliferation of live gated CD19 B cells was measured by dye dilution by flow cytometry. The % of proliferating ROR1$^+$ and ROR1$^-$ B cells is shown. The graph depicts the results from 2 experiments.

function. ROR1-specific CAR has to be engineered in T cells to recognize and kill ROR1$^+$ target cells. Also, endogenous T cells have to be activated by BiTEs to act on ROR1$^+$ tumor cells. Additionally, ROR1-specific monoclonal antibody therapy may require NK cells to mediate cytotoxicity. Therefore, an *in vivo* model consisting of human ROR1$^+$ target cells and autologous immune cells would be a valuable tool to evaluate these therapies. Our data indicate that huNSG

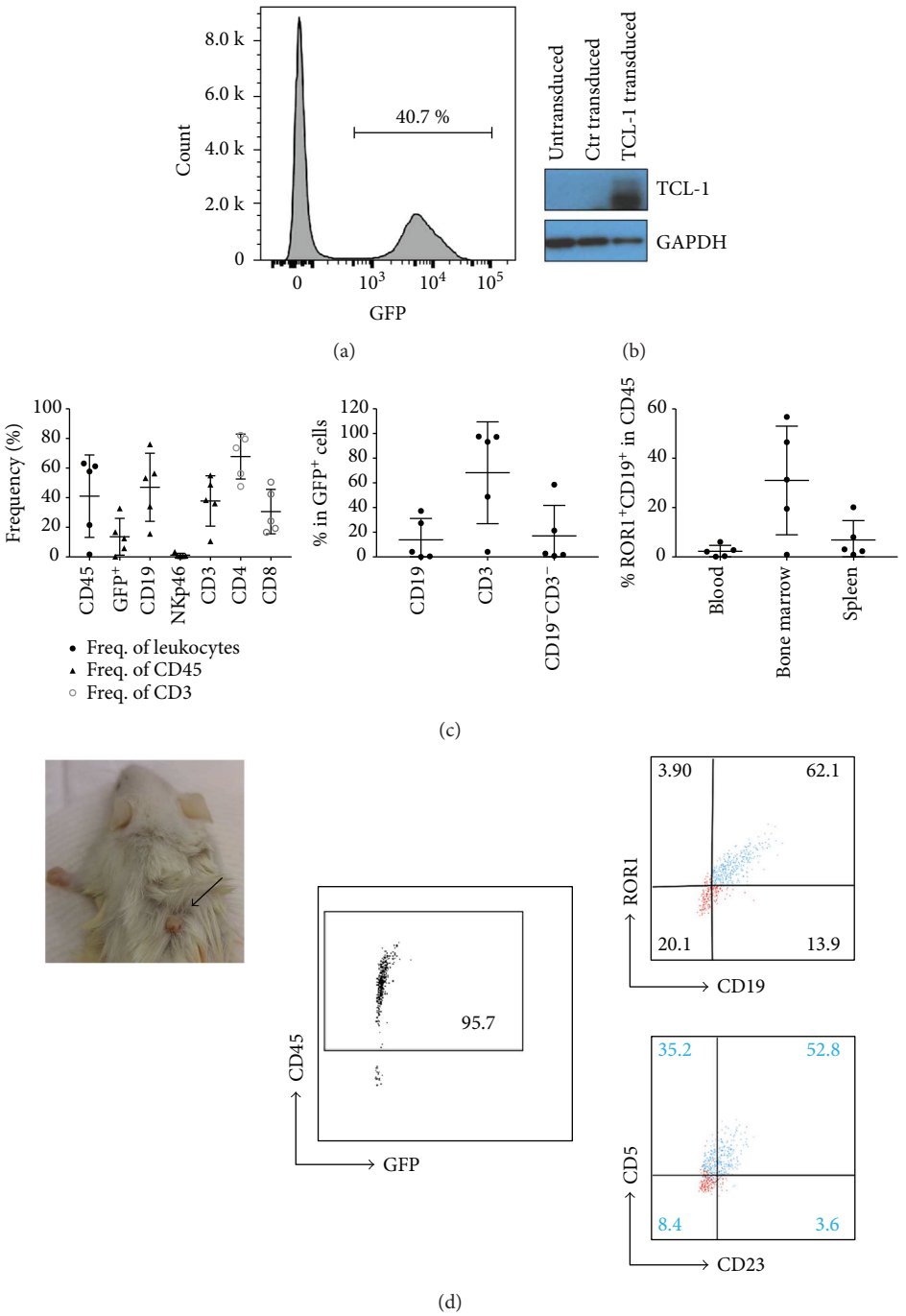

Figure 5: Engraftment of TCL-1-transduced human CD34$^+$ cells in NSG mice could induce ROR1-expressing tumors. (a) Human CD34$^+$ cells isolated from fetal liver tissues were transduced with lentivirus expressing TCL-1 GFP. Frequency of GFP-positive CD34$^+$ cells after 4 days of lentiviral transduction is shown. (b) CD34$^+$ cells transduced with lentivirus expressing TCL-1 (TCL-1 transduced) and control lentivirus (Ctr transduced) or untransduced were harvested and lysed 4 days after infection. Protein lysates were separated by gel electrophoresis, transferred to PVDF membranes by Western blotting, and probed with TCL-1-specific antibody. The blot was also probed for GAPDH as a loading control. (c) Peripheral blood from NSG mice transplanted with lentiviral-transduced CD34$^+$ cells was analyzed 3 months after reconstitution. The frequencies of different immune cell compartments are indicated. Frequencies of human CD45$^+$ cells within the leukocyte gate, frequencies of GFP$^+$ cells, CD19$^+$ B cells, NKp46$^+$ NK cells, and CD3$^+$ T cells within human CD45$^+$ cells, and frequencies of CD4$^+$ and CD8$^+$ T cells within CD3$^+$ cells are shown (left). The composition of the GFP$^+$ cells is shown (middle), and the frequency of CD19$^+$ and ROR1$^+$ cells within human CD45$^+$ cells in the blood, bone marrow, and spleen of the mice is presented (right). Horizontal lines represent mean and SD. Data are from 2 different reconstitution cohorts with CD34$^+$ cells derived from the same donor. (d) The mouse with the highest GFP$^+$ cells in the blood developed a tumor-like lump at the back as pointed by the arrow (left). Cells isolated from the tumor-like lump were analyzed by flow cytometry for the expression of human CD45 and GFP (left). The gated human CD45$^+$ cells were further analyzed for CD19, ROR1, CD5, and CD23 expression. The ROR1$^+$CD19$^+$ cell population is represented in blue.

mice have a stable proportion of ROR1$^+$ B cells in the peripheral blood, spleen, and bone marrow, together with functional autologous T cells and NK cells. It has been shown that huNSG T cells can be transduced and adoptively transferred back to the same host to control viral infection [33]. With this, ROR1-specific CAR T cells could be generated from huNSG mice and the efficacy can be evaluated by the removal of ROR1$^+$ cells in the host. As we can deplete different subsets of immune cells in huNSG mice [15, 34], this model enables a better study of the immunotherapies.

ROR1 surface expression in B cells is detected in more than 95% of CLL cases [1]. Though we found a high percentage of huNSG B cells expressing this oncofetal antigen, these were mainly immature B cells and had a very different phenotype compared to CLL B cells. It has been reported that surface ROR1 is present at an early stage of normal B cell differentiation in human bone marrow [10]. While ROR1-expressing CLL B cells are CD5$^+$CD23$^+$ mature cells [35], ROR1$^+$ B cells in huNSG mice are mainly CD5$^-$CD23$^-$ immature nonneoplastic B cells. That limits the potential use of this model to study antitumor efficacy. Moreover, this model should not be used for safety study of ROR1-directed immunotherapies because huNSG mice have a much higher frequency of ROR1$^+$ immature B cells than humans.

We attempted to generate an *in vivo* CLL model by manipulating the CD34$^+$ human hematopoietic progenitor cells. As the first transgenic mouse model of CLL was generated by overexpressing the human TCL-1 gene under the control of the immunoglobulin heavy chain variable region promoter and immunoglobulin heavy chain enhancer [19], we transduced CD34$^+$ human hematopoietic progenitor cells with TCL-1-expressing lentivirus before injecting these cells into the neonatal mice. The reconstituted mice did not develop a CLL-like disease or other leukemic diseases. This may be due to the following reasons. First, the reconstituted GFP-positive cells, representing the engraftment of TCL-1-transduced CD34$^+$ cells, were at a relatively low level, with the highest only at 32% of CD45$^+$ cells in one of the five mice. Second, the TCL-1 transgenic mouse model of CLL has a delayed disease development, in which CLL-like disease is usually developed at 8–12 months of age [36], whereas our mice were only at 6-7 months of age. Third, the TCL-1 gene was expressed under the EF1α promoter in our model. Future study should examine if TCL-1 overexpression under the control of the immunoglobulin heavy chain variable region promoter and immunoglobulin heavy chain enhancer could lead to a CLL-like phenotype.

Although the reconstituted mice did not develop CLL-like disease, the mouse with the highest reconstituted GFP-positive cells in the blood developed a tumor-like lump. Cells isolated from the lump were human CD45$^+$, and the majority were ROR1-expressing B cells. More than half of these cells coexpressed CD5 and CD23, hinting that they might be neoplastic B cells. However, these cells did not express GFP, suggesting that they might not be derived from the TCL-1-transduced CD34$^+$ cells, and how TCL-1 affected the interaction of the immune cells in huNSG mice and led to the development of this tumor-like lump remains to be determined.

In order to generate a consistent ROR1$^+$ tumor model in huNSG mice, we have to improve the transduction efficiency of CD34$^+$ cells and achieve a higher engraftment of TCL-1-transduced CD34$^+$ cells [37]. The oncogenic nature of TCL-1 is well documented [38], but the addition of ROR1 overexpression in the CD34$^+$ cells should be able to promote and drive tumorigenesis in huNSG mice [39]. Moreover, it has been shown that introducing genetic changes to CD34$^+$ human hematopoietic progenitor cells before injecting these cells into immunodeficient mice could generate a humanized mouse leukemic model that has recapitulating features of primary leukemia [40]. Introducing the genetic deletion of the chromosomal region 13q14, a common cytogenetic abnormality in CLL [41], could be considered.

In summary, we have shown that ROR1 protein was highly expressed in a proportion of B cells in huNSG mice; the majority of these cells were immature B cells. Transplantation of TCL-1-transduced CD34$^+$ human hematopoietic progenitor cells in neonatal NSG mice did not increase the frequency of ROR1-expressing B cells, but the mouse with the highest engraftment of transduced cells developed a tumor-like lump consisting of a high percentage of ROR1-expressing B cells. Further work would be required to induce frequent and consistent ROR1$^+$ tumors in huNSG mice for studying immunotherapies targeting ROR1.

Disclosure

This study was presented in the poster session A (A78) at the Tumor Immunology and Immunotherapy Conference organized by the American Association for Cancer Research in October 2017.

Conflicts of Interest

The author declares no competing financial interests.

Acknowledgments

This work was supported by a fellowship from the Swiss National Science Foundation (P300P3_155374) to Carol S. Leung. The author would like to thank Mrs. Emma Knights (University College London) for her frequent checking of the general health of mice and Dr. Maria Notaridou (Autolus Limited), Dr. Xiao Qin (University College London), and Dr. Jingyi Ma (University of Oxford) for their technical help on the experiments.

References

[1] S. Baskar, K. Y. Kwong, T. Hofer et al., "Unique cell surface expression of receptor tyrosine kinase ROR1 in human B-cell chronic lymphocytic leukemia," *Clinical Cancer Research*, vol. 14, no. 2, pp. 396–404, 2008.

[2] V. T. Bicocca, B. H. Chang, B. K. Masouleh et al., "Crosstalk between ROR1 and the pre-B cell receptor promotes survival of t(1;19) acute lymphoblastic leukemia," *Cancer Cell*, vol. 22, no. 5, pp. 656–667, 2012.

[3] G. Barna, R. Mihalik, B. Timár et al., "ROR1 expression is not a unique marker of CLL," *Hematological Oncology*, vol. 29, no. 1, pp. 17–21, 2011.

[4] A. H. Daneshmanesh, A. Porwit, M. Hojjat-Farsangi et al., "Orphan receptor tyrosine kinases ROR1 and ROR2 in hematological malignancies," *Leukemia & Lymphoma*, vol. 54, no. 4, pp. 843–850, 2013.

[5] S. Zhang, L. Chen, J. Wang-Rodriguez et al., "The oncoembryonic antigen ROR1 is expressed by a variety of human cancers," *The American Journal of Pathology*, vol. 181, no. 6, pp. 1903–1910, 2012.

[6] A. Gentile, L. Lazzari, S. Benvenuti, L. Trusolino, and P. M. Comoglio, "Ror1 is a pseudokinase that is crucial for Met-driven tumorigenesis," *Cancer Research*, vol. 71, no. 8, pp. 3132–3141, 2011.

[7] M. K. Hasan, J. Yu, L. Chen et al., "Wnt5a induces ROR1 to complex with HS1 to enhance migration of chronic lymphocytic leukemia cells," *Leukemia*, vol. 31, no. 12, pp. 2615–2622, 2017.

[8] A. Balakrishnan, T. Goodpaster, J. Randolph-Habecker et al., "Analysis of ROR1 protein expression in human cancer and normal tissues," *Clinical Cancer Research*, vol. 23, no. 12, pp. 3061–3071, 2017.

[9] A. H. Daneshmanesh, M. Hojjat-Farsangi, A. S. Khan et al., "Monoclonal antibodies against ROR1 induce apoptosis of chronic lymphocytic leukemia (CLL) cells," *Leukemia*, vol. 26, no. 6, pp. 1348–1355, 2012.

[10] M. Hudecek, T. M. Schmitt, S. Baskar et al., "The B-cell tumor–associated antigen ROR1 can be targeted with T cells modified to express a ROR1-specific chimeric antigen receptor," *Blood*, vol. 116, no. 22, pp. 4532–4541, 2010.

[11] S. Meixlsperger, C. S. Leung, P. C. Ramer et al., "CD141$^+$ dendritic cells produce prominent amounts of IFN-α after dsRNA recognition and can be targeted via DEC-205 in humanized mice," *Blood*, vol. 121, no. 25, pp. 5034–5044, 2013.

[12] L. Zitvogel, J. M. Pitt, R. Daillere, M. J. Smyth, and G. Kroemer, "Mouse models in oncoimmunology," *Nature Reviews Cancer*, vol. 16, no. 12, pp. 759–773, 2016.

[13] C. Leung, O. Chijioke, C. Gujer et al., "Infectious diseases in humanized mice," *European Journal of Immunology*, vol. 43, no. 9, pp. 2246–2254, 2013.

[14] E. Seung and A. M. Tager, "Humoral immunity in humanized mice: a work in progress," *The Journal of Infectious Diseases*, vol. 208, Suppl 2, pp. S155–S159, 2013.

[15] T. Strowig, C. Gurer, A. Ploss et al., "Priming of protective T cell responses against virus-induced tumors in mice with human immune system components," *Journal of Experimental Medicine*, vol. 206, no. 6, pp. 1423–1434, 2009.

[16] J. Lang, M. Kelly, B. M. Freed et al., "Studies of lymphocyte reconstitution in a humanized mouse model reveal a requirement of T cells for human B cell maturation," *The Journal of Immunology*, vol. 190, no. 5, pp. 2090–2101, 2013.

[17] I. Bekeredjian-Ding, S. Foermer, C. J. Kirschning, M. Parcina, and K. Heeg, "Poke weed mitogen requires Toll-like receptor ligands for proliferative activity in human and murine B lymphocytes," *PLoS One*, vol. 7, no. 1, article e29806, 2012.

[18] S. Crotty, R. D. Aubert, J. Glidewell, and R. Ahmed, "Tracking human antigen-specific memory B cells: a sensitive and generalized ELISPOT system," *Journal of Immunological Methods*, vol. 286, no. 1-2, pp. 111–122, 2004.

[19] R. Bichi, S. A. Shinton, E. S. Martin et al., "Human chronic lymphocytic leukemia modeled in mouse by targeted *TCL1* expression," *Proceedings of the National Academy of Sciences of the United States of America*, vol. 99, no. 10, pp. 6955–6960, 2002.

[20] L. D. Shultz, B. L. Lyons, L. M. Burzenski et al., "Human lymphoid and myeloid cell development in NOD/LtSz-*scid IL2R*γ^{null} mice engrafted with mobilized human hemopoietic stem cells," *The Journal of Immunology*, vol. 174, no. 10, pp. 6477–6489, 2005.

[21] S. Biswas, H. Chang, P. T. N. Sarkis, E. Fikrig, Q. Zhu, and W. A. Marasco, "Humoral immune responses in humanized BLT mice immunized with West Nile virus and HIV-1 envelope proteins are largely mediated via human CD5$^+$ B cells," *Immunology*, vol. 134, no. 4, pp. 419–433, 2011.

[22] E. Matutes, K. Owusu-Ankomah, R. Morilla et al., "The immunological profile of B-cell disorders and proposal of a scoring system for the diagnosis of CLL," *Leukemia*, vol. 8, no. 10, pp. 1640–1645, 1994.

[23] H. E. Broome, L. Z. Rassenti, H. Y. Wang, L. M. Meyer, and T. J. Kipps, "ROR1 is expressed on hematogones (non-neoplastic human B-lymphocyte precursors) and a minority of precursor-B acute lymphoblastic leukemia," *Leukemia Research*, vol. 35, no. 10, pp. 1390–1394, 2011.

[24] A. Audigé, M. A. Rochat, D. Li et al., "Long-term leukocyte reconstitution in NSG mice transplanted with human cord blood hematopoietic stem and progenitor cells," *BMC Immunology*, vol. 18, no. 1, p. 28, 2017.

[25] J. C. Biancotti and T. Town, "Increasing hematopoietic stem cell yield to develop mice with human immune systems," *BioMed Research International*, vol. 2013, Article ID 740892, 11 pages, 2013.

[26] R. Vuyyuru, J. Patton, and T. Manser, "Human immune system mice: current potential and limitations for translational research on human antibody responses," *Immunologic Research*, vol. 51, no. 2-3, pp. 257–266, 2011.

[27] Y. Watanabe, T. Takahashi, A. Okajima et al., "The analysis of the functions of human B and T cells in humanized NOD/shi-scid/γc^{null} (NOG) mice (hu-HSC NOG mice)," *International Immunology*, vol. 21, no. 7, pp. 843–858, 2009.

[28] H. Yu, C. Borsotti, J. N. Schickel et al., "A novel humanized mouse model with significant improvement of class-switched, antigen-specific antibody production," *Blood*, vol. 129, no. 8, pp. 959–969, 2017.

[29] S. Jangalwe, L. D. Shultz, A. Mathew, and M. A. Brehm, "Improved B cell development in humanized NOD-*scid IL2R*γ^{null} mice transgenically expressing human stem cell factor, granulocyte-macrophage colony-stimulating factor and interleukin-3," *Immunity, Inflammation and Disease*, vol. 4, no. 4, pp. 427–440, 2016.

[30] M. Shabani, J. Naseri, and F. Shokri, "Receptor tyrosine kinase-like orphan receptor 1: a novel target for cancer immunotherapy," *Expert Opinion on Therapeutic Targets*, vol. 19, no. 7, pp. 941–955, 2015.

[31] J. Yang, S. Baskar, K. Y. Kwong, M. G. Kennedy, A. Wiestner, and C. Rader, "Therapeutic potential and challenges of targeting receptor tyrosine kinase ROR1 with monoclonal antibodies in B-cell malignancies," *PLoS One*, vol. 6, no. 6, article e21018, 2011.

[32] S. H. Gohil, S. R. Paredes-Moscosso, M. Harrasser et al., "An ROR1 bi-specific T-cell engager provides effective targeting

and cytotoxicity against a range of solid tumors," *OncoImmunology*, vol. 6, no. 7, article e1326437, 2017.

[33] O. Antsiferova, A. Müller, P. C. Rämer et al., "Adoptive transfer of EBV specific $CD8^+$ T cell clones can transiently control EBV infection in humanized mice," *PLoS Pathogens*, vol. 10, no. 8, article e1004333, 2014.

[34] O. Chijioke, A. Müller, R. Feederle et al., "Human natural killer cells prevent infectious mononucleosis features by targeting lytic Epstein-Barr virus infection," *Cell Reports*, vol. 5, no. 6, pp. 1489–1498, 2013.

[35] J. Hulkkonen, L. Vilpo, M. Hurme, and J. Vilpo, "Surface antigen expression in chronic lymphocytic leukemia: clustering analysis, interrelationships and effects of chromosomal abnormalities," *Leukemia*, vol. 16, no. 2, pp. 178–185, 2002.

[36] T. Enzler, A. P. Kater, W. Zhang et al., "Chronic lymphocytic leukemia of Eμ-*TCL1* transgenic mice undergoes rapid cell turnover that can be offset by extrinsic CD257 to accelerate disease progression," *Blood*, vol. 114, no. 20, pp. 4469–4476, 2009.

[37] N. Uchida, M. M. Hsieh, J. Hayakawa, C. Madison, K. N. Washington, and J. F. Tisdale, "Optimal conditions for lentiviral transduction of engrafting human $CD34^+$ cells," *Gene Therapy*, vol. 18, no. 11, pp. 1078–1086, 2011.

[38] Y. Pekarsky, A. Drusco, P. Kumchala, C. M. Croce, and N. Zanesi, "The long journey of *TCL1* transgenic mice: lessons learned in the last 15 years," *Gene Expression*, vol. 16, no. 3, pp. 129–135, 2015.

[39] G. F. Widhopf, B. Cui, E. M. Ghia et al., "ROR1 can interact with TCL1 and enhance leukemogenesis in Eμ-TCL1 transgenic mice," *Proceedings of the National Academy of Sciences of the United States of America*, vol. 111, no. 2, pp. 793–798, 2014.

[40] H. Qin, S. Malek, J. K. Cowell, and M. Ren, "Transformation of human CD34+ hematopoietic progenitor cells with DEK-NUP214 induces AML in an immunocompromised mouse model," *Oncogene*, vol. 35, no. 43, pp. 5686–5691, 2016.

[41] U. Klein, M. Lia, M. Crespo et al., "The *DLEU2*/*miR-15a*/*16-1* cluster controls B cell proliferation and its deletion leads to chronic lymphocytic leukemia," *Cancer Cell*, vol. 17, no. 1, pp. 28–40, 2010.

Hindawi
Journal of Immunology Research
Volume 2018, Article ID 2386187, 10 pages
https://doi.org/10.1155/2018/2386187

Review Article

Immunotherapy with CAR-Modified T Cells: Toxicities and Overcoming Strategies

Shangjun Sun,[1,2] He Hao,[1,3] Ge Yang,[4] Yi Zhang,[5] and Yang Fu[1]

[1]*Department of Gastroenterology, The First Affiliated Hospital of Zhengzhou University, Zhengzhou, Henan 450052, China*
[2]*Department of Oncology, Ansteel Group Hospital, Anshan, Liaoning 114000, China*
[3]*Department of Orthopedics, Ansteel Group Hospital, Anshan, Liaoning 114000, China*
[4]*Department of Ophthalmology, The First Affiliated Hospital of Zhengzhou University, Zhengzhou, Henan 450052, China*
[5]*Biotherapy Center, The First Affiliated Hospital of Zhengzhou University, Zhengzhou, Henan 450052, China*

Correspondence should be addressed to Yi Zhang; yizhang@zzu.edu.cn and Yang Fu; fuyang@zzu.edu.cn

Received 28 August 2017; Accepted 7 February 2018; Published 17 April 2018

Academic Editor: Martin Holland

T cells modified via chimeric antigen receptors (CARs) have emerged as a promising treatment modality. Unparalleled clinical efficacy recently demonstrated in refractory B-cell malignancy has brought this new form of adoptive immunotherapy to the center stage. Nonetheless, its current success has also highlighted its potential treatment-related toxicities. The adverse events observed in the clinical trials are described in this review, after which, some innovative strategies developed to overcome these unwanted toxicities are outlined, including suicide genes, targeted activation, and other novel strategies.

1. Introduction

Cell-based therapies have risen to the forefront of treatment approaches for cancer [1]. Progress in synthetic biology and gene transfer enables a rapid and efficient redirection of polyclonal T lymphocytes [2]. T cells modified via synthetic CARs have made remarkable achievements in eliminating chemotherapy-resistant acute lymphoblastic leukemia [3–7], chronic lymphocytic leukemia [8, 9], and non-Hodgkin lymphoma [10, 11]. In light of their promise, there has formed a broad wave of CAR-modified T cells for cancer immunotherapy, including the challenging solid tumors [12–15].

CARs commonly composed of an extracellular antigen-binding moiety (i.e., single-chain variable fragment of antibody) fused to intracellular signaling domains can reprogram specificity against the targeted molecules of a selected cell and outsmart HLA restriction [16, 17]. Upon antigen ligand engagement, CAR T cells can produce cytokines, kill targeted cells, and stimulate the proliferation of T cells, resulting in a highly amplified response and the consequent eradication of a huge quantity of tumor cells within weeks. Despite CAR T cells being promising, toxicities have been associated with most of the clinical responses, and fatal complications have been observed in some patients treated with gene-modified T cells [18–22]. The aim of this review is to provide a framework for the classification of different toxicities and highlight state-of-the-art potential overcoming strategies.

2. Toxicities of T Cells Genetically Modified with CARs

A brisk immune response can be a double-edged weapon. The efficacy of T cells genetically modified with CARs against cancer is greatly improved at the expense of enhanced toxicities; therefore, it will be useful to classify the multifaceted adverse events in trials, clearly dividing them into five categories, i.e., on-target on-tumor, on-target off-tumor, off-target, neurotoxicity, and other toxicities (Figure 1).

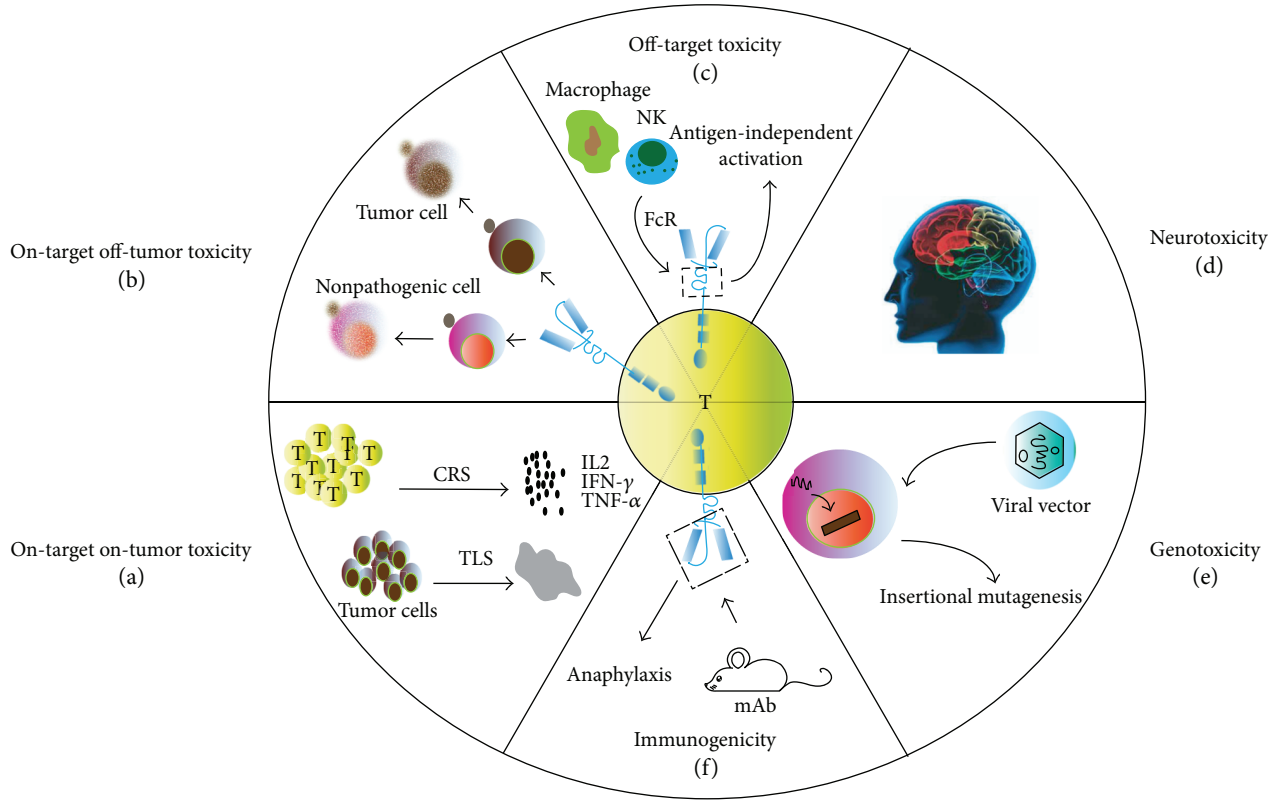

Figure 1: Toxicities of T cells genetically modified with CARs. (a) On-target on-tumor toxicity. (a1) Effector T-cell activation and excessive cytokine release may result in cytokine release syndrome (CRS). (a2) High tumor load leads to massive destruction of tumor tissue, resulting in tumor lysis syndrome (TLS). (b) On-target off-tumor toxicity: the shared target antigen is also expressed on nonpathogenic cell, subsequently damaging healthy tissue. (c) Off-target toxicity: the extracellular crystallizable fragment (Fc) of CARs can interact with the Fc receptor (FcR) expressed on innate immune cells, leading to antigen-independent activation. (d) Neurotoxicity: manifestation ranges from confusion, delirium, aphasia to some degree of myoclonus, and seizure. (e) Genotoxicity: integrating viral vectors used to facilitate the stable expression in primary T cells may pose a potential risk of oncogenic insertional mutagenesis. (f) Immunogenicity: single-chain variable fragments (scFvs) derive from mouse monoclonal antibodies (mAbs), leading to severe immune response.

2.1. On-Target On-Tumor Toxicity. When it comes to the toxicity specific to the administration of T cells itself, the most common toxicity is the on-target on-tumor type, which is triggered by excessive cytokine release or tumor cell necrosis (Figure 1(a)). The underlying premise of immunotherapy is to activate effector T cell and achieve cytokine release. However, excessive cytokine release may result in cytokine release syndrome (CRS), which can vary from mild moderate to severe potentially fatal forms [18–20]. Furthermore, the rapid devastation of large quantities of tumor cells can also trigger tumor lysis syndrome (TLS), which can bring out an array of systemic metabolic disturbances with an overlap in symptoms with CRS and is characterized by elevated levels of phosphate, potassium, and uric acid in serum [8, 21]. Emerging evidence suggests that the severity of CRS and TLS depends upon disease burden [3, 22]; splitting the initial dose and strictly monitoring the vital parameters can mitigate the risk [5, 23]. Additionally, considering that CRS manifests as a rapid immune reaction driven by the massive release of cytokines, including IFN-γ, IL-6, and IL-10, the administration of high-dose corticosteroids and corresponding antagonist mAb (e.g., IL-6 receptor antagonist mAb and tocilizumab) can also be effective therapeutic interventions [24–26].

2.2. On-Target Off-Tumor Toxicity. The most striking toxicity specific to genetically targeted T cells is "on-target off-tumor," resulting from a direct attack on normal tissues that have the shared expression of the targeted antigen (Figure 1(b)). Considering the potency of redirected T cells, toxicity on nonpathogenic tissues expressing low levels of the antigen can be highly detrimental. For example, Erasmus University's earliest trials described the occurrence of cholestasis in renal cell carcinoma patients infused with T cells modified with a CAR specific for carbonic anhydrase IX, which is physiologically expressed on bile duct epithelial cells [27, 28]. Similarly, low-level ERBB2 expression on lung epithelia might have precipitated the reported case of fatal lung toxicity [29]. With these toxicities in mind, the selection of target antigen, which is strictly specific to the tumor (e.g., EphA2 [30] and mutated EGFRvIII [31, 32]) or on the category of nonessential tissues (e.g., thymic stromal lymphopoietin [33, 34] and CD33 [35, 36]), is probably the most critical determinant to broaden the application. Indeed, such

antigens have been difficult to identify, particularly in the settings of solid malignancies. Moreover, a study proved that the substantial dose of infused CAR T cells (1×10^{10}) could potentially provoke this toxicity, and lower doses of HER2/neu-specific CAR T cells (without prior conditioning chemotherapy) were safe [13]. Hence, given the known background expression of the target antigen, it becomes extremely important to determine whether levels are over the threshold that can cause this toxicity and to determine the potential severity thereof in humans.

2.3. Off-Target Toxicity. Off-target toxicity occurs when the transduced T-cell population unexpectedly attacks an antigen other than the intended one or activates themselves independently from their specificity (Figure 1(c)). The majority of CAR T cells recognize antigens through single-chain variable fragments derived from monoclonal antibodies (mAbs). However, the safety of some mAbs profile is uncertain. The data *in vitro* suggested that the artificial synthetic constructs themselves may carry some risks of off-target recognition. For example, the toxicity profile of the mAbs has been illustrated in the case of trastuzumab (anti-HER2/neu), in which CARs carrying the IgG1-derived CH2CH3 domain as extracellular spacer may interact with the Fc receptor expressed on innate immune cells (e.g., macrophages and NK cells), leading to antigen-independent activation [29]. Fortunately, the off-target recognition of cross-reactive antigens has not been evident in CAR T-cell trials to date. Nonetheless, fatal cardiac toxicity has been seen in 2/2 patients infused with autologous T cells engineered to express an enhanced affinity T-cell receptor (TCR) directed against the testis antigen MAGE-A3 [37, 38], of which the cross-reactivity occurred against titin only expressing in cardiac tissue [39]. Therefore, this possibility has to be kept in mind for future developments when CAR T cells target novel tumor-associated antigen.

2.4. Neurotoxicity. Neurotoxicity is another potentially serious toxicity observed in patients receiving CD19-specific CAR T-cell therapy, and its manifestation ranges from confusion, delirium, and aphasia to some degree of myoclonus and seizure (Figure 1(d)). What is not clear is the causative pathophysiology of these neurologic side effects. Although a clear expression of CD19 in the affected brain areas has not been shown, some groups have documented the infiltration of CAR T cells into the cerebrospinal fluid (CSF) in most patients with neurotoxicity [3–5, 40]. Lee et al. particularly found that 6/21 patients who had neurotoxicity had higher concentrations of CSF CAR T cells. However, magnetic resonance imaging scans often did not show abnormalities. Furthermore, a similar constellation of symptoms has also been observed in patients treated with blinatumomab [41, 42]. Therefore, it is uncertain if the toxicity arises from direct CAR T cells attack on the CNS tissue or generalized cytokine-mediated inflammation [43]. To date, the neurologic toxicity in all but the rare fatal cases has been reversible and self-limited. Understanding the mechanisms behind it will be critical for safer CAR T-cell therapy as well as for more effective management of these adverse effects.

2.5. Other Toxicities. Besides the toxicities mentioned above, there are some others as follows: (1) Immunosuppression: Immunosuppressive pretreating to the recipients prior to T-cell infusion is associated with much greater antitumor efficacy [44]. Unfortunately, the lymphodepleting and nonmyeloablative regimen comes along with the well-known toxicities of anemia, coagulopathy, and neutropenic sepsis. The mortality of this toxicity is approximately 1% and constitutes the major fatal risk of adoptive T-cell therapy in the National Cancer Institute Surgery Branch experience [45, 46]. (2) Immunogenicity: The majority of the antigen recognition region used in a genetically modified T cell is derived from mouse mAb [47], of which the foreign potential immunogenicity may lead to severe anaphylaxis [48–50] (Figure 1(f)). The mesothelin-specific CAR T cell had been reported to cause severe cardiac dysfunction [51], which was ultimately attributed to the formation of anti-mouse antibody triggered by allergic reaction. Therefore, diligent surveillance, prompt recognition, and immediate treatment must be adhered to, to control this life-threatening toxicity, whenever possible, and especially, if repeated dosing is planned, humanizing scFvs rather than mouse mAbs should be used [52]. (3) Genotoxicity: Integrating viral vectors used to facilitate the stable expression in primary T cells may pose a potential risk of oncogenic insertional mutagenesis, including the disruption of normal gene expression as observed in the therapy for SCID-X1 on the account of an uncontrollable LMO2 gene [53, 54] (Figure 1(e)). Though no such toxicity of vector-induced immortalization, clonal expansion, or enrichment for integration sites has been reported in CAR therapy to date [55], it is clearly an important consideration for the future when CAR T cells may prevail for the lifetime of the treated patient.

3. Overcoming Strategies of Related Toxicities

In light of the different spectrums of toxicities associated with the administration of T cells, it is logical to find a fine balance between tumor elimination and unexpected toxicities. To achieve this, innovative strategies have been implemented to offer compelling opportunities, including suicide gene, targeted activation, and other innovative gene therapy strategies.

3.1. Suicide Gene Therapy. To manage unexpected toxicities or to eliminate transduced T cells after an eradication of the disease, coexpressing a conditional safety switch is a potentially effective tool. A suicide gene is a gene-encoding molecule, which allows the selective destruction of expressing cells upon the administration of a nontoxic prodrug and the elimination of the symptoms of treatment-driven toxicities (Figure 2); however, the clinical impact on their activation is unknown at present. The HSV-tk suicide gene has been utilized in most clinical settings, rendering target cells susceptible to GCV-mediated elimination [56–58] (Figure 2(a)). While limited by the immunogenicity of viral enzymes and the long time (several days) to reach full effect [59, 60], it may not be acceptable in the face of toxicities, which pose immediate threat to live. Alternative safety switches are based on the well-characterized, targetable surface

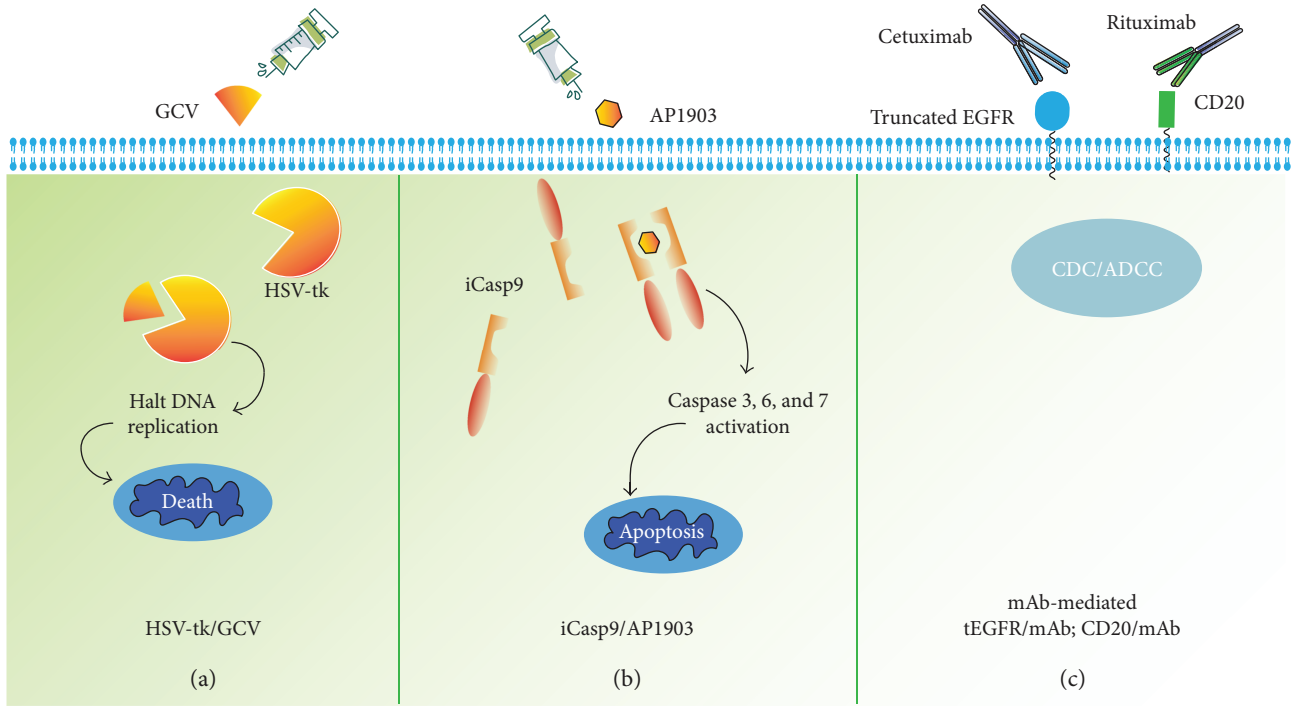

Figure 2: Summary of overcoming toxicities by the suicide gene co-expression in T cells. (a) HSV-tk turns the nontoxic prodrug GCV into GCV-triphosphate, leading to cell death by halting DNA replication. (b) iCasp9 can bind to the small molecule AP1903 and result in dimerization, which activates the intrinsic apoptotic pathway. (c) Targetable surface antigen expressed in the transduced T cells (e.g., CD20 and truncated EGFR), allowing eliminating the modified cells efficiently through complement/antibody-dependent cellular cytotoxicity (CDC/ADCC) after administration of the associated monoclonal antibody.

antigen expressed in the transduced T cells, such as CD20 [61, 62] and truncated EGFR [63, 64], allowing eliminating the modified cells efficiently through complement/antibody-dependent cellular cytotoxicity (CDC/ADCC) after the administration of the associated monoclonal antibody (Figure 2(c)). Despite the preponderance of the system in nonimmunogenicity and dual-purpose nature of the additional transgene (which can also be used to measure the persistence of the transduced T cells), its efficacy and kinetics as a CAR T-cell elimination system have not been tested in the settings of clinical toxicities.

The inducible caspase 9 (iCasp9)/AP1903 suicide system is perhaps the most advanced and effective solution, which is based on the fusion of caspase 9 and a drug-sensitive FK-modified binding protein [60, 65]. Upon being exposed to the synthetic molecule AP1903, the fusion protein dimerizes and leads to the rapid apoptosis of T cells (Figure 2(b)). The efficacy and safety of iCasp9/AP1903 have been first demonstrated in allogeneic hematopoietic stem cell transplantation studies [66, 67]. When the GvHD occurred, AP1903 administration could eliminate iCasp9-expressing T cells within 30 min from the end of AP1903 administration (2 hours of infusion), followed by the permanent abrogation of symptoms without recurrence [68]. This response has also been replicated in preclinical models using CAR T cells along with coexpressing iCasp9 [69–71]. However, this represents the least preferred strategy, since the depletion of the CAR T cell will also mean abrogating its therapeutic potential, and the modulated activation of the switch and multiple administration of CAR T cells are potential strategies to overcome this issue.

3.2. Targeted Activation

3.2.1. Targeting Two Tumor-Associated Antigens. Considering the prematurely attenuated therapeutic potential of suicide genes, there is a considerable interest in developing T cells whose activation can be controlled through combinatorial antigen-targeting activation with separated signals. These include dual targeting CAR strategies in which T cells are modified to express two CARs with different tumor-associated antigens to ensure that their activation occurs only on tumor cells [72–74]. It is achieved by "splitting" the activation signal and the endocostimulatory signal in different CAR constructs (Figure 3(a)). Likewise, this has also been proven in principle for Tan-CARs [75, 76], a single CAR that has specificity for two antigens owing to the expression of two tandemly arranged scFvs coupled to the same signaling domain (Figure 3(b)). Alternatively, if the presentation of antigens is exclusive to normal tissue, the inclusion of inhibitory CARs (iCARs) mediated by the physiological checkpoint molecule (PD-1 and CTLA-4) is another approach [77, 78]. The binding of iCARs bind to antigens found on normal cells can result in the inhibition of the CAR T-cell function, allowing a dynamic, self-regulating switch to target malignant tissue (expressing one antigen) while the normal tissue is spared [79] (Figure 3(c)). Recently, an novel dual-receptor AND-gate CAR called synthetic Notch (synNotch)

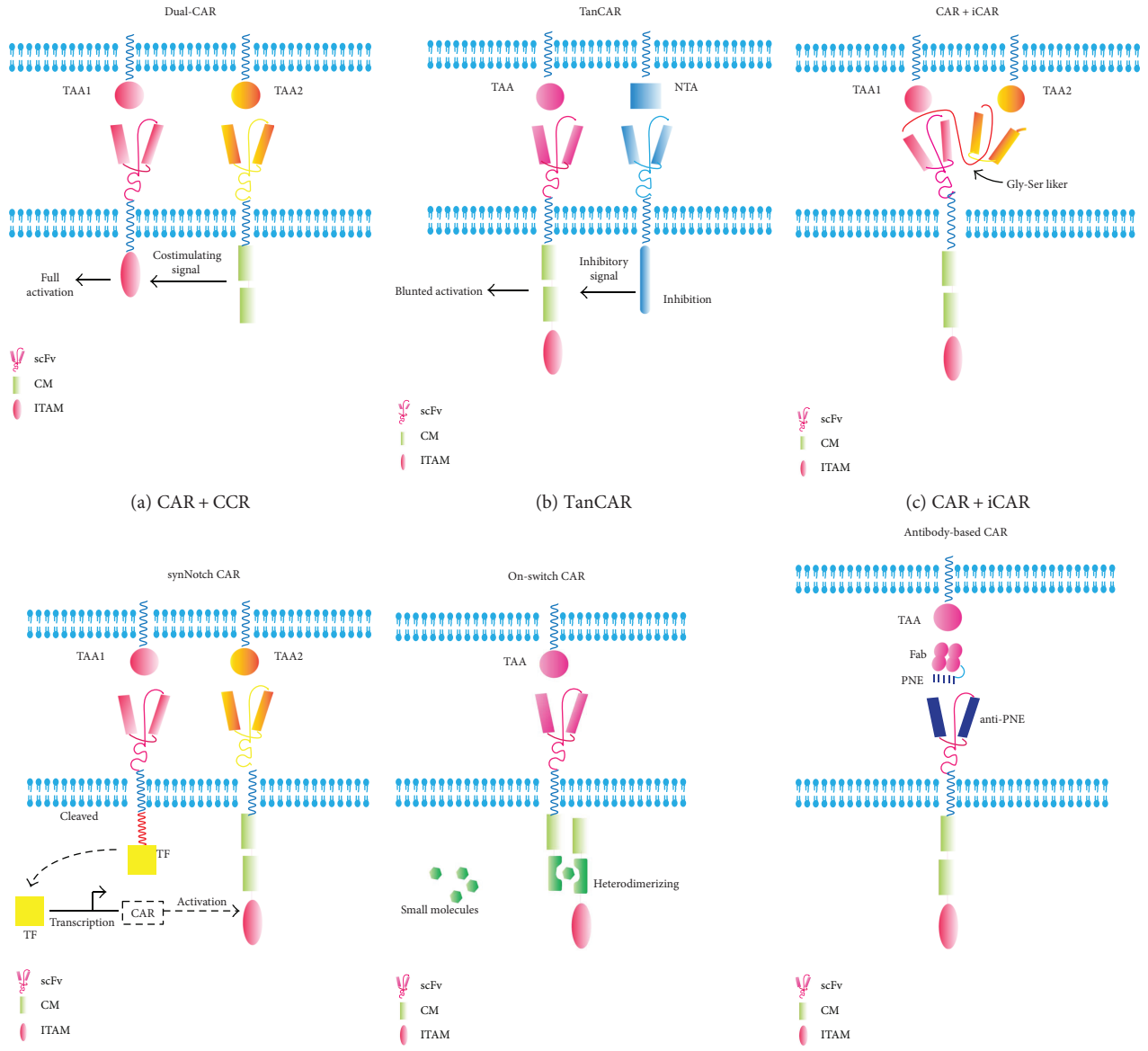

FIGURE 3: Summary of the targeted activation strategies for T cells to overcome toxicities. (a) In the dual targeting CAR-modified T cells, the T cells are transduced with both a CAR that provides suboptimal activation upon binding of one antigen and a chimeric costimulatory receptor (CCR) that recognizes a second antigen. (b) T cells are designed with a bispecific tandem CAR (TanCAR), in which two distinct antigen recognition domains are present in tandem by a Gly-Ser linker. (c) T cells can be engineered with an inhibitory receptor, carrying an intracellular domain from PD1 or CTLA-4, which can be triggered by an antigen expressed on normal cells, allowing T-cell inhibition outside the tumor. (d) Design of a synNotch AND-gate circuit that requires T cells to sense two antigens to activate. It works in two sequential steps: (1) The synNotch receptor is engineered to allow the T cell to recognize TAA1. Upon ligand recognition by the synNotch receptor, an orthogonal transcription factor is cleaved from the cytoplasmic tail, and (2) the T cell expresses a CAR directed towards TAA2. The cleaved transcription factor primes CAR expression. If A and B are present, the T cells can activate and kill the target tumor. (e) The on-switch CAR design distributes key components from the conventional CAR into two physically separate polypeptides that can be conditionally reassembled when a heterodimerizing small-molecule agent is present. Only in the presence of a heterodimerizing small molecule can they conditionally reassemble. (f) Antibody-based switches are engineered by the introduction of peptide neo-epitopes (PNE) at defined locations in an antigen-specific antibody. Given that the PNE is not an endogenous tissue or antigen , the activation of the sCAR-T cell is therefore strictly dependent on the presence of the switch. scFV: single-chain variable fragment of antibody; CM: costimulatory molecule; ITAM: immune-receptor tyrosine-based activation motif; TAA: tumor-associated antigen; NTA: normal tissue antigen; CAR: chimeric antigen receptor; CCR: chimeric costimulatory receptor; iCAR: inhibitory CAR; TanCAR: tandem CAR; synNotch CAR: synthetic notch CAR; TF: transcription factor; PNE: peptide neo-epitope; Fab: fragment of antigen binding.

has been developed in the lab of Wendell Lima, which consists of an engineered antigen-recognition domain towards an antigen of interest (e.g., CD19 or surface GFP), a Notch core, and an artificial transcription factor [80, 81]. Upon ligand recognition by the synNotch receptor, an orthogonal transcription factor (e.g., TetR-VP64 or Gal4-VP64) is cleaved from the cytoplasmic tail that regulates a custom genetic circuit, and the cleaved transcription factor primes CAR expression. Only when both antigens are present can it work orthogonally and requires no signaling intermediates, providing an extraordinary flexible way to regulate customized cascades in a wide variety of applications [82] (Figure 3(d)). However, the immunogenicity of the nonhuman transcription factors remains to be investigated [83].

3.2.2. Switch-Mediated Activation

(1) On-Switch CAR. Overriding strategies by the inclusion of an "on-off" switch in CAR design enable the precise regulation of the location, duration, and intensity of therapeutic activities. Wu et al. [84] described an approach that gated cellular functions by clinician-prescribed small molecule inputs, making a major step. The authors distributed the conventional CAR into two parts by expressing the extracellular antigen-binding domain separately from the intracellular signal-transducing domain. Only in the presence of a heterodimerizing small molecule can they conditionally reassemble (Figure 3(e)). This approach has great potential for clinical application. Similarly, Juillerat et al. described a strategy to create a "transient" CAR T cells with a new architecture in CARs that are directly dimerized at the hinge domain with the addition of a small molecule. They finally confirmed that it can offer a basic framework to use alternative split-CARs and show a more controlled and potentially safer way towards the development of the engineered CAR T cell [85]. In summary, both exogenous control behaviors based on small molecules below can be implemented for the modified T cell to alter conventional T cells into smart T cells whose therapeutic behaviors are precise and effective and subject to user control [86].

(2) Recombinant Antibodies as Switches. With the rapid development of the bispecific antibodies in cancer immunotherapy [87, 88], the titratable recombinant antibody-based switches also enable the precise control geometry and stoichiometry of complex formation between the target cells and T cells. Examples of these switches include TAA-specific monoclonal antibodies that elicit antitumor activity from Fc-specific CAR T cells [89] and chemically or enzymatically modified antibody-hapten conjugates that redirect antihapten CAR T cells [90, 91]. Rodgers et al. reported the tumor antigen-specific Fab molecule engrafted with a peptide neoepitope (PNE) that is bound exclusively by a PNE-specific switchable CAR T cell [92] (Figure 3(f)), and Kim et al. demonstrated the redirection of anti-FITC CAR T cells with a heterobifunctional small-molecule switch, folate-FITC, which selectively targets folate receptor-overexpressing cancers [93]. Overall, these switchable CAR T-cell dosing regimens could be tuned to provide efficacy comparable to that of the corresponding conventional CAR T cells targeting CD19, characterized by lower cytokine levels and broader range of antigens targeting. Therefore, this may offer a method of mitigating CRS, as well as a strategy for targeting other types of cancer, including solid tumors.

3.3. Other Strategies. In addition to the strategies mentioned above, it is possible to tune down the intrinsic potency of genetically targeted T cells by controlling the expression time or modulating the affinity of TCRs/CARs. The transient expression of CARs in T cells using nonviral methods (e.g., mRNA electroporation [12] and sleeping beauty transposition [94]) and the stimulation of activation-induced T-cell inhibitory proteins (e.g., PD-1 [95]) ensure the limited persistence of the redirected T cells; conversely, the regulation of affinity may be achieved via high-affinity TCR/CAR detection [96]. A fully human CAR comprised of the human C4 folate receptor-alpha (αFR)-specific scFv has been developed with lower affinity for αFR protein and less recognition of normal cells expressing low levels of αFR, which may overcome the issues of transgene immunogenicity and "on-target off-tumor" toxicity [97]. However, affinity tuning may decrease the threshold for CAR T-cell activation, which may change the therapeutic window of CAR T cells to tissues that express only high levels of antigen [98].

Besides, directing CAR T-cell delivery on the tumor sites anatomically may also limit toxicity and enhance therapeutic efficacy, which may be achieved by intratumoral or local intralymphatic delivery [99] and/or by engineering CAR T cells to express receptors of tumor-secreted chemokines [100, 101]. The "fourth-generation" CAR (or TRUCK) T cells with inducible release of IL-12 attract and activate innate immune cells to the targeted tumor lesion, which in turn eliminate cancer cells not recognized by CAR T cells [102, 103]. It offers a strategy to locally achieve therapeutic concentrations freed from systemic toxicity and prevent tumor relapse by residual cancer cells. Last but not least, the type of T cells used for adoptive transfer is critical, with T cells displaying a less differentiated phenotype potentially delivering improved therapy in vivo [104]. The CAR expressed in Vα24-invariant natural killer T- (NKT-) cells can build on the natural antitumor properties of these cells while their restriction by monomorphic CD1d limits toxicity [105], and the CD19-transduced T memory stem cells cultured in IL-7 and IL-15 cytokines expanded more efficiently and showed more potent survival and more powerful antitumor effect in preclinical models [106].

4. Perspectives

Over the last decade, CAR-modified T-cell therapy has progressed rapidly, and dramatic benefits in patients with refractory hematological malignancies have formed a powerful trend in developing this therapy. The unparalleled efficacy was, however, frequently associated with toxicities that were not fully anticipated by preclinical studies. As better medical management of the associated adverse events has been put into effect and more innovative gene therapy strategies have been developed, we can expect that the era with improved

control of toxicities with resulting superior outcomes and applicability of CAR T-cell approaches is not far away. The challenge will be to see whether in the next 5–10 years, the CAR T-cell approach will be more widely applied as the first-line treatment in a wider array of hematologic malignancies and other neoplasms.

Conflicts of Interest

The authors declare that they have no conflict of interest.

Authors' Contributions

Shangjun Sun and He Hao wrote the first draft of the review after consulting a large number of reviews and articles; Ge Yang designed the three figures; and Yang Fu and Yi Zhang participated extensively in revising and determining the content contained in the review. Shangjun Sun and He Hao contributed equally to this work.

Acknowledgments

This study was supported by the Chinese National Natural Science Foundation of Youth Fund (nos. 81401944 and 81602154), the National Natural Science Foundation of China (nos. 81171986 and 81271815), the National Key Research and Development Program of China (2016YFC1303501), the Project of Henan Health Department (no. 201401004), the Basic and Advanced Technology Research Projects of Henan Science and Technology Department (nos. 142300410378, 1611003101000, and 162102410060), and the Key Scientific Research Projects of Colleges and Universities of Henan Province Department of Education (no. 15A320014).

References

[1] M. A. Fischbach, J. A. Bluestone, and W. A. Lim, "Cell-based therapeutics: the next pillar of medicine," *Science Translational Medicine*, vol. 5, no. 179, article 179ps7, 2013.

[2] M. C. Jensen, "Synthetic immunobiology boosts the IQ of T cells," *Science*, vol. 350, no. 6260, pp. 514-515, 2015.

[3] S. L. Maude, N. Frey, P. A. Shaw et al., "Chimeric antigen receptor T cells for sustained remissions in leukemia," *The New England Journal of Medicine*, vol. 371, no. 16, pp. 1507–1517, 2014.

[4] D. W. Lee, J. N. Kochenderfer, M. Stetler-Stevenson et al., "T cells expressing CD19 chimeric antigen receptors for acute lymphoblastic leukaemia in children and young adults: a phase 1 dose-escalation trial," *The Lancet*, vol. 385, no. 9967, pp. 517–528, 2015.

[5] M. L. Davila, I. Riviere, X. Wang et al., "Efficacy and toxicity management of 19-28z CAR T cell therapy in B cell acute lymphoblastic leukemia," *Science Translational Medicine*, vol. 6, no. 224, article 224ra225, 2014.

[6] C. J. Turtle, L. A. Hanafi, C. Berger et al., "CD19 CAR-T cells of defined $CD4^+$:$CD8^+$ composition in adult B cell ALL patients," *The Journal of Clinical Investigation*, vol. 126, no. 6, pp. 2123–2138, 2016.

[7] S. A. Grupp, M. Kalos, D. Barrett et al., "Chimeric antigen receptor–modified T cells for acute lymphoid leukemia," *The New England Journal of Medicine*, vol. 368, no. 16, pp. 1509–1518, 2013.

[8] D. L. Porter, W. T. Hwang, N. V. Frey et al., "Chimeric antigen receptor T cells persist and induce sustained remissions in relapsed refractory chronic lymphocytic leukemia," *Science Translational Medicine*, vol. 7, no. 303, article 303ra139, 2015.

[9] D. L. Porter, B. L. Levine, M. Kalos, A. Bagg, and C. H. June, "Chimeric antigen receptor–modified T cells in chronic lymphoid leukemia," *The New England Journal of Medicine*, vol. 365, no. 8, pp. 725–733, 2011.

[10] J. N. Brudno, R. P. Somerville, V. Shi et al., "Allogeneic T cells that express an anti-CD19 chimeric antigen receptor induce remissions of B-cell malignancies that progress after allogeneic hematopoietic stem-cell transplantation without causing graft-versus-host disease," *Journal of Clinical Oncology*, vol. 34, no. 10, pp. 1112–1121, 2016.

[11] J. N. Kochenderfer, M. E. Dudley, S. H. Kassim et al., "Chemotherapy-refractory diffuse large B-cell lymphoma and indolent B-cell malignancies can be effectively treated with autologous T cells expressing an anti-CD19 chimeric antigen receptor," *Journal of Clinical Oncology*, vol. 33, no. 6, pp. 540–549, 2015.

[12] G. L. Beatty, A. R. Haas, M. V. Maus et al., "Mesothelin-specific chimeric antigen receptor mRNA-engineered T cells induce antitumor activity in solid malignancies," *Cancer immunology research*, vol. 2, no. 2, pp. 112–120, 2014.

[13] N. Ahmed, V. S. Brawley, M. Hegde et al., "Human epidermal growth factor receptor 2 (HER2)–specific chimeric antigen receptor–modified T cells for the immunotherapy of HER2-positive sarcoma," *Journal of Clinical Oncology*, vol. 33, no. 15, pp. 1688–1696, 2015.

[14] L. M. Whilding, A. C. Parente-Pereira, T. Zabinski et al., "Targeting of aberrant $\alpha v\beta$ 6 integrin expression in solid tumors using chimeric antigen receptor-engineered T cells," *Molecular Therapy*, vol. 25, no. 1, pp. 259–273, 2017.

[15] S. Yu, A. Li, Q. Liu et al., "Chimeric antigen receptor T cells: a novel therapy for solid tumors," *Journal of Hematology & Oncology*, vol. 10, no. 1, p. 78, 2017.

[16] G. Dotti, S. Gottschalk, B. Savoldo, and M. K. Brenner, "Design and development of therapies using chimeric antigen receptor-expressing T cells," *Immunological reviews*, vol. 257, no. 1, pp. 107–126, 2014.

[17] J. Maher, "Immunotherapy of malignant disease using chimeric antigen receptor engrafted T cells," *ISRN Oncology*, vol. 2012, Article ID 278093, 23 pages, 2012.

[18] P. J. Bugelski, R. Achuthanandam, R. J. Capocasale, G. Treacy, and E. Bouman-Thio, "Monoclonal antibody-induced cytokine-release syndrome," *Expert Review of Clinical Immunology*, vol. 5, no. 5, pp. 499–521, 2009.

[19] D. W. Lee, R. Gardner, D. L. Porter et al., "Current concepts in the diagnosis and management of cytokine release syndrome," *Blood*, vol. 124, no. 2, pp. 188–195, 2014.

[20] J. C. Fitzgerald, S. L. Weiss, S. L. Maude et al., "Cytokine release syndrome after chimeric antigen receptor T cell therapy for acute lymphoblastic leukemia," *Critical Care Medicine*, vol. 45, no. 2, pp. e124–e131, 2017.

[21] S. C. Howard, D. P. Jones, and C. H. Pui, "The tumor lysis syndrome," *The New England Journal of Medicine*, vol. 364, no. 19, pp. 1844–1854, 2011.

[22] R. J. Brentjens, M. L. Davila, I. Riviere et al., "CD19-targeted T cells rapidly induce molecular remissions in adults with chemotherapy-refractory acute lymphoblastic leukemia," *Science Translational Medicine*, vol. 5, no. 177, article 177ra138, 2013.

[23] C. L. Bonifant, H. J. Jackson, R. J. Brentjens, and K. J. Curran, "Toxicity and management in CAR T-cell therapy," *Molecular Therapy Oncolytics*, vol. 3, article 16011, 2016.

[24] D. T. Teachey, S. R. Rheingold, S. L. Maude et al., "Cytokine release syndrome after blinatumomab treatment related to abnormal macrophage activation and ameliorated with cytokine-directed therapy," *Blood*, vol. 121, no. 26, pp. 5154–5157, 2013.

[25] S. L. Maude, D. Barrett, D. T. Teachey, and S. A. Grupp, "Managing cytokine release syndrome associated with novel T cell-engaging therapies," *Cancer Journal*, vol. 20, no. 2, pp. 119–122, 2014.

[26] F. De Benedetti, H. I. Brunner, N. Ruperto et al., "Randomized trial of tocilizumab in systemic juvenile idiopathic arthritis," *The New England Journal of Medicine*, vol. 367, no. 25, pp. 2385–2395, 2012.

[27] C. H. Lamers, S. Sleijfer, A. G. Vulto et al., "Treatment of metastatic renal cell carcinoma with autologous T-lymphocytes genetically retargeted against carbonic anhydrase IX: first clinical experience," *Journal of Clinical Oncology*, vol. 24, no. 13, pp. e20–e22, 2006.

[28] C. H. Lamers, S. Sleijfer, S. van Steenbergen et al., "Treatment of metastatic renal cell carcinoma with CAIX CAR-engineered T cells: clinical evaluation and management of on-target toxicity," *Molecular Therapy*, vol. 21, no. 4, pp. 904–912, 2013.

[29] H. A, A. A. Hombach, and H. Abken, "Adoptive immunotherapy with genetically engineered T cells: modification of the IgG1 Fc 'spacer' domain in the extracellular moiety of chimeric antigen receptors avoids 'off-target' activation and unintended initiation of an innate immune response," *Gene Therapy*, vol. 17, no. 10, pp. 1206–1213, 2010.

[30] K. T. Coffman, M. Hu, K. Carles-Kinch et al., "Differential EphA2 epitope display on normal *versus* malignant cells," *Cancer Research*, vol. 63, no. 22, pp. 7907–7912, 2003.

[31] J. H. Sampson, A. B. Heimberger, G. E. Archer et al., "Immunologic escape after prolonged progression-free survival with epidermal growth factor receptor variant III peptide vaccination in patients with newly diagnosed glioblastoma," *Journal of Clinical Oncology*, vol. 28, no. 31, pp. 4722–4729, 2010.

[32] H. K. Gan, A. W. Burgess, A. H. Clayton, and A. M. Scott, "Targeting of a conformationally exposed, tumor-specific epitope of EGFR as a strategy for cancer therapy," *Cancer Research*, vol. 72, no. 12, pp. 2924–2930, 2012.

[33] D. M. Davies and J. Maher, "TSLPR: a new CAR in the showroom for B-ALL," *Blood*, vol. 126, no. 5, pp. 567–569, 2015.

[34] H. Qin, M. Cho, W. Haso et al., "Eradication of B-ALL using chimeric antigen receptor-expressing T cells targeting the TSLPR oncoprotein," *Blood*, vol. 126, no. 5, pp. 629–639, 2015.

[35] S. S. Kenderian, M. Ruella, O. Shestova et al., "CD33-specific chimeric antigen receptor T cells exhibit potent preclinical activity against human acute myeloid leukemia," *Leukemia*, vol. 29, no. 8, pp. 1637–1647, 2015.

[36] C. O'Hear, J. F. Heiber, I. Schubert, G. Fey, and T. L. Geiger, "Anti-CD33 chimeric antigen receptor targeting of acute myeloid leukemia," *Haematologica*, vol. 100, no. 3, pp. 336–344, 2015.

[37] B. J. Cameron, A. B. Gerry, J. Dukes et al., "Identification of a titin-derived HLA-A1–presented peptide as a cross-reactive target for engineered MAGE A3–directed T cells," *Science Translational Medicine*, vol. 5, no. 197, article 197ra103, 2013.

[38] G. P. Linette, E. A. Stadtmauer, M. V. Maus et al., "Cardiovascular toxicity and titin cross-reactivity of affinity-enhanced T cells in myeloma and melanoma," *Blood*, vol. 122, no. 6, pp. 863–871, 2013.

[39] S. Kotter, C. Andresen, and M. Kruger, "Titin: central player of hypertrophic signaling and sarcomeric protein quality control," *Biological Chemistry*, vol. 395, no. 11, pp. 1341–1352, 2014.

[40] Y. Hu, J. Sun, Z. Wu et al., "Predominant cerebral cytokine release syndrome in CD19-directed chimeric antigen receptor-modified T cell therapy," *Journal of Hematology & Oncology*, vol. 9, no. 1, p. 70, 2016.

[41] M. S. Topp, N. Gockbuget, and A. S. Stein, "Safety and activity of blinatumomab for adult patients with relapsed or refractory B-precursor acute lymphoblastic leukaemia: a multicentre, single-arm, phase 2 study," *The Lancet Oncology*, vol. 16, no. 1, pp. 57–66, 2015.

[42] M. E. Goebeler, S. Knop, A. Viardot et al., "Bispecific T-cell engager (BiTE) antibody construct blinatumomab for the treatment of patients with relapsed/refractory non-Hodgkin lymphoma: final results from a phase I study," *Journal of Clinical Oncology*, vol. 34, no. 10, pp. 1104–1111, 2016.

[43] H. Mei, H. Jiang, Y. Wu et al., "Neurological toxicities and coagulation disorders in the cytokine release syndrome during CAR-T therapy," *British Journal of Haematology*, 2017.

[44] M. E. Dudley, J. R. Wunderlich, P. F. Robbins et al., "Cancer regression and autoimmunity in patients after clonal repopulation with antitumor lymphocytes," *Science*, vol. 298, no. 5594, pp. 850–854, 2002.

[45] M. E. Dudley, J. C. Yang, R. Sherry et al., "Adoptive cell therapy for patients with metastatic melanoma: evaluation of intensive myeloablative chemoradiation preparative regimens," *Journal of Clinical Oncology*, vol. 26, no. 32, pp. 5233–5239, 2008.

[46] M. E. Dudley, C. A. Gross, R. P. Somerville et al., "Randomized selection design trial evaluating $CD8^+$-enriched versus unselected tumor-infiltrating lymphocytes for adoptive cell therapy for patients with melanoma," *Journal of Clinical Oncology*, vol. 31, no. 17, pp. 2152–2159, 2013.

[47] K. J. Curran, H. J. Pegram, and R. J. Brentjens, "Chimeric antigen receptors for T cell immunotherapy: current understanding and future directions," *The Journal of Gene Medicine*, vol. 14, no. 6, pp. 405–415, 2012.

[48] M. H. Kershaw, J. A. Westwood, L. L. Parker et al., "A phase I study on adoptive immunotherapy using gene-modified T cells for ovarian cancer," *Clinical Cancer Research*, vol. 12, no. 20, pp. 6106–6115, 2006.

[49] M. C. Jensen, L. Popplewell, L. J. Cooper et al., "Antitransgene rejection responses contribute to attenuated persistence of adoptively transferred CD20/CD19-specific chimeric antigen receptor redirected T cells in humans," *Biology of Blood and Marrow Transplantation*, vol. 16, no. 9, pp. 1245–1256, 2010.

[50] C. H. Lamers, R. Willemsen, P. van Elzakker et al., "Immune responses to transgene and retroviral vector in patients treated with ex vivo–engineered T cells," *Blood*, vol. 117, no. 1, pp. 72–82, 2011.

[51] M. V. Maus, S. A. Grupp, D. L. Porter, and C. H. June, "Antibody-modified T cells: CARs take the front seat for hematologic malignancies," *Blood*, vol. 123, no. 17, pp. 2625–2635, 2014.

[52] M. Casucci, R. E. Hawkins, G. Dotti, and A. Bondanza, "Overcoming the toxicity hurdles of genetically targeted T cells," *Cancer Immunology, Immunotherapy*, vol. 64, no. 1, pp. 123–130, 2015.

[53] S. Hacein-Bey-Abina, C. Von Kalle, M. Schmidt et al., "*LMO2*-associated clonal T cell proliferation in two patients after gene therapy for SCID-X1," *Science*, vol. 302, no. 5644, pp. 415–419, 2003.

[54] S. Hacein-Bey-Abina, A. Garrigue, G. P. Wang et al., "Insertional oncogenesis in 4 patients after retrovirus-mediated gene therapy of SCID-X1," *The Journal of Clinical Investigation*, vol. 118, no. 9, pp. 3132–3142, 2008.

[55] J. Scholler, T. L. Brady, G. Binder-Scholl et al., "Decade-long safety and function of retroviral-modified chimeric antigen receptor T cells," *Science Translational Medicine*, vol. 4, no. 132, article 132ra153, 2012.

[56] C. Bordignon, C. Bonini, S. Verzeletti et al., "Transfer of the HSV-tk gene into donor peripheral blood lymphocytes for in vivo modulation of donor anti-tumor immunity after allogeneic bone marrow transplantation," *Human Gene Therapy*, vol. 6, no. 6, pp. 813–819, 1995.

[57] C. Bonini, G. Ferrari, S. Verzeletti et al., "HSV-TK gene transfer into donor lymphocytes for control of allogeneic graft-versus-leukemia," *Science*, vol. 276, no. 5319, pp. 1719–1724, 1997.

[58] B. S. Jones, L. S. Lamb, F. Goldman, and A. Di Stasi, "Improving the safety of cell therapy products by suicide gene transfer," *Frontiers in Pharmacology*, vol. 5, p. 254, 2014.

[59] D. Chalmers, C. Ferrand, J. F. Apperley et al., "Elimination of the truncated message from the herpes simplex virus thymidine kinase suicide gene," *Molecular Therapy*, vol. 4, no. 2, pp. 146–148, 2001.

[60] K. C. Straathof, M. A. Pule, P. Yotnda et al., "An inducible caspase 9 safety switch for T-cell therapy," *Blood*, vol. 105, no. 11, pp. 4247–4254, 2005.

[61] M. Griffioen, E. H. van Egmond, M. G. Kester, R. Willemze, J. H. Falkenburg, and M. H. Heemskerk, "Retroviral transfer of human CD20 as a suicide gene for adoptive T-cell therapy," *Haematologica*, vol. 94, no. 9, pp. 1316–1320, 2009.

[62] B. Philip, E. Kokalaki, L. Mekkaoui et al., "A highly compact epitope-based marker/suicide gene for easier and safer T-cell therapy," *Blood*, vol. 124, no. 8, pp. 1277–1287, 2014.

[63] M. Koneru, R. O'Cearbhaill, S. Pendharkar, D. R. Spriggs, and R. J. Brentjens, "A phase I clinical trial of adoptive T cell therapy using IL-12 secreting MUC-16^{ecto} directed chimeric antigen receptors for recurrent ovarian cancer," *Journal of Translational Medicine*, vol. 13, no. 1, p. 102, 2015.

[64] P. J. Paszkiewicz, S. P. Fräßle, S. Srivastava et al., "Targeted antibody-mediated depletion of murine CD19 CAR T cells permanently reverses B cell aplasia," *The Journal of Clinical Investigation*, vol. 126, no. 11, pp. 4262–4272, 2016.

[65] T. Gargett and M. P. Brown, "The inducible caspase-9 suicide gene system as a "safety switch" to limit on-target, off-tumor toxicities of chimeric antigen receptor T cells," *Frontiers in pharmacology*, vol. 5, 2014.

[66] A. Di Stasi, S. K. Tey, G. Dotti et al., "Inducible apoptosis as a safety switch for adoptive cell therapy," *The New England Journal of Medicine*, vol. 365, no. 18, pp. 1673–1683, 2011.

[67] X. Zhou, A. Di Stasi, S. K. Tey et al., "Long-term outcome after haploidentical stem cell transplant and infusion of T cells expressing the inducible caspase 9 safety transgene," *Blood*, vol. 123, no. 25, pp. 3895–3905, 2014.

[68] X. Zhou, G. Dotti, R. A. Krance et al., "Inducible caspase-9 suicide gene controls adverse effects from alloreplete T cells after haploidentical stem cell transplantation," *Blood*, vol. 125, no. 26, pp. 4103–4113, 2015.

[69] L. E. Budde, C. Berger, Y. Lin et al., "Combining a CD20 chimeric antigen receptor and an inducible caspase 9 suicide switch to improve the efficacy and safety of T cell adoptive immunotherapy for lymphoma," *PLoS One*, vol. 8, no. 12, article e82742, 2013.

[70] V. Hoyos, B. Savoldo, C. Quintarelli et al., "Engineering CD19-specific T lymphocytes with interleukin-15 and a suicide gene to enhance their anti-lymphoma/leukemia effects and safety," *Leukemia*, vol. 24, no. 6, pp. 1160–1170, 2010.

[71] K. Minagawa, M. O. Jamil, M. Al-Obaidi et al., "*In vitro* pre-clinical validation of suicide gene modified anti-CD33 redirected chimeric antigen receptor T-cells for acute myeloid leukemia," *PLoS One*, vol. 11, no. 12, article e0166891, 2016.

[72] C. C. Kloss, M. Condomines, M. Cartellieri, M. Bachmann, and M. Sadelain, "Combinatorial antigen recognition with balanced signaling promotes selective tumor eradication by engineered T cells," *Nature Biotechnology*, vol. 31, no. 1, pp. 71–75, 2013.

[73] S. Wilkie, M. C. van Schalkwyk, S. Hobbs et al., "Dual targeting of ErbB2 and MUC1 in breast cancer using chimeric antigen receptors engineered to provide complementary signaling," *Journal of Clinical Immunology*, vol. 32, no. 5, pp. 1059–1070, 2012.

[74] E. Lanitis, M. Poussin, A. W. Klattenhoff et al., "Chimeric antigen receptor T cells with dissociated signaling domains exhibit focused antitumor activity with reduced potential for toxicity *in vivo*," *Cancer Immunology Research*, vol. 1, no. 1, pp. 43–53, 2013.

[75] Z. Grada, M. Hegde, T. Byrd et al., "TanCAR: a novel bispecific chimeric antigen receptor for cancer immunotherapy," *Molecular Therapy Nucleic Acids*, vol. 2, article e105, 2013.

[76] H. J. Pegram, J. H. Park, and R. J. Brentjens, "CD28z CARs and armored CARs," *The Cancer Journal*, vol. 20, no. 2, pp. 127–133, 2014.

[77] A. Im and S. Z. Pavletic, "Immunotherapy in hematologic malignancies: past, present, and future," *Journal of Hematology & Oncology*, vol. 10, no. 1, p. 94, 2017.

[78] C. Y. Ok and K. H. Young, "Checkpoint inhibitors in hematological malignancies," *Journal of Hematology & Oncology*, vol. 10, no. 1, p. 103, 2017.

[79] V. D. Fedorov, M. Themeli, and M. Sadelain, "PD-1– and CTLA-4–based inhibitory chimeric antigen receptors (iCARs) divert off-target immunotherapy responses," *Science Translational Medicine*, vol. 5, no. 215, article 215ra172, 2013.

[80] L. Morsut, K. T. Roybal, X. Xiong et al., "Engineering customized cell sensing and response behaviors using synthetic Notch receptors," *Cell*, vol. 164, no. 4, pp. 780–791, 2016.

[81] K. T. Roybal, J. Z. Williams, L. Morsut et al., "Engineering T cells with customized therapeutic response programs using synthetic Notch receptors," *Cell*, vol. 167, no. 2, pp. 419–432.e16, 2016.

[82] K. T. Roybal, L. J. Rupp, L. Morsut et al., "Precision tumor recognition by T cells with combinatorial antigen-sensing circuits," *Cell*, vol. 164, no. 4, pp. 770–779, 2016.

[83] J. E. Jaspers and R. J. Brentjens, "Development of CAR T cells designed to improve antitumor efficacy and safety," *Pharmacology & Therapeutics*, vol. 178, pp. 83–91, 2017.

[84] C. Y. Wu, K. T. Roybal, E. M. Puchner, J. Onuffer, and W. A. Lim, "Remote control of therapeutic T cells through a small molecule–gated chimeric receptor," *Science*, vol. 350, no. 6258, article aab4077, 2015.

[85] A. Juillerat, A. Marechal, J. M. Filhol et al., "Design of chimeric antigen receptors with integrated controllable transient functions," *Scientific Reports*, vol. 6, no. 1, article 18950, 2016.

[86] E. Zhang and H. Xu, "A new insight in chimeric antigen receptor-engineered T cells for cancer immunotherapy," *Journal of Hematology & Oncology*, vol. 10, no. 1, p. 1, 2017.

[87] J. Wu, J. Fu, M. Zhang, and D. Liu, "Blinatumomab: a bispecific T cell engager (BiTE) antibody against CD19/CD3 for refractory acute lymphoid leukemia," *Journal of Hematology & Oncology*, vol. 8, no. 1, p. 104, 2015.

[88] G. Fan, Z. Wang, M. Hao, and J. Li, "Bispecific antibodies and their applications," *Journal of Hematology & Oncology*, vol. 8, no. 1, p. 130, 2015.

[89] K. Kudo, C. Imai, P. Lorenzini et al., "T lymphocytes expressing a CD16 signaling receptor exert antibody-dependent cancer cell killing," *Cancer Research*, vol. 74, no. 1, pp. 93–103, 2014.

[90] K. Tamada, D. Geng, Y. Sakoda et al., "Redirecting gene-modified T cells toward various cancer types using tagged antibodies," *Clinical Cancer Research*, vol. 18, no. 23, pp. 6436–6445, 2012.

[91] K. Urbanska, E. Lanitis, M. Poussin et al., "A universal strategy for adoptive immunotherapy of cancer through use of a novel T-cell antigen receptor," *Cancer Research*, vol. 72, no. 7, pp. 1844–1852, 2012.

[92] D. T. Rodgers, M. Mazagova, E. N. Hampton et al., "Switch-mediated activation and retargeting of CAR-T cells for B-cell malignancies," *Proceedings of the National Academy of Sciences of the United States of America*, vol. 113, no. 4, pp. E459–E468, 2016.

[93] M. S. Kim, J. S. Ma, H. Yun et al., "Redirection of genetically engineered CAR-T cells using bifunctional small molecules," *Journal of the American Chemical Society*, vol. 137, no. 8, pp. 2832–2835, 2015.

[94] D. C. Deniger, J. Yu, M. H. Huls et al., "Sleeping beauty transposition of chimeric antigen receptors targeting receptor tyrosine kinase-like orphan receptor-1 (ROR1) into diverse memory T-cell populations," *PLoS One*, vol. 10, no. 6, article e0128151, 2015.

[95] L. Cherkassky, A. Morello, J. Villena-Vargas et al., "Human CAR T cells with cell-intrinsic PD-1 checkpoint blockade resist tumor-mediated inhibition," *The Journal of Clinical Investigation*, vol. 126, no. 8, pp. 3130–3144, 2016.

[96] C. J. Turtle, L. A. Hanafi, C. Berger et al., "Immunotherapy of non-Hodgkin's lymphoma with a defined ratio of $CD8^+$ and $CD4^+$ CD19-specific chimeric antigen receptor–modified T cells," *Science Translational Medicine*, vol. 8, no. 355, article 355ra116, 2016.

[97] D. G. Song, Q. Ye, M. Poussin, L. Liu, M. Figini, and D. J. Powell Jr., "A fully human chimeric antigen receptor with potent activity against cancer cells but reduced risk for off-tumor toxicity," *Oncotarget*, vol. 6, no. 25, pp. 21533–21546, 2015.

[98] M. V. Maus and D. J. Powell Jr., "Chimeric antigen receptor T-cells: new approaches to improve their efficacy and reduce toxicity," *The Cancer Journal*, vol. 21, no. 6, pp. 475–479, 2015.

[99] P. S. Adusumilli, L. Cherkassky, J. Villena-Vargas et al., "Regional delivery of mesothelin-targeted CAR T cell therapy generates potent and long-lasting CD4-dependent tumor immunity," *Science Translational Medicine*, vol. 6, no. 261, article 261ra151, 2014.

[100] A. Di Stasi, B. De Angelis, C. M. Rooney et al., "T lymphocytes coexpressing CCR4 and a chimeric antigen receptor targeting CD30 have improved homing and antitumor activity in a Hodgkin tumor model," *Blood*, vol. 113, no. 25, pp. 6392–6402, 2009.

[101] J. A. Craddock, A. Lu, A. Bear et al., "Enhanced tumor trafficking of GD2 chimeric antigen receptor T cells by expression of the chemokine receptor CCR2b," *Journal of immunotherapy*, vol. 33, no. 8, pp. 780–788, 2010.

[102] M. Chmielewski, A. A. Hombach, and H. Abken, "Of CARs and TRUCKs: chimeric antigen receptor (CAR) T cells engineered with an inducible cytokine to modulate the tumor stroma," *Immunological Reviews*, vol. 257, no. 1, pp. 83–90, 2014.

[103] M. Chmielewski and H. Abken, "TRUCKs: the fourth generation of CARs," *Expert Opinion on Biological Therapy*, vol. 15, no. 8, pp. 1145–1154, 2015.

[104] L. Gattinoni, C. A. Klebanoff, and N. P. Restifo, "Paths to stemness: building the ultimate antitumour T cell," *Nature Reviews Cancer*, vol. 12, no. 10, pp. 671–684, 2012.

[105] A. Heczey, D. Liu, G. Tian et al., "Invariant NKT cells with chimeric antigen receptor provide a novel platform for safe and effective cancer immunotherapy," *Blood*, vol. 124, no. 18, pp. 2824–2833, 2014.

[106] Y. Xu, M. Zhang, C. A. Ramos et al., "Closely related T-memory stem cells correlate with in vivo expansion of CAR.CD19-T cells and are preserved by IL-7 and IL-15," *Blood*, vol. 123, no. 24, pp. 3750–3759, 2014.

Hindawi
Journal of Immunology Research
Volume 2018, Article ID 3525302, 13 pages
https://doi.org/10.1155/2018/3525302

Research Article

Mycobacterium tuberculosis Protein Rv3841 Activates Dendritic Cells and Contributes to a T Helper 1 Immune Response

Seunga Choi,[1,2] Han-Gyu Choi,[1,2] Ki-Won Shin,[1,2] Yong Woo Back,[1,2] Hye-Soo Park,[1,2] Jae Hwi Lee,[1,2] and Hwa-Jung Kim[1,2]

[1]*Department of Microbiology, College of Medicine, Chungnam National University, Daejeon, Republic of Korea*
[2]*Department of Medical Science, College of Medicine, Chungnam National University, Daejeon, Republic of Korea*

Correspondence should be addressed to Hwa-Jung Kim; hjukim@cnu.ac.kr

Received 7 August 2017; Revised 2 January 2018; Accepted 10 January 2018; Published 15 March 2018

Academic Editor: Angelika Riemer

The attenuated vaccine *Mycobacterium bovis* BCG (Bacille Calmette Guerin) has limited protective efficacy against TB. The development of more effective TB vaccines has focused on the mycobacterial antigens that cause strong T helper 1 (Th1) responses. Mtb protein Rv3841 (bacterioferritin B; BfrB) is known to play a crucial role in the growth of Mtb. Nonetheless, it is unclear whether Rv3841 can induce protective immunity against Mtb. Here, we studied the action of Rv3841 in maturation of dendritic cells (DCs) and its engagement in the development of T-cell immunity. We found that Rv3841 functionally activated DCs by upregulating costimulatory molecules and increased secretion of proinflammatory cytokines. Activation of DCs by Rv3841 was mediated by Toll-like receptor 4 (TLR4), followed by triggering of mitogen-activated protein kinase and nuclear factor-κB signaling pathways. In addition, Rv3841-matured DCs effectively proliferated and polarized Th1 immune response of naïve $CD4^+$ and $CD8^+$ T-cells. Moreover, Rv3841 specifically caused the expansion of $CD4^+CD44^{high}CD62L^{low}$ T-cells from Mtb-infected mice; besides, the T-cells activated by Rv3841-matured DCs inhibited intracellular mycobacterial growth. Our data suggest that Rv3841 induces DC maturation and protective immune responses, a finding that may provide candidate of effective TB vaccines.

1. Introduction

For tuberculosis (TB) to be removed from the top rank of global health problems within any practical time frame, transformative tools and projects will need to be developed [1]. The currently licensed anti-TB vaccine *Mycobacterium bovis* Bacille Calmette Guerin (BCG) confers insufficient protection from pulmonary TB in adolescents and adults [2]. Effective vaccines in latently infected individuals and adults are strongly needed.

The immunological mode of action of an effective TB vaccine involves driving the immunodominant $CD4^+$ and $CD8^+$ T-cell responses that can eliminate the invading bacteria. Priming and expansion of the antigen-specific T-cells after a primary *Mycobacterium tuberculosis* (Mtb) infection occur in regional lymph nodes that drain the lungs, and these responses are initiated by Mtb-infected dendritic cells (DCs) trafficking from the lungs [3, 4]. On the other hand, it has been reported that Mtb modulates the infected DCs to inhibit antigen presentation to T-cells, thus delaying recruitment of activated T-cells into the lungs from lymph nodes [5]. Therefore, effective DC activation and migration are necessary to eliminate Mtb via an adaptive immune response.

DCs are the most potent antigen-presenting cells in terms of activation of naïve T-cells and play a critical role in the initiation of both primary and secondary immune responses to pathogens [6, 7]. DCs express diverse cell surface markers, and phenotypic analysis broadly classifies DCs into immature and mature stages [8]. Mature DCs show high expression of costimulatory molecules, such as CD40, CD80, and CD86, as well as MHC class II antigens [9]. This maturation can be caused by stimuli, such as tumor necrosis factor α

(TNF-α), interleukin-1β (IL-1β), and components of infectious agents. Many stimuli, related maturation, induce phosphorylation of mitogen-activated protein kinases (MAPKs), such as p38 MAPK, c-Jun N-terminal kinases (JNKs), and extracellular signal-regulated kinases (ERKs). Then, the MAPK signaling pathways have obvious functions in the DC maturation [9]. Recent studies suggest that MAPK signaling pathways differentially regulate appearances of phenotypic maturation, cytokine production, and functional differentiation of DCs [10–12]. Thus, distinct maturation of DCs may be induced by modulating the balance of phosphorylation of MAPKs.

Immature DCs can capture and internalize mycobacterial antigens that engage surface-expressed receptors, such as Toll-like receptors (TLRs) [13]. The innate immune response prompt by involvement of TLRs implicates recruitment of cytoplasmic adaptor proteins and signaling molecules, resulting in phagosome maturation and the production of proinflammatory cytokines [13, 14]. Many studies have shown that mycobacterial antigens participate in innate recognition and responses through TLR signaling [15–17]. TLR receptors activate signal transduction cascades that sequentially activate the adaptor protein myeloid differentiation factor 88 (MyD88) and tumor necrosis factor receptor 6, eventually promoting the translocation of NF-κB and activation of MAPKs [18].

Critical players in antimycobacterial immune responses are T lymphocytes and antigen-presenting cells including macrophages and DCs. The mycobacterial antigen-activated DCs may preferentially drive $CD4^+$ T helper cells to polarize into T helper 1 (Th1) or Th2 cell types, thereby controlling the development of type 1 or type 2 immune responses [19, 20]. Immunological control of Mtb infection is based on a type 1 T-cell response [21]. IL-12 is induced after phagocytosis of Mtb by macrophages and DCs [22, 23]; this process drives the development of a Th1 response with production of IFN-γ. Th1 immune responses are relevant to containment and control of Mtb replication and involve IFN-γ-producing or polyfunctional (IL-2-, IFN-γ-, and TNF-α-producing) $CD4^+$ and $CD8^+$ T lymphocytes [24]. Although many mycobacterial proteins that cause DCs to secrete proinflammatory cytokines have been identified [17], DC-activating antigens with a proven protective effect against Mtb are rarely reported. We hypothesized that the proteins that induce maturation of DCs and a Th1 immune response can be potential candidate for use in vaccines against Mtb.

Protein Rv3841 (also known as BfrB, Mtb ferritin B) is involved in iron storage. Ferritins are known as important participant in iron storage and detoxification processes linked to Mtb's growth and pathogenicity [25–27]. Therefore, we theorized that Rv3841 is a good target for the development antitubercular drugs and vaccine candidates. In this study, we report that recognition of recombinant Rv3841 by DCs causes these cells to mature and to promote a Th1 immune response. Our results suggest that by acting on antigen-presenting cells, such as DCs, recombinant Rv3841 proteins may regulate immune responses to Mtb and the relevant host defense mechanism.

2. Materials and Methods

2.1. Animals. 5-6 weeks of age, female C57BL/6 TLR2 knockout (KO) mice, TLR4 KO mice, C57BL/6 OT-I mice, and OT-II T TCR transgenic mice were purchased from the Jackson Laboratory (Bar Harbor, ME, USA). All animals were maintained under specific pathogen-free (SPF) barrier conditions at Preclinical Research Center (PCRC) of Chungnam National University Hospital, Daejeon, Korea. All mice used are in accordance with the guide for care and used of the Korean Food and Drug Administration (KFDA). All animal studies used were licensed by the Ethics Committee and Institutional Animal Care and Use Committee (Permit number 2014-0197-3) of the Laboratory Animal Research Center at IACUC (CNU-00284) of Chungnam National University (Daejeon, Korea).

2.2. Generation of Mouse Bone Marrow-Derived Dendritic Cells and Macrophages. Bone marrow-derived dendritic cells (BMDCs) and bone marrow-derived macrophages (BMDMs) were differentiated in vitro from isolated bone marrow cells from uninfected 5-6-week-old C57BL/6 mice. The cells were generated and cultured as recently described [28]. Briefly, using BMDC differentiation method, bone marrow cells collected from mouse femurs and tibias were incubated for 7 d in RPMI media supplemented with 10% fetal bovine serum (FBS), penicillin/streptomycin (100 unit/mL), nonessential amino acids (0.1 mM), β-mercaptoethanol (50 μM), sodium pyruvate (1 mM), GM-CSF (20 ng/mL), and IL-4 (10 ng/mL). For the differentiation of BMDMs, bone marrow cells were cultured in DMEM media containing 10% FBS and 20 ng/mL of M-CSF for 6 d.

2.3. Purification of Rv3841 Protein and Confirmation of LPS Decontamination. Rv3841 (BfrB) gene was amplified by PCR using the Mtb H37Rv ATCC27294 genomic DNA as a template and the following primers: Rv3841 forward, 5′-CA TATGACAGAATACGAAGGGCCTAAG-3′, and reverse, 5′-AAGCTTGAGGCGGCCCCCGGCAGCGTG-3′. The PCR product of Rv3841 was cloned with the pET22b (+) (Novagen, Madison, WI, USA) with His tagged at the C-terminus. *E. coli* BL21 bacteria carrying Rv3841 expressed plasmid was induced with IPTG (isopropyl-β-D-thiogalactopyranoside). His-tagged recombinant Rv3841 protein was purified with Ni-NTA columns (Qiagen, Valencia, CA). The purification protocol was performed as previously described [29]. To confirm the contaminating endotoxins or LPS in protein purification, digestion with proteinase K (Sigma), pretreatment with polymyxin B (PmB) (Sigma), and heat denaturation were performed.

2.4. Flow Cytometry Analysis. To investigate the cytotoxic effect of Rv3841 on the DCs, DCs (1×10^6 cells/mL) were incubated with 10 μg/mL Rv3841 for 24 h. After 24 h of treatment, the cells were stained with FITC-conjugated annexin V and PI from R&D Systems (Minneapolis, MN, USA). Cell toxicity was detected according to the manufacturer's instructions. Then, samples were detected on the FACSCanto II with FACSDiva and analyzed using the

FlowJo software (Tree Star, Ashland, OR, USA). To investigate the surface molecules, after 24 h of Rv3841 protein treatment, the cells were stained with PE-conjugated anti-CD80, anti-CD86, anti-H-2Kb (MHC class I), and anti-I-Ab (MHC class II) with FITC-conjugated anti-CD11c antibodies from eBioscience (San Diego, CA, USA) for 30 min at 4°C. The fluorescence was measured by flow cytometry.

2.5. Immunoblotting Analysis. Immunoblotting (IB) was performed as described previously [29]. Briefly, cells seeded at 10^6 cells/mL in 6-well plates were treated with or without LPS or Rv3841 protein. At 24 h incubation, the cells were harvested and lysed in cell lysis buffer (50 mM Tris HCl, pH 8.0; 137 mM NaCl; 1 mM EDTA; 1% (vol/vol) Triton X-100; 10% (vol/vol) glycerol; 1 mM PMSF; 1 μg/mL each of aprotinin, leupeptin, and pepstatin; 1 mM Na3VO4; and 1 mM NaF). The cell lysates from each sample were subjected to SDS-PAGE followed by the transfer of proteins to PVDF membranes. ECL reagents (Millipore) were applied for immune blot analysis.

2.6. Treatment of DCs with Pharmacological Inhibitors of Signaling Pathways. All the pharmacological inhibitors were purchased from Calbiochem (San Diego, CA, USA). Dimethyl sulfoxide (Sigma) was added to cultures at 0.1% (vol/vol) as a solvent control. Inhibitors were used at the following concentrations: U0126 (10 μM), SB203580 (20 μM), SP600125 (10 μM), and Bay11-7082 (20 μM). A tested concentration was used after determining the viability of DCs in titration experiments using an MTT assay. In experiments with inhibitors, the cells were treated with a given inhibitor for 1 h before treatments with proteins.

2.7. In Vitro T-Cell Proliferation Assay. For T-cell proliferation assay, OVA-specific $CD4^+$ and $CD8^+$ T-cells were isolated using a MACS column (Miltenyi Biotec, Bergisch Gladbach, Germany) from splenocytes of OT-I and OT-II transgenic mice. Then, these T-cells were stained with 1 μM CFSE (Invitrogen). T-cell proliferation assay was performed as recently described [28]. Briefly, DCs were treated with the OVA peptide from Peptron (Daejeon, Korea) and 10 μg/mL of Rv3841 for 24 h. After that, Rv3841-activated DCs were cocultured with CFSE-stained T-cells at DC : T-cell ratios of 1 : 10. After 3 d of coculture, each T-cell batch was stained with anti-$CD4^+$ mAb or anti-$CD8^+$ mAb from eBioscience analyzed by flow cytometry. The supernatants were harvested and measured by ELISAs from eBioscience.

2.8. Bacteria, Mtb Infection in Mice, and Cell Preparation. Virulent Mtb strain H37Rv ATCC 27294 and the avirulent strain H37Ra ATCC 25177 were purchased from American Type Culture Collection (ATCC, Manassas, VA). All mycobacteria were provided from the International Tuberculosis Research Center (ITRC, Changwon, Gyeongsangnam-do, South Korea). These strains were cultured in Middlebrook 7H9 broth (Difco Laboratories, Detroit, MI) supplemented with 0.02% glycerol and 10% (vol/vol) oleic acid-albumin-dextrose-catalase (OADC, Becton Dickinson, Sparks, MD) for 25–28 days at 37°C. Age- and sex-matched C57BL/6 mice were infected with Mtb H37Ra, and the mycobacteria preparation protocol was performed as previously described [29]. Briefly, 6-week-old mice per group were intravenous initial infectious dose with 10^7 CFU Mtb H37Ra. The infected mice were euthanized at 6 weeks after infection to analyze immune responses. $CD4^+$ T-cells were isolated from the spleens of H37Ra-infected mice using a MACS column.

2.9. Analysis of the Activation of Effector/Memory T-Cells. For memory response analysis, C57BL/6 mice at 6 weeks of age were infected with Mtb H37Ra as described above. DCs (2×10^5 cells/well) isolated from WT C57BL/6 mice were treated with Rv3841 for 24 h followed by extensive washing and were cocultured with 2×10^6 splenocytes from Mtb-infected mice at DC : T-cell ratios of 1 : 10. On 4 days of coculture, the cells were stained with PerCP-Cy5.5-conjugated anti-$CD4^+$ mAb, FITC-conjugated anti-CD62L mAb, and PE-conjugated anti-CD44 mAb from eBioscience and analyzed by flow cytometry.

2.10. Analysis of Cytokines. Cytokines were quantified in culture supernatants using a sandwich enzyme-linked immunosorbent assay (ELISA) as described previously [28].

2.11. Intracellular Staining Assays. The cells were harvested and stained for cell surface antigens CD4. After washing, cells were fixed and permeabilized, using Cytofix/Cytoperm kit (BD Biosciences), and then stained for T-bet, GATA-3, and Foxp3 fluorescein-conjugated antibodies from eBiosciences. The cells were analyzed by means of a flow cytometer.

2.12. Bacterial Counts. Intracellular Mtb growth assays were performed as described previously [28]. Briefly, BMDMs were seeded at 2×10^5 cells/well in 24-well plates and further were infected with Mtb at MOI = 1 for 4 h. The infected BMDMs were added with 200 μg/mL amikacin for 2 h to remove extracellular mycobacteria after infection. After that, a prepared T-cell mixture was added to each well and incubated for 3 d. The T-cell mixture was $CD4^+$ T-cells cocultured for 3 d with antigen-activated DCs (DC : T-cell ratio = 1 : 10). The number of internalized mycobacteria within the BMDM was measured by lysing the infected cells. The bacterial counts were inspected by serial dilution on 7H10 agar (Difco Laboratories) supplemented with 0.05% glycerol and 10% OADC at 37°C. At the end of the 3 weeks, colony-forming units (CFUs) were counted from the number of colonies in plate.

2.13. Statistical Analysis. All experiments were performed at least three times. Statistical significance between samples was assessed with one-way ANOVA followed by Tukey's multiple comparison test using statistical software (GraphPad Prism Software, version 5.01; GraphPad Software, San Diego, CA, USA). The data represent the mean ± SEM. $^*p < 0.05$, $^{**}p < 0.01$, and $^{***}p < 0.001$ were considered statistically significant.

3. Results

3.1. Purification and Cytotoxicity of the Recombinant Rv3841 Protein. Rv3841 was expressed as a His-tagged protein in *E.*

coli and purified by Ni-NTA affinity chromatography. The SDS-PAGE and Western blot analysis of the purified recombinant Rv3841 are shown in Figure S1A. The purified protein appeared as a major band of approximately 25 kDa, which is the expected size, according to the calculated molecular weight corresponding to the full-length amino acid sequence. To remove any contaminating endotoxins from the protein preparations, the purified Rv3841 was passed through a polymyxin B agarose column for all the experiments. The purity of Rv3841 was quantified by Quantity One software (Bio-Rad, Hercules, CA, USA) and calculated by dividing the intensity per square millimeter of the Rv3841-specific band by that of all the protein bands in the preparation lane. Rv3841 had 95% purity when 20 μg of the protein preparation was stained by Coomassie staining. To determine whether Rv3841 cytotoxicity was affected DC maturation, we tested the Rv3841 protein-induced cytotoxicity in DCs by treating cells with 1, 5, and 10 μg/mL Rv3841 for 24 h, then staining with annexin V, and propidium iodide to assess cell viability. Rv3841 was not cytotoxic at a concentration of 10 μg/mL, indicating that a concentration below 10 μg/mL would not skew the subsequent experiments (Figure S1B). Consequently, endotoxin content was measured by an LAL assay and was below 15 pg/mL (<0.1 UE/mL) in Rv3841 preparations (Figure S2A).

3.2. Rv3841 Induces DC Maturation. We first tested whether the recombinant Rv3841 could promote maturation of DCs. Immature bone marrow-derived dendritic cells were prepared by culturing for 7 days with granulocyte macrophage colony-stimulating factor (GM-CSF) and IL-4 under standard conditions and then maturated by 24 h incubation in the presence of 1, 5, or 10 μg/mL Rv3841 or LPS (as a positive control). Because maturation of DCs and T-cell polarization are influenced by a variety of cytokines secreted by DCs, the levels of secretion of immunomodulatory cytokines after stimulation of immature DCs with Rv3841 were determined. We found that Rv3841 indeed caused DCs to secrete the immunomodulatory cytokines, including TNF-α, IL-1β, and IL-12p70 in a dose-dependent manner (Figure 1(a)). Nevertheless, the level of IL-10 production in Rv3841-treated DCs did not increase. We next analyzed the phenotypic alteration of DCs by analyzing the expression of various cell surface markers of DC maturation. Significant upregulation of some surface markers, including CD80, CD86, MHC class I, and MHC class II, was induced by the stimulation of DCs with Rv3841 in a concentration-dependent manner (Figure 1(b)). These results suggested that Rv3841-induced DC maturation is a potent activator of the Th1 immune response.

Several lines of evidence indicated that Rv3841-induced DC maturation was not due to contaminating endotoxins or lipopolysaccharide (LPS). For all the experiments, we used purified Rv3841 protein preparations that were passed through a polymyxin B agarose column. Furthermore, we assessed endotoxin or LPS contamination by heat denaturation and treatment with proteinase K or polymyxin B. Heat denaturation and proteinase K pretreatment abrogated the ability of the Rv3841 protein to induce DC maturation. Polymyxin B treatment did not affect the functionality of the Rv3841 protein but changed the functionality of LPS (Figure S2B). These results indicated that the maturation of DCs was induced by the intact Rv3841 protein and not by contaminating endotoxins.

3.3. Activation of the MAPK and NF-κB Pathways Is Necessary for Rv3841-Mediated Maturation of DCs. It has been reported that the mycobacterial antigen-mediated DC maturation is driven by activation of NF-κB and MAPK pathways [10, 12]. We examined the activation of NF-κB and MAPKs in response to Rv3841 treatment. Phosphorylation of MAPKs and phosphorylation and degradation of IκB-α in DCs stimulated with Rv3841 were analyzed at the indicated time points (Figure 2). As shown in Figure 2(a), Rv3841 triggered the activation of JNK, ERK1/2, and p38. In addition, Rv3841 induced the phosphorylation and degradation of IκB-α. The functions of these kinases in the DC maturation were corroborated by means of specific pharmacological inhibitors. Rv3841-induced expression of surface molecules (CD80 and CD86; Figure 2(b)) and proinflammatory-cytokine production (TNF-α, IL-1β, and IL-12p70; Figure 2(c)) were significantly inhibited in the cells pretreated with a p38 inhibitor (SB203580), ERK1/2 inhibitor (U0126), JNK inhibitor (SP600125), or NF-κB inhibitor (Bay 11-0782) for 60 min. These findings clearly indicate that activation of MAPK and KF-κB is required for the production of proinflammatory cytokines and expression of costimulatory molecules during Rv3841-mediated DC maturation.

3.4. Rv3841-Induced DC Maturation Is Mediated by TLR4. Mtb and its components encounter innate immunity, which operates through a variety of germline-encoded pattern recognition receptors including Toll-like receptors (TLRs) for recognition of various molecular patterns of mycobacteria [13, 17]. Therefore, we tested whether Rv3841 could be recognized by and act through TLRs in DCs. To identify TLRs interacting with Rv3841, DCs isolated from WT, TLR2$^{-/-}$, or TLR4$^{-/-}$ mice were stimulated with the Rv3841 protein. The expression of CD86 and MHC class II molecules (Figures 3(a) and 3(b)) and production of proinflammatory cytokines (Figure 3(c)) in TLR4$^{-/-}$ DCs stimulated with Rv3841 were significantly weaker when compared to WT or TLR2$^{-/-}$ DCs stimulated with Rv3841. These results clearly indicated that Rv3841 induced DC maturation in a TLR4-dependent manner.

3.5. Rv3841-Stimulated DCs Promote Naïve T-Cell Proliferation and Th1 Polarization. DCs are currently considered the most efficient inducers of activation of naïve T-cells [30]. It is now clear that cessation of bacterial growth correlates with the arrival of IFN-γ-producing Th1-polarized CD4$^+$ T-cells [31, 32] in the lungs and that a loss of CD4$^+$ T-cells increases the likelihood of succumbing to tuberculosis [30, 33]. To precisely characterize the effect of T-cells interacting with Rv3841-activated DCs, we examined a T-cell proliferation assay using OT-I mouse TCR transgenic CD8$^+$ T-cells and OT-II mouse TCR transgenic CD4$^+$ T-cells. Transgenic CFSE-labeled OVA-specific CD4$^+$ and CD8$^+$

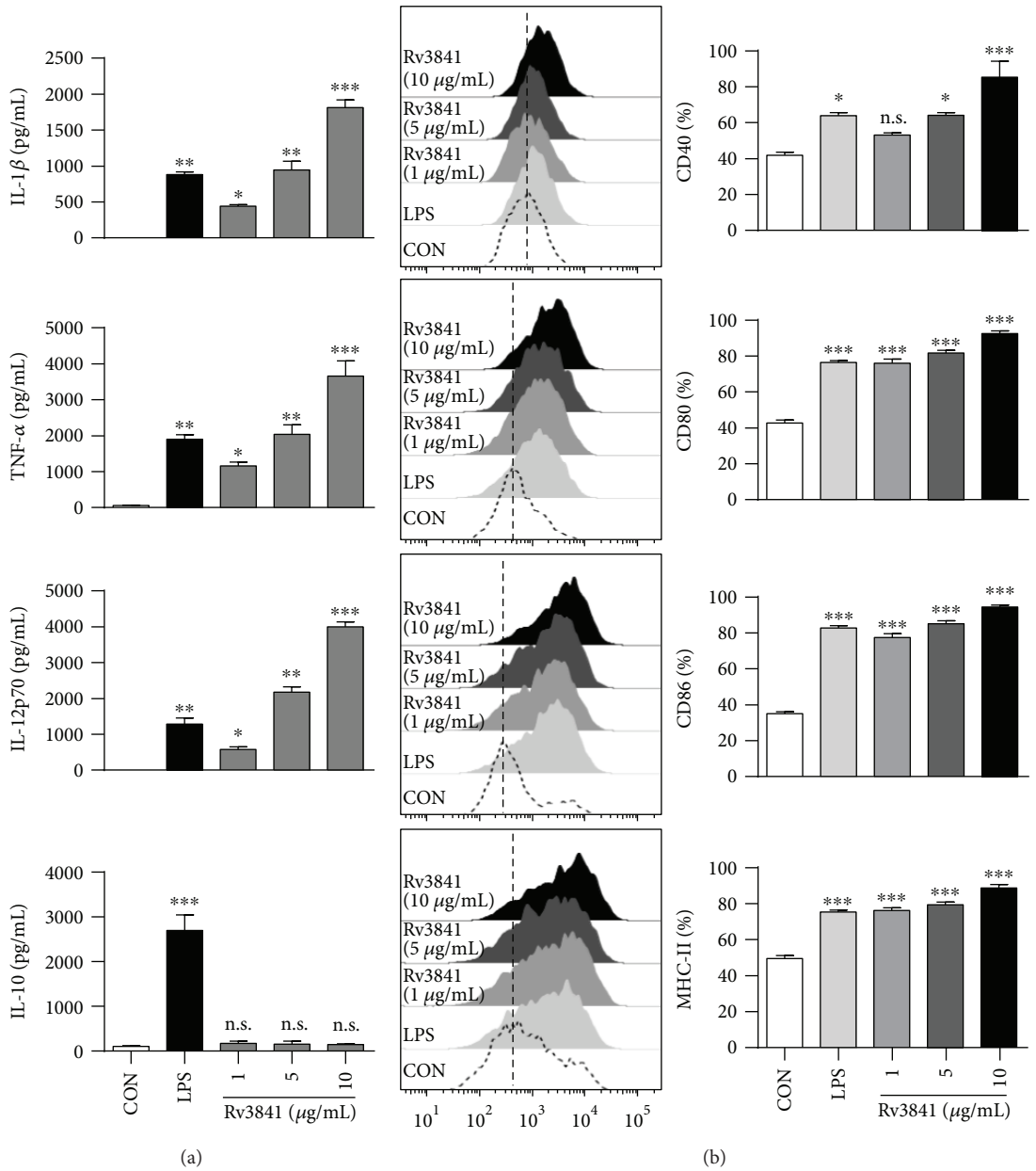

Figure 1: Rv3841 induces DC maturation. (a) Rv3841 induced functional activation of DCs in a dose-dependent manner. Immature DCs (10^6 cells/mL) were cultured in the presence of 1, 5, or 10 μg/mL Rv3841 or 100 ng/mL LPS for 24 h. The quantities of TNF-α, IL-1β, IL-10, and IL-12p70 in the culture supernatant were determined by ELISAs. All the data were expressed as mean ± SD ($n = 3$). The levels of significance ($^*p < 0.05$, $^{**}p < 0.01$, or $^{***}p < 0.001$ determined by one-way ANOVA) of the differences between the treatment data and the control data are indicated; treatments that were not significantly different are indicated by "*n.s.*" (b) Rv3841 induced phenotypic and functional activation of DCs in a dose-dependent manner, and the cells were analyzed for the expression of surface markers by flow cytometry. The cells were gated on $CD11c^+$. The DCs were stained with an anti-CD80, anti-CD86, anti-MHC class I, or anti-MHC class II antibody. The percentage of positive cells is shown in each panel. The bar graphs depict data as mean ± SD ($n = 3$). The levels of significance ($^*p < 0.05$ or $^{***}p < 0.001$, determined by one-way ANOVA) of the differences between the treatment data and the control data are indicated. Treatments without a significant effect are indicated by "n.s."

T-cells cocultured with Rv3841-treated DCs pulsed with peptide $OVA_{257–264}$ or $OVA_{323–339}$ proliferated to a significantly greater extent than did the same T-cells cocultured with DCs without Rv3841 treatment but pulsed with $OVA_{257–264}$ or $OVA_{323–339}$ (Figure 4). In addition, the secretion of IFN-γ and IL-2—as a consequence of priming of naïve $CD4^+$ T and $CD8^+$ T-cells by Rv3841-treated DCs—also significantly increased, whereas a comparable level of IL-4 secretion was not detected regardless of Rv3841 stimulation (Figure 4). FACS analysis also revealed that naïve $CD4^+$ T-cells in the presence of Rv3841-treated DCs showed an increased percentage of IFN-γ-positive cells as compared to incubation with untreated DCs, whereas no change was observed in IL-4-positive cells (Figure S3).

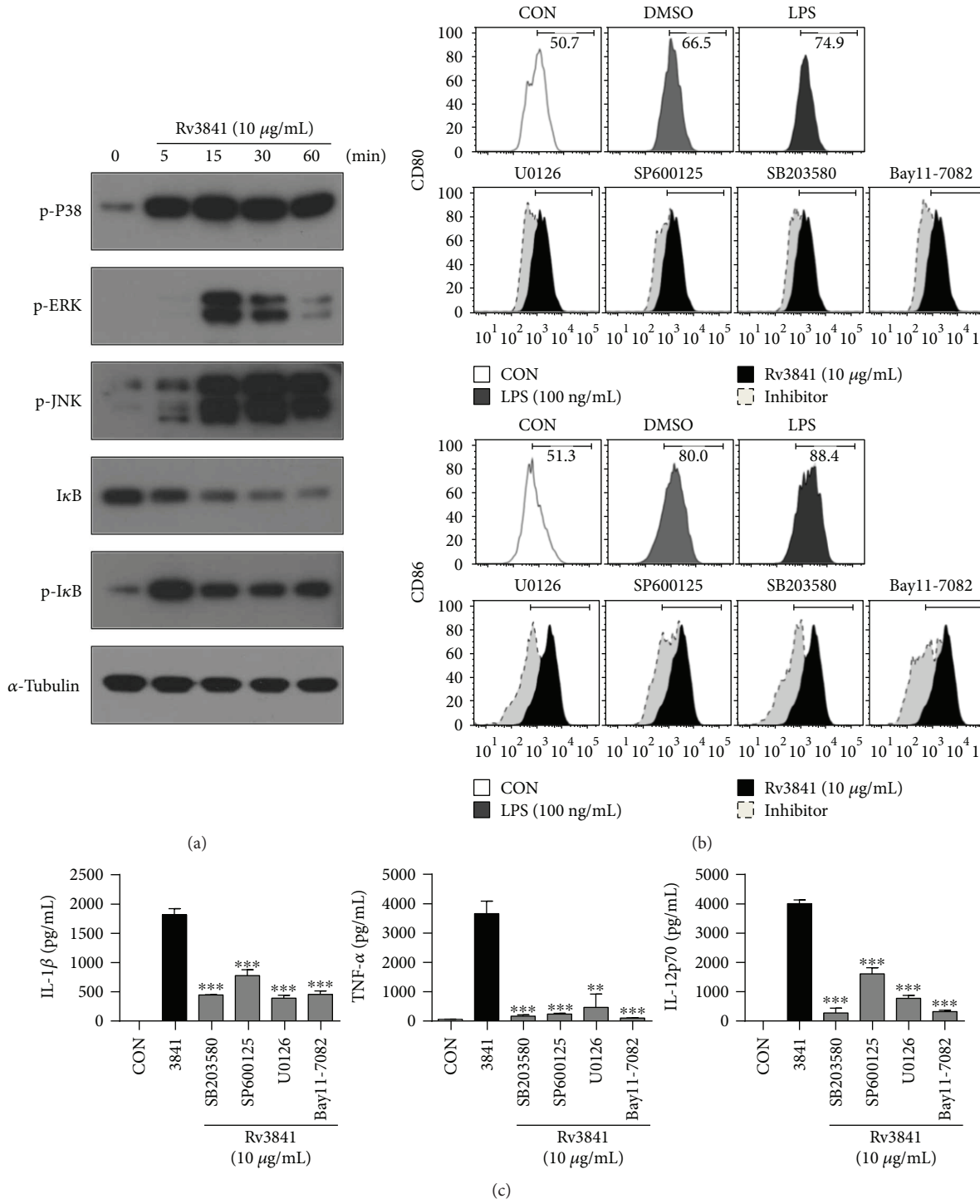

Figure 2: DC maturation triggered by Rv3841 involves activation of MAPKs and NF-κB. (a) Protein production over time by DCs treated with 10 μg/mL Rv3841. Cell lysates were subjected to SDS-PAGE, and immunoblotting analysis was carried out by means of antibodies specific to phospho-p38 (p-p38), p-ERK1/2, p-JNK, p-IκB-α, and IκB-α. α-Tubulin served as the loading control for the cytosolic proteins. Representative blots from five independent experiments are shown. (b, c) DCs were treated with pharmacological inhibitors of p38 (SB203580, 20 μM), ERK1/2 (U0126, 10 μM), JNK (SP600125, 20 μM), or NF-κB (Bay 11-7082, 20 μM) or with DMSO (vehicle control) for 1 h prior to treatment with 10 μg/mL Rv3841 for 24 h. (b) The expression of costimulatory molecules was determined by flow cytometry. (c) The concentrations of TNF-α, IL-1β, and IL-12p70 in the culture media were determined by ELISAs. Mean values ± SD ($n = 3$) are shown; $^{**}p < 0.01$ or $^{***}p < 0.001$: a significant difference from Rv3841-treated DCs, as determined by unpaired Student's t-test.

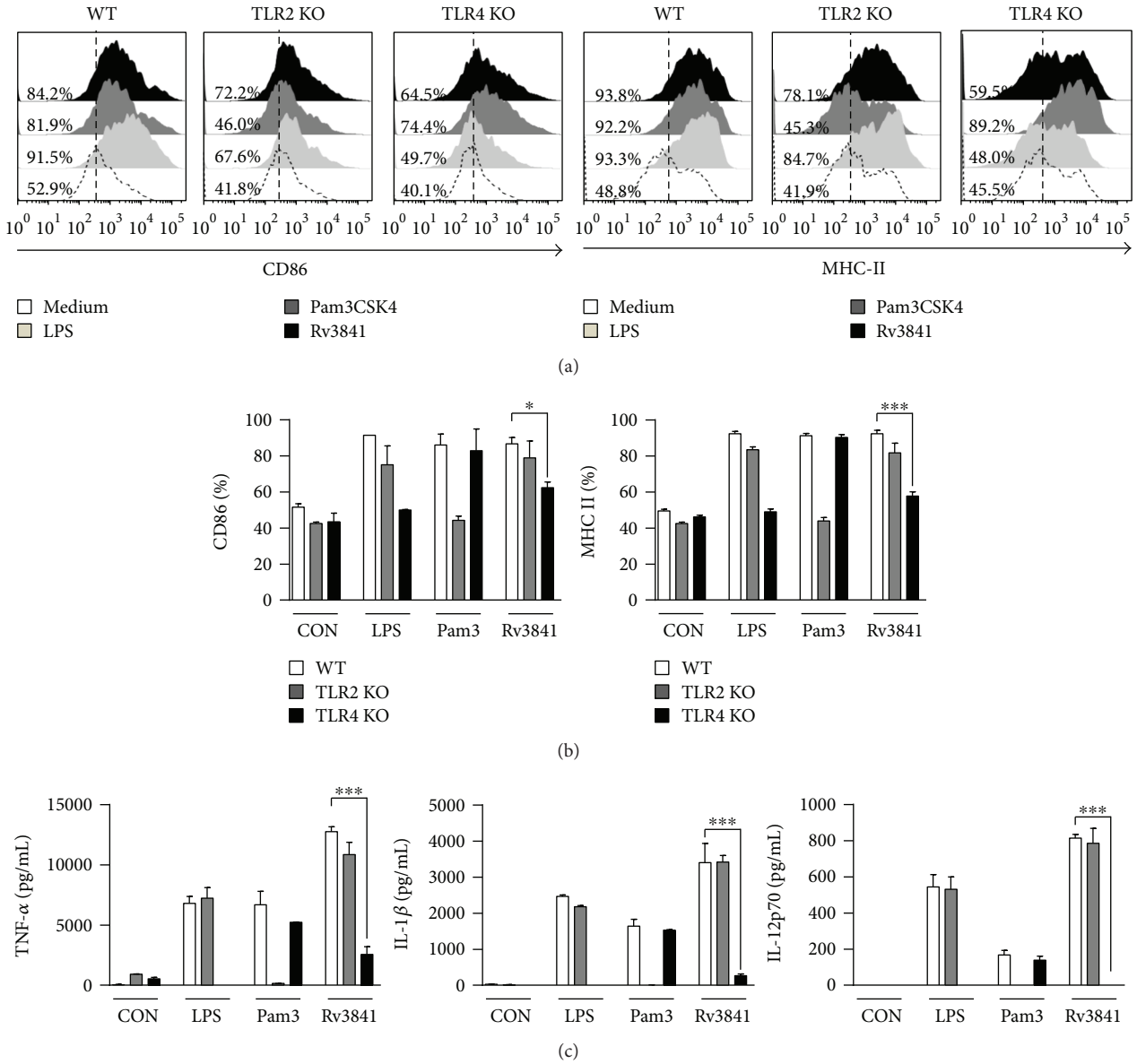

Figure 3: Rv3841 induces DC activation via TLR4. (a, b) Bar graphs showing the level of CD86 or MHC class II expression on Rv3841-treated $CD11c^+$-gated DCs derived from WT, $TLR2^{-/-}$, or $TLR4^{-/-}$ mice. DCs derived from WT, $TLR2^{-/-}$, or $TLR4^{-/-}$ mice were treated with Rv3841 (10 μg/mL) for 24 h. The percentage of positive cells is shown in each panel. The bar graphs present the mean percentage ± SEM for each surface molecule on $CD11c^+$ cells across three independent experiments. $^{***}p < 0.001$, as determined by one-way ANOVA. (c) DCs derived from WT, $TLR2^{-/-}$, or $TLR4^{-/-}$ mice were treated with Rv3841 (10 μg/mL) or LPS (100 ng/mL) for 24 h. The TNF-α, IL-1β, or IL-12p70 production of Rv3841- or LPS-treated DCs derived from WT, $TLR2^{-/-}$, or $TLR4^{-/-}$ mice was quantified by ELISAs. All the data were expressed as mean ± SD ($n = 3$); $^{*}p < 0.05$ or $^{***}p < 0.001$: a significant difference of Rv3841-treated $TLR4^{-/-}$ DC groups from Rv3841-treated WT DC control groups and other controls, as determined by one-way ANOVA.

Furthermore, we found that Rv3841-stimulated DCs elevated the expression of T-bet, which is a Th1-specific transcription factor, whereas the expression of GATA3, which is essential for Th2 development, was not observed (Figure 5(a)). We next analyzed the differentiation of $CD4^{+-}$ $CD25^+Foxp3^+$ regulatory T-cells (Treg cells) under the influence of Rv3841-stimulated DCs. Rv3841-treated DCs did not affect the regulatory T-cell population (Figure 5(b)). These findings suggested that Rv3841-matured DC promoted proliferation of naïve T-cells and pushed them toward a Th1 phenotype.

3.6. Rv3841-Stimulated DCs Induce Development of Effector/Memory T-Cells. To validate the properties of Rv3841 as a T-cell antigen, we determined whether Rv3841-stimulated DCs can induce expansion of the effector/memory $CD4^+$ T-cell populations in Mtb-infected mice. We analyzed the surface expression of CD62L and CD44 on $CD4^+$ T-cells using flow cytometry. The $CD4^+$ T-cells from the spleen of Mtb-infected mice at 6 weeks postinfection were cocultured with Rv3841-treated DCs. Ag85B served as a positive control antigen because it is expressed primarily during the early stages of Mtb infection and is recognized by T-cells [34]. As shown

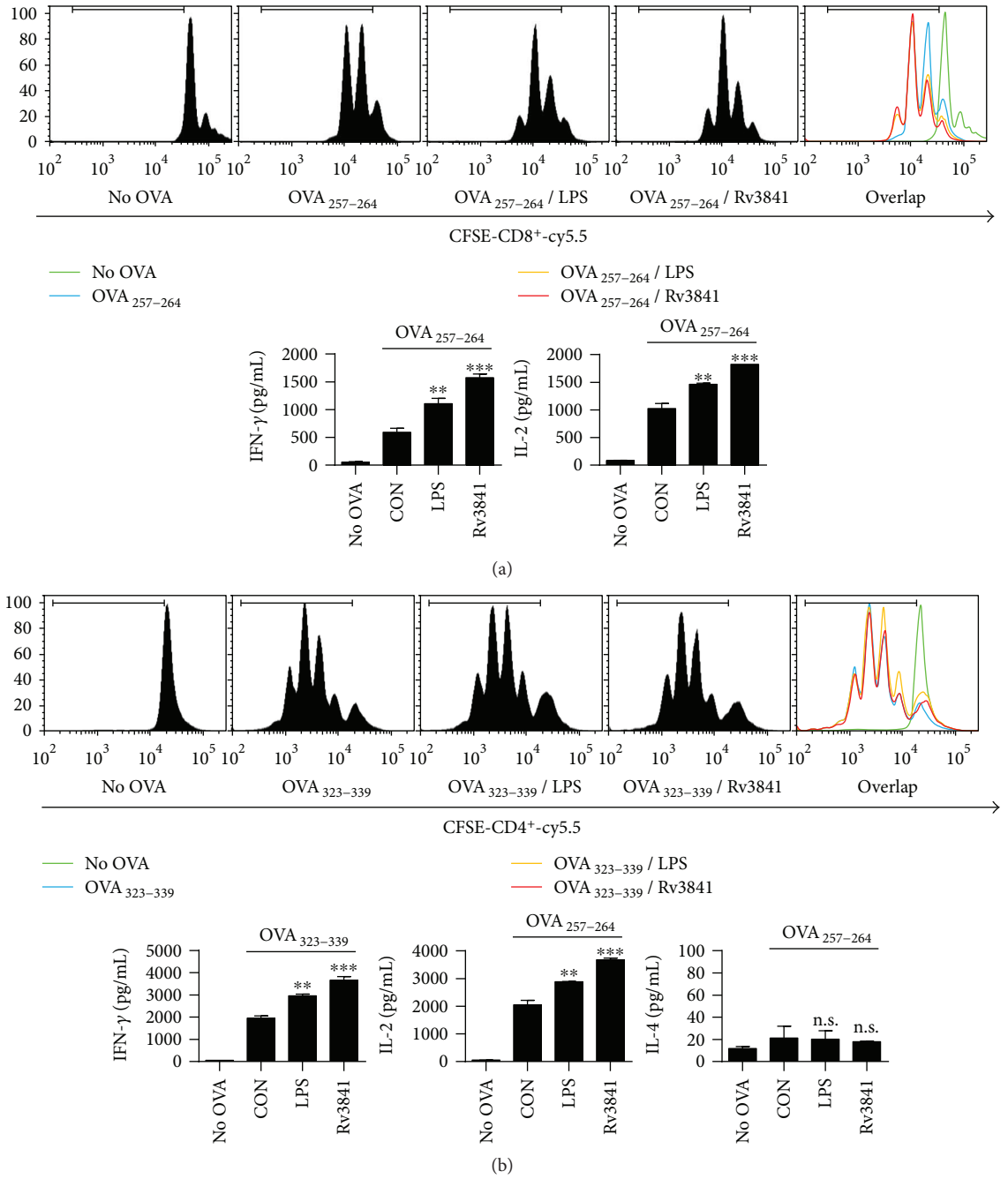

Figure 4: Rv3841-treated DCs stimulate T-cells to produce Th1 cytokines. (a, b) Transgenic OVA-specific $CD4^+$ T-cells were isolated using MACS from OT-I and OT-II mouse splenocytes, were stained with CFSE, and were cocultured for 96 h with DCs that had been treated with Rv3841 (10 μg/mL) or LPS (100 ng/mL) and then pulsed with $OVA_{257–264}$ (1 μg/mL) or $OVA_{323–339}$ (1 μg/mL) to produce OVA-specific $CD4^+$ T-cells. (a) The proliferation of OT-I T-cells was then assessed by flow cytometry. T-cells alone or T-cells cocultured with untreated DCs served as the controls. Representative histograms from three independent experiments are shown. Culture supernatants were harvested after 96 h, and the IFN-γ, IL-2, and IL-4 concentrations were determined by ELISAs. The mean values ± SD ($n = 3$) are shown; $^{**}p < 0.01$ or $^{***}p < 0.001$: a significant difference of treatment groups from the appropriate controls (T-cells + $OVA_{257–264}$-pulsed DCs or T-cells + $OVA_{323–339}$-pulsed DCs), as determined by one-way ANOVA. Treatments without a significant effect are indicated by "n.s."

in Figures 6(a) and 6(b), the Rv3841-treated DCs specifically induced the expansion of effector/memory T-cells by significantly downregulating CD62L and upregulating CD44 in $CD4^+$ T-cells from the spleen of Mtb-infected mice when compared with untreated DCs or Ag85B- or LPS-treated DCs. In addition, the production of IFN-γ by the T-cells cocultured with Rv3841-treated DCs was significantly higher in comparison with T-cells cocultured with untreated DCs or LPS-stimulated DCs. IL-2 production by T-cells cocultured with Rv3841-treated DCs was significantly higher than that by T-cells cocultured with Ag85B- or LPS-treated DCs (Figure 6(c)). In contrast, IL-4 production by T-cells

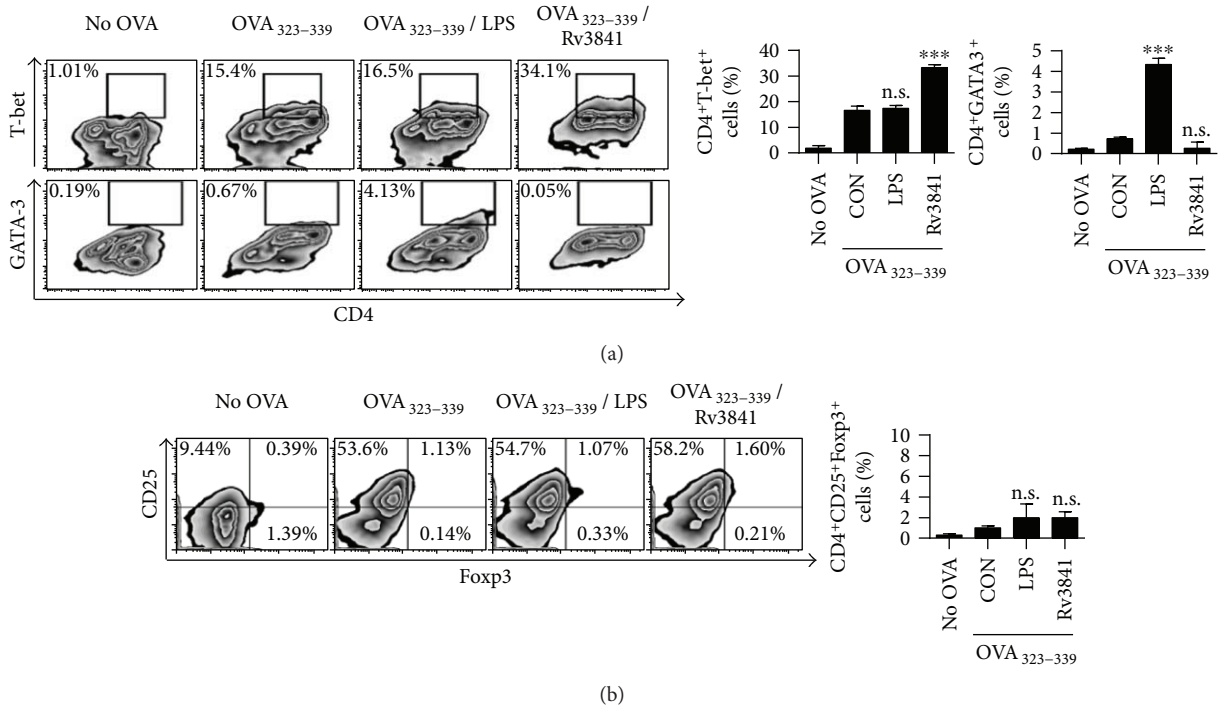

Figure 5: Rv3841-treated DCs stimulate T-cells to differentiate into the Th1 but not Th2 or Treg lineage. Transgenic OVA-specific $CD4^+$ T-cells were isolated using MACS from OT-II mouse splenocytes and were cocultured for 72 h with DCs that were pretreated with Rv3841 (10 μg/mL) or LPS (100 ng/mL) and then pulsed with $OVA_{323-339}$ (1 μg/mL) to produce OVA-specific $CD4^+$ T-cells. T-cells alone or T-cells cocultured with untreated DCs served as controls. (a, b) The expression of transcription factors was then assessed using intracellular FACS analysis. The mean values ± SD ($n = 3$) are shown; $^{***}p < 0.001$: a significant difference of treatment groups from the appropriate controls (T-cells+$OVA_{323-339}$-pulsed DCs), as determined by one-way ANOVA. Treatments without a significant effect are indicated by "n.s."

cocultured with Rv3841 or Ag85B-stimulated DCs remained at a baseline level. Recent studies have revealed that adaptive immune responses to *Mycobacterium tuberculosis* are delayed, including a delayed migration of dendritic cells from the lungs to the local lymph node and subsequent interaction with regulatory T-cells [3, 35–37]. Therefore, we determined whether Rv3841-stimulated DCs can induce effector/memory $CD4^+$ T-cells from the lymph nodes of Mtb-infected mice (Figure S4). Interestingly, our results showed that Rv3841-stimulated DCs specifically expanded a population of $CD62L^{low}CD44^{high}CD4^+$ effector/memory T-cells from lymph nodes of Mtb-infected mice like splenic T-cells. Although the onset of adaptive immune responses in Mtb infection is considerably delayed, our results showed that Rv3841 can act as a specific recall antigen during the course of Mtb infection. These data suggest that Rv3841-stimulated DCs induced the development of effector/memory T-cells and drive Th1 memory responses during mycobacterial infection.

3.7. T-Cells Activated by Rv3841-Stimulated DCs Inhibit Intracellular Mycobacterial Growth. On the basis of the above results, to confirm the involvement of Rv3841-stimulated DCs in the control of intracellular mycobacterial growth, we examined that T-cells activated by Rv3841-stimulated DCs could inhibit the bacterial growth within macrophages. Splenic $CD4^+$ T-cells from Mtb-infected mice were activated by Rv3841-stimulated DCs for 3 d and then added to BMDMs. The plain addition of unactivated T-cells caused appreciable inhibition of intracellular mycobacterial growth. Of note, T-cells activated by Rv3841-stimulated DCs significantly inhibited the mycobacterial growth in BMDMs as compared to T-cells activated by control or LPS-stimulated DCs (Figure 7(a)). The importance of IFN-γ and nitric oxide (NO) in the control of mycobacterial growth is well established [38, 39]. Furthermore, IFN-γ and NO production, which are involved to antimycobacterial activity, were significantly elevated after the addition of T-cells activated by Rv3841-stimulated DCs in comparison with T-cells activated by control or LPS-stimulated DCs (Figure 7(b)). These results suggested that Rv3841-stimulated DCs can control intracellular mycobacterial growth via T-cell activation.

4. Discussion

The most important strategy for the development of a TB subunit vaccine is to identify the reliable antigens that can be included in the antigen combination. We have been reporting that the proteins activating DCs or macrophages are promising candidates for the development of an effective TB subunit vaccine [28, 29, 40]. In the present study, we demonstrate that the Rv3841 protein induces maturation of DCs and Th1 polarization of T-cells. PE_PGRS proteins induce maturation of DCs via the TLR2 pathway and stimulate $CD4^+$ T-cell responses [16, 17]. Proteins Rv0315 and Rv0577 induce maturation and activation of DCs thus

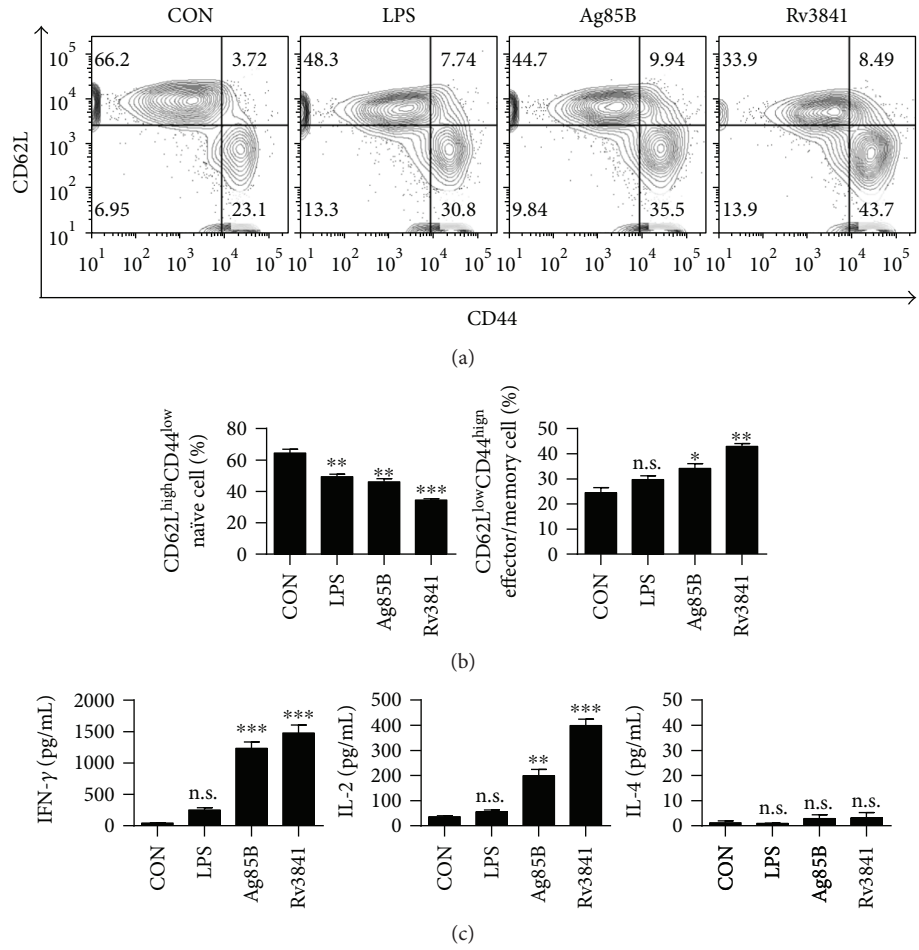

Figure 6: Rv3841-treated DCs induce expansion of the effector/memory T-cell population. DCs from WT mice were treated with Rv3841 (10 μg/mL) or LPS (100 ng/mL) and then cocultured for 3 days with T-cells from Mtb-infected mice at the DC to T-cell ratio of 1 : 10. Splenocytes were stained with anti-CD4, anti-CD62L, and anti-CD44 monoclonal antibodies. (a, b) A histogram is shown for gating of the labeled T-cells. Bar graphs show $CD62L^{low}CD44^{high}$ T-cells or $CD62L^{high}CD44^{low}$ T-cell populations among the spleen cells. (c) Culture supernatants were harvested after 96 h, and IFN-γ, IL-2, and IL-4 concentrations were measured by ELISAs. The mean values ± SD ($n = 3$) are shown; $^{*}p < 0.05$, $^{**}p < 0.01$ or $^{***}p < 0.001$: a significant difference of treatment groups from the appropriate controls, as determined by one-way ANOVA test. Treatments without a significant effect are indicated by "n.s."

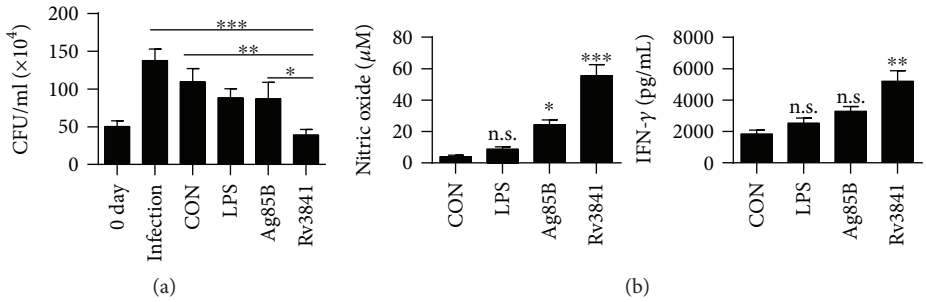

Figure 7: T-cells activated by Rv3841-treated DCs inhibit intracellular Mtb growth. Splenic T-cells or T-cells from Mtb-infected mice activated by unstimulated DCs, LPS-stimulated DCs, Ag85B-stimulated DCs, or Rv3841-stimulated DCs at a DC : T-cell ratio of 1 : 10 for 3 days were cocultured with BMDMs infected with Mtb. (a) Intracellular Mtb growth in BMDMs was determined at time point 0 (day 0) and 3 days after culturing with T-cells or without T-cells (control). (b) The NO and IFN-γ levels in culture supernatants were determined. The data are shown as mean ± SD ($n = 3$); $^{*}p < 0.05$, $^{**}p < 0.01$, or $^{***}p < 0.001$: a significant difference of BMDMs cocultured with T-cells from control BMDMs. n.s.: no significant difference.

increasing the expression of proinflammatory cytokines and surface molecules involved in antigen presentation, leading to a Th1 immune response [41, 42]. In addition, a recent study showed that PE27 induces Th1-polarized immune responses of memory T-cells through functional activation of DCs [43]. Our previous study also showed that Rv2299c-maturated DCs promote Th1 immunere-sponse with bactericidal activity and that a Rv2299c-fused protein has a vaccination potential [28]. Therefore, myco-bacterial antigens inducing activation of DCs may lead to enhanced protective immunity against Mtb. For these rea-sons, using multidimensional fractionation of Mtb culture filtrate proteins, we have identified the proteins that have effects on DCs or macrophages [28, 29, 40]. Rv3841 was one of the active mycobacterial proteins identified during these experiments.

Mtb Rv3841 is a ferritin B participating in iron storage. The iron acquisition and iron storage pathways in Mtb perform crucial functions in the growth, virulence, and latency [25–27]. Rv3841 and Rv1876 (BfrA) exclusively work in iron homeostasis and storage and are upregulated under iron-rich and downregulated under iron-deprived conditions [44]. Accordingly, Rv3841 has an important role in iron storage and detoxification processes [25, 26]. A recent paper indicates that overexpression of the Rv3841 protein may be important for the survival and pathogenesis of aminoglycoside-resistant Mtb strains by modulating the effects of amikacin and kanamycin [45]. These observations suggest that Rv3841 is related to drug-resistant TB, which can be prevented just as XDR-TB can. Although Rv3841 is considered a causative antigen of TB pathogenesis, little is known about the cellular immune responses triggered by the Rv3841 protein. Our data show that a recombinant Rv3841 protein functionally induced maturation of DCs by augmenting the expression of cell surface markers and pro-duction of proinflammatory cytokines, which are down-stream effects of the TLR4-related signaling pathways including MAPK and NF-κB signal transduction. Further-more, Rv3841-treated DCs (i) activated naïve T-cells, (ii) effectively polarized $CD4^+$ and $CD8^+$ T-cells so that they secrete IFN-γ and IL-2, and (iii) induced T-cell proliferation (Figure 4). Rv3841-maturated DCs specifically expanded a population of $CD44^{high}CD62L^{low}CD4^+$ effector/memory cells among splenic T-cells collected from Mtb-infected mice, indicating that Rv3841 acts as a recall antigen in a Th1 mem-ory response (Figure 6). Although a number of antigens from Mtb are known for their interaction with host cells, to the best of our knowledge, this is the first report showing that functions and signaling mechanisms of action of Rv3841 in DCs activate T-cell immunity. IFN-γ mediates antimicrobial action by activating phagocytes [46]—so that they rapidly ingest and degrade pathogenic microbes—and by activating inducible nitric oxide synthase (iNOS), which promotes microbicidal NO production [38, 47]. Our study indicates that the Rv3841-stimulated DCs can induce IFN-γ produc-tion in T-cells. T-cells activated by Rv3841-stimulated DCs enhanced NO production in infected macrophages. NO pro-duction is a part of the host defense against Mtb, particularly in the murine immune system [48]. These results suggest that Rv3841-stimulated DCs are important for a protective immune response against Mtb.

Collectively, our data reveal that Rv3841 enhances the immunostimulatory capacity of DCs to promote a Th1-polarized T-cell response in a TLR4-dependent pathway. Even if we did not supply direct evidence for vaccine effect of the recombinant Rv3841 protein, Rv3841 may be an excel-lent target for the rational design of effective TB vaccines.

This study offers novel data indicating that Rv3841 can drive Th1-polarized immune responses through DC matura-tion. Furthermore, Rv3841 induced a Th1-polarized memory $CD4^+$ T-cell response during Mtb infection, suggesting that Rv3841 has a possibility as a successful vaccine candidate against TB.

Conflicts of Interest

The authors declare that there is no conflict of interests regarding the publication of this paper.

Authors' Contributions

Seunga Choi and Han-Gyu Choi contributed equally to this work.

Acknowledgments

This study was supported by the Basic Science Research Pro-gram through the National Research Foundation of Korea (NRF) funded by the Ministry of Science, ICT and Future Planning (2013R1A1A2063064 and 2016R1E1A1A02921580).

Supplementary Materials

Supplementary 1. Figure S1: recombinant Rv3841 induces DC maturation. (a) The purified recombinant Rv3841 pro-tein was analyzed by SDS-PAGE with Coomassie blue stain-ing (a) and Western blot analysis using an anti-His tag antibody (b). DCs were activated by the indicated concen-tration of Rv3841 or LPS (100 ng/mL) for 24 h. Bone marrow-derived dendritic cells (BMDCs) treated with the indicated concentration of Rv3841 for 24 h were analyzed by flow cytometry involving staining with an anti-CD11c antibody, annexin V, and PI. Staurosporine treatment served as a positive control. The results are representative of three experiments.

Supplementary 2. Figure S2: confirmation of endotoxin decontamination of the purified Rv3841. (A) The amount of residual LPS in the Rv3841 preparation was estimated using the Limulus amoebocyte lysate (LAL) test according to the manufacturer's instructions. (B) DCs were stimulated with Rv3841 denatured by boiling for 1 h at 100°C or digested with proteinase K (PK, 10 μg/mL) for 1 h at 37°C. Alterna-tively, DCs were pretreated with polymyxin B (50 μg/mL) for 1 h prior to stimulation of the DCs. LPS treatment (100 ng/mL) served as a control. After 24 h, the quantities of TNF-α, IL-1β, and IL-6 in the culture supernatant were measured by ELISAs. All the data are expressed as mean $\pm$ SD ($n = 3$), and statistical significance ($^{***}p < 0.001$) is

indicated for treatments compared to the controls, whereas treatments that showed no significant effect are indicated as "*n.s.*"

Supplementary 3. Figure S3: Rv3841-treated DCs stimulate T-cells to differentiate into the Th1 but not Th2 or Treg lineage. Transgenic OVA-specific $CD4^+$ T-cells were isolated using MACS from OT-II mouse splenocytes and cocultured for 72 h with DCs pretreated with Rv3841 (10 μg/mL) or LPS (100 ng/mL) and then pulsed with $OVA_{323-339}$ (1 μg/mL) to produce OVA-specific $CD4^+$ T-cells. T-cells alone and T-cells cocultured with untreated DCs served as controls. Cytokine production was then assessed using intracellular FACS staining. The mean values ± SD ($n = 3$) are shown; $^*p < 0.05$, $^{**}p < 0.01$, or $^{***}p < 0.001$: a significant difference of treatment groups from the appropriate controls (T-cells + $OVA_{323-339}$-pulsed DCs), as determined by one-way ANOVA. Treatments without a significant effect are indicated by "*n.s.*"

Supplementary 4. Figure S4: Rv3841-treated DCs induce expansion of the effector/memory T-cell population from lymph nodes of Mtb-infected mice. DCs from WT mice were treated with Rv3841 (10 μg/mL) or LPS (100 ng/mL) and then cocultured for 3 days with T-cells from lymph nodes in Mtb-infected mice at the DC to T-cell ratio of 1 : 10. T-cells were stained with anti-CD4, anti-CD62L, and anti-CD44 monoclonal antibodies. A histogram is shown for gating of the labeled T-cells. Bar graphs show $CD62L^{low}CD44^{high}$ T-cells or $CD62L^{high}CD44^{low}$ T-cell populations. The mean values ± SD ($n = 3$) are shown; $^*p < 0.05$, $^{**}p < 0.01$, or $^{***}p < 0.001$: a significant difference of treatment groups from the appropriate controls, as determined by one-way ANOVA test. Treatments without a significant effect are indicated by "*n.s.*"

References

[1] C. L. Karp, C. B. Wilson, and L. M. Stuart, "Tuberculosis vaccines: barriers and prospects on the quest for a transformative tool," *Immunological Reviews*, vol. 264, no. 1, pp. 363–381, 2015.

[2] S. H. E. Kaufmann, T. G. Evans, and W. A. Hanekom, "Tuberculosis vaccines: time for a global strategy," *Science Translational Medicine*, vol. 7, no. 276, article 276fs278, p. 276fs8, 2015.

[3] A. J. Wolf, L. Desvignes, B. Linas et al., "Initiation of the adaptive immune response to *Mycobacterium tuberculosis* depends on antigen production in the local lymph node, not the lungs," *The Journal of Experimental Medicine*, vol. 205, no. 1, pp. 105–115, 2008.

[4] C. Nunes-Alves, M. G. Booty, S. M. Carpenter, P. Jayaraman, A. C. Rothchild, and S. M. Behar, "In search of a new paradigm for protective immunity to TB," *Nature Reviews Microbiology*, vol. 12, no. 4, pp. 289–299, 2014.

[5] C. V. Harding and W. H. Boom, "Regulation of antigen presentation by *Mycobacterium tuberculosis*: a role for Toll-like receptors," *Nature Reviews Microbiology*, vol. 8, no. 4, pp. 296–307, 2010.

[6] C. Reis e Sousa, "Dendritic cells as sensors of infection," *Immunity*, vol. 14, no. 5, pp. 495–498, 2001.

[7] J. A. Villadangos and P. Schnorrer, "Intrinsic and cooperative antigen-presenting functions of dendritic-cell subsets *in vivo*," *Nature Reviews Immunology*, vol. 7, no. 7, pp. 543–555, 2007.

[8] C. Reis e Sousa, "Dendritic cells in a mature age," *Nature Reviews Immunology*, vol. 6, no. 6, pp. 476–483, 2006.

[9] J. Banchereau, F. Briere, C. Caux et al., "Immunobiology of dendritic cells," *Annual Review of Immunology*, vol. 18, no. 1, pp. 767–811, 2000.

[10] J. S. Schorey and A. M. Cooper, "Macrophage signalling upon mycobacterial infection: the MAP kinases lead the way," *Cellular Microbiology*, vol. 5, no. 3, pp. 133–142, 2003.

[11] T. Nakahara, Y. Moroi, H. Uchi, and M. Furue, "Differential role of MAPK signaling in human dendritic cell maturation and Th1/Th2 engagement," *Journal of Dermatological Science*, vol. 42, no. 1, pp. 1–11, 2006.

[12] D. Dowling, C. M. Hamilton, and S. M. O'Neill, "A comparative analysis of cytokine responses, cell surface marker expression and MAPKs in DCs matured with LPS compared with a panel of TLR ligands," *Cytokine*, vol. 41, no. 3, pp. 254–262, 2008.

[13] K. Natarajan, M. Kundu, P. Sharma, and J. Basu, "Innate immune responses to *M. tuberculosis* infection," *Tuberculosis*, vol. 91, no. 5, pp. 427–431, 2011.

[14] V. Sundaramurthy and J. Pieters, "Interactions of pathogenic mycobacteria with host macrophages," *Microbes and Infection*, vol. 9, no. 14–15, pp. 1671–1679, 2007.

[15] S. Basu, S. K. Pathak, A. Banerjee et al., "Execution of macrophage apoptosis by PE_PGRS33 of *Mycobacterium tuberculosis* is mediated by Toll-like receptor 2-dependent release of tumor necrosis factor-α," *The Journal of Biological Chemistry*, vol. 282, no. 2, pp. 1039–1050, 2007.

[16] K. Bansal, S. R. Elluru, Y. Narayana et al., "PE_PGRS antigens of *Mycobacterium tuberculosis* induce maturation and activation of human dendritic cells," *Journal of Immunology*, vol. 184, no. 7, pp. 3495–3504, 2010.

[17] J. Basu, D. M. Shin, and E. K. Jo, "Mycobacterial signaling through toll-like receptors," *Frontiers in Cellular and Infection Microbiology*, vol. 2, no. 145, 2012.

[18] T. K. Means, D. T. Golenbock, and M. J. Fenton, "The biology of Toll-like receptors," *Cytokine & Growth Factor Reviews*, vol. 11, no. 3, pp. 219–232, 2000.

[19] C. Reis e Sousa, A. Sher, and P. Kaye, "The role of dendritic cells in the induction and regulation of immunity to microbial infection," *Current Opinion in Immunology*, vol. 11, no. 4, pp. 392–399, 1999.

[20] C. Demangel and W. J. Britton, "Interaction of dendritic cells with mycobacteria: where the action starts," *Immunology and Cell Biology*, vol. 78, no. 4, pp. 318–324, 2000.

[21] J. L. Flynn and J. Chan, "Immunology of tuberculosis," *Annual Review of Immunology*, vol. 19, no. 1, pp. 93–129, 2001.

[22] C. H. Ladel, G. Szalay, D. Riedel, and S. H. Kaufmann, "Interleukin-12 secretion by *Mycobacterium tuberculosis*-infected macrophages," *Infection and Immunity*, vol. 65, no. 5, pp. 1936–1938, 1997.

[23] R. A. Henderson, S. C. Watkins, and J. L. Flynn, "Activation of human dendritic cells following infection with Mycobacterium tuberculosis," *The Journal of Immunology*, vol. 159, no. 2, pp. 635–643, 1997.

[24] F. Bozzano, F. Marras, and A. De Maria, "Immunology of tuberculosis," *Mediterranean Journal of Hematology and Infectious Diseases*, vol. 6, no. 1, article e2014027, 2014.

[25] F. Bou-Abdallah, "The iron redox and hydrolysis chemistry of the ferritins," *Biochimica et Biophysica Acta (BBA) - General Subjects*, vol. 1800, no. 8, pp. 719–731, 2010.

[26] G. Khare, V. Gupta, P. Nangpal, R. K. Gupta, N. K. Sauter, and A. K. Tyagi, "Ferritin structure from *Mycobacterium tuberculosis*: comparative study with homologues identifies extended C-terminus involved in ferroxidase activity," *PLoS One*, vol. 6, no. 4, article e18570, 2011.

[27] G. M. Rodriguez and I. Smith, "Mechanisms of iron regulation in mycobacteria: role in physiology and virulence," *Molecular Microbiology*, vol. 47, no. 6, pp. 1485–1494, 2003.

[28] H. G. Choi, S. Choi, Y. W. Back et al., "Rv2299c, a novel dendritic cell-activating antigen of *Mycobacterium tuberculosis*, fused-ESAT-6 subunit vaccine confers improved and durable protection against the hypervirulent strain HN878 in mice," *Oncotarget*, vol. 8, no. 12, pp. 19947–19967, 2017.

[29] H. G. Choi, S. Choi, Y. W. Back et al., "*Mycobacterium tuberculosis* Rv2882c protein induces activation of macrophages through TLR4 and exhibits vaccine potential," *PLoS One*, vol. 11, no. 10, article e0164458, 2016.

[30] A. M. Cooper, "Cell-mediated immune responses in tuberculosis," *Annual Review of Immunology*, vol. 27, no. 1, pp. 393–422, 2009.

[31] A. A. Chackerian, T. V. Perera, and S. M. Behar, "Gamma interferon-producing $CD4^+$ T lymphocytes in the lung correlate with resistance to infection with *Mycobacterium tuberculosis*," *Infection and Immunity*, vol. 69, no. 4, pp. 2666–2674, 2001.

[32] Y. J. Jung, L. Ryan, R. LaCourse, and R. J. North, "Properties and protective value of the secondary versus primary T helper type 1 response to airborne *Mycobacterium tuberculosis* infection in mice," *The Journal of Experimental Medicine*, vol. 201, no. 12, pp. 1915–1924, 2005.

[33] D. V. Havlir and P. F. Barnes, "Tuberculosis in patients with human immunodeficiency virus infection," *The New England Journal of Medicine*, vol. 340, no. 5, pp. 367–373, 1999.

[34] B. J. Rogerson, Y. J. Jung, R. LaCourse, L. Ryan, N. Enright, and R. J. North, "Expression levels of *Mycobacterium tuberculosis* antigen-encoding genes versus production levels of antigen-specific T cells during stationary level lung infection in mice," *Immunology*, vol. 118, no. 2, pp. 195–201, 2006.

[35] K. B. Urdahl, S. Shafiani, and J. D. Ernst, "Initiation and regulation of T-cell responses in tuberculosis," *Mucosal Immunology*, vol. 4, no. 3, pp. 288–293, 2011.

[36] W. W. Reiley, M. D. Calayag, S. T. Wittmer et al., "ESAT-6-specific CD4 T cell responses to aerosol *Mycobacterium tuberculosis* infection are initiated in the mediastinal lymph nodes," *Proceedings of the National Academy of Sciences of the United States of America*, vol. 105, no. 31, pp. 10961–10966, 2008.

[37] S. Shafiani, G. Tucker-Heard, A. Kariyone, K. Takatsu, and K. B. Urdahl, "Pathogen-specific regulatory T cells delay the arrival of effector T cells in the lung during early tuberculosis," *The Journal of Experimental Medicine*, vol. 207, no. 7, pp. 1409–1420, 2010.

[38] J. Chan, Y. Xing, R. S. Magliozzo, and B. R. Bloom, "Killing of virulent *Mycobacterium tuberculosis* by reactive nitrogen intermediates produced by activated murine macrophages," *The Journal of Experimental Medicine*, vol. 175, no. 4, pp. 1111–1122, 1992.

[39] J. L. Flynn, J. Chan, K. J. Triebold, D. K. Dalton, T. A. Stewart, and B. R. Bloom, "An essential role for interferon gamma in resistance to Mycobacterium tuberculosis infection," *The Journal of Experimental Medicine*, vol. 178, no. 6, pp. 2249–2254, 1993.

[40] H. G. Choi, W. S. Kim, Y. W. Back et al., "*Mycobacterium tuberculosis* RpfE promotes simultaneous Th1- and Th17-type T-cell immunity via TLR4-dependent maturation of dendritic cells," *European Journal of Immunology*, vol. 45, no. 7, pp. 1957–1971, 2015.

[41] E. H. Byun, W. S. Kim, A. R. Shin et al., "Rv0315, a novel immunostimulatory antigen of *Mycobacterium tuberculosis*, activates dendritic cells and drives Th1 immune responses," *Journal of Molecular Medicine*, vol. 90, no. 3, pp. 285–298, 2012.

[42] E. H. Byun, W. S. Kim, J. S. Kim et al., "Mycobacterium tuberculosis Rv0577, a novel TLR2 agonist, induces maturation of dendritic cells and drives Th1 immune response," *The FASEB Journal*, vol. 26, no. 6, pp. 2695–2711, 2012.

[43] W. S. Kim, J. S. Kim, S. B. Cha et al., "*Mycobacterium tuberculosis* PE27 activates dendritic cells and contributes to Th1-polarized memory immune responses during *in vivo* infection," *Immunobiology*, vol. 221, no. 3, pp. 440–453, 2016.

[44] S. A. Hwang and J. K. Actor, "Lactoferrin modulation of BCG-infected dendritic cell functions," *International Immunology*, vol. 21, no. 10, pp. 1185–1197, 2009.

[45] D. Sharma, M. Lata, M. Faheem et al., "*M. tuberculosis* ferritin (Rv3841): potential involvement in amikacin (AK) & kanamycin (KM) resistance," *Biochemical and Biophysical Research Communications*, vol. 478, no. 2, pp. 908–912, 2016.

[46] S. B. Corradin, Y. Buchmuller-Rouiller, and J. Mauel, "Phagocytosis enhances murine macrophage activation by interferon-γ and tumor necrosis factor-α," *European Journal of Immunology*, vol. 21, no. 10, pp. 2553–2558, 1991.

[47] D. J. Stuehr and M. A. Marletta, "Induction of nitrite/nitrate synthesis in murine macrophages by BCG infection, lymphokines, or interferon-gamma," *The Journal of Immunology*, vol. 139, no. 2, pp. 518–525, 1987.

[48] J. MacMicking, Q. W. Xie, and C. Nathan, "Nitric oxide and macrophage function," *Annual Review of Immunology*, vol. 15, no. 1, pp. 323–350, 1997.

Hindawi
Journal of Immunology Research
Volume 2018, Article ID 3487095, 8 pages
https://doi.org/10.1155/2018/3487095

Research Article

Parenterally Administered Norovirus GII.4 Virus-Like Particle Vaccine Formulated with Aluminum Hydroxide or Monophosphoryl Lipid A Adjuvants Induces Systemic but Not Mucosal Immune Responses in Mice

Suvi Heinimäki, Maria Malm, Timo Vesikari, and Vesna Blazevic

Vaccine Research Center, University of Tampere, Tampere, Finland

Correspondence should be addressed to Vesna Blazevic; vesna.blazevic@uta.fi

Received 31 August 2017; Accepted 16 January 2018; Published 28 February 2018

Academic Editor: Nejat K. Egilmez

Norovirus (NoV) is a main cause of acute gastroenteritis across all ages worldwide. NoV vaccine candidates currently in clinical trials are based on noninfectious highly immunogenic virus-like particles (VLPs) delivered intramuscularly (IM). Since NoV is an enteric pathogen, it is likely that mucosal immunity has a significant role in protection from infection in the intestine. Due to the fact that IM delivery of NoV VLPs does not generate mucosal immunity, we investigated whether NoV genotype GII.4 VLPs coadministered with aluminum hydroxide ($Al(OH)_3$) or monophosphoryl lipid A (MPLA) would induce mucosal antibodies in mice. Systemic as well as mucosal IgG and IgA antibodies in serum and intestinal and nasal secretions were measured. As expected, strong serum IgG, IgG1, and IgG2a antibodies as well as a dose sparing effect were induced by both $Al(OH)_3$ and MPLA, but no mucosal IgA antibodies were detected. In contrast, IN immunization with GII.4 VLPs without an adjuvant induced systemic as well as mucosal IgA antibody response. These results indicate that mucosal delivery of NoV VLPs is needed for induction of mucosal responses.

1. Introduction

The need for norovirus (NoV) vaccine is apparent, as NoV is the most common cause of acute viral gastroenteritis worldwide with approximately 200,000 annual deaths [1]. It infects humans of all ages, but children <5 years of age, the elderly, and immunocompromised individuals are at the highest risk. The most advanced NoV vaccine in phase II clinical trials is based on virus-like particles (VLPs) administered intramuscularly (IM) with aluminum hydroxide ($Al(OH)_3$) [2] or a combination of $Al(OH)_3$ and monophosphoryl lipid A (MPLA) [3–6]. Alternative intranasal (IN) administration of NoV VLPs has previously been evaluated as well [7, 8]. Despite the lack of the definite vaccine-associated correlate of protection for NoV, mucosal immunity is known to play a significant role in protection from infection and disease caused by enteric pathogens, including NoV [9–12].

At present, there are only a few adjuvants approved for human use, and none for mucosal delivery [13, 14]. Aluminum salts (Alum) and MPLA are adjuvants commonly included in the formulation of licensed protein subunit vaccines, such as VLP-based vaccines against human papilloma virus (Cervarix®, Gardasil®) and hepatitis B virus (Engerix-B®, Recombivax HB®). Alum, the first and predominant adjuvant in human vaccines, is employed to stabilize the vaccine antigen and also as a delivery system [13, 15]. MPLA, a new-generation toll-like receptor- (TLR-) based adjuvant, is a TLR4 agonist, which activates innate immunity [16, 17], thereby influencing the development of adaptive immunity. Recently, alum has been described to possess immunomodulatory features as well [18]. Both of these adjuvants stimulate systemic immune responses, when administered parenterally with the vaccine antigens. However, their effect on antigen-specific mucosal immunity is not known.

We have recently shown that NoV GII.4 VLPs induce protective IgA antibodies in mucosal lavages of mice immunized via intranasal (IN), but not IM, route [9]. Here, we investigated if IM delivery of NoV GII.4 VLPs formulated with commonly used adjuvants, $Al(OH)_3$ or MPLA, has an effect on generation of NoV-specific mucosal immunity.

2. Materials and Methods

2.1. Recombinant NoV VLP Production. NoV GII.4-1999 (reference strain accession number AF080551) VLPs used for immunization and as antigen in immunological assays were produced by recombinant baculovirus technology in Sf9 insect cells and purified as described in detail elsewhere [19].

2.2. Immunization and Sample Preparation. Female 7-week-old BALB/c OlaHsd mice (5–8 mice/experimental group) (Envigo, Horst, the Netherlands) were immunized IM two times (at study weeks 0 and 3) with 0.3 μg dose of GII.4 VLPs alone or formulated with 100 μg of $Al(OH)_3$ (Alhydrogel; InvivoGen, San Diego, CA) or 5 μg of MPLA from *S. minnesota R595* (InvivoGen). In addition, two groups of mice received a combination vaccine [20] containing 10 μg GII.4 VLPs via IM and IN delivery. Mice administered IM or IN with a carrier (sterile PBS only) served as control groups. Immunizations were performed under general anesthesia induced with a mixture of ketamine (Ketalar®; Pfizer Ltd., NY) and medetomidine (Dorbene®; Syva, Leon, Spain).

To test the kinetics of the antibody responses in sera, tail blood samples (diluted 1 : 200 in PBS at the time of collection) were collected at study weeks 0 (prebleed, nonimmune sera) and 3. Mice were sacrificed at study week 5 by decapitation, when whole blood, intestinal secretions (feces), nasal washes (NWs), and mesenteric lymph nodes (MLNs) were collected. Preparation of blood samples and lymphoid tissues was conducted according to the previously published procedures [21], except a single-cell suspension from group-wise pooled MLNs was prepared without a lysis step of red blood cells. Fecal pellets and NWs were processed as previously published [9, 22]. All of the experimental procedures conducted were in accordance with the regulations and guidelines of the Finnish National Experiment Board.

2.3. Detection of NoV-Specific Serum and Mucosal Antibodies by ELISA. Serum samples of individual mice were serially diluted two-fold from 1 : 200 (for IgG) or 1 : 20 (for IgA) and tested in ELISA for the presence of NoV GII.4-specific IgG, IgG1, IgG2a, and IgA antibodies as described elsewhere [10, 21]. Fecal suspensions (10%) and NWs were two-fold serially diluted from 1 : 5 and studied for IgG and IgA antibodies. Briefly, 96-well half-area polystyrene plates (Corning Inc., Corning, NY) were coated with 50 ng of GII.4 VLPs per well. Sample dilutions were added on the plates, and the bound antibodies were detected with horseradish peroxidase- (HRP-) conjugated anti-mouse IgG (Sigma-Aldrich, St. Louis, MO), IgG1 (Invitrogen, Carlsbad, CA), IgG2a (Invitrogen) or IgA (Sigma-Aldrich), and SIGMAFAST OPD substrate (Sigma-Aldrich). Optical density (OD) values at 490 nm were measured by a microplate reader (Victor^2 1420; PerkinElmer, Waltham, MA). A sample was considered positive if the OD_{490} was above the cut-off value (mean $OD_{490} + 3 \times SD$ of the control mice and $OD_{490} > 0.1$). The end-point titer was defined as the reciprocal of the highest dilution with an OD_{490} above the cut-off value. For negative samples with the OD_{490} below the cut-off limit, a half of the starting dilution was assigned for the titer.

2.4. Detection of NoV-Specific Antibody Secretion by MLN Cells. Group-wise pooled MLN cells (4×10^6 cell/ml) from immunized mice were stimulated *in vitro* [23, 24] with 5 μg/ml of GII.4 VLPs or culture medium (RPMI 1640 supplemented with 10% FBS, 100 U/ml penicillin, 100 μg/ml streptomycin, 50 μM 2-mercaptoethanol, and 2 mM L-glutamine; all from Sigma-Aldrich) only. After incubation at 37°C for 10 days, supernatants were collected and stored at −20°C until analyzed in ELISA for anti-GII.4 IgG and IgA antibodies as described above.

2.5. Statistical Analyses. Fisher's exact test was employed to assess the intergroup differences in the IgG and IgA end-point titers. The Mann–Whitney *U* test and Kruskal-Wallis test were used to compare differences between the nonparametric observations of two or more independent groups. All analyses were conducted by IBM SPSS Statistics for Windows Version 23.0 (IBM Corp., Armonk, NY). The statistically significant difference was defined as $p \leq 0.05$.

3. Results

3.1. Induction of NoV GII.4-Specific Serum IgG and IgA Antibodies. Effect of two commonly used adjuvants on NoV GII.4-specific serum IgG and IgA antibody responses was investigated by immunizing the experimental mice twice IM with 0.3 or 10 μg of GII.4 VLPs alone or 0.3 μg dose combined with $Al(OH)_3$ or MPLA. For comparison, one group of mice received 10 μg GII.4 VLPs via IN delivery. IM immunization with 0.3 μg of GII.4 VLPs did not elicit a significant serum IgG response (geometric mean titer, GMT = 119; 95% CI = 74–192), whereas coadministration of 0.3 μg VLPs with $Al(OH)_3$ or MPLA resulted in robust (GMTs > 5log10) NoV GII.4-specific IgG levels (Figures 1(a) and 1(b)). Also, IM and IN administration of 10 μg dose of VLPs induced high levels of anti-GII.4 IgG antibodies (Figures 1(a) and 1(b)). No significant difference ($p = 0.87$) was observed in the magnitude of the responses induced by 0.3 μg dose of VLPs with either of the adjuvants and 10 μg dose of VLPs via IM or IN route.

Parenteral delivery of VLPs without an adjuvant did not elicit detectable serum anti-NoV IgA antibodies, but very low serum IgA was observed in 1/5 mice after immunizations with 0.3 μg dose formulated with $Al(OH)_3$ (GMT = 13; 95% CI = 6–27) or MPLA (GMT = 11; 95% CI = 8–17) (Figures 1(c) and 1(d)). In contrast, IN administration of the GII.4 VLPs alone generated a significantly higher ($p = 0.006$) IgA response (GMT = 119; 95% CI = 73–194) compared with IM administration of the adjuvanted VLP formulations (Figures 1(c) and 1(d)). No GII.4-specific

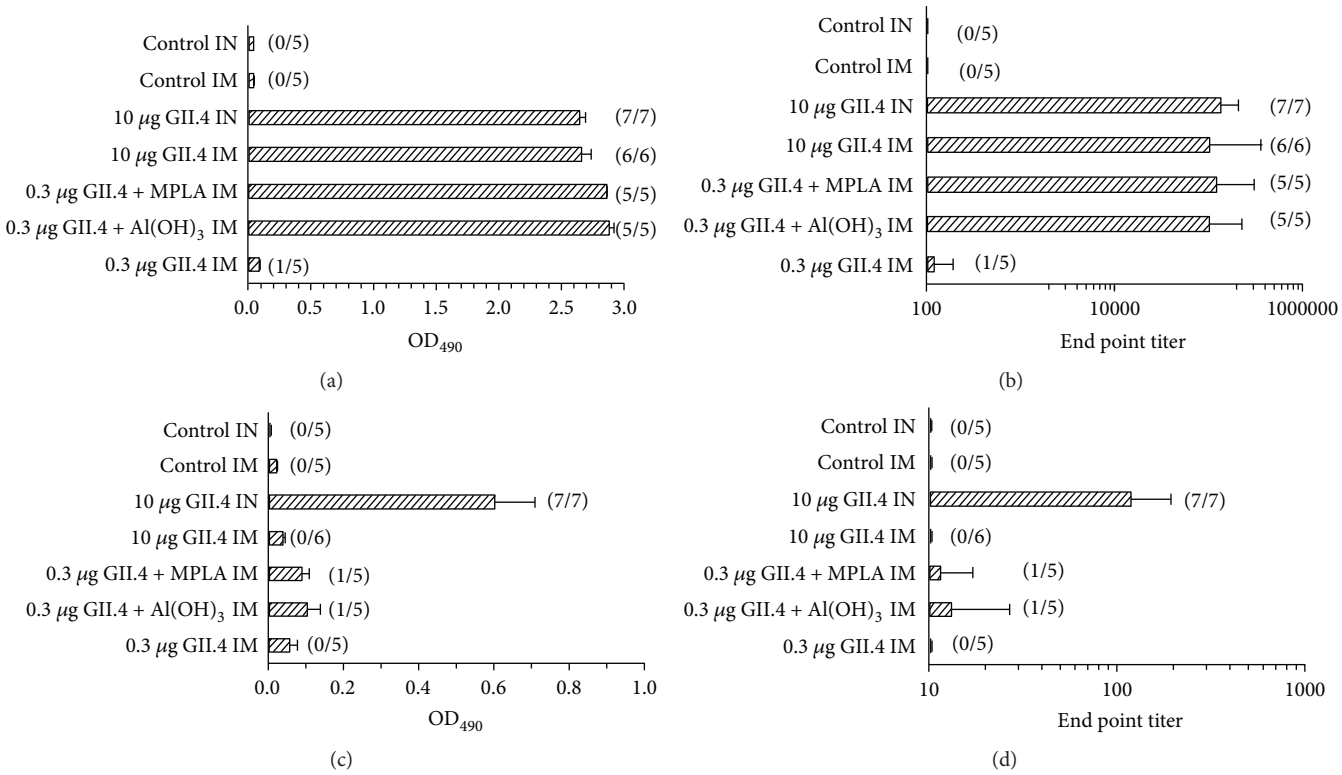

Figure 1: NoV GII.4-specific systemic IgG (a, b) and IgA (c, d) antibody responses after IM immunization with 0.3 or 10 μg of NoV GII.4 VLPs alone or 0.3 μg of VLPs combined with $Al(OH)_3$ or MPLA, or IN immunization with 10 μg of VLPs alone. Group mean OD_{490} values with standard error of the means of IgG (a) and IgA (c) antibodies in 1 : 200 (a) and 1 : 20 (c) diluted sera of experimental mice. Control mice received PBS only. End-point titers of IgG (b) and IgA (d) antibodies in sera of the experimental groups. Bars represent reciprocal of $\log_{10}$ geometric mean titers with 95% confidence intervals. The number of positive/tested mice is denoted on each figure in parenthesis.

IgG or IgA antibodies were detected in sera of control mice (Figures 1(a)–1(d)).

3.2. Kinetics and Th1/Th2 Dichotomy Induced by $Al(OH)_3$ and MPLA. To study the effect of $Al(OH)_3$ and MPLA on kinetics of serum NoV GII.4-specific antibody responses, 1 : 200 diluted sera from mice immunized IM on a two-dose schedule at an interval of three weeks were tested for IgG antibodies. After the first immunization, 0.3 μg dose of GII.4 VLPs formulated with $Al(OH)_3$ or MPLA as well as 10 μg dose of VLPs alone resulted in comparable IgG responses ($p = 0.679$) (Figure 2(a)). The second dose of these antigenic formulations delivered at week 3 enhanced the already established strong responses in all experimental groups ($p = 0.176$), as observed at week 5 (Figure 2(a)). Control mice remained negative for GII.4-specific IgG ($OD_{490} < 0.1$) during the study period (Figure 2(a)).

Determination of IgG subtype titers showed generation of both IgG1 (a marker of a Th2-type response) (Figure 2(b)) and IgG2a (a marker of a Th1 type response) (Figure 2(c)) antibodies by both adjuvanted GII.4 VLP formulations. No statistical difference was detected in the IgG1 titers ($p = 0.122$) induced by 0.3 μg of VLPs in the presence of $Al(OH)_3$ or MPLA or 10 μg of VLPs alone (Figure 2(b)). In contrast, IgG2a titers differed between the experimental groups (Figure 2(c)), $Al(OH)_3$ adjuvanted group having significantly lower titers compared to other groups ($p = 0.039$). End-point titer IgG1/IgG2a (Th2/Th1) ratio was 2 : 1 for mice immunized with a combination of VLPs and MPLA and 10 : 1 for VLPs and $Al(OH)_3$. No GII.4-specific IgG subtype antibodies were detected in sera of control mice (Figures 2(b) and 2(c)).

3.3. Induction of NoV GII.4-Specific Antibodies in Mucosal Secretions. In order to investigate if NoV VLPs coadministered with $Al(OH)_3$ or MPLA induced antibodies at mucosal surfaces, 10% fecal suspensions and NW samples of experimental animals were tested for the presence of anti-GII.4 IgG and IgA antibodies. As expected, mice immunized IM with 0.3 μg dose of GII.4 VLPs alone did not develop intestinal IgG antibodies (Figure 3(a)). Instead, all other experimental groups had similar levels of IgG ($p = 0.277$) in the intestines (Figure 3(a)).

IM delivery of VLPs in the absence of adjuvants did not generate intestinal IgA antibodies (GMT = 2.5), but fecal IgA response was detected in 1/5 and 2/5 mice after coadministration of 0.3 μg dose with $Al(OH)_3$ (GMT = 3; 95% CI = 2–7) or MPLA (GMT = 5; 95% CI = 2–15) (Figure 3(b)), corroborating serum IgA response (Figure 1(d)). Significantly greater level of IgA in the intestine ($p = 0.023$) was elicited by mucosal IN delivery of 10 μg of VLPs (GMT = 25; 95% CI = 12–53) (Figure 3(b)).

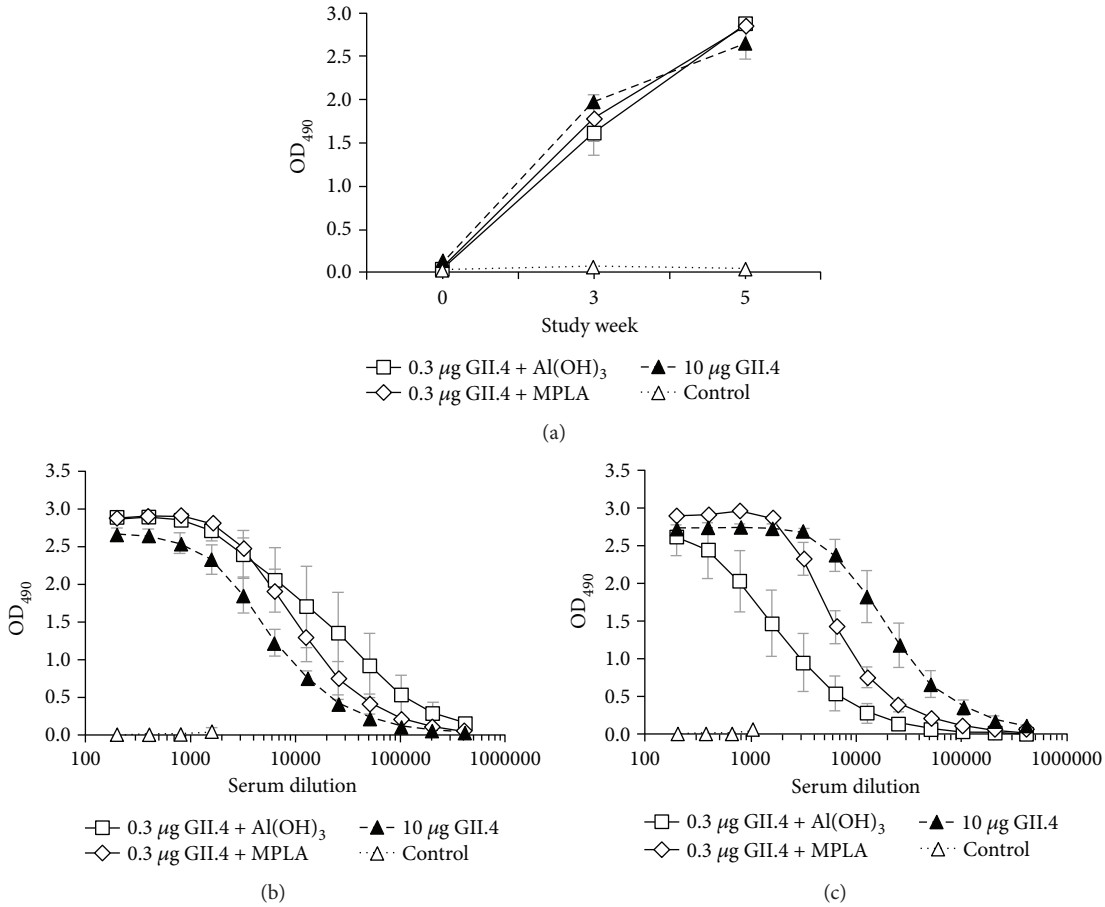

Figure 2: Development of IgG (a) and IgG subtype antibodies (b, c) in mice immunized IM with 0.3 μg of GII.4 VLPs formulated with $Al(OH)_3$ or MPLA or 10 μg of GII.4 VLPs alone. (a) Kinetics of NoV GII.4-specific total IgG antibodies in sera of mice immunized with the antigenic formulations at study weeks 0 and 3. Control mice received PBS only. Group mean OD_{490} values with standard error of the means of individual tail blood samples collected at indicated study weeks and termination sera at week 5 are shown. End-point titrations of anti-GII.4 IgG1 (b) and IgG2a (c) antibodies in termination sera at week 5. Mean titration curves with standard errors of the mean of the experimental groups are shown.

Nasal lavages from experimental groups with intestinal antibodies were also tested for the presence of GII.4-specific IgG and IgA antibodies. Similar to fecal specimens, comparable IgG levels ($p = 0.902$) were induced by 0.3 μg of VLPs in the presence of $Al(OH)_3$ (GMT = 6; 95% CI = 2–15) or MPLA (GMT = 6; 95% CI = 4–8) via IM delivery, or by 10 μg of VLPs alone via IM (GMT = 7; 95% CI = 3–16) or IN delivery (GMT = 12; 95% CI = 4–33) (Figure 4(a)). In contrast, only IN administration of VLPs resulted in generation of IgA antibodies (GMT = 30; 95% CI = 9–102) in the nasal secretions (Figure 4(b)).

3.4. $Al(OH)_3$ or MPLA Induced No Production of IgA Antibodies by MLN Cells. In order to confirm a lack of mucosal IgA antibodies induced by the two adjuvants in mucosal secretions (Figures 3 and 4), MLN cells from $Al(OH)_3$ and MPLA immunized mice were tested for the production of IgG and IgA antibodies. Cells from mice receiving VLPs in the presence of $Al(OH)_3$ or MPLA via IM delivery responded with considerable IgG production to *in vitro* stimulation with GII.4 VLPs (Figures 5(a) and 5(b)). On the contrary, neither of the adjuvanted formulations induced IgA production by MLN cells (Figures 5(a) and 5(b)), indicating that MLNs were not inductive sites of IgA responses detected in the intestinal secretions after IM immunization. No anti-GII.4 IgG or IgA production was detected when MLN cells were stimulated with the culture medium only (data not shown).

4. Discussion

Protection against pathogens at mucosal surfaces is largely dependent on secretory IgA effectively induced by IN immunization [25, 26]. Because of NoV transmission through intestinal mucosa, induction of mucosal immunity to NoV is likely a pivotal factor to be taken into consideration in NoV vaccine development. Although parenteral immunization routes are not generally considered potent inducers of mucosal immunity [9, 10, 27–29], we investigated if mucosal antibodies are induced by IM immunization of BALB/c mice with NoV GII.4 VLPs formulated with the widely used systemic adjuvants $Al(OH)_3$, a gold standard delivery system, or MPLA, a TLR4 agonist. It has been recently demonstrated

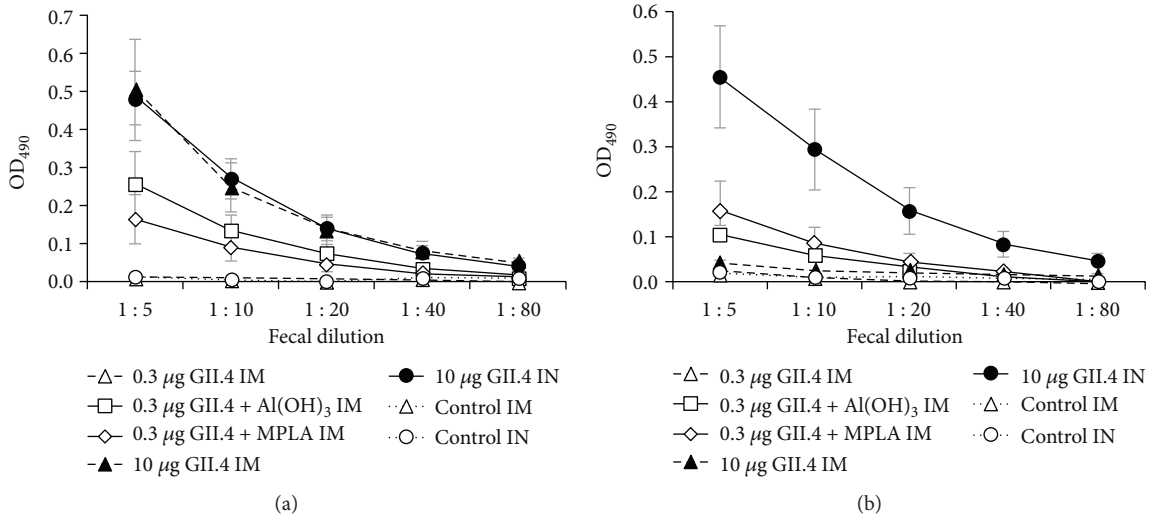

Figure 3: NoV GII.4-specific fecal antibody responses after IM immunization with 0.3 or 10 μg of NoV GII.4 VLPs alone or 0.3 μg of VLPs combined with $Al(OH)_3$ or MPLA, or IN immunization with 10 μg of VLPs alone. End-point titrations of anti-GII.4 IgG (a) and IgA (b) antibodies in 10% fecal suspensions of experimental mice. Control mice received PBS only. Mean titration curves with standard errors of the mean of the experimental groups are shown.

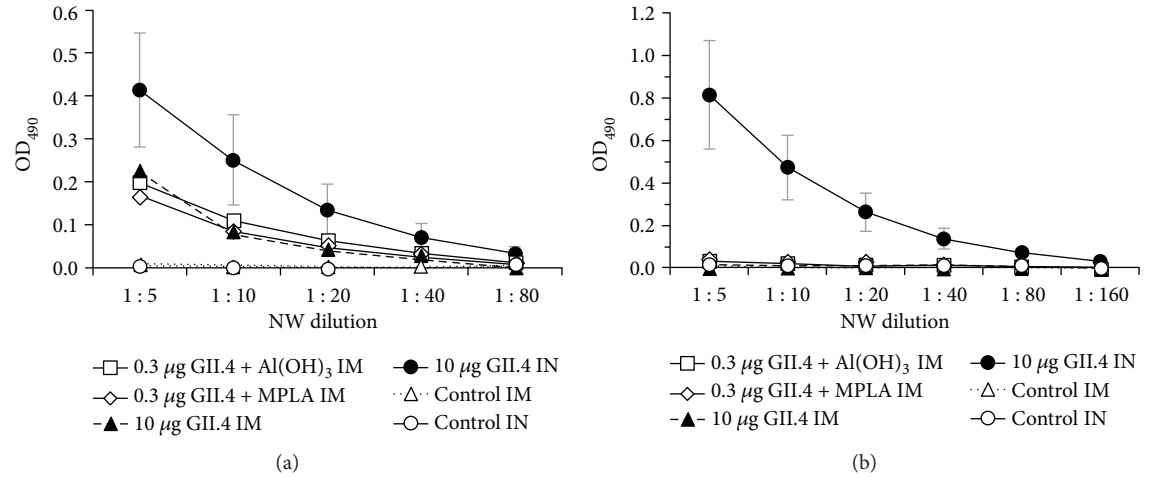

Figure 4: Mucosal antibody responses in nasal washes after IM immunization with 0.3 μg of NoV GII.4 VLPs formulated with $Al(OH)_3$ or MPLA, or IM or IN immunization with 10 μg of VLPs alone. End-point titrations of anti-GII.4 IgG (a) and IgA (b) antibodies in nasal washes (NWs) of experimental mice. Control mice received PBS only. Mean titration curves with standard errors of the mean of the experimental groups are shown.

that TLR ligands (TLR3/TLR4) alter migration patterns of dendritic cells *in vivo* and promote induction of mucosal responses to codelivered antigens as a consequence of antigen-loaded dendritic cells migrating to both draining and nondraining lymph nodes [30]. Therefore, we also investigated if IM immunization of NoV VLP antigens codelivered with these adjuvants causes lymphoid cell dissemination to remote sites like MLN.

The current NoV VLP vaccine candidate in the most advanced phases of clinical trials is administered IM in a formulation with MPLA and/or $Al(OH)_3$, being effective in inducing high systemic antibody responses [3–6]. After the challenge, protection was seen against moderate to severe forms of acute gastroenteritis, without significant reductions in NoV shedding [6]. Mucosal responses, namely, antibody-secreting cells (ASCs) with mucosal homing phenotype, derived from a recall of the mucosal response primed by prior exposures to NoV may be responsible for the observed protection [31]. In gnotobiotic calves, fecal IgA-mediated protection from virulent bovine NoV challenge was demonstrated only after mucosal (IN) immunization with bovine NoV VLPs [32]. Several other reports have also shown importance of mucosal immunity, especially IgA, in protection from NoV infection [9, 11, 12]. Similarly, parenterally delivered inactivated polio vaccine (IPV) generates protective serum antibodies but not local intestinal mucosal antibodies in the gut, therefore being sufficient to protect against disease but insufficient to prevent wild poliovirus from replicating in intestines and spreading to the environment [33, 34].

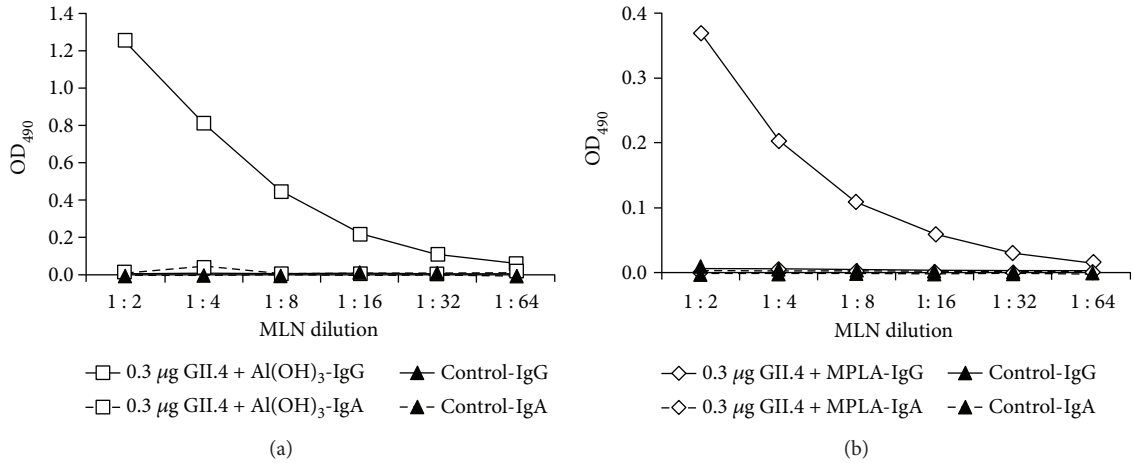

Figure 5: IgG and IgA antibodies in cells from mesenteric lymph nodes after IM immunization with 0.3 μg of NoV GII.4 VLPs formulated with $Al(OH)_3$ (a) or MPLA (b). End-point titration curves of anti-GII.4 IgG and IgA antibodies in cell culture supernatants from pooled mesenteric lymph nodes (MLNs) of experimental groups stimulated *in vitro* with 5 μg GII.4 VLPs. Control mice received PBS only.

In this study, high levels of serum IgG antibodies were induced by both adjuvants. $Al(OH)_3$ and MPLA promoted >30-fold dose sparing above nonadjuvanted dose (0.3 μg versus 10 μg dose, resp.) and induced considerable levels of IgG1, a marker of Th2 response, as well as IgG2a, a marker of Th1 response. Although MPLA promotes a Th1 bias [17, 35], our data showed induction of a balanced Th1/Th2-type response by this adjuvant. In contrast, $Al(OH)_3$ stimulated Th2-biased response, which is in concordance with previous observations [13, 36, 37]. A biased response depends on several factors such as the route of delivery, animal strain, and the vaccine antigen used, thereby explaining apparent discrepancies of our results. Despite different mechanisms of the two adjuvants employed in the present study, one being primarily a delivery or depot system and another an immunostimulator [13], our data indicate that $Al(OH)_3$ and MPLA work similarly for IM delivered NoV VLPs in terms of the dose sparing, kinetics, and generation of systemic IgG antibodies.

Our recent study demonstrated that IgA levels in mucosal tissues correlated with blocking activity, suggesting that IgA, but not IgG, was the main antibody neutralizing NoV on the mucosal surfaces [9]. In concordance with [9], current results show that mucosal IgA antibodies were induced by IN, but not IM, administration of NoV VLPs without an adjuvant. Only low level of fecal IgA was detected in a few mice immunized IM with NoV GII.4 VLPs and either of the adjuvants. Because of the similarly low IgA levels in sera of these animals, the detected antibody is likely a systemic IgA passively exuded from serum to mucosal secretions. In order to ensure that no NoV GII.4-specific secretory IgA response in mucosa was missed, we also tested NWs and vaginal washes (data not shown) for the presence of IgA antibodies. Only IN delivery of GII.4 NoV VLPs induced IgA antibodies in these secretions. In addition, in support to the serum origin of IgA, no IgA ASCs were detected in MLN cells of mice immunized with NoV VLP vaccine formulated with $Al(OH)_3$ or MPLA adjuvant. Similarly, Bessa and colleagues have detected IgG, but not IgA, ASCs in MLN after subcutaneous immunization of mice with a vaccine platform based on VLPs [38].

Our results clearly demonstrate the lack of the mucosal IgA antibody generation in naïve animals after IM delivery of NoV VLPs regardless of the adjuvants $Al(OH)_3$ or MPLA used. Others have shown that parenteral delivery (IM and intradermal) of vaccine antigens with mucosal adjuvant dmLT (a detoxified form of the heat-labile enterotoxin of *E. coli*) promotes mucosal immunity [24], likely by inducing mucosal homing receptors on B cells and their migration to mucosal compartments [39], although the exact mechanism is not completely understood. Therefore, the field of NoV vaccine development should consider mucosal delivery of NoV VLP vaccines [40], or at least inclusion of mucosal adjuvants or components targeted to mucosal trafficking, to immunize naïve individuals, such as infants and young children, to ensure induction of mucosal responses in the gut, the port of entry for enteric viruses like NoV.

5. Conclusions

The present study demonstrates that IM administration of NoV GII.4 VLPs formulated with $Al(OH)_3$ or MPLA does not induce significant mucosal IgA antibodies in mice. Instead, IN immunization with GII.4 VLPs alone elicited NoV-specific mucosal immunity. These results underline the importance of mucosal delivery route in induction of potent mucosal responses.

Conflicts of Interest

The authors declare that they have no conflicts of interest.

Acknowledgments

The authors acknowledge the technical assistance given by the laboratory personnel of the Vaccine Research Center. Special thanks are due to Dr. Kirsi Tamminen, Eeva Jokela, Sanna Kavén, and Marianne Karlsberg.

References

[1] M. M. Patel, M. A. Widdowson, R. I. Glass, K. Akazawa, J. Vinje, and U. D. Parashar, "Systematic literature review of role of noroviruses in sporadic gastroenteritis," *Emerging Infectious Diseases*, vol. 14, no. 8, pp. 1224–1231, 2008.

[2] F. Baehner, H. Bogaerts, and R. Goodwin, "Vaccines against norovirus: state of the art trials in children and adults," *Clinical Microbiology and Infection*, vol. 22, Supplement 5, pp. S136–S139, 2016.

[3] J. J. Treanor, R. L. Atmar, S. E. Frey et al., "A novel intramuscular bivalent norovirus virus-like particle vaccine candidate—reactogenicity, safety, and immunogenicity in a phase 1 trial in healthy adults," *The Journal of Infectious Diseases*, vol. 210, no. 11, pp. 1763–1771, 2014.

[4] S. Ramani, F. H. Neill, J. Ferreira et al., "B-cell responses to intramuscular administration of a bivalent virus-like particle human norovirus vaccine," *Clinical and Vaccine Immunology*, vol. 24, no. 5, article e00571-16, 2017.

[5] R. L. Atmar, F. Baehner, J. P. Cramer et al., "Rapid responses to 2 virus-like particle norovirus vaccine candidate formulations in healthy adults: a randomized controlled trial," *The Journal of Infectious Diseases*, vol. 214, no. 6, pp. 845–853, 2016.

[6] D. I. Bernstein, R. L. Atmar, G. M. Lyon et al., "Norovirus vaccine against experimental human GII.4 virus illness: a challenge study in healthy adults," *The Journal of Infectious Diseases*, vol. 211, no. 6, pp. 870–878, 2015.

[7] R. L. Atmar, D. I. Bernstein, C. D. Harro et al., "Norovirus vaccine against experimental human Norwalk virus illness," *The New England Journal of Medicine*, vol. 365, no. 23, pp. 2178–2187, 2011.

[8] S. S. El-Kamary, M. F. Pasetti, P. M. Mendelman et al., "Adjuvanted intranasal Norwalk virus-like particle vaccine elicits antibodies and antibody-secreting cells that express homing receptors for mucosal and peripheral lymphoid tissues," *The Journal of Infectious Diseases*, vol. 202, no. 11, pp. 1649–1658, 2010.

[9] K. Tamminen, M. Malm, T. Vesikari, and V. Blazevic, "Mucosal antibodies induced by intranasal but not intramuscular immunization block norovirus GII.4 virus-like particle receptor binding," *Viral Immunology*, vol. 29, no. 5, pp. 315–319, 2016.

[10] M. Malm, K. Tamminen, T. Vesikari, and V. Blazevic, "Comparison of intramuscular, intranasal and combined administration of norovirus virus-like particle subunit vaccine candidate for induction of protective immune responses in mice," *Journal of Clinical & Cellular Immunology*, vol. 6, no. 284, 2015.

[11] L. Lindesmith, C. Moe, S. Marionneau et al., "Human susceptibility and resistance to Norwalk virus infection," *Nature Medicine*, vol. 9, no. 5, pp. 548–553, 2003.

[12] S. Ramani, F. H. Neill, A. R. Opekun et al., "Mucosal and cellular immune responses to Norwalk virus," *The Journal of Infectious Diseases*, vol. 212, no. 3, pp. 397–405, 2015.

[13] S. Apostolico Jde, V. A. Lunardelli, F. C. Coirada, S. B. Boscardin, and D. S. Rosa, "Adjuvants: classification, modus operandi, and licensing," *Journal of Immunology Research*, vol. 2016, Article ID 1459394, 16 pages, 2016.

[14] N. Lycke, "Recent progress in mucosal vaccine development: potential and limitations," *Nature Reviews Immunology*, vol. 12, no. 8, pp. 592–605, 2012.

[15] T. R. Ghimire, R. A. Benson, P. Garside, and J. M. Brewer, "Alum increases antigen uptake, reduces antigen degradation and sustains antigen presentation by DCs *in vitro*," *Immunology Letters*, vol. 147, no. 1-2, pp. 55–62, 2012.

[16] V. Mata-Haro, C. Cekic, M. Martin, P. M. Chilton, C. R. Casella, and T. C. Mitchell, "The vaccine adjuvant monophosphoryl lipid a as a TRIF-biased agonist of TLR4," *Science*, vol. 316, no. 5831, pp. 1628–1632, 2007.

[17] C. R. Casella and T. C. Mitchell, "Putting endotoxin to work for us: monophosphoryl lipid a as a safe and effective vaccine adjuvant," *Cellular and Molecular Life Sciences*, vol. 65, no. 20, pp. 3231–3240, 2008.

[18] M. Kool, V. Petrilli, T. De Smedt et al., "Cutting edge: alum adjuvant stimulates inflammatory dendritic cells through activation of the NALP3 inflammasome," *The Journal of Immunology*, vol. 181, no. 6, pp. 3755–3759, 2008.

[19] L. Huhti, V. Blazevic, K. Nurminen, T. Koho, V. Hytönen, and T. Vesikari, "A comparison of methods for purification and concentration of norovirus GII-4 capsid virus-like particles," *Archives of Virology*, vol. 155, no. 11, pp. 1855–1858, 2010.

[20] K. Tamminen, S. Lappalainen, L. Huhti, T. Vesikari, and V. Blazevic, "Trivalent combination vaccine induces broad heterologous immune responses to norovirus and rotavirus in mice," *PLoS One*, vol. 8, no. 7, article e70409, 2013.

[21] K. Tamminen, L. Huhti, T. Koho et al., "A comparison of immunogenicity of norovirus GII-4 virus-like particles and P-particles," *Immunology*, vol. 135, no. 1, pp. 89–99, 2012.

[22] V. Blazevic, S. Lappalainen, K. Nurminen, L. Huhti, and T. Vesikari, "Norovirus VLPs and rotavirus VP6 protein as combined vaccine for childhood gastroenteritis," *Vaccine*, vol. 29, no. 45, pp. 8126–8133, 2011.

[23] C. O. Elson and W. Ealding, "Generalized systemic and mucosal immunity in mice after mucosal stimulation with cholera toxin," *The Journal of Immunology*, vol. 132, no. 6, pp. 2736–2741, 1984.

[24] E. B. Norton, D. L. Bauer, W. C. Weldon, M. S. Oberste, L. B. Lawson, and J. D. Clements, "The novel adjuvant dmLT promotes dose sparing, mucosal immunity and longevity of antibody responses to the inactivated polio vaccine in a murine model," *Vaccine*, vol. 33, no. 16, pp. 1909–1915, 2015.

[25] N. Lycke, "T cell and cytokine regulation of the IgA response," *Chemical Immunology*, vol. 71, pp. 209–234, 1998.

[26] P. A. Kozlowski, S. B. Williams, R. M. Lynch et al., "Differential induction of mucosal and systemic antibody responses in women after nasal, rectal, or vaginal immunization: influence of the menstrual cycle," *The Journal of Immunology*, vol. 169, no. 1, pp. 566–574, 2002.

[27] Z. Moldoveanu, M. L. Clements, S. J. Prince, B. R. Murphy, and J. Mestecky, "Human immune responses to influenza virus vaccines administered by systemic or mucosal routes," *Vaccine*, vol. 13, no. 11, pp. 1006–1012, 1995.

[28] S. Sasaki, K. Sumino, K. Hamajima et al., "Induction of systemic and mucosal immune responses to human immunodeficiency virus type 1 by a DNA vaccine formulated with QS-21 saponin adjuvant via intramuscular and intranasal routes," *Journal of Virology*, vol. 72, no. 6, pp. 4931–4939, 1998.

[29] T. M. Herremans, J. H. Reimerink, A. M. Buisman, T. G. Kimman, and M. P. Koopmans, "Induction of mucosal immunity by inactivated poliovirus vaccine is dependent on previous mucosal contact with live virus," *The Journal of Immunology*, vol. 162, no. 8, pp. 5011–5018, 1999.

[30] E. Y. Enioutina, D. Bareyan, and R. A. Daynes, "TLR ligands that stimulate the metabolism of vitamin D3 in activated murine dendritic cells can function as effective mucosal adjuvants to subcutaneously administered vaccines," *Vaccine*, vol. 26, no. 5, pp. 601–613, 2008.

[31] A. Sundararajan, M. Y. Sangster, S. Frey et al., "Robust mucosal-homing antibody-secreting B cell responses induced by intramuscular administration of adjuvanted bivalent human norovirus-like particle vaccine," *Vaccine*, vol. 33, no. 4, pp. 568–576, 2015.

[32] M. G. Han, S. Cheetham, M. Azevedo, C. Thomas, and L. J. Saif, "Immune responses to bovine norovirus-like particles with various adjuvants and analysis of protection in gnotobiotic calves," *Vaccine*, vol. 24, no. 3, pp. 317–326, 2006.

[33] T. R. Hird and N. C. Grassly, "Systematic review of mucosal immunity induced by oral and inactivated poliovirus vaccines against virus shedding following oral poliovirus challenge," *PLoS Pathogens*, vol. 8, no. 4, article e1002599, 2012.

[34] P. L. Ogra, D. T. Karzon, F. Righthand, and M. MacGillivray, "Immunoglobulin response in serum and secretions after immunization with live and inactivated poliovaccine and natural infection," *The New England Journal of Medicine*, vol. 279, no. 17, pp. 893–900, 1968.

[35] L. Vernacchio, H. Bernstein, S. Pelton et al., "Effect of monophosphoryl lipid A (MPL®) on T-helper cells when administered as an adjuvant with pneumococcoccal–CRM_{197} conjugate vaccine in healthy toddlers," *Vaccine*, vol. 20, no. 31-32, pp. 3658–3667, 2002.

[36] J. M. Brewer, "(How) do aluminium adjuvants work?," *Immunology Letters*, vol. 102, no. 1, pp. 10–15, 2006.

[37] E. B. Lindblad, "Aluminium compounds for use in vaccines," *Immunology and Cell Biology*, vol. 82, no. 5, pp. 497–505, 2004.

[38] J. Bessa, N. Schmitz, H. J. Hinton, K. Schwarz, A. Jegerlehner, and M. F. Bachmann, "Efficient induction of mucosal and systemic immune responses by virus-like particles administered intranasally: implications for vaccine design," *European Journal of Immunology*, vol. 38, no. 1, pp. 114–126, 2008.

[39] J. D. Clements and L. C. Freytag, "Parenteral vaccination can be an effective means of inducing protective mucosal responses," *Clinical and Vaccine Immunology*, vol. 23, no. 6, pp. 438–441, 2016.

[40] J. P. Ball, M. J. Springer, Y. Ni et al., "Intranasal delivery of a bivalent norovirus vaccine formulated in an *in situ* gelling dry powder," *PLoS One*, vol. 12, no. 5, article e0177310, 2017.

Hindawi
Journal of Immunology Research
Volume 2018, Article ID 3710961, 9 pages
https://doi.org/10.1155/2018/3710961

Research Article

Leaf-Encapsulated Vaccines: Agroinfiltration and Transient Expression of the Antigen *Staphylococcal Endotoxin* B in Radish Leaves

Pei-Feng Liu,[1] Yanhan Wang,[1] Robert G. Ulrich,[2] Christopher W. Simmons,[3] Jean S. VanderGheynst,[3] Richard L. Gallo,[1] and Chun-Ming Huang[1,4]

[1]*Department of Dermatology, University of California, San Diego, CA 92161, USA*
[2]*Department of Immunology, Army Medical Research Institute of Infectious Diseases, Frederick, MD 21703, USA*
[3]*Department of Biological & Agricultural Engineering, University of California, Davis, CA 95616, USA*
[4]*Department of Dermatology and Moores Cancer Center, University of California, San Diego, CA 92161, USA*

Correspondence should be addressed to Chun-Ming Huang; chunming@ucsd.edu

Received 26 February 2017; Revised 24 September 2017; Accepted 10 October 2017; Published 7 February 2018

Academic Editor: Stuart Berzins

Transgene introgression is a major concern associated with transgenic plant-based vaccines. Agroinfiltration can be used to selectively transform nonreproductive organs and avoid introgression. Here, we introduce a new vaccine modality in which Staphylococcal enterotoxin B (SEB) genes are agroinfiltrated into radishes (*Raphanw sativus* L.), resulting in transient expression and accumulation of SEB *in planta*. This approach can simultaneously express multiple antigens in a single leaf. Furthermore, the potential of high-throughput vaccine production was demonstrated by simultaneously agroinfiltrating multiple radish leaves using a multichannel pipette. The expression of SEB was detectable in two leaf cell types (epidermal and guard cells) in agroinfiltrated leaves. ICR mice intranasally immunized with homogenized leaves agroinfiltrated with SEB elicited detectable antibody to SEB and displayed protection against SEB-induced interferon-gamma (IFN-γ) production. The concept of encapsulating antigens in leaves rather than purifying them for immunization may facilitate rapid vaccine production during an epidemic disease.

1. Introduction

Transgenic plants have emerged as a promising technology to generate recombinant biopharmaceutical proteins and vaccines [1, 2]. Plants produce full-length mammalian proteins that appear to be processed correspondingly to their native counterpart with appropriate folding, assembly, and posttranslational modifications [3]. Although stably transformed transgenic plants have been widely created to deliver edible vaccines [4, 5] and have proven success in clinical trials [6, 7], the fact that transgenes are permanently incorporated into the genomes of transgenic plants raises many concerns, such as the environmental release of genetically modified plants and the possibility of transgene introgression into nonmodified counterparts [8]. In addition, immunization with edible vaccines derived from transgenic plants may carry a risk of inducing oral tolerance due to immunization with multidoses within a long period of time. Transient expression of recombinant proteins in leaf tissue avoids transgene introgression and provides a fast platform for protein production without an effort-exhaustive process to generate stably transformed transgenic plants [9].

Currently, there are at least four approaches to transforming and inducing transient expression in plants: (1) delivery of "naked" DNA by particle bombardment [10], (2) infection with modified viral vectors [6, 10, 11], (3) agroinfiltration of plant tissues with *Agrobacteria* [10, 12], and (4) polyethylene glycol- (PEG-) mediated gene transfer and electroporation of protoplasts [13]. Agroinfiltration accommodates transforming plants with large genes encoding complex proteins, such

as antibodies. Moreover, agroinfiltration-induced transient expression can yield high levels of recombinant protein [14]. Vacuum and syringe infiltration are two major methods of promoting agroinfiltration and expressing proteins/antigens in plants [15, 16]. Unlike the vacuum infiltration, syringe infiltration can be easily applied for infiltrating multiple antigens on the same leaf. Syringe infiltration, where a needle-less syringe is placed at the surface of a leaf and used to push a suspension of *A. tumefaciens* into the leaf interior, provides a high level of control over which tissues are transformed. In contrast to agroinfiltration, the efficiency of particle bombardment using a gene gun is relatively low since transgenes are successfully delivered to only few target cells [14]. Furthermore, transient expression using plant virus infection shows many disadvantages, such as biosafety and construct-size limitation [2]. Protoplast transformation involves a care-intensive, complicated procedure of isolating protoplasts from leaf mesophylls. Protoplasts can also respond differently from intact cells and may not be suitable for certain types of expression analysis [17].

Staphylococcal enterotoxin B (SEB) is one of the several toxins produced by *Staphylococcus aureus* bacteria [18, 19]. The toxin commonly causes outbreaks of food poisoning. Also, SEB has been studied as a potential biological warfare agent because it can easily be aerosolized, is very stable, and can cause shortness of breath, widespread systemic damage, and even shock and death when inhaled at very high dosages [20–22]. Molecularly, SEB acts as a superantigen, binding to class II major histocompatibility complex proteins and stimulating T cells to induce inflammation and cytokine (e.g., tumor necrosis factor alpha and interferon-gamma (IFN-γ)) release [23]. Considering the toxicity and potential weaponization of SEB, there is an urgent need to have anti-SEB vaccines that can be produced in an effortless and timely manner during SEB outbreaks.

Here, we generate SEB vaccines by agroinfiltrating SEB genes into radish leaves. Intranasal immunization of mice with SEB-expressing leaves in conjunction with adjuvant cholera toxin (CT) elicited systemic antibodies to SEB and offered protective immunity against SEB-induced IFN-γ production. We also demonstrate that two different antigens (SEB and a tetanus toxin C fragment (TetC)) can be simultaneously agroinfiltrated and transiently expressed within the same leaf. Notably, we here highlight the concept of stamping antigens onto leaves to generate vaccines by using agroinfiltration. The technique shows that agroinfiltration can be used to rapidly induce transient expression of antigens in leaf tissue, which can be used for immunization in a way that eliminates complicated purification procedures commonly associated with recombinant antigens. This work illustrates that agroinfiltrated/stamped leaves can not only act as bioreactors for antigen production but may also serve as capsulated vaccines containing one or more antigens for patient immunization.

2. Materials and Methods

2.1. Plant Materials. Japanese radish sprouts (Kaiware-daikon) (*Raphanus sativus* L.) and lettuce (*Lactuca sativa*) were obtained from a commercial supplier (ICREST International, JCP, Carson, CA). Japanese radish sprouts that were 9 cm in length with two leaflets were used. *Arabidopsis thaliana* seeds were kindly provided by Professor Nigel Crawford at University of California, San Diego. All plants were grown at room temperature under a 23-watt fluorescent bulb (Philips, Portland, OR) and were sprayed with water daily.

2.2. Vector Construction and Agrobacterium tumefaciens Transformation. The methods of vector construction and transformation were according to a modified protocol described in our previous publication. Briefly, the binary vector pBI121 carrying the reporter GUS driven by the CaMV 35S promoter was used [24, 25]. A forward primer (5′-GATTCTAGAATGGAGAGTCAACCAGATCCTAAAC CAGA-3′) and a reverse primer (5′-TCGCCCGGGCGCTT TTTCTTTGTCGTAAGATAAACTTC-3′) were utilized for polymerase chain reaction (PCR) to amplify the open reading frame of detoxified SEB cDNA with three mutations (National Center for Biotechnology Information (NCBI) accession number M11118) [26]. A forward primer (5′-GGATCTAGAATGGAAAATCTGGATTGTT GGG-3′) and a reverse primer (5′-AATCCCGGGCG GTCGTTGGTCCAACCTTC-3′) were added into a PCR reaction to amplify the TetC cDNA (NCBI accession number AM412776). PCR products were cloned into polylinker sites of pBI121 vectors to generate 35S::*SEB-GUS* and 35S::*TetC-GUS* constructs [25]. These two constructs were then transformed into *Agrobacterium tumefaciens* strain LBA4404 according to a liquid nitrogen freeze-thaw method.

2.3. Agroinfiltration of 35S::SEB-GUS and 35S::TetC-GUS Constructs into Radish Leaves. A single colony of *A. tumefaciens* transformants was cultured in 2 ml of YEP media (10 mg/ml Bacto™ Tryptone (DIFCO, Detroit, MI), 10 mg/ml yeast extract (DIFCO, Detroit, MI), and 5 mg/ml NaCl (Sigma, St. Louis, MO; pH 7.5)) containing 50 μg/ml kanamycin and streptomycin at 28°C until optical density (OD) at 600 nm (OD_{600}) reached 0.5. Nontransformed *Agrobacterium* served as a negative control. For syringe infiltration, as previously described [25], 0.1 ml of *Agrobacterium* bacterial suspension (5×10^7 CFU) was injected into the wounded lower epidermis site for five days. For high-throughput agroinfiltration, six radish leaves were concurrently infiltrated with 0.1 ml of bacterial suspension containing the 35S::*SEB-GUS* construct using a multichannel pipette with open (2.2 mm diameter) tips. The infiltrated leaves were next placed in a dish containing wet cloths and incubated overnight.

2.4. Histochemical GUS Assays. Agroinfiltrated leaves were stained using a histochemical GUS assay solution consisting of 0.1 M $NaPO_4$ (pH 7.0), 0.5 mM $K_3Fe(CN)_6$, 0.5 mM $K_4Fe(CN)_6$, 0.1% (*v*/*v*) Triton X-100, and 0.05% (*w*/*v*) X-Gluc (Sigma, St. Louis, MO) [27]. Leaves were submerged in the staining solution and incubated at 37°C in the dark overnight. After incubation, leaves were removed from the staining solution and immersed in a stop solution containing

42.5% (*v*/*v*) ethanol, 10% (*v*/*v*) formaldehyde, and 5% (*v*/*v*) acetic acid [28]. Stained leaves were embedded in OCT compound (Miles Inc., Diagnostics Division, Elkhart, IN) and cut with a glass knife on a cryogenic ultramicrotome (7 μm thick). Fresh-mounted OCT sections were examined under bright-field microscopy (Olympus America, Inc., Melville, NY).

2.5. Intranasal Immunization with Homogenized Leaves Containing Recombinant SEB. Our previous study indicated that intranasal immunization of mice with ground leaves expressing CAMP factor elicits detectable antibodies to *P. acnes* CAMP factor, indicating that intranasal administration of whole plant leaves may be a new regimen for vaccination [25]. In the study, female ICR (Institute of Cancer Research) mice (3 to 6 weeks old; Harlan, Indianapolis, IN) were utilized for intranasal immunization. Intranasal immunization holds the potential to induce a mucosal immune response that recapitulates the natural SEB infection across the respiratory tract [29]. All mice used in the study were maintained in accordance to institutional IACUC guidelines. The central areas (25 mm^2) of five radish leaves expressing SEB-GUS or GUS alone were excised using a sterile scalpel. Leaf sections were then pooled and homogenized under liquid nitrogen followed by addition of 700 μl ddH_2O and then sterilized by an ultraviolet crosslinker (Spectronics, Westbury, NY) at 7000 J/m^2 for 30 min. Inactivation of sterilized *Agrobacterium* was confirmed by their inability to form colonies on YEP agar plates (data not shown). Twenty-five microliter homogenized leaves containing either SEB-GUS or GUS alone (as a negative control) mixed with a CT adjuvant (Sigma-Aldrich, St. Louis, MO) which has been used to boost the mucosal immunogenicity (5 μg/25 μl of ground leaf materials as described below) were then intranasally inoculated into the nasal cavities of ICR mice (25 μl of ground leaf materials). Three boosts at the same dose were performed at 1, 2, and 4 weeks after the first immunization [30].

2.6. Western Blotting. Twenty μg of homogenized leaves expressing either SEB-GUS or GUS alone were loaded into a 10% SDS-PAGE for antigen detection. After electrophoretically transferring SDS-PAGE to nitrocellulose membranes, the membranes were incubated with mouse monoclonal anti-SEB antibody (1 : 1000 dilution) (Toxin Technology, Sarasota, FL). To detect the production of antibodies in immunized mice, recombinant SEB (15 μg) (Toxin Technology, Sarasota, FL) was subject to a 10% SDS-PAGE and transferred to a nitrocellulose membrane which was subsequently immunoreacted to four-week serum (1 : 500 dilution) obtained from mice immunized with whole leaf containing SEB-GUS. Immunoglobulin G (IgG) antibodies were detected with anti-mouse horseradish peroxidase-conjugated IgG (1 : 5000 dilution, Promega, Madison, WI). A Western Lighting™ Chemiluminescence kit (PerkinElmer, Boston, MA) was used to visualize the peroxidase activity.

2.7. Titration of Antibodies. The antibody titer of SEB was quantified by ELISA. Eight mice were used per group. Sera were collected 4 weeks after first immunization with L-GUS or L-SEB-GUS. Purified recombinant SEB (0.1 μg/well) was diluted with PBS buffer and coated onto a 96-well ELISA plate (Corning, Lowell, MA) at 4°C overnight. The plate was washed with PBS containing 0.05% (*w*/*v*) Tween-20 and blocked with PBS containing 1% (*w*/*v*) bovine-serum albumin and 0.05% (*w*/*v*) Tween-20 for 2 h at room temperature. Pooled antisera obtained from eight immunized mice with L-GUS or L-SEB-GUS were serially diluted by 10-fold and separately added to the wells and incubated for 2 h. A goat anti-mouse IgG-HRP conjugate (Promega, Madison, WI) (1 : 5000 dilution) was added and incubated for 2 h before washing. HRP activity was determined with an OptEIA™ Reagent Set (BD Biosciences). The OD of each well was measured at 490 nm. The endpoint was defined as the dilution of sera producing the same OD at 490 nm as a 1/100 dilution of preimmune sera. Sera negative at the lowest dilution tested were assigned endpoint titers of 100. The data was presented as geometric mean endpoint ELISA titers as previously described [31].

2.8. Measurement of SEB-Induced IFN-γ Production in Immunized Mice. Naïve mice and immunized mice after the third boost were challenged intranasally with recombinant SEB (40 μg/mouse) for overnight. Eight mice were used per group. After trachea cannulation, the lungs were lavaged twice with 0.5 ml of phosphate-buffered saline, and BAL fluids were pooled. After centrifugation at 1300g, IFN-γ in fluids pooled from eight mice per group was measured by an ELISA kit as directed by the manufacturer (BD Biosciences, San Diego, CA) [31].

3. Results and Discussion

3.1. Agroinfiltration, Transient Expression, and Encapsulation of β-Glucuronidase (GUS) Protein in a Model Plant and Two Edible Crops. Many plants, including *Arabidopsis*, a model plant, are able to express proteins [32] via either stable genetic or transient transformation [33]. *Agrobacterium* has been utilized as a vector to deliver foreign DNA and induce transient expression of recombinant proteins in various plants [34]. In this study, *Arabidopsis* and two edible crops, lettuce and radish, were used as platforms to transiently express GUS and/or antigens. Leaves of these plants were bombarded with *Agrobacterium* harboring a 35S::*GUS* construct via a pressure infiltration. Five days post-infiltration, spatial expression of GUS within the leaves was detected by histochemical GUS staining. Infiltration of radish, lettuce, and *Arabidopsis* leaves with *A. tumefaciens* harboring 35S::GUS constructs resulted in GUS expression in all three plants. Control infiltrations, in which *A. tumefaciens* lacking 35S::GUS constructs was used, did not yield detectable GUS expression (Figure 1). These results confirm the versatility of agroinfiltration for inducing transient expression of transgenes in a variety of plants. Radishes, being edible and easily grown, were used for all following transient expression experiments. As presented in Figure 1, GUS can be agroinfiltrated and transiently expressed in *Arabidopsis*, lettuce, and radish, demonstrating *A. tumefaciens*' broad host

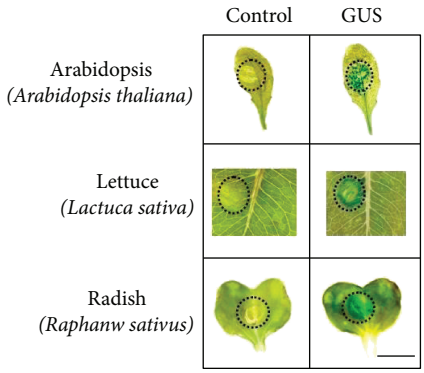

Figure 1: Transient expression of agroinfiltrated GUS in *Arabidopsis*, lettuce, and radish leaves. Transient encapsulation of GUS in leaves of three different plants. In an effort to transiently encapsulate GUS, leaves of *Arabidopsis thaliana*, the first selected to decipher its genome sequences, and two edible crops (lettuce (*Lactuca sativa*) and radish (*Raphanw sativus L.*)) were infiltrated with *A. tumefaciens* (LBA4404 strains, 5×10^7 CFU) transforming a 35S::*GUS* construct (pBI121). Plant leaves infiltrated with nontransformed LBA4404 cells (control, 5×10^7 CFU) served as negative controls. Dotted circles indicate locations of syringe infiltration with *A. tumefaciens*. GUS was detected using a histochemical staining procedure. Blue-stained areas indicate GUS activity. Bar = 6 mm.

range [35]. The Japanese radish (*Raphanus sativus L.*) is an edible leaf vegetable that is grown and consumed throughout the world. Recently, it has been reported that the Japanese radish is the vegetable with the highest per capita consumption within the *Brassicaceae* family. Moreover, it is rich in antioxidant constituents that can potentially prevent several human diseases [36]. Due to its easy growth and edibility, Japanese radish was selected for transient expression of GUS and/or SEB-GUS. Histochemical GUS assays demonstrated that GUS expression is detectable in radish five days after agroinfiltration (Figure 1). Detection of GUS activity using 4-methylumbelliferyl-D-glucuronide (4-MUG) as a substrate indicated that the amount of GUS expression was dramatically elevated to the 0.45 U/mg five days after agroinfiltration [25], which may predict the kinetics or amount of transient protein expression in agroinfiltrated leaves although *in planta* transient transgene expression has not been well quantified [37].

3.2. Agroinfiltration of SEB-GUS into Radish Leaves. SEB has been categorized as a biological threat agent in bioterrorism and epidemic outbreaks of food poisoning. Development of a modality that can produce vaccines against SEB in a quick and undemanding way may be an effective strategy to block the SEB spread. In this study, the action of agroinfiltration stamping was displayed by means of pressure infiltration of leaves with an *Agrobacterium*-loaded syringe (Figure 2(a)). Infiltration of radish leaves with *Agrobacterium* containing a 35S::*SEB-GUS* construct resulted in recombinant SEB-GUS encapsulation within leaves, as indicated by GUS histochemical staining in the central part of the leaf (Figure 2(b), SEB-GUS). Control leaves agroinfiltrated with *A. tumefaciens* lacking the 35S::*SEB-GUS* construct did not exhibit any staining (Figure 2(b)). Infiltrating each leaflet of a single radish leaf with different *Agrobacterium* transformants, specifically, one containing a 35S::*SEB-GUS* construct another containing 35S::*TetC-GUS*, allowed a single radish leaf to express two different antigens (SEB and TetC) with distinct spatial encapsulation of the antigens within the leaf (Figure 2(b), SEB-GUS + TetC-GUS), demonstrating the simplicity of using agroinfiltration stamping to create a bivalent vaccine in plants [38]. The throughput of syringe infiltration was increased by using a multichannel pipette to infiltrate six harvested radish leaves in parallel (Figure 2(c)). *A. tumefaciens* either harboring or lacking the 35S::*SEB-GUS* construct was loaded into tips on the multichannel pipette and pressure infiltrated into leaves in a manner similar to that used with syringes. SEB-GUS was detected in the leaves agroinfiltrated with the 35S::*SEB-GUS* construct, as indicated by histochemical staining (Figure 2(d)).

In this study, we emphasized the concept of using agroinfiltration stamping to transiently express and encapsulate antigens in radish leaves. The agroinfiltration stamping was illustrated by applying pressure infiltration of *A. tumefaciens* suspension into leaf tissue, accomplished with either a syringe or a multichannel pipette (Figure 2), avoided more complicated techniques like microparticle bombardment [39], which requires gene guns [40] and coating DNA on gold particles. Unlike agroinfiltration stamping, microparticle bombardment will thus make it difficult to simultaneously transfer multiple antigens into a single leaf as well as to bombard antigens in a high-throughput manner. Agroinfiltration is an efficient method for inducing transient expression of multiple antigen transgenes in plant tissue. The concept of high-throughput agroinfiltration system in the study could be applied for producing high level and variety of antigens in the future [41]. Moreover, agroinfiltration can provide milligram amounts of a recombinant protein within a week [42]. This is an important issue because it dramatically accelerates the development of plant lines producing recombinant therapeutics. Importantly, agroinfiltration may even prove suitable for preclinical trials without the need for production of stably transformed plants [14].

3.3. Cellular Distribution of SEB-GUS Transient Expression in Radish Leaves. To examine the cellular distributions of GUS and SEB expression, Tissue-Tek Optimal Cutting Temperature- (OCT-) embedded tissue sections of agroinfiltrated radish leaves were stained with 5-bromo-4-chloro-3-indolyl-β-D-glucuronic acid cyclohexylammonium salt (X-Gluc). No GUS expression was detected when leaves were infiltrated with nontransformant *A. tumefaciens* (control). GUS expression (indicated by a blue precipitate after X-Gluc treatment) was condensed in the wounded area of radish leaves infiltrated with *A. tumefaciens* carrying a 35S::*GUS* construct (Figure 3(a)). The GUS or SEB-GUS was detectable in epidermal cells, but predominantly expressed in guard cells in the wounded area agroinfiltrated with 35S::*GUS* or 35S::*SEB-GUS* constructs, respectively (Figure 3(b)). GUS expression was used as an indicator for SEB expression since constructs were designed to have the SEB coding sequence upstream of the GUS coding sequence in SEB-GUS fusions.

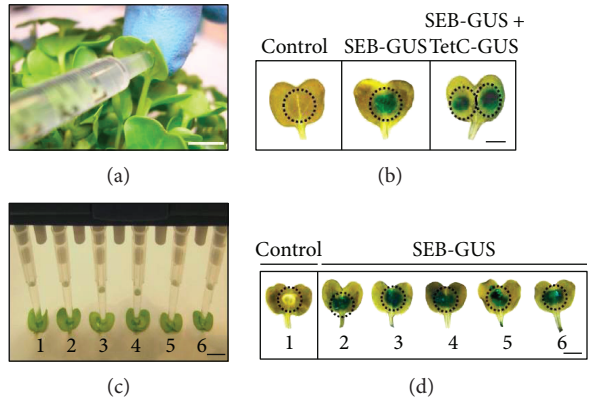

Figure 2: Agroinfiltration of SEB-GUS and TetC-GUS genes into radish leaves. (a) Syringe infiltration of *A. tumefaciens* into radish leaves. Bar = 6 mm. (b) Histochemical staining of radish leaves agroinfiltrated with *A. tumefaciens* (5×10^7 CFU) containing no construct (as a control), 35S::*SEB-GUS* construct, or both 35S::*SEB-GUS* plus 35S::*TetC-GUS* constructs. To simultaneously express two antigens *in planta*, the left half of a single radish leaf was infiltrated with *A. tumefaciens* harboring a 35S::*SEB-GUS* construct while the right half was infiltrated with *A. tumefaciens* harboring a 35S::*TetC-GUS* construct. (c) For higher throughput antigen expression, six isolated radish leaves were concurrently infiltrated with nontransformed *A. tumefaciens* (number 1) as a control and *A. tumefaciens* carrying a 35S::*SEB-GUS* construct (numbers 2–6) using a multichannel pipette. Bar = 12 mm. (d) Histochemical staining of leaves simultaneously infiltrated using the multichannel pipette to indicate GUS expression one day after pipetting. Bar = 6 mm.

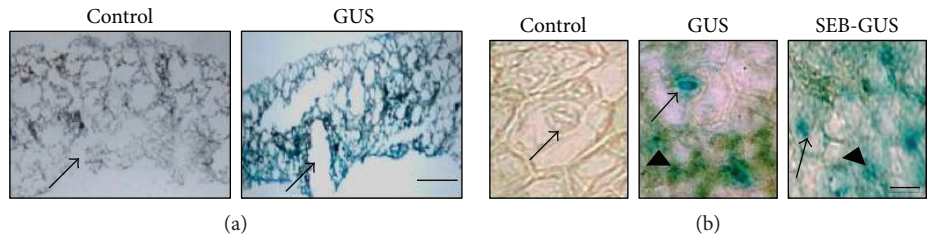

Figure 3: Cellular distributions of transient expression and encapsulation of GUS and SEB-GUS in radish leaves. (a) The majority of GUS-positive cells (blue) were located in the wounded area (arrows) of radish leaves infiltrated with *A. tumefaciens* (5×10^7 CFU) carrying a 35S::*GUS* construct, but not with nontransformed *A. tumefaciens* (control, 5×10^7 CFU). Bar = 0.5 mm. (b) Amplification of wounded areas indicated that GUS or SEB-GUS was detectable in the epidermal (arrowheads) cells, but predominantly expressed in guard cells (arrows) of infiltrated leaves. Bar = 10 μm.

Additionally, SEB-GUS expression was detected by a Western blot analysis. Proteins in agroinfiltrated radish leaves were separated using 10% sodium dodecyl sulfate polyacrylamide gel electrophoresis (SDS-PAGE) and reacted with a mouse monoclonal anti-SEB antibody. A band at 96 kDa corresponding to the expression of a SEB- (28 kDa) GUS (68 kDa) fusion protein appeared for leaves infiltrated with *A. tumefaciens* carrying a 35S:*SEB:GUS* construct (Figure 4). Although several protein bands were recognized by a mouse monoclonal anti-SEB antibody, the 96 kDa band is not detected in leaves infiltrated with nontransformant *Agrobacterium* (control). Future work will extract SEB-GUS from infiltrated leaves [43] and conduct Western blot analysis to validate the expression of SEB in leaves. Data from Figures 3 and 4 indicate that SEB-GUS was expressed and encapsulated in radish leaves after agroinfiltration. Through advances in molecular and genetic techniques, protein expression in plants has been optimized for high-level production [44]. Recently, synthesis of codon-optimized bacteria gene in plants is powerful and common [45]. It is conceivable that pathogens and radish sprouts have very different tRNA pools. Thus, synthesis of a codon-optimized gene ought to enhance the production of in plant cells [46]. Moreover, transient expression levels can be elevated by using the cauliflower mosaic virus (CaMV) 35S promoter to drive transgene expression in plants [47]. Previous studies demonstrated the cell type-specific expression of a CaMV 35S-GUS gene in transgenic plants [48]. Here, we showed that epidermal cells and guard cells in CaMV 35S-GUS-transformed radish leaves expressed GUS most readily (Figure 3), which is consistent with GUS expression patterns seen in transgenic tobacco leaves [49].

3.4. SEB Immunogenicity and Protective Immunity against IFN-γ Production. The functionality of SEB-GUS encapsulated in radish leaves as a vaccine was tested. Without purifying SEB from leaves, whole leaves infiltrated with *A. tumefaciens* carrying a 35S::*SEB-GUS* (L-SEB-GUS) or a 35S::*GUS* (L-GUS) construct were ground in sterile water, ultraviolet-inactivated, and mixed with cholera toxin, a common adjuvant used for intranasal immunization [50]. The ground leaves were subsequently inoculated into nasal

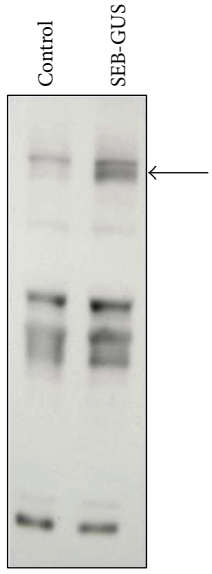

Figure 4: Confirmation of SEB-GUS expression by Western blot analysis. Ground radish leaves (20 μg) infiltrated with *A. tumefaciens* (5×10^7 CFU) carrying a 35S::*GUS* construct (SEB-GUS) or nontransformed *A. tumefaciens* (control, 5×10^7 CFU) were run on a 10% (*w*/*v*) SDS-PAGE and blotted onto a nitrocellulose membrane. The membranes were then probed with mouse monoclonal anti-SEB antibodies. An arrow indicates the molecular weight (96 kDa) of SEB-GUS.

cavities of ICR mice for intranasal immunization. The anti-SEB-GUS antibodies were measurable by a Western blot assay in mouse serum four weeks after intranasal immunization with leaves containing SEB-GUS (Figure 5(a)). Data from enzyme-linked immunosorbent assay (ELISA) indicated that mice immunized with L-SEB-GUS elicited antibody to SEB (Figure 5(b)). No antibodies against SEB were detected in mice immunized with GUS alone. This result demonstrates that SEB expressed in radish leaves can act as a vaccine to confer immunity against SEB. It has been reported that levels of IFN-γ in bronchoalveolar lavage (BAL) fluids dramatically increase in mice during SEB-induced inflammation [20]. We intranasally inoculated naïve mice with 40 μg of recombinant SEB or the same volume of phosphate-buffered saline (PBS). The challenge of recombinant SEB significantly augmented the production of IFN-γ in BAL fluids (Figure 5(c)). To assess the protective effects of SEB vaccines encapsulated in radish leaves, we next intranasally challenged SEB into mice and measured the change of IFN-γ levels in BAL fluids. In mice that had previously been inoculated with leaves containing only GUS, BAL fluid IFN-γ levels were 2345.49 ± 64.65 pg/ml after being challenged with SEB. However, in mice that had previously been inoculated with leaves containing SEB-GUS, IFN-γ levels in BAL fluid dropped to 586.18 ± 30.69 pg/ml (Figure 5(c)). This result illustrates that SEB vaccine encapsulated in radish leaves confers protection against SEB-induced IFN-γ production.

Recently, a number of studies have demonstrated the capability of agroinfiltration to generate recombinant proteins as antigens [51, 52]. These studies focused on increasing recombinant protein yields for purification [53]. Indeed, the antigenicity of proteins relies not only on the protein amounts but also on the protein structures. However, low amounts of protein can provide sufficiently high immunogenicity [54]. In this study, we used homogenized radish leaves expressing SEB, rather than purified recombinant SEB, for immunization. The production of SEB antibodies in immunized mice (Figure 5(a)) demonstrated that agroinfiltration and *in planta* transient expression of SEB is sufficient for leaf tissue to exhibit SEB immunogenicity. Notably, the use of minimally prepared homogenized leaves containing SEB as vaccines can eliminate sophisticated procedures for antigen purification. In fact, agroinfiltration is adding lipopolysaccharide (LPS) from the *Agrobacterium*, which in itself may be a molecule capable of impacting the immune responses [55]. Further works should focus on performing control data for the LPS responses like using SEB from non-LPS sources as a control and comparing its immune response to that from LPS sources. Furthermore, using Western blot and ELISA assays, antibodies against SEB were detectable in mice immunized with homogenized leaves expressing SEB without the addition of an exogenous CT adjuvant (data not shown). This result supports other evidence indicating that leaves contain natural adjuvants such as phyto-saponins [56]. Unfortunately, these immunized mice are unable to suppress SEB-induced IFN-γ production (data not shown). Conversely, intranasal immunization of mice with SEB-expressing leaves in conjunction with adjuvant CT not only elicited systemic antibodies to SEB but also offered protective immunity against SEB-induced IFN-γ production although it was shown that CT may induce Bell's palsy [57]. Thus, other safe mucosal adjuvants should be analyzed in the future.

GUS has been shown to be an immunogenic protein [58]. In addition, several leaf proteins are antigenic in mice as well [59]. The immunogenicities of GUS and radish proteins in mice immunized with whole leaves containing GUS are undetermined in this study. However, in comparison with immunizations using leaves containing SEB-GUS, mice immunized with leaves containing only GUS elicited high levels of IFN-γ after SEB challenge (Figure 5(b)), suggesting that the background of GUS and leaf proteins present in leaves did not inhibit or confound SEB immunogenicity.

4. Conclusion

The argoinfiltration stamping was exploited as a novel modality to generate monovalent or bivalent vaccines. Argoinfiltrating gene (SEB and TetC) into radish leaves provides a simple approach for transiently expressing and encapsulating antigens in leaf tissue. This approach avoids the issue of transgene introgression and offers means to generate vaccines in a rapid manner. Moreover, the coexpression of antigens could be applied for analyzing multiple immunological responses to provide new means of vaccine manufacture and delivery without the complicated codelivery procedure following mixing of many expressed antigens. Increased awareness about the prospects of global epidemics and bioterrorism has motivated the development of techniques to create inexpensive vaccines on a rapid, massive

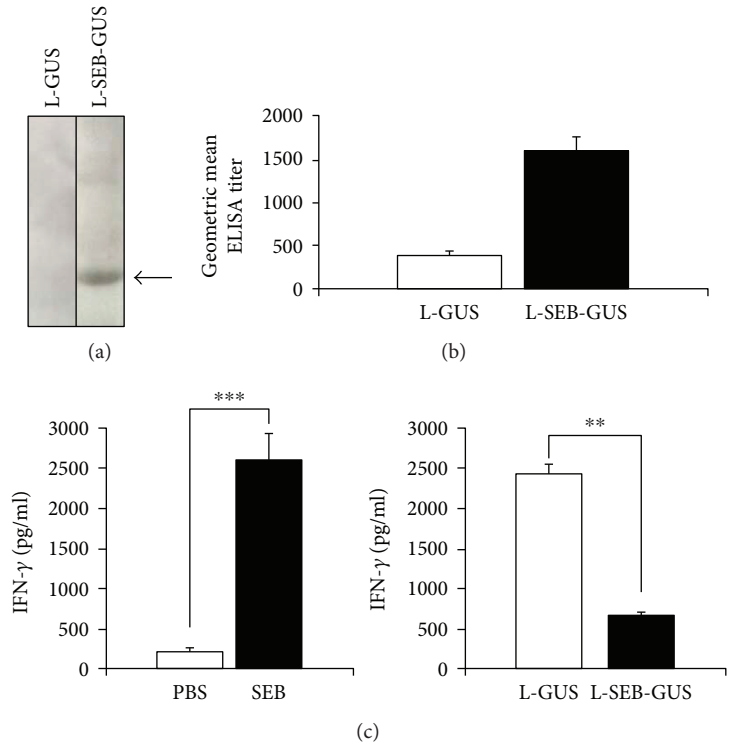

Figure 5: SEB immunogenicity and protective immunity against SEB-induced IFN-γ production. (a) Recombinant SEB (15 μg) run on a 10% (w/v) SDS-PAGE was blotted onto a nitrocellulose membrane and immunoreacted to sera obtained from mice immunized with 25 μl homogenized leaves expressing SEB-GUS (L-SEB-GUS) or GUS (L-GUS) mixed with a CT adjuvant (5 μg/25 μl whole leaves). Recombinant SEB reactive to serum from L-SEB-GUS-immunized mice produces a band (arrow) at approximately 28 kDa, verifying the immunogenicity of SEB. (b) Titers of pooled anti-SEB antibodies from eight immunized mice were qualified by ELISA. The geometric means of ELISA titers were presented. (c) Eight naïve mice were challenged intranasally with 40 μg of recombinant SEB or PBS as a negative control, and the levels of IFN-γ in BAL fluids were measured by ELISA. Mice immunized with L-SEB-GUS or L-GUS were challenged intranasally with 40 μg of recombinant SEB overnight. The levels of collected IFN-γ in BAL fluids of L-SEB-GUS- and L-GUS-immunized mice were compared by an ELISA assay. Experiments were performed in triplicate. Data were analyzed statistically by Student's t-test and presented as mean ± SD ($^{**}p < 0.005$; $^{***}p < 0.0005$ by Student's t-test).

scale if necessary [60]. As shown with SEB, transient expression of antigens in plant tissue offers one such method of rapid production. Intranasal immunization with minimally prepared homogenized leaves containing recombinant antigens eliminates the cost and time requirements of antigen purification and avoids the intrinsic problems associated with needle injections. Also, intranasal immunization of mice with ground leaves expressing SEB elicits detectable antibodies to *S. aurues* SEB. However, it had been reported that vaccination via an intranasal route can cause facial nerve paralysis [61]. Therefore, the safety of intranasal administration is worthy to be investigated since the human respiratory tract is not exposed to plant leaves on a routine basis [7]. In addition, the concept of encapsulating proteins/antigens in the leaves instead of purifying them for immunization may benefit vaccine production in the developing countries where cold chain facilities are lacking and emerge as a commercially viable approach for urgent vaccine development.

Conflicts of Interest

The authors declare no conflict of interest.

Acknowledgments

This work was supported by a grant (1R41AR056169-01) from the National Institutes of Health in US and grants (105-2314-B-008-001 and 105-2320-B-008-001) from the Ministry of Science and Technology (MOST) in Taiwan. The authors thank Mandy Kao for critical reading of the manuscript.

References

[1] D. A. Goldstein and J. A. Thomas, "Biopharmaceuticals derived from genetically modified plants," *Quarterly Journal of Medicine*, vol. 97, no. 11, pp. 705–716, 2004.

[2] R. Fischer, E. Stoger, S. Schillberg, P. Christou, and R. M. Twyman, "Plant-based production of biopharmaceuticals," *Current Opinion Plant Biology*, vol. 7, no. 2, pp. 152–158, 2004.

[3] V. Gomord and L. Faye, "Posttranslational modification of therapeutic proteins in plants," *Current Opinion Plant Biology*, vol. 7, no. 2, pp. 171–181, 2004.

[4] J. Hammond, P. McGarvey, and V. Yusibov, *Plant Biotechnology-New Products and Applications*, Springer-Verlag, Berlin, Heidelberg, 1999.

[5] I. A. Dreesen, G. Charpin-El Hamri, and M. Fussenegger, "Heat-stable oral alga-based vaccine protects mice from *Staphylococcus aureus* infection," *Journal of Biotechnology*, vol. 145, no. 3, pp. 273–280, 2010.

[6] A. A. McCormick, S. Reddy, S. J. Reinl et al., "Plant-produced idiotype vaccines for the treatment of non-Hodgkin's lymphoma: safety and immunogenicity in a phase I clinical study," *Proceedings of the National Academy of Sciences*, vol. 105, no. 29, pp. 10131–10136, 2008.

[7] E. P. Rybicki, "Plant-made vaccines for humans and animals," *Plant Biotechnology Journal*, vol. 8, no. 5, pp. 620–637, 2010.

[8] D. Castle and J. Dalgleish, "Cultivating fertile ground for the introduction of plant-derived vaccines in developing countries," *Vaccine*, vol. 23, no. 15, pp. 1881–1885, 2005.

[9] L. B. Andrews and W. R. Curtis, "Comparison of transient protein expression in tobacco leaves and plant suspension culture," *Biotechnology Progress*, vol. 21, no. 3, pp. 946–952, 2005.

[10] V. Negrouk, G. Eisner, H. I. Lee, K. Han, D. Taylor, and H. C. Wong, "Highly efficient transient expression of functional recombinant antibodies in lettuce," *Plant Science*, vol. 169, no. 2, pp. 433–438, 2005.

[11] Y. Gleba, V. Klimyuk, and S. Marillonnet, "Viral vectors for the expression of proteins in plants," *Current Opinion Biotechnology*, vol. 18, no. 2, pp. 134–141, 2007.

[12] S. Marillonnet, C. Thoeringer, R. Kandzia, V. Klimyuk, and Y. Gleba, "Systemic *Agrobacterium tumefaciens*-mediated transfection of viral replicons for efficient transient expression in plants," *Nature Biotechnology*, vol. 23, no. 6, pp. 718–723, 2005.

[13] S. Abel and A. Theologis, "Transient transformation of *Arabidopsis* leaf protoplasts: a versatile experimental system to study gene expression," *The Plant Journal*, vol. 5, no. 3, pp. 421–427, 1994.

[14] R. Fischer and N. Emans, "Molecular farming of pharmaceutical proteins," *Transgenic Research*, vol. 9, no. 4-5, pp. 279–299, 2000.

[15] N. Bechtold, J. Ellis, and G. Pelletier, "In planta *Agrobacterium*-mediated gene transfer by infiltration of adult *Arabidopsis thaliana* plants," *CR Academy Science Paris Life Science*, vol. 316, pp. 1194–1199, 1993.

[16] S. R. Scofield, C. M. Tobias, and J. P. Rathjen, "Molecular basis of gene-for-gene specificity in bacterial speck disease of tomato," *Science*, vol. 274, no. 5295, pp. 2063–2065, 1996.

[17] M. W. Lee and Y. Yang, "Transient expression assay by agroinfiltration of leaves," *Methods in Molecular Biology*, vol. 323, pp. 225–229, 2006.

[18] F. Niedergang, A. Hemar, C. R. Hewitt, M. J. Owen, A. Dautry-Varsat, and A. Alcover, "The *Staphylococcus aureus* enterotoxin B superantigen induces specific T cell receptor down-regulation by increasing its internalization," *Journal of Biological Chemistry*, vol. 270, no. 21, pp. 12839–12845, 1995.

[19] P. F. Liu, C. W. Lo, C. H. Chen, M. F. Hsieh, and C. M. Huang, "Use of nanoparticles as therapy for methicillin-resistant Staphylococcus aureus infections," *Current Drug Metabolism*, vol. 10, no. 8, pp. 875–884, 2009.

[20] G. Rajagopalan, K. Iijima, M. Singh, H. Kita, R. Patel, and C. S. David, "Intranasal exposure to bacterial superantigens induces airway inflammation in HLA class II transgenic mice," *Infection and Immunology*, vol. 74, no. 2, pp. 1284–1296, 2006.

[21] A. Casadevall, "Passive antibody administration (immediate immunity) as a specific defense against biological weapons," *Emerging Infectious Diseases*, vol. 8, no. 8, pp. 833–841, 2002.

[22] G. H. Lowell, R. W. Kaminski, and S. Grate, "Intranasal and intramuscular proteosome-staphylococcal enterotoxin B (SEB) toxoid vaccines: immunogenicity and efficacy against lethal SEB intoxication in mice," *Infection and Immunology*, vol. 64, no. 5, pp. 1706–1713, 1996.

[23] M. Nagaki, Y. Muto, and H. Ohnishi, "Hepatic injury and lethal shock in galactosamine-sensitized mice induced by the superantigen staphylococcal enterotoxin B," *Gastroenterology*, vol. 106, no. 2, pp. 450–458, 1994.

[24] R. A. Jefferson, "Assaying chimeric genes in plants: the GUS gene fusion system," *Plant Molecular Biology Reporter*, vol. 5, no. 4, pp. 387–405, 1987.

[25] P. F. Liu, T. Nakatsuji, W. Zhu, R. L. Gallo, and C. M. Huang, "Passive immunoprotection targeting a secreted CAMP factor of *Propionibacterium* acnes as a novel immunotherapeutic for acne vulgaris," *Vaccine*, vol. 29, no. 17, pp. 3230–3238, 2011.

[26] J. D. Coffman, J. Zhu, J. M. Roach, S. Bavari, R. G. Ulrich, and S. L. Giardina, "Production and purification of a recombinant Staphylococcal enterotoxin B vaccine candidate expressed in *Escherichia coli*," *Protein Expression and Purification*, vol. 24, no. 2, pp. 302–312, 2002.

[27] P. F. Liu, W. C. Chang, Y. K. Wang, H. Y. Chang, and R. L. Pan, "Signaling pathways mediating the suppression of *Arabidopsis thaliana* Ku gene expression by abscisic acid," *Biochimica et Biophysica Acta (BBA) - Gene Regulatory Mechanisms*, vol. 1779, no. 3, pp. 164–174, 2008.

[28] P. F. Liu, Y. K. Wang, W. C. Chang, H. Y. Chang, and R. L. Pan, "Regulation of *Arabidopsis thaliana Ku* genes at different developmental stages under heat stress," *Biochimica et Biophysica Acta (BBA) - Gene Regulatory Mechanisms*, vol. 1779, no. 6-7, pp. 402–407, 2008.

[29] N. J. Mantis, "Vaccines against the category B toxins: Staphylococcal enterotoxin B, epsilon toxin and ricin," *Advanced Drug Delivery Reviews*, vol. 57, no. 9, pp. 1424–1439, 2005.

[30] P. F. Liu, S. K. Haake, R. L. Gallo, and C. M. Huang, "A novel vaccine targeting *Fusobacterium nucleatum* against abscesses and halitosis," *Vaccine*, vol. 27, no. 10, pp. 1589–1595, 2009.

[31] P. F. Liu, W. Shi, W. Zhu et al., "Vaccination targeting surface FomA of *Fusobacterium nucleatum* against bacterial co-aggregation: implication for treatment of periodontal infection and halitosis," *Vaccine*, vol. 28, no. 19, pp. 3496–3505, 2010.

[32] S. Schillberg, R. M. Twyman, and R. Fischer, "Opportunities for recombinant antigen and antibody expression in transgenic plants—technology assessment," *Vaccine*, vol. 23, no. 15, pp. 1764–1769, 2005.

[33] H. S. Mason, H. Warzecha, T. Mor, and C. J. Arntzen, "Edible plant vaccines: applications for prophylactic and therapeutic molecular medicine," *Trends in Molecular Medicine*, vol. 8, no. 7, pp. 324–329, 2002.

[34] A. Bendahmane, M. Querci, K. Kanyuka, and D. C. Baulcombe, "*Agrobacterium* transient expression system as a tool for the isolation of disease resistance genes: application to the *Rx2* locus in potato," *The Plant Journal*, vol. 21, no. 1, pp. 73–81, 2000.

[35] K. Lindsey, *Transgenic Plant Research*, p. 19, Harwood Academic, Amsterdam, 1998.

[36] A. Papi, M. Orlandi, G. Bartolini et al., "Cytotoxic and antioxidant activity of 4-methylthio-3-butenyl isothiocyanate from

Raphanus sativus L. (Kaiware Daikon) sprouts," *Journal of Agricultural and Food Chemistry*, vol. 56, no. 3, pp. 875–883, 2008.

[37] C. W. Simmons, J. S. VanderGheynst, and S. K. Upadhyaya, "A model of *Agrobacterium tumefaciens* vacuum infiltration into harvested leaf tissue and subsequent in planta transgene transient expression," *Biotechnology and Bioengineering*, vol. 102, no. 3, pp. 965–970, 2009.

[38] R. Greco, M. Michel, and D. Guetard, "Production of recombinant HIV-1/HBV virus-like particles in *Nicotiana tabacum* and *Arabidopsis thaliana* plants for a bivalent plant-based vaccine," *Vaccine*, vol. 25, no. 49, pp. 8228–8240, 2007.

[39] K. Vongpaseuth, E. Nims, M. St Amand, E. L. Walker, and S. C. Roberts, "Development of a particle bombardment-mediated transient transformation system for *Taxus* spp. cells in culture," *Biotechnology Progress*, vol. 23, no. 5, pp. 1180–1185, 2007.

[40] C. Tan, S. Qin, Q. Zhang, P. Jiang, and F. Zhao, "Establishment of a micro-particle bombardment transformation system for *Dunaliella salina*," *Journal of Microbiology*, vol. 43, no. 4, pp. 361–365, 2005.

[41] E. P. Rybicki, "Third international conference on plant-based vaccines and antibodies," *Expert Review of Vaccines*, vol. 8, no. 9, pp. 1151–1155, 2009.

[42] C. Vaquero, M. Sack, and J. Chandler, "Transient expression of a tumor-specific single-chain fragment and a chimeric antibody in tobacco leaves," *Proceedings of the National Academy of Sciences*, vol. 96, no. 20, pp. 11128–11133, 1999.

[43] L. D. Joh, K. A. McDonald, and J. S. VanderGheynst, "Evaluating extraction and storage of a recombinant protein produced in agroinfiltrated lettuce," *Biotechnology Progress*, vol. 22, no. 3, pp. 723–730, 2006.

[44] S. P. Fletcher, M. Muto, and S. P. Mayfield, "Optimization of recombinant protein expression in the chloroplasts of green algae," *Advances in Experimental Medicine and Biology*, vol. 616, pp. 90–98, 2007.

[45] R. Jabeen, M. S. Khan, Y. Zafar, and T. Anjum, "Codon optimization of cry1Ab gene for hyper expression in plant organelles," *Molecular Biology Reports*, vol. 37, no. 2, pp. 1011–1017, 2010.

[46] J. Zhang, Z. Shi, and F. K. Kong, "Topical application of *Escherichia coli*-vectored vaccine as a simple method for eliciting protective immunity," *Infection and Immunology*, vol. 74, no. 6, pp. 3607–3617, 2006.

[47] G. Sunilkumar, L. Mohr, E. Lopata-Finch, C. Emani, and K. S. Rathore, "Developmental and tissue-specific expression of CaMV 35S promoter in cotton as revealed by GFP," *Plant Molecular Biology*, vol. 50, no. 3, pp. 463–479, 2002.

[48] N. S. Yang and P. Christou, "Cell type specific expression of a CaMV 35S-GUS gene in transgenic soybean plants," *Genesis*, vol. 111, pp. 289–293, 1990.

[49] P. Dupree, K. H. Pwee, and J. C. Gray, "Expression of photosynthesis gene-promoter fusions in leaf epidermal cells of transgenic tobacco plants," *The Plant Journal*, vol. 1, no. 1, pp. 115–120, 1991.

[50] G. B. Patel, H. Zhou, A. Ponce, G. Harris, and W. Chen, "Intranasal immunization with an archaeal lipid mucosal vaccine adjuvant and delivery formulation protects against a respiratory pathogen challenge," *PLoS One*, vol. 5, no. 12, article e15574, 2010.

[51] A. Meyers, E. Chakauya, and E. Shephard, "Expression of HIV-1 antigens in plants as potential subunit vaccines," *BMC Biotechnology*, vol. 8, no. 1, p. 53, 2008.

[52] A. K. Hull, C. J. Criscuolo, and V. Mett, "Human-derived, plant-produced monoclonal antibody for the treatment of anthrax," *Vaccine*, vol. 23, no. 17-18, pp. 2082–2086, 2005.

[53] A. Varsani, A. L. Williamson, D. Stewart, and E. P. Rybicki, "Transient expression of human papillomavirus type 16 L1 protein in *Nicotiana benthamiana* using an infectious tobamovirus vector," *Virus Research*, vol. 120, no. 1-2, pp. 91–96, 2006.

[54] H. Wang, M. N. Griffiths, D. R. Burton, and P. Ghazal, "Rapid antibody responses by low-dose, single-step, dendritic cell-targeted immunization," *Proceedings of the National Academy of Sciences*, vol. 97, no. 2, pp. 847–852, 2000.

[55] C. De Castro, A. Molinaro, R. Lanzetta, A. Silipo, and M. Parrilli, "Lipopolysaccharide structures from *Agrobacterium* and *Rhizobiaceae* species," *Carbohydrate Research*, vol. 343, no. 12, pp. 1924–1933, 2008.

[56] B. P. Chapagain and Z. Wiesman, "Phyto-saponins as a natural adjuvant for delivery of agromaterials through plant cuticle membranes," *Journal of Agricultural and Food Chemistry*, vol. 54, no. 17, pp. 6277–6285, 2006.

[57] R. B. Couch, "Nasal vaccination, *Escherichia coli* enterotoxin, and Bell's palsy," *The New England Journal of Medicine*, vol. 350, no. 9, pp. 860-861, 2004.

[58] C. Vogler, B. Levy, and J. H. Grubb, "Overcoming the blood-brain barrier with high-dose enzyme replacement therapy in murine mucopolysaccharidosis VII," *Proceedings of the National Academy of Sciences*, vol. 102, no. 41, pp. 14777–14782, 2005.

[59] S. B. Lehrer, M. McCants, L. Aukrust, and J. E. Salvaggio, "Analysis of tobacco leaf allergens by crossed radioimmunoelectrophoresis," *Clinical & Experimental Allergy*, vol. 15, no. 4, pp. 355–361, 1985.

[60] K. Hefferon and Y. L. Fan, "Expression of a vaccine protein in a plant cell line using a geminivirus-based replicon system," *Vaccine*, vol. 23, no. 3, pp. 404–410, 2004.

[61] P. Sendi, R. Locher, B. Bucheli, and M. Battegay, "Intranasal influenza vaccine in a working population," *Clinical Infectious Diseases*, vol. 38, no. 7, pp. 974–980, 2004.

Hindawi
Journal of Immunology Research
Volume 2017, Article ID 6940546, 9 pages
https://doi.org/10.1155/2017/6940546

Review Article

A Comprehensive Review of US FDA-Approved Immune Checkpoint Inhibitors in Urothelial Carcinoma

Fu-Shun Hsu,[1,2] Chun-Hung Su,[3] and Kou-How Huang[4]

[1]*Department of Urology, New Taipei City Hospital, New Taipei City, Taiwan*
[2]*Graduate Institute of Clinical Medicine, National Taiwan University College of Medicine, No. 7 Chung San South Road, Taipei 10002, Taiwan*
[3]*Genomics Research Center, Academia Sinica, No. 128, Academia Rd., Sec. 2, Taipei 11529, Taiwan*
[4]*Department of Urology, National Taiwan University Hospital, No. 1, Jen-Ai Rd., Sec. 1, Taipei 10051, Taiwan*

Correspondence should be addressed to Kou-How Huang; khhuang123@ntu.edu.tw

Received 17 August 2017; Accepted 31 October 2017; Published 10 December 2017

Academic Editor: Eyad Elkord

Few effective treatment options are available for patients with advanced or metastatic urothelial carcinoma (UC) after unsuccessful first-line platinum-based chemotherapy. To date, immune checkpoint inhibitors are novel therapeutic agents for UC treatment. From May 2016 to May 2017, five anti-PD-1/PD-L1 monoclonal antibodies received accelerated or regular approval from the US Food and Drug Administration (FDA) for the treatment of patients with locally advanced or metastatic UC. The present comprehensive review presents the background information of these five US FDA-approved anticancer agents to provide a basic but concise understanding of these agents for advanced studies. We summarize their immune checkpoint mechanisms, clinical efficacy, recommended usage protocols, adverse events, and the limitations of the PD-L1 biomarker assays.

1. Introduction

Urothelial carcinoma (UC) is one of the top ten leading causes of cancer death worldwide. UC tumorigenesis is thought to be associated with environmental carcinogenic exposure such as cigarette smoking and chemical exposure [1]. The pathological sites of UC include the renal pelvis and ureter in the upper tract as well as bladder and urethra in the lower tract. Among them, the bladder is the most common site of UC occurrence. In the United States, it was estimated that 79,030 new cases and 16,870 deaths were due to bladder UC in 2017 [2].

Bacillus Calmette–Guérin (BCG), an attenuated live strain of *Mycobacterium bovis*, has been used for treatment in patients with nonmuscle invasive bladder UC since the 1990s. The benefits from intravesical BCG instillation have been proven, including lowering the risk of disease recurrence and disease progression [3]. BCG is the standard treatment for patients with nonmuscle invasive bladder UC following transurethral resection of bladder tumors for decades, but underlying mechanism of its antitumor effect remains unclear. BCG induces a local inflammatory response and recruits immune cells to destroy tumor cells and, therefore, plays a vital role in bladder cancer immunotherapy. There are some limitations in BCG treatment, including high failure rate and risk of systemic infection.

Cisplatin-based systemic chemotherapy remains the mainstay of treatment in patients with metastatic UC [4]. There are still 30% to 50% of advanced UC cases that are not responsive to cisplatin-based chemotherapy. Although some new chemotherapy regimens have been developed, the prognosis for patients with metastatic UC remains poor [5]. Other limiting factors associated with standard regimen are the substantial toxicity and patients' physical conditions [6]. Treatment-related deaths occurred in 2% to 4% of patients, especially in the elderly [4, 7]. The median overall survival (OS) of patients with metastatic UC who received first-line platinum-based chemotherapy ranges from 12 to 15 months, and only approximately 5% of these patients have a 5-year survival [8–10]. The systemic salvage therapy for

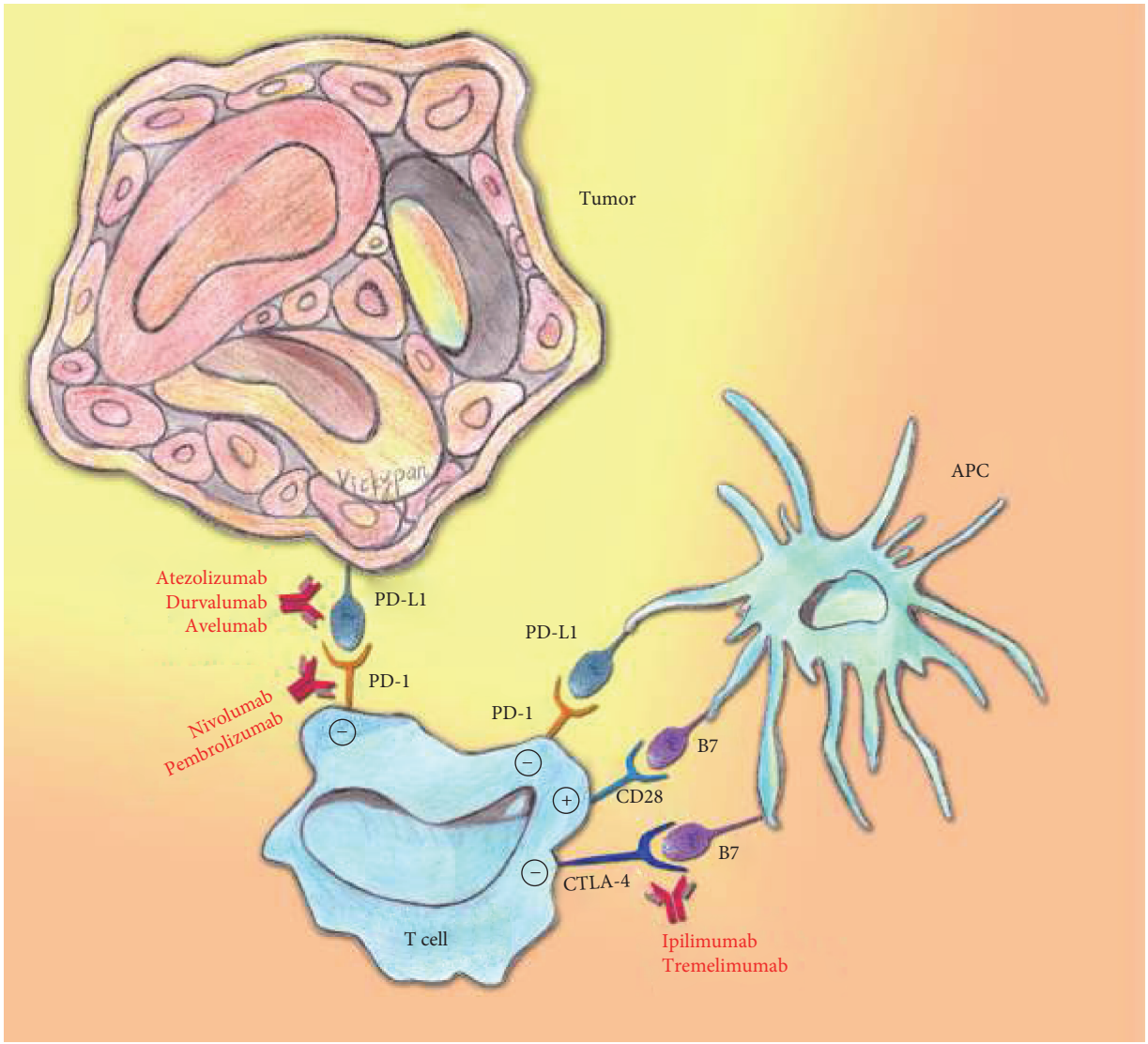

Figure 1: Illustration of anticheckpoint immunotherapy. The immune system is maintained and functions in homeostasis. Once CD28 binds to its ligand, B7, on the surface of antigen-presenting cells (APCs), T cell proliferation is activated to enhance immunity. On the other hand, cytotoxic T lymphocyte antigen-4 (CTLA-4) and programmed death-1 (PD-1) on APCs or tumor cells transmit inhibitory signals, while binding to their ligands, B7 and PD-L1, respectively. In general, the immune cells could recognize tumor cells and then destroy them. However, the tumor cells can escape from the host antitumor activities by suppressing the activation of immune cells. The anticheckpoint antibodies are developed to block the inhibitory pathways and then restore T cell immunity against tumors.

patients with advanced UC lasts only 6 to 8 months [11]. Unlike patients with other cancers, such as non-small-cell lung cancer (NSCLC) [12–14], breast cancer [15, 16], and leukemia [17], who can benefit from many targeted agents, including small molecule inhibitors or anticancer antibodies, patients with UC are still awaiting effective targeted drug treatments. Therefore, there is an urgent need to develop a novel therapy to improve therapeutic efficacy and patient survival or to reduce side effects for patients with locally advanced or metastatic UC.

2. Immune Checkpoint Therapy

The immune system defends the body from an invasion by foreign etiological agents. The presentation of antigens to T cells by antigen-presenting cells (APCs) is a critical process (Figure 1). Several protein molecules involved in the regulation of immune processes and for homeostatic maintenance of the immune system have been identified. CD28 was the first protein to be identified as a coreceptor that transmits stimulatory signals to T cells. After CD28 binds to its ligand, the B7 protein, on the surface of APCs, T cell proliferation is activated to enhance immunity (Figure 1). Cytotoxic T lymphocyte antigen-4 (CTLA-4) and programmed death-1 (PD-1) transmit inhibitory signals when bound to their ligands, B7-1/B7-2 and PD-L1 (B7-H1)/PD-L2 (B7-DC), respectively, on APCs or tumors (Figure 1). Such protein molecules involved in immune regulation are referred to as immune checkpoints. Typically, the immune system is capable of recognizing and destroying tumor cells; however, tumor cells can exploit the

Table 1: Background information on US FDA-approved PD-1/PD-L1 inhibitors for the treatment of urothelial carcinoma.

Target	Generic name	Antibody class	Trade name	Development name(s)	Company	Recommended dose and schedule	Date of approval
PD-1	Nivolumab	Human IgG4	Opdivo	BMS-936558, MDX-1106, ONO-4538	Bristol-Myers Squibb Co.	240 mg, every 2 weeks	2 Feb. 2017
	Pembrolizumab	Humanized IgG4	Keytruda	MK-3475, lambrolizumab	Merck and Co. Inc.	200 mg, every 3 weeks	18 May 2017
PD-L1	Atezolizumab	Human IgG1k	Tecentriq	MPDL3280A, RG7446	Genentech Inc.	1200 mg, every 3 weeks	18 May 2016
	Durvalumab	Humanized IgG1k	Imfinzi	MEDI-4736	AstraZeneca UK Limited	10 mg/kg, every 2 weeks	1 May 2017
	Avelumab	Human IgG1	Bavencio	MSB0010718C, MSB0010682	EMD Serono Inc.	10 mg/kg, every 2 weeks	9 May 2017

All are for the patients with locally advanced or metastatic urothelial carcinoma and who has the prior platinum-based chemotherapy.

inhibitory mechanism and evade the host antitumor activity by suppressing the proliferation of immune cells, subsequently survive, and continue to proliferate.

Immune checkpoint inhibitors were developed to control immune escape tumors. The most widely studied immune checkpoint inhibitors are anti-CTLA-4, anti-PD-1, and anti-PD-L1 monoclonal antibodies [18–20] (Figure 1) which target the T cell regulatory pathways to augment antitumor immune responses [21]. These inhibitors have shown promising efficacy in melanoma [22], renal cell carcinoma [23], NSCLC [24, 25], and bladder UC [26]. As in the case with immunotherapy for other types of cancers, these drugs show limited response rate, but the efficacy in achieving long-lasting benefits for some patients has changed the paradigm of cancer treatment. Due to the milestone discovery of the role of PD-1 [27], PD-L1 [28], and CTLA-4 [29] in inhibiting carcinogenesis, the 2017 Warren Alpert Foundation Prize was awarded to Drs. T. Honjo, L. Chen, James P. Allison, and colleagues to honor their significant contributions in the field of cancer immunotherapy [29]. This review focuses on the FDA-approved PD-1 and PD-L1 inhibitors in urothelial carcinoma.

3. US Food and Drug Administration-Approved Immune Checkpoint Inhibitors in Urothelial Carcinoma

The first checkpoint inhibitor approved for bladder UC was atezolizumab (Tecentriq) in 2016, which was the second-line therapy for patients who had received platinum-based chemotherapy. Response rates were around 15% with median survival of 7.9 months [30–32]. Other approved drugs that followed atezolizumab include durvalumab (Imfinzi) [33–35], nivolumab (Opdivo) [36], and avelumab (Bavencio) [37], and the latest is pembrolizumab (Keytruda) [38, 39]. All these US FDA-approved agents were approved for the treatment of patients with locally advanced or metastatic UC who experienced disease progression during or after platinum-based chemotherapy, or within 12 months of neoadjuvant or adjuvant treatment with platinum-based chemotherapy [30–42]. The clinical efficacy, adverse events, and recommended usage of these drugs are as follows.

3.1. Efficacy. Atezolizumab was the first immune checkpoint inhibitor approved by the US FDA on May 18, 2016, for the treatment of patients who experienced unsuccessful first-line platinum-based chemotherapy (Table 1). Atezolizumab is a human IgG1k antibody against the PD-L1 checkpoint. The US FDA-accelerated approval was obtained by the results of the IMvigor-210 study, a multicenter, single-arm trial of 310 patients with UC [30–32]. The IMvigor-210 study stratified patients with UC by PD-L1 expression levels in the tumor-infiltrating immune cells. Patients with ≥5% of tumor-infiltrating immune cells stained by PD-L1 in the tumor were categorized as a PD-L1-positive group. In this study, a total of 100 (32%) and 210 (68%) patients were categorized into PD-L1 positive and PD-L1 negative, respectively. The trial excluded patients with a history of autoimmune diseases or those who required systemic immunosuppressive medications. All patients received 1200 mg of atezolizumab intravenously every 3 weeks. The efficacy was evaluated by Response Evaluation Criteria in Solid Tumors version 1.1 (RECIST v1.1). The objective response rate (ORR) of all patients was 14.8% (Table 2) [30, 31]. The median duration of response ranged from 2.1 to 13.8 months. The ORR for patients with PD-L1 positive versus those were negative was 26.0% and 9.5%, respectively (Table 2) [30, 31].

Durvalumab is a humanized IgG1k antibody also against the PD-L1 checkpoint (Table 1) [33]. The US FDA granted accelerated approval to durvalumab for the treatment of patients with advanced or metastatic UC on May 1, 2017. The approval was based on a single-arm study of patients with UC who had unsuccessful first-line platinum-based chemotherapy [33, 34]. Recently, the results from the durvalumab trial involving 191 patients with UC have been updated [35]. Durvalumab (10 mg/kg every 2 weeks) was administered to patients intravenously. The efficacy was assessed using RECIST v1.1 criteria. The median duration of response ranged from 0.9 to 19.9 months. The trial also stratified patients with UC by PD-L1 expression levels. The ORR was 17.8% for all patients ($n = 191$) and was 27.6% ($n = 27$)

Table 2: Efficacy outcomes of all tested patients with urothelial carcinoma in US FDA-approved PD-1/PD-L1 inhibitor trials.

Inhibitor target	Treatment regimen	Trial code	NCT identifier	Trial phase	Patient number	ORR (95% CI)	DoR/month (range)	PFS/month (95% CI)	OS/month (95% CI)	Reference
PD-1	Nivolumab	CheckMate-275	NCT02387996	Phase 2	265	19.6% (15.1, 24.9)	10.3	2.0 (1.87, 2.63)	8.74 (6.05, NR)	[36]
	Pembrolizumab	KEYNOTE-045	NCT02256436	Phase 3	542	21% (16.4, 26.5)	—	2.1 (2.0, 2.2)	10.3 (8.0, 11.8)	[38, 39]
		KEYNOTE-052	NCT02335424	Phase 2	370	28.6% (24, 34)	NR (1.4+, 17.8+)	—	—	[40]
PD-L1	Atezolizumab	IMvigor-210	NCT02108652	Phase 2	310	14.8% (11.1, 19.3)	NR (2.1+, 13.8+)	2.1 (2.1, 2.1)	7.90 (6.6, 9.3)	[30, 31]
	Durvalumab	Study 1108	NCT01693562	Phase 1/2	191	17.8 (12.7, 24.0)	NR (0.9+, 19.9+)	1.5 (1.4, 1.9)	18.2 (8.1, NR)	[35]
	Avelumab	JAVELIN	NCT01772004	Phase 1	44	*13.3% (9.1, 18.4) **16.1% (10.8, 22.8)	NR (1.4+, 17.4+)	2.9 (1.53, 4.35)	13.7 (8.5, NE)	[37]

ORR: objective response rate; DoR: median duration of response; PFS: median progression-free survival; OS: median overall survival; HR: hazard ratio; CI: confidence interval; NR: not reached; NE: not estimable; *follow-up at least 13 weeks; **follow-up at least 6 months.

Table 3: Treatment-related adverse events of US FDA-approved PD-1/PD-L1 inhibitors in patients with urothelial carcinoma.

Target	Inhibitor name	Treatment-related adverse events	Immune-related adverse events
PD-1	Nivolumab	Fatigue, decreased appetite, nausea, musculoskeletal pain, diarrhea, rash	Pneumonitis, hepatitis, colitis, endocrinopathies, nephritis, renal dysfunction, encephalitis, rash
	Pembrolizumab	Fatigue, decreased appetite, nausea, musculoskeletal pain, diarrhea, rash, pruritus, constipation	Pneumonitis, hepatitis, colitis, endocrinopathies, nephritis, renal dysfunction
PD-L1	Atezolizumab	Fatigue, decreased appetite, nausea, urinary tract infection, pyrexia, constipation	Pneumonitis, hepatitis, colitis, endocrinopathies (thyroid disease, adrenal insufficiency, hypophysitis, type 1 diabetes), meningitis/encephalitis, pancreatitis, dermatitis/rash
	Durvalumab	Fatigue, decreased appetite, nausea, urinary tract infection, diarrhea, musculoskeletal pain, constipation, peripheral edema	Pneumonitis, hepatitis, colitis, endocrinopathies (thyroid disease, adrenal insufficiency, hypophysitis, type 1 diabetes), nephritis
	Avelumab	Fatigue, decreased appetite, nausea, urinary tract infection, musculoskeletal pain	Pneumonitis, hepatitis, colitis, endocrinopathies, nephritis, renal dysfunction

and 5.1% ($n = 4$) in PD-L1 high expression and low (or negative) expression groups, respectively. The median OS was 18.2 months for all patients and was 20.0 months and 8.1 months in PD-L1 high expression and low (or negative) expression groups, respectively (Table 2) [35].

Avelumab is a human IgG1 antibody against the PD-L1 checkpoint. Avelumab received US FDA-accelerated approval on May 9, 2017, based on the results of the open-label, single-arm, multicenter JAVELIN study (Table 1) [37]. Avelumab was approved for the treatment of patients with UC who had disease progression after first-line platinum-based chemotherapy. In the JAVELIN trial, patients received avelumab (10 mg/kg every 2 weeks) intravenously until disease progression or intolerable toxicity. Before avelumab administration, all patients received antihistamine and acetaminophen. The ORRs at 13-week ($n = 30$) and 6-month ($n = 26$) follow-ups were 13.3% and 16.1%, respectively. The median duration of response ranged from 1.4 to 17.4 months (Table 2) [37].

Nivolumab is a human IgG4 antibody against the PD-1 checkpoint. Based on a single-arm clinical study, CheckMate-275 [36], the US FDA granted accelerated approval to nivolumab on February 2, 2017, for the treatment of UC after unsuccessful first-line platinum-based chemotherapy (Table 1). Nivolumab was also the first immune checkpoint inhibitor approved in the European Union for UC treatment on June 4, 2017. In the CheckMate-275 trial, nivolumab was administered to 270 patients with UC (3 mg/kg every 2 weeks) until disease progression or intolerable toxicity. The ORR following RECIST criteria was 19.6%. Seven patients (2.6%) had complete responses, whereas 46 (17%) had a partial response. The median duration of response was 10.3 months, and the median overall survival (OS) was 8.7 months (Table 2) [36].

Pembrolizumab is a humanized IgG4 antibody against the PD-1 checkpoint. Pembrolizumab is the latest immune checkpoint inhibitor approved by the US FDA on May 18, 2017, for the treatment of patients with UC (Table 1). In addition to the approval of second-line indication, pembrolizumab also received US FDA-accelerated approval for first-line indication for UC treatment. The first- and second-line indications were approved based on KEYNOTE-052 [40] and KEYNOTE-045 [38, 39] trials, respectively. In the KEYNOTE-052 trial, 370 patients with UC who were not eligible for cisplatin-based chemotherapy were enrolled and administered with pembrolizumab (200 mg every 3 weeks). The median follow-up was 7.8 months, and the ORR was 28.6%. The median duration of response ranged from 1.4 to 17.8 months. In the KEYNOTE-045 trial, 542 patients with UC were randomly assigned to receive either pembrolizumab (200 mg every 3 weeks; $n = 270$) or the investigator's choice of a chemotherapy regimen (every 3 weeks, $n = 272$) [38]. This trial produced significant improvements in the median OS and ORRs in both pembrolizumab- and chemotherapy-treated groups. The median OS was 10.3 and 7.4 months in pembrolizumab- and chemotherapy-treated groups, respectively (hazard ratio: 0.73; 95% CI: 0.59–0.91; $p = 0.004$). The ORRs were 21% and 11% for pembrolizumab- and chemotherapy-treated groups, respectively ($p = 0.002$). However, no significant differences were observed in the progression-free survival between the two regimen groups (Table 2) [38, 39].

3.2. Adverse Events. Table 3 presents the adverse events of the five US FDA-approved PD-1/PD-L1 inhibitors for patients with UC [30–38, 40, 43–47]. The most common treatment-related adverse events observed in about 15–20% of treated patients include fatigue, decreased appetite, nausea, and musculoskeletal pain. Urinary tract infection was reported in patients treated with the three PD-L1 inhibitors. Constipation was observed in the atezolizumab-, durvalumab-, and pembrolizumab-treated groups. In addition, pyrexia and peripheral edema were reported in the atezolizumab- and durvalumab-treated groups, respectively. Furthermore, the pembrolizumab-treated group had pruritus and rash. Diarrhea is commonly seen in PD-L1- and durvalumab-treated patients.

In addition, immune-targeted agents that can cause dysimmune toxicities in any tissue but mainly affect the lung, liver, gut, endocrine glands, and skin caused immune-related adverse events (IRAEs) [48]. Although severe IRAEs are rare, once occurred, they can be life-threatening if

Table 4: Selected new or ongoing clinical trials of PD-1/PD-L1 inhibitors for the treatment of urothelial carcinoma.

NCT identifier	Interventions	Recruitment	Phases	Locations
NCT03113266	Anti-PD-1 monoclonal antibody	Recruiting	Phase 2	China
NCT03287050	Pembrolizumab/radiation	Not yet recruiting	Early phase 1	United States
NCT03240016	Pembrolizumab/abraxane	Not yet recruiting	Phase 2	United States
NCT02807636	Atezolizumab/carboplatin/gemcitabine/cisplatin/placebo	Recruiting	Phase 3	Globe
NCT02853305	Pembrolizumab/cisplatin/carboplatin/gemcitabine	Recruiting	Phase 3	Globe
NCT03219775	Nivolumab/ipilimumab	Recruiting	Phase 2	Germany
NCT02500121	Pembrolizumab/placebo	Recruiting	Phase 2	United States
NCT02450331	Atezolizumab	Recruiting	Phase 3	Globe
NCT03115801	Atezolizumab/radiation	Recruiting	Phase 2	United States
NCT03244384	Pembrolizumab/clinical observation/biomarker analysis	Recruiting	Phase 3	United States
NCT02451423	Atezolizumab dose level 1/dose level 2/dose level 3	Recruiting	Phase 2	United States
NCT02897765	NEO-PV-01/nivolumab/adjuvant	Recruiting	Phase 1	United States
NCT02845323	Nivolumab + urelumab/nivolumab monotherapy	Recruiting	Phase 2	United States
NCT02736266	Pembrolizumab	Recruiting	Phase 2	Italy
NCT03237780	Atezolizumab/eribulin mesylate/biomarker analysis	Not yet recruiting	Phase 2	United States

managed inappropriately [49]. Table 3 lists the common IRAEs of checkpoint inhibitor-treated patients. All five checkpoint inhibitor-treated groups might have pneumonitis, hepatitis, colitis, and endocrinopathies (e.g., thyroid disease, adrenal insufficiency, hypophysitis, and type 1 diabetes). Nephritis and renal dysfunction were commonly observed in all drug-treated groups except the atezolizumab-treated group. Meningitis/encephalitis and dermatitis/rash were observed in the atezolizumab- and nivolumab-treated groups. Pancreatitis may also in the atezolizumab-treated group. Other details of the IRAEs caused by checkpoint inhibitors are described elsewhere [6, 43–47].

3.3. Recommended Usage. Table 1 presents the recommended usage of the US FDA-approved immune checkpoint inhibitors for UC treatment. These antibodies are administered intravenously. The recommended doses and schedules for atezolizumab, nivolumab, durvalumab, avelumab, and pembrolizumab are 1200 mg every 3 weeks, 240 mg every 2 weeks, 10 mg/kg every 2 weeks, 10 mg/kg over a 60-minute influx every 2 weeks, and 200 mg over a 30-minute influx every 3 weeks, respectively, until disease progression or intolerable toxicity [30–40].

4. Discussion

Although upper tract urothelial carcinoma (UTUC) was identified with molecular profiling approaches that were different from those for bladder UC [50], the immune checkpoint inhibitors performed with promising efficacy in both UTUC and bladder UC [51]. However, many concerns remain. For example, the exact mechanism underlying the dominant role of PD-L1 expression in the efficacy of anti-PD-1/PD-L1 antibodies remains unclear. Furthermore, the influence of patients' genetic backgrounds, particularly racial differences, warrants further investigation.

According to our review of the relevant literature, previous studies did not provide the nucleotide sequence or protein compositions of PD-1/PD-L1 immune checkpoints in patients with UC. The relationships between the antigen-binding sites (paratopes) on the therapeutic monoclonal antibody inhibitors and the antibody-binding sites (epitopes) on the checkpoint proteins remain unclear. Nonetheless, UC has been identified as the tumor with high and heterogeneous mutation burden [52]. The genetic characteristics affect the efficacy of anticancer agents. The observation on tyrosine kinase inhibitor (TKI) treatments for NSCLC demonstrated a paradigm shift on the associations between mutation type and drug efficacy; moreover, even a single site mutation could have a substantial influence on drug sensitivity or resistance [53]. There is an urgent need to identify a biomarker as a clinical outcome predictor for patients with UC who can benefit from the anti-PD-1/PD-L1 immunotherapy.

Currently, PD-L1 is regarded as a biomarker in PD-1/PD-L1 inhibitor trials [20, 54–56] trials although the exact role of PD-L1 expression in the therapeutic efficacy of PD-1/PD-L1 inhibitors remains controversial [57]. For clinical practice, PD-L1 expression level of patients with metastatic melanoma or NSCLC is typically examined to determine whether the patients are suitable for treatment of anti-PD-1/PD-L1 immunotherapy [58]. For patients with UC, VENTANA PD-L1 SP142 and SP263 assays were used to classify them into PD-L1-positive or PD-L1-negative cohorts in atezolizumab and durvalumab trials, respectively [30, 31, 33, 35]. Those trials indicated patients with higher PD-L1 expression exhibiting improved efficacy compared to those with lower PD-L1 expression. However, of the variations in techniques, platforms, diverse specimens, tumor and immune microenvironment and the positive cutoff of PD-L1 expression complicate the standardization of decision-making in clinical applications [57]. Therefore, the classification of PD-L1-positive and PD-L1-negative groups for cancer patients is usually defined dynamically based on different assays or

cutoffs. Currently, we suggest using PD-L1 expression level for outcome assessments but not for patient selections. Hence, the optimization of biomarker assays to identify the ideal population for anti-PD-1/PD-L1 immunotherapy is crucial for clinical practice [57, 58]. Alternatively, stratifying patients with UC based on the epitope sequences of their checkpoints and then applying the subtypes of the epitopes to develop the corresponding anti-PD-1/PD-L1 antibodies may contribute to the optimization of personalized and precision medicine.

Additionally, these PD-1/PD-L1 inhibitors may exert synergistic effects with other anticancer agents to prolong patients' survival or reduce side effects. Table 4 shows selected new or ongoing clinical studies of PD-1/PD-L1 inhibitors for the treatment of UC. Those interventions are monotherapy of PD-1/PD-L1 inhibitors or combination therapy with anti-CTLA-4 antibodies, chemotherapy agents, or radiotherapy. Some studies are designed to discover the relationships between biomarker and the efficacy of PD-1/PD-L1 inhibitors as well as the effect of difference dosage levels. Their results may provide new clues or strategies in winning the fight against UC in the future.

In this compact but comprehensive review, we summarized the background information of the five US FDA approved PD-1 and PD-L1 checkpoint inhibitors as well as elucidate their mechanism of actions (MOA). We outlined their drug efficacy, safety, and adverse events from the clinical trials of patients with UC. These therapeutic antibodies have shown promising results in their respective FDA-approved trials and have given new hope to those who are suffering from advanced or metastatic UC. Further large-scale clinical trials of checkpoint inhibitor will reveal the optimal administration of these drugs and allow more patients with UC to benefit from immunotherapy treatments.

Conflicts of Interest

The authors declare that they have no financial or commercial conflicts of interest related to the subject matter or materials discussed in the manuscript.

Acknowledgments

This review article was partially supported by Taiwan Maple Urological Association. The authors thank Chun-I Pan for the illustration of the figure. This article has been proofread by An-Chi Chen (Tamkang University, Taiwan).

References

[1] O. Sanli, J. Dobruch, M. A. Knowles et al., "Bladder cancer," *Nature Reviews Disease Primers*, vol. 3, article 17022, 2017.

[2] R. L. Siegel, K. D. Miller, and A. Jemal, "Cancer statistics, 2017," *CA: a Cancer Journal for Clinicians*, vol. 67, no. 1, pp. 7–30, 2017.

[3] J. C. Park and N. M. Hahn, "Emerging role of immunotherapy in urothelial carcinoma-future directions and novel therapies," *Urologic Oncology*, vol. 34, no. 12, pp. 566–576, 2016.

[4] S. A. Hussain and N. D. James, "The systemic treatment of advanced and metastatic bladder cancer," *Lancet Oncology*, vol. 4, no. 8, pp. 489–497, 2003.

[5] J. J. Kim, "Recent advances in treatment of advanced urothelial carcinoma," *Current Urology Reports*, vol. 13, no. 2, pp. 147–152, 2012.

[6] D. P. Petrylak, "Immunotherapy: the wave of the future in bladder cancer?," *Clinical Genitourinary Cancer*, vol. 15, no. 3, pp. S3–S17, 2017.

[7] B. J. Roth and D. F. Bajorin, "Advanced bladder cancer: the need to identify new agents in the post-M-VAC (methotrexate, vinblastine, doxorubicin and cisplatin) world," *The Journal of Urology*, vol. 153, no. 3, pp. 894–900, 1995.

[8] J. D. Ramos and E. Y. Yu, "Making urothelial carcinomas less immune to immunotherapy," *Urologic Oncology*, vol. 34, no. 12, pp. 534–537, 2016.

[9] J. García-Donas, A. Font, B. Pérez-Valderrama et al., "Maintenance therapy with vinflunine plus best supportive care versus best supportive care alone in patients with advanced urothelial carcinoma with a response after first-line chemotherapy (MAJA; SOGUG 2011/02): a multicentre, randomised, controlled, open-label, phase 2 trial," *Lancet Oncology*, vol. 18, no. 5, pp. 672–681, 2017.

[10] S. Gupta, D. Gill, A. Poole, and N. Agarwal, "Systemic immunotherapy for urothelial cancer: current trends and future directions," *Cancers*, vol. 9, no. 2, article E15, 2017.

[11] G. Sonpavde, B. S. Jones, J. Bellmunt, T. K. Choueiri, and C. N. Sternberg, "Future directions and targeted therapies in bladder cancer," *Hematology/Oncology Clinics of North America*, vol. 29, no. 2, pp. 361–376, 2015.

[12] S. Wang, Y. Song, and D. Liu, "EAI045: the fourth-generation EGFR inhibitor overcoming T790M and C797S resistance," *Cancer Letters*, vol. 385, pp. 51–54, 2017.

[13] M. Friese-Hamim, F. Bladt, G. Locatelli, U. Stammberger, and A. Blaukat, "The selective c-Met inhibitor tepotinib can overcome epidermal growth factor receptor inhibitor resistance mediated by aberrant c-Met activation in NSCLC models," *American Journal of Cancer Research*, vol. 7, no. 4, pp. 962–972, 2017.

[14] T. Kurata, A. Nakaya, T. Yokoi et al., "Phase I/II study of erlotinib, carboplatin, pemetrexed, and bevacizumab in chemotherapy-naïve patients with advanced non-squamous non-small cell lung cancer harboring epidermal growth factor receptor mutation," *Genes and Cancer*, vol. 8, no. 5-6, pp. 559–565, 2017.

[15] H. R. Kourie, E. El Rassy, F. Clatot, E. de Azambuja, and M. Lambertini, "Emerging treatments for HER2-positive early-stage breast cancer: focus on neratinib," *OncoTargets and Therapy*, vol. 10, pp. 3363–3372, 2017.

[16] C. Chung and M. S. Lam, "Pertuzumab for the treatment of human epidermal growth factor receptor type 2-positive metastatic breast cancer," *American Journal of Health-System Pharmacy*, vol. 70, no. 18, pp. 1579–1587, 2013.

[17] M. Miura, "Therapeutic drug monitoring of imatinib, nilotinib, and dasatinib for patients with chronic myeloid leukemia," *Biological & Pharmaceutical Bulletin*, vol. 38, no. 5, pp. 645–654, 2015.

[18] E. I. Buchbinder and A. Desai, "CTLA-4 and PD-1 pathways: similarities, differences, and implications of their inhibition," *American Journal of Clinical Oncology*, vol. 39, no. 1, pp. 98–106, 2016.

[19] J. Wang, R. Yuan, W. Song, J. Sun, D. Liu, and Z. Li, "PD-1, PD-L1 (B7-H1) and tumor-site immune modulation therapy: the historical perspective," *Journal of Hematology & Oncology*, vol. 10, no. 1, p. 34, 2017.

[20] W. Ma, B. M. Gilligan, J. Yuan, and T. Li, "Current status and perspectives in translational biomarker research for PD-1/PD-L1 immune checkpoint blockade therapy," *Journal of Hematology & Oncology*, vol. 9, no. 1, p. 47, 2016.

[21] P. Sharma and J. P. Allison, "The future of immune checkpoint therapy," *Science*, vol. 348, no. 6230, pp. 56–61, 2015.

[22] M. Sanlorenzo, I. Vujic, C. Posch et al., "Melanoma immunotherapy," *Cancer Biology & Therapy*, vol. 15, no. 6, pp. 665–674, 2014.

[23] M. C. Ornstein and B. I. Rini, "The safety and efficacy of nivolumab for the treatment of advanced renal cell carcinoma," *Expert Review of Anticancer Therapy*, vol. 16, no. 6, pp. 577–584, 2016.

[24] S. L. Topalian, F. S. Hodi, J. R. Brahmer et al., "Safety, activity, and immune correlates of anti-PD-1 antibody in cancer," *New England Journal of Medicine*, vol. 366, no. 26, pp. 2443–2454, 2012.

[25] J. R. Brahmer, S. S. Tykodi, L. Q. Chow et al., "Safety and activity of anti-PD-L1 antibody in patients with advanced cancer," *New England Journal of Medicine*, vol. 366, no. 26, pp. 2455–2465, 2012.

[26] T. Powles, J. P. Eder, G. D. Fine et al., "MPDL3280A (anti-PD-L1) treatment leads to clinical activity in metastatic bladder cancer," *Nature*, vol. 515, no. 7528, pp. 558–562, 2014.

[27] Y. Ishida, Y. Agata, K. Shibahara, and J. Honjo, "Induced expression of PD-1, a novel member of the immunoglobulin gene superfamily, upon programmed cell death," *The EMBO Journal*, vol. 11, no. 11, pp. 3887–3895, 1992.

[28] H. Dong, G. Zhu, K. Tamada, and L. Chen, "B7-H1, a third member of the B7 family, co-stimulates T-cell proliferation and interleukin-10 secretion," *Nature Medicine*, vol. 5, no. 12, pp. 1365–1369, 1999.

[29] "2017 Warren Alpert Foundation Prize Recipients Announced," https://warrenalpert.org/news/2017-warren-alpert-foundation-prize-recipients-announced.

[30] J. E. Rosenberg, J. Hoffman-Censits, T. Powles et al., "Atezolizumab in patients with locally advanced and metastatic urothelial carcinoma who have progressed following treatment with platinum-based chemotherapy: a single-arm, multicentre, phase 2 trial," *Lancet*, vol. 387, no. 10031, pp. 1909–1920, 2016.

[31] Y. M. Ning, D. Suzman, V. E. Maher et al., "FDA approval summary: atezolizumab for the treatment of patients with progressive advanced urothelial carcinoma after platinum-containing chemotherapy," *The Oncologist*, vol. 22, no. 6, pp. 743–749, 2017.

[32] A. Markham, "Atezolizumab: first global approval," *Drugs*, vol. 76, no. 12, pp. 1227–1232, 2016.

[33] C. Massard, M. S. Gordon, S. Sharma et al., "Safety and efficacy of durvalumab (MEDI4736), an anti-programmed cell death ligand-1 immune checkpoint inhibitor, in patients with advanced urothelial bladder cancer," *Journal of Clinical Oncology*, vol. 34, no. 26, pp. 3119–3125, 2016.

[34] V. Brower, "Anti-PD-L1 inhibitor durvalumab in bladder cancer," *Lancet Oncology*, vol. 17, no. 7, article e275, 2016.

[35] T. Powles, P. H. O'Donnell, C. Massard et al., "Efficacy and safety of durvalumab in locally advanced or metastatic urothelial carcinoma: updated results from a phase 1/2 open-label study," *JAMA Oncology*, vol. 3, no. 9, article e172411, 2017.

[36] P. Sharma, M. Retz, A. Siefker-Radtke et al., "Nivolumab in metastatic urothelial carcinoma after platinum therapy (CheckMate 275): a multicentre, single-arm, phase 2 trial," *Lancet Oncology*, vol. 18, no. 3, pp. 312–322, 2017.

[37] C. R. Heery, G. O'Sullivan-Coyne, R. A. Madan et al., "Avelumab for metastatic or locally advanced previously treated solid tumours (JAVELIN solid tumor): a phase 1a, multicohort, dose-escalation trial," *Lancet Oncology*, vol. 18, no. 5, pp. 587–598, 2017.

[38] J. Bellmunt, R. de Wit, D. J. Vaughn et al., "Pembrolizumab as second-line therapy for advanced urothelial carcinoma," *New England Journal of Medicine*, vol. 376, no. 11, pp. 1015–1026, 2017.

[39] J. M. Lavoie, S. Bidnur, P. C. Black, and B. J. Eigl, "Expanding immunotherapy options for bladder cancer," *Urology*, vol. 106, no. 9, pp. 1-2, 2017.

[40] A. Balar, J. Bellmunt, P. H. O'Donnell et al., "Pembrolizumab (pembro) as first-line therapy for advanced/unresectable or metastatic urothelial cancer: preliminary results from the phase 2 KEYNOTE-052 study," *Annals of Oncology*, vol. 27, Supplement_6, 2016.

[41] C. Zichi, M. Tucci, G. Leone et al., "Immunotherapy for patients with advanced urothelial cancer: current evidence and future perspectives," *BioMed Research International*, vol. 2017, p. 5618174, 2017.

[42] M. S. Farina, K. T. Lundgren, and J. Bellmunt, "Immunotherapy in urothelial cancer: recent results and future perspectives," *Drugs*, vol. 77, no. 10, pp. 1077–1089, 2017.

[43] "FDA Highlights of Prescribing Information: Atezolizumab," https://www.accessdata.fda.gov/drugsatfda_docs/label/2016/761034s000lbl.pdf.

[44] "FDA Highlights of Prescribing Information: Durvalumab," https://www.accessdata.fda.gov/drugsatfda_docs/label/2017/761069s000lbl.pdf.

[45] "FDA Highlights of Prescribing Information: Avelumab," https://www.accessdata.fda.gov/drugsatfda_docs/label/2017/761078s000lbl.pdf.

[46] "FDA Highlights of Prescribing Information: Nivolumab," https://www.accessdata.fda.gov/drugsatfda_docs/label/2017/125554s024lbl.pdf.

[47] "FDA Highlights of Prescribing Information: Pembrolizumab," https://www.accessdata.fda.gov/drugsatfda_docs/label/2017/125514s017s018lbl.pdf.

[48] J. M. Michot, C. Bigenwald, S. Champiat et al., "Immune-related adverse events with immune checkpoint blockade: a comprehensive review," *European Journal of Cancer*, vol. 54, pp. 139–148, 2016.

[49] S. Champiat, O. Lambotte, E. Barreau et al., "Management of immune checkpoint blockade dysimmune toxicities: a collaborative position paper," *Annals of Oncology*, vol. 27, no. 4, pp. 559–574, 2016.

[50] R. Mathieu and S. F. Shariat, "Building bridges in urothelial carcinoma to face common challenges," *Translational Andrology and Urology*, vol. 5, no. 5, pp. 745–748, 2016.

[51] J. B. Aragon-Ching, "Challenges and advances in the diagnosis, biology, and treatment of urothelial upper tract and bladder carcinomas," *Urologic Oncology*, vol. 35, no. 7, pp. 462–464, 2017.

[52] S. A. Mullane and J. Bellmunt, "Cancer immunotherapy: new applications in urologic oncology," *Current Opinions in Urology*, vol. 26, no. 6, pp. 556–563, 2016.

[53] S. Wang, S. Cang, and D. Liu, "Third-generation inhibitors targeting EGFR T790M mutation in advanced non-small cell lung cancer," *Journal of Hematology & Oncology*, vol. 9, no. 1, p. 34, 2016.

[54] A. I. Daud, K. Loo, M. L. Pauli et al., "Tumor immune profiling predicts response to anti-PD-1 therapy in human melanoma," *The Journal of Clinical Investigation*, vol. 126, no. 9, pp. 3447–3452, 2016.

[55] M. Callea, L. Albiges, M. Gupta et al., "Differential expression of PD-L1 between primary and metastatic sites in clear-cell renal cell carcinoma," *Cancer Immunology Research*, vol. 3, no. 10, pp. 1158–1164, 2015.

[56] C. Y. Yang, M. W. Lin, Y. L. Chang, C. T. Wu, and P. C. Yang, "Programmed cell death-ligand 1 expression in surgically resected stage I pulmonary adenocarcinoma and its correlation with driver mutations and clinical outcomes," *European Journal of Cancer*, vol. 50, no. 7, pp. 1361–1369, 2014.

[57] D. Liu, S. Wang, and W. Bindeman, "Clinical applications of PD-L1 bioassays for cancer immunotherapy," *Journal of Hematology & Oncology*, vol. 10, no. 1, p. 110, 2017.

[58] L. P. Diggs and E. C. Hsueh, "Utility of PD-L1 immunohistochemistry assays for predicting PD-1/PD-L1 inhibitor response," *Biomarker Research*, vol. 5, no. 1, p. 12, 2017.

Hindawi
Journal of Immunology Research
Volume 2017, Article ID 7983217, 12 pages
https://doi.org/10.1155/2017/7983217

Research Article

Targeting of Immune Cells by Dual TLR2/7 Ligands Suppresses Features of Allergic Th2 Immune Responses in Mice

Jonathan Laiño,[1] Andrea Wangorsch,[1] Frank Blanco,[1] Sonja Wolfheimer,[1] Maren Krause,[1] Adam Flaczyk,[1] Tobias-Maximilian Möller,[1] Mindy Tsai,[2] Stephen Galli,[2,3] Stefan Vieths,[1] Masako Toda,[1] Stephan Scheurer,[1] and Stefan Schülke[1]

[1]*Vice President's Research Group 1: Molecular Allergology, Paul-Ehrlich-Institut, Langen, Germany*
[2]*Department of Pathology and The Sean N. Parker Center for Allergy and Asthma Research, Stanford University School of Medicine, Stanford, CA, USA*
[3]*Department of Microbiology and Immunology, Stanford University School of Medicine, Stanford, CA, USA*

Correspondence should be addressed to Stefan Schülke; stefan.schuelke@pei.de

Received 17 May 2017; Revised 16 August 2017; Accepted 5 September 2017; Published 24 October 2017

Academic Editor: Carol Leung

Background. TLR ligands can promote Th1-biased immune responses, mimicking potent stimuli of viruses and bacteria. *Aim*. To investigate the adjuvant properties of dual TLR2/7 ligands compared to those of the mixture of both single ligands. *Methods*. Dual TLR2/7 ligands: CL401, CL413, and CL531, including CL264 (TLR7-ligand) and Pam_2CysK_4 (TLR2-ligand), were used. Immune-modulatory capacity of the dual ligands with the individual ligands alone or as a mixture in mouse BMmDCs, BMmDC:TC cocultures, or BMCMCs was compared and assessed in naïve mice and in a mouse model of OVA-induced intestinal allergy. *Results*. CL413 and CL531 induced BMmDC-derived IL-10 secretion, suppressed rOVA-induced IL-5 secretion from OVA-specific DO11.10 $CD4^+$ TCs, and induced proinflammatory cytokine secretion *in vivo*. In contrast, CL401 induced considerably less IL-10 secretion and led to IL-17A production in BMmDC:TC cocultures, but not BMCMC IL-6 secretion, or IL-6 or TNF-α production *in vivo*. No immune-modulating effects were observed with single ligands. All dual TLR2/7 ligands suppressed DNP-induced IgE-and-Ag-specific mast cell degranulation. Compared to vaccination with OVA, vaccination with the mixture CL531 and OVA, significantly suppressed OVA-specific IgE production in the intestinal allergy model. *Conclusions*. Based on beneficial immune-modulating properties, CL413 and CL531 may have utility as potential adjuvants for allergy treatment.

1. Introduction

Th1-promoting adjuvants are promising candidates to improve the efficacy of allergy treatments. Studies have shown that exposure to bacterial or viral infections during early childhood may reduce the risk for the development of allergies later in life "hygiene hypothesis" [1]. Therefore, virus- or bacteria-derived PAMPs (pathogen-associated molecular patterns) which are able to shift an allergy-causing Th2 immune response towards a more tolerant Th1/Tr1-dominated phenotype are being investigated as vaccine components for improved allergy treatment.

In this context, TLR7 ligands are especially promising since they induce robust Th1-biased immune responses [2]. Cream containing the TLR7 ligand Imiquimod was shown to have a low irritating potential upon skin application and is undergoing extensive clinical testing as an adjuvant for topical treatment of human papillomavirus- (HPV-) induced warts, actinic keratosis, basal cell carcinoma, lentigo maligna, and molluscum contagiosum [2–4]. In the setting of basal cell carcinoma, Imiquimod induced both cytotoxic T cell responses and a pronounced proinflammatory cytokine secretion (TNF-α, IFN-α, IL-6, and IL-12) [5]. Coapplication of Imiquimod also was found to enhance antitumor responses in various mouse models [2]. However, Imiquimod treatment can result in toxic and inflammatory systemic symptoms such as fatigue, fever, malaise, pain, headache, nausea, diarrhea, and influenza-like symptoms [6]. Furthermore, studies

have indicated a limited bioavailability of TLR7 ligands due to the rapid extracellular and intracellular degradation of purified TLR7 ligands by RNAses [7]. Therefore, intracellular TLR7 activation by purified TLR7 ligands in the target cell compartment is restricted. To circumvent this toxicity and reduced bioavailability, new approaches need to be developed that improve the efficacy of TLR7 ligand-based adjuvants that include improving their stability and their delivery inside the cell of interest.

In contrast to this, bacterial lipopeptides such as the TLR2/6 ligand Pam_2CysK_4 have been shown to be stable and potent adjuvants that induce tolerogenic DC and regulatory T cell responses [8, 9]. Moreover, they can induce a Th1-promoting cytokine milieu and enhance Ag presentation of endogenous peptides [10, 11]. Chemical conjugation of the TLR2 ligand Pam_3CysK_4 to OVA-derived $CD8^+$ TC peptide sequences resulted in a rapid and enhanced uptake in DCs [12]. Additionally, TLR2 stimulation of mouse Th1 cells induced IFN-γ production, cell proliferation, and cell survival without additional TCR stimulation [13], while IL-5, IL-13, and IFN-γ responses in cells derived from human house dust mite-allergic patients were inhibited by Pam_3CysK_4 [14]. These properties suggest that TLR2/6 ligands may have utility in the treatment of allergies.

In an attempt to improve the bioavailability and to leverage the Th1-inducing potential of TLR2 and TLR7 ligands, we investigated three different, commercially available, synthetic dual TLR2/7 ligands: CL401, CL413, and CL531. These dual TLR2/7 ligands contain CL264, a TLR7-activating 9-benzyl-8-hydroxyadenine which is conjugated to different positions of the TLR2/6 ligand Pam_2CysK_4: CL401 combines CL264 directly with Pam_2Cys, whereas for CL413, and CL531, CL264 is conjugated to the terminal acid function or to the lateral chain of the second lysine of Pam_2CysK_4, respectively (Repository Figure 1 available online at https://doi.org/10.1155/2017/7983217) [15].

In a mouse B16 melanoma model, intratumoral administration of CL401 and CL413 into established tumors resulted in reduced tumor growth and enhanced survival [15]. Moreover, after the initial submission of the present manuscript, Gutjahr and coworkers recently published that coapplication of a similar dual TLR2/7 ligand PamadiFectin (CL307) and HIV-1 antigen p24-coated nanoparticles can efficiently boost HIV-specific antibody responses while also inducing a balanced Th1/Th2 profile in mice [16]. We hypothesized that chemical conjugation of different TLR ligands could be used to create dual TLR2/7 ligands which can promote TLR-mediated Th1-biased immune responses. This new class of adjuvants may be able to mimic the potent immune stimuli of viruses and bacteria and may facilitate penetration of the TLR7 ligand into the cell by TLR2-mediated uptake and trafficking. However, there is currently very little data concerning the immune-activating properties of these novel adjuvants.

Here, we evaluated three different dual TLR2/7 ligands and compared their immune-modulating capacity to equimolar amounts of the two-component ligands, either tested alone or provided as a mixture. We analyzed their effects on mouse bone marrow-derived myeloid dendritic cells (BMmDCs), BMmDC:TC cocultures, and bone marrow-cultured mast cells (BMCMCs). Moreover, we also investigated their immune-activating potential in naïve mice as well as the immune-modulating effect of CL531 upon prophylactic vaccination in combination with OVA in a mouse model of OVA-induced intestinal allergy.

2. Materials and Methods

2.1. Mice. BALB/c, OVA-TCR transgenic DO11.10 (BALB/c background), and C57BL/6 mice (Jackson Laboratories, Bar Harbor, Maine, USA) were bred under specific pathogen-free conditions at the animal facilities of the Paul-Ehrlich-Institut and Stanford University Medical School, respectively.

2.2. Antigens and TLR Ligands. Recombinant ovalbumin (OVA) was produced according to Schülke et al. [17]. CL264, CL401, CL413, CL531 (all with an endotoxin level < 0.001 EU/μg), and Pam_2CysK_4 (absence of endotoxins controlled by HEK-Blue™ TLR4 cells by the manufacturer) were purchased from InvivoGen (Toulouse, France).

2.3. Epithelial Cell Activation. Mouse lung epithelial cells (LA-4, ATTC® CCL-196) were cultured in DMEM (Lonza, Basel, Switzerland) containing L-glutamine (1 mM), penicillin (100 U/mL), streptomycin (100 μg/mL), and 15% fetal calf serum (FCS, Sigma-Aldrich, Steinheim, Germany). For stimulation assays, cells were harvested, taken up in medium containing 2% FCS, and 6.5×10^5 cells were cultivated in 24-well plates (Thermo Fisher Scientific, Langenselbold, Germany) at 37°C in a humidified atmosphere of 5% CO_2 overnight. Nonadherent cells were removed by replacing the medium, and cells were stimulated with equimolar amounts of Pam_2CysK_4, CL264, Pam_2CysK_4 plus CL264, CL401, CL413, or CL531 in a total volume of 0.5 mL for 24 h. Levels of CCL2 were determined 24 h poststimulation using the CCL2 Ready-SET-Go! ELISA Kit (eBiosciences, Frankfurt, Germany).

2.4. In Vitro Generation of Mouse Bone Marrow-Derived Dendritic Cells. Mouse myeloid dendritic cells (referred to herein as BMmDCs) and plasmacytoid dendritic cells (referred to herein as BMpDCs) were generated as described previously [17, 18]. Briefly, bone marrow cells were isolated from the femurs and tibias of BALB/c mice and differentiated into BMmDCs using GM-CSF or into BMpDC using Flt-3L (both R&D Systems, Minneapolis, USA) for eight days.

2.5. Dendritic Cell Activation. BALB/c BMmDCs or BMpDCs were seeded at 3.2×10^5 cells/mL in 24-well plates (Thermo Fisher Scientific) and stimulated with equimolar amounts of Pam_2CysK_4, CL264, Pam_2CysK_4 plus CL264, CL401, CL413, or CL531 for 24 h. Supernatants were analyzed for cytokine secretion by ELISA using BD Opteia ELISA sets (BD Biosciences, Heidelberg, Germany).

2.6. Preparation of BMmDC and $CD4^+$ T Cell Cocultures. Splenic $CD4^+$ T cells were isolated from OVA-TCR transgenic DO11.10 mice using the CD4 T Cell Isolation Kit (Miltenyi Biotec, Bergisch Gladbach, Germany). BALB/c-derived BMmDCs (3.2×10^5 cells/mL) were either cultured alone or together with DO11.10 $CD4^+$ T cells (8.0×10^5

cells/mL, >95% purity) and stimulated with equimolar amounts of Pam_2CysK_4, CL264, Pam_2CysK_4 plus CL264, CL401, CL413, or CL531 in the presence or absence of 20 μg/mL rOVA for 72 h. Subsequently, concentrations of IL-1β, IL-2, IL-4, IL-5, IL-6, IL-10, IL-13, IL-17A, TNF-α, and IFN-γ in the supernatants were measured by either BD OptEIA™ ELISA (BD Biosciences) or Ready-SET-Go! ELISA Sets (eBiosciences).

2.7. Mast Cell Generation and Functional Analysis. C57BL/6 and BALB/c bone marrow cells were differentiated into bone marrow-derived cultured mast cells (BMCMCs) by using 20% WEHI-3-conditioned, complete CMLESS medium (DMEM 10% FCS, 2 mM L-glutamine, 5×10^{-5} M β-mercaptoethanol, and 1% antibiotic/antimycotic) for 6 weeks. 1×10^6 C57BL/6 BMCMCs were stimulated with the indicated equimolar amounts of Pam_2CysK_4, CL264, Pam_2CysK_4 plus CL264, CL401, CL413, or CL531 for 24 h in 24-well plates in a total volume of 1 mL complete CMLESS medium conditioned with 20% WEHI-3-supernatant. 50 ng/mL PMA plus 10 μM A23187 calcium ionophore (both Sigma-Aldrich) was used as positive control. After 24 h, plates were centrifuged at 400 g at RT for 5 min and supernatants were removed and analyzed for IL-6 secretion by ELISA using the BD OptEIA IL-6 ELISA set according to the manufacturer's recommendations (BD Biosciences). BMCMCs were analyzed for cell viability by propidium iodide (Life Technologies, Carlsbad, CA) incorporation 24 h poststimulation.

To investigate the influence of the different TLR ligands on mast cell (MC) degranulation, C57.1 mouse MCs were maintained in complete CMLESS medium at a concentration of 5×10^5 cells/mL. For degranulation assays, 2×10^5 C57.1 MCs were sensitized with 2 μg/mL anti-DNP IgE [19] overnight and stimulated with 10 ng/mL of DNP-HSA (30–40 mol DNP per mol albumin, Sigma-Aldrich) in the presence or absence of the indicated amounts of Pam_2CysK_4, CL264, Pam_2CysK_4 plus CL264, CL401, CL413, or CL531 for 1 h in a total volume of 50 μL 1x Tyrode's buffer. 50 ng/mL PMA plus 10 μM A23187 calcium ionophore was used as positive control (Sigma-Aldrich). Subsequently, 10 μL of both cell supernatant and cell lysate was analyzed for β-hexosaminidase content using p-NAG (Sigma-Aldrich) as substrate. Secretion of β-hexosaminidase was calculated as % release = OD (sup.)/(($OD_{sup.} + OD_{lysate}$)/100).

2.8. Analysis of ERK1/2 Phosphorylation in BMCMCs. For detection of phosphorylated ERK1/2, C57BL/6-derived BMCMCs were stimulated with 50 ng/mL PMA plus 10 μM A23187 calcium ionophore or 5 μM of either Pam_2CysK_4, CL264, Pam_2CysK_4 plus CL264, CL401, CL413, or CL531 for 5 min at 37°C and 5% CO_2. Additionally 5×10^5 BMCMCs/mL were sensitized with 2 μg/mL anti-DNP IgE [19] overnight and stimulated with 10 ng/mL DNP-HSA for 5 min at 37°C 5% CO_2. Subsequently, cells were fixed with 4% PFA for 15 min, permeabilized with cold methanol for 30 min, and stained for CD117 (APC-conjugate, eBiosciences) and pERK1/2 using an AF647-conjugated anti-pERK1/2 (Thr202/Tyr204) antibody (Cell Signaling Technologies, Danvers, MA) for 2 h. For pERK1/2 analysis, BMCMC preparations were gated on CD117-positive mast cells.

2.9. In Vivo Administration of TLR Ligands. For measurements of cytokine secretion *in vivo*, BALB/c mice ($n = 5$ per group) were injected i.p. with 0.2 mM of the different ligands in a final volume of 0.2 mL PBS. Blood samples were drawn by cardiac puncture 8 h postinjection and collected in Z-gel tubes (Sarstedt, Nümbrecht, Germany). Levels of IL-1β, IL-6, IL-12p70, and TNF-α in mouse sera were measured using BD Opteia ELISA sets (BD Biosciences). Levels of IFN-α were measured using the VeriKine™ Mouse IFN Alpha ELISA Kit (pbl Assay Science, New Jersey, USA) according to the manufacturer's recommendations. All animal experiments were performed in compliance with approved protocols by the German Animal Protection Law (local approval number: F107/131) or Stanford University.

2.10. Prophylactic Vaccination in a Mouse Model of Intestinal Allergy. For prophylactic vaccination, BALB/c mice (female, 8–12 weeks) were vaccinated three times in three-day intervals by i.n. administration of the following substances (all in 30 μl volume): (a) nontreated mice (Mock group)—received PBS as mock vaccination; (b) nonvaccinated allergic positive control group (PBS)—mice that received PBS; (c) OVA group (OVA)—10 μg rOVA; (d) TLR2 ligand group (Pam_2CysK_4 + OVA)—0.5 mM Pam_2CysK_4 + 10 μg rOVA; (e) TLR7 ligand group (CL264 + OVA)—0.5 mM CL264 + 10 μg rOVA; (f) TLR2/7 dual-ligand group (CL531 + OVA)—0.5 mM CL531 + 10 μg rOVA; and (g) TLR2/7 dual-ligand control (no OVA) group (CL531)—0.5 mM CL531 (for comparison of experimental groups see also Repository Figure 5).

One week after the last vaccination, mice from PBS, OVA, Pam_2CysK_4 + OVA, CL264 + OVA, CL531 + OVA, and CL531 groups were sensitized to OVA twice in a biweekly interval by i.p. injection of 10 μg OVA (grade V) absorbed to 2 mg aluminum-hydroxide adjuvant (Pierce, Solingen, Germany) in 200 μL sterile PBS (OVA/A). Mice in the Mock group received PBS as mock sensitization.

For induction of intestinal allergy, two weeks after the second sensitization, mice were challenged by being fed an egg white diet containing OVA for 8 days (PBS, OVA, Pam_2CysK_4 + OVA, CL264 + OVA, CL531 + OVA, and CL531 groups) or by being fed a conventional diet (PBS group) free from OVA as control [20]. Blood samples were collected after vaccination (day 14) and after sensitization (day 42) via the tail vein and on the final day of EW diet, by cardiac puncture under deep ketamine/rompun anaesthesia (Figure 5(a)). All animal experiments were performed in compliance with approved protocols by the German Animal Protection Law (local approval number: F107/131).

2.11. Detection of OVA-Specific IgG1, IgG2a, and IgE Levels in Mouse Sera and Detection of Mediator Release from RBL 2H3 Cells. For measurement of OVA-specific IgG1, IgG2a, and IgE antibody titers in mouse sera, ELISA plates (Greiner Bio-One, Solingen-Wald, Germany) were coated with 5 μg/well OVA (OVA grade V, Sigma) in coating buffer (50 mM

Na_2CO_3/$NaHCO_3$, pH 9.6) overnight at 4°C. Serum samples (50 μL/well) were diluted by serial dilution (for IgE: $1 \times 1:10$, then $6 \times 1:5$, for IgG1 and IgG2a: $1 \times 1:100$, then $6 \times 1:10$) and incubated at 4°C overnight (IgE) or for 2 h at room temperature (IgG1, IgG2a). Levels of OVA-specific antibodies were measured using 50 μL secondary detection antibody diluted in PBS supplemented with 10% FCS (IgE: rat anti-mouse IgE biotin conjugated, BD Biosciences, Heidelberg, Germany 1 : 1000; IgG1: goat anti-mouse IgG1γ1 HRP-conjugated, 1 : 8000; and IgG2a: rabbit anti-mouse IgG2a, 1 : 8000—all Invitrogen, Darmstadt, Germany—incubation time: 1.5 h for IgG1 and IgG2a and overnight for IgE) in combination with a streptavidin-HRP antibody (for IgE detection, 50 μL diluted 1 : 2000 in PBS supplemented with 10% FCS, BD Biosciences) applied for 30 min at room temperature. Development was performed with 100 μL/well TMB substrate solution (BD Biosciences) for up to 30 min. The reaction was stopped by the addition of 50 μL/well 25% sulfuric acid and analyzed using a SpectraMAX340PC (Molecular Devices, CA) reading the absorbance at 450 nm. Data were analyzed using Excel and Graphpad Prism (GraphPad Software, La Jolla, CA, USA). Measurement of mediator release from RBL-2H3 cells was performed by sensitizing RBL 2H3 cells with pooled sera and by quantifying of β-hexosaminidase release according to [20]. In short, 1.5×10^5 RBL 2H3 cells/well were seeded in 96-well plates overnight. The next day, medium was removed by aspiration, pool sera were diluted 1 to 10 in medium, 50 μL serum dilution per well were added to the cells in triplicates, and cells were sensitized for 1 h at 37°C. Subsequently, plates were washed with 1x Tyrode's buffer (137 mM NaCl, 2.7 mM KCl, 0.4 mM NaH_2PO_4, 0.5 mM $MgCl_2^*6H_2O$, 1 mM $CaCl_2$, 0.1% BSA, 0.1% glucose, 10 mM HEPES, pH 7.45), 100 μL of the indicated amounts of OVA (grade V, Sigma-Aldrich) in 1x Tyrode's buffer was added to the cells, and plates were incubated at 37°C. After one hour, 30 μL of supernatant was transferred to a new 96-well plate and mixed with 50 μL/well substrate solution (0.1 M pNAG, pH 4.5 in Na_2HPO_4). Plates were incubated for 45 minutes at 37°C and stopped with 100 μL/well stop solution (0.2 M glycine, pH 10.7).

2.12. Statistical Analysis. Comparison between different treatment groups was performed by means of 2-way ANOVA analysis. Confidence intervals for the estimated differences between treatment groups as well as p values were adjusted using the Bonferroni method in order to restrict the overall type I error α (false-positive results, that is, false significant differences) to 5%. p values < 0.05, <0.01, and <0.001 were designated with $*$, $**$, and $***$, respectively. The statistical analyses were performed with GraphPad Prism 6 software for Mac, version 6.0f.

3. Results

3.1. The Dual TLR2/7 Ligands CL413 and CL531 Induce Strong Secretion of IL-10 by BMmDCs and Suppress rOVA-Induced Th2 Cytokine Secretion. First, we checked the potential of the different TLR ligands to induce the activation of mouse bone marrow-derived myeloid dendritic cells (BMmDCs) since these cells are highly important in the establishment of adaptive immune responses when applying these adjuvants in a vaccination setting. When analyzing the activation profile of *in vitro* differentiated BMmDCs (Figure 1, gating strategy and phenotype shown in Repository Figure 2), we observed that, compared to Pam_2CysK_4 alone or mixed with CL264, the dual TLR2/7 ligands CL413 and CL531 resulted in significantly reduced IL-1β secretion, even when applied in higher concentrations. CL264 and CL401 dose-dependently induced IL-1β secretion, at lower levels than Pam_2CysK_4. In contrast, IL-6 secretion at low-stimulation doses (0.2 and 0.1 μM) was similar among Pam_2CysK_4-, Pam_2CysK_4 + CL264-, and CL531-stimulated cells, whereas CL413 stimulation resulted in a significantly higher IL-6 secretion than the other ligands. For CL264 and CL401, at least 0.5 μM of each ligand was required to induce levels of IL-6 secretion similar to those of the other dual TLR2/7 ligands. Most interestingly, only CL413 and CL531 induced a highly significant induction of the anti-inflammatory cytokine IL-10, especially notable at low concentrations of the agents.

We also investigated cytokine secretion induced by the different ligands from Flt-3L-cultures containing approximately 10% bone marrow-derived plasmacytoid dendritic cells (BMpDCs) (Repository Figure 3, gating strategy and phenotype shown in Repository Figure 2). While dendritic cells within Flt-3L-cultures did not secrete high amounts of IL-1β upon stimulation with any of the tested ligands, we were able to detect high levels of IL-6 secretion upon stimulation with either Pam_2CysK_4, Pam_2CysK_4 + CL264, CL413, or CL531, but not CL264 or CL401 (Repository Figure 3). Here, in lower stimulation concentrations (0.1 and 0.5 μM), CL413 and CL531 tended to induce slightly higher (although not significantly higher) levels of IL-10 production than Pam_2Cysk_4 and CL264 (Repository Figure 3).

CL413 and CL531 also enhanced BMmDC-derived IL-10 secretion in BMmDC:DO11.10 $CD4^+$ TC coculture (Figure 2). Here, this IL-10 secretion did not reach statistical significance. While only slightly reducing rOVA-induced IFN-γ secretion, costimulation with CL413 or CL531 resulted in significantly reduced IL-13 and IL-5 levels compared to stimulation with rOVA alone (Figure 2). In contrast, CL401 had no effect on rOVA-induced IL-5 secretion, but induced significantly elevated levels of IL-17A (Figure 2).

In mouse LA-4 epithelial cells, stimulation with Pam_2CysK_4 (with or without CL264), CL413, or CL531 induced similar levels of CCL2 production whereas CL401-induced CCL2 secretion was only observed at higher doses and CL264 was without detectable effect (Repository Figure 4).

In summary, these results suggest that the dual TLR2/7 ligands CL413 and CL531 might be of potential value as adjuvants for the treatment of allergic diseases because of their capacity to induce tolerogenic IL-10 secretion from BMmDCs and to suppress the secretion of Th2-cytokines from allergen-specific T cells.

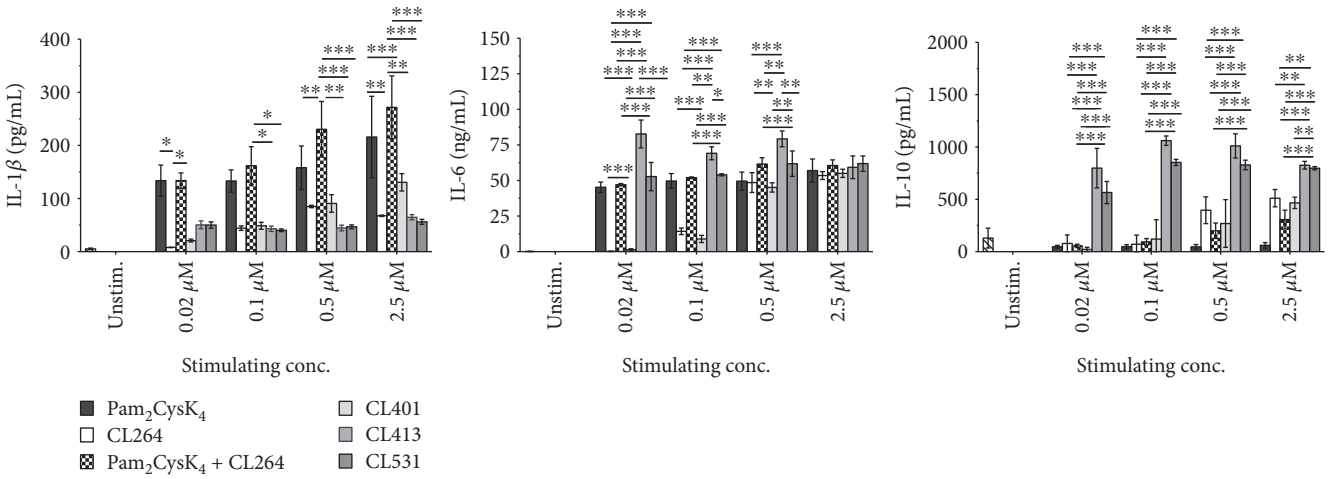

Figure 1: The dual TLR2/7 ligands CL413 and CL531 induce a strong BMmDC IL-10 secretion. Cytokine secretion from stimulated BALB/c BMmDCs. Data are mean results of three independent experiments ± SD. $^{*}P < 0.05$; $^{**}P < 0.01$; $^{***}P < 0.001$.

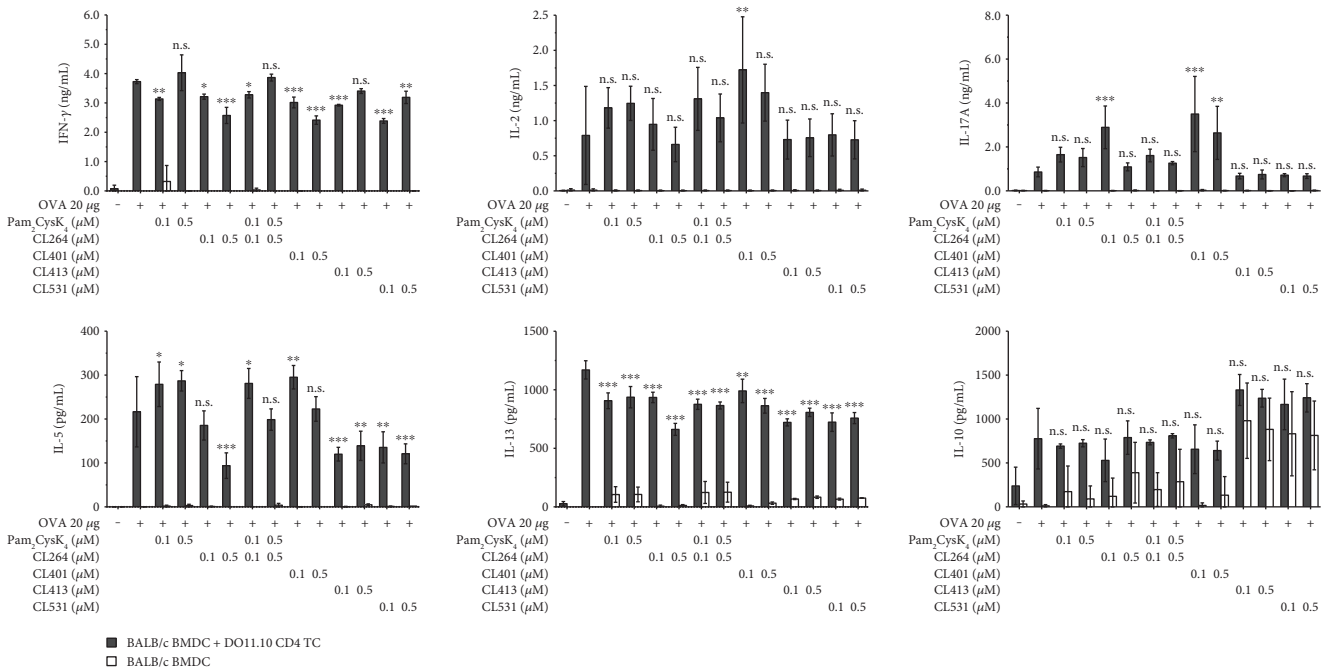

Figure 2: The dual TLR2/7 ligands CL413 and CL531 suppress rOVA-induced Th2 cytokine secretion while CL401 induces IL-17A secretion. Cytokine secretion from stimulated BALB/c BMmDC:DO11.10 $CD4^{+}$ TC cocultures. Data are mean results of two independent experiments ± SD. n.s. / * / ** / *** : statistical significance compared to the OVA 20 μg group.

3.2. Dual TLR2/7 Ligands Induce Limited Mast Cell Activation. Next, we evaluated the potential of the different ligands to induce direct mast cell activation and degranulation. Direct mast cell activation is a hallmark feature of allergic reactions and potential adjuvants for the treatment of allergies should neither induce mast cell degranulation by themselves nor enhance mast cell degranulation upon coapplication with an allergen. When stimulating BALB/c (Figure 3(a)) or C57BL/6 (Figure 3(b)) bone marrow-derived cultured mast cells (BMCMCs) with the different ligands, we observed a dose-dependent BMCMC activation with all ligands except CL264 in BALB/c-derived BMCMCs (Figure 3(a)), while IL-6 secretion was less pronounced for all activators in C57BL/6-derived BMCMCs (Figure 3(b)). We also observed initial toxic effects upon stimulation with the highest dose (5 μM) of Pam_2CysK_4, CL413, and CL531 in BMCMCs derived from either strain (Figure 3(b)). In this experimental setting, for all tested concentrations, no upregulation of ICOS-L or OX-40L and no secretion of IL-4, IL-10, IL-12, or GM-CSF was detected in BALB/c or C57BL/6 BMCMCs stimulated with the different TLR2 and TLR7 ligands (data not shown).

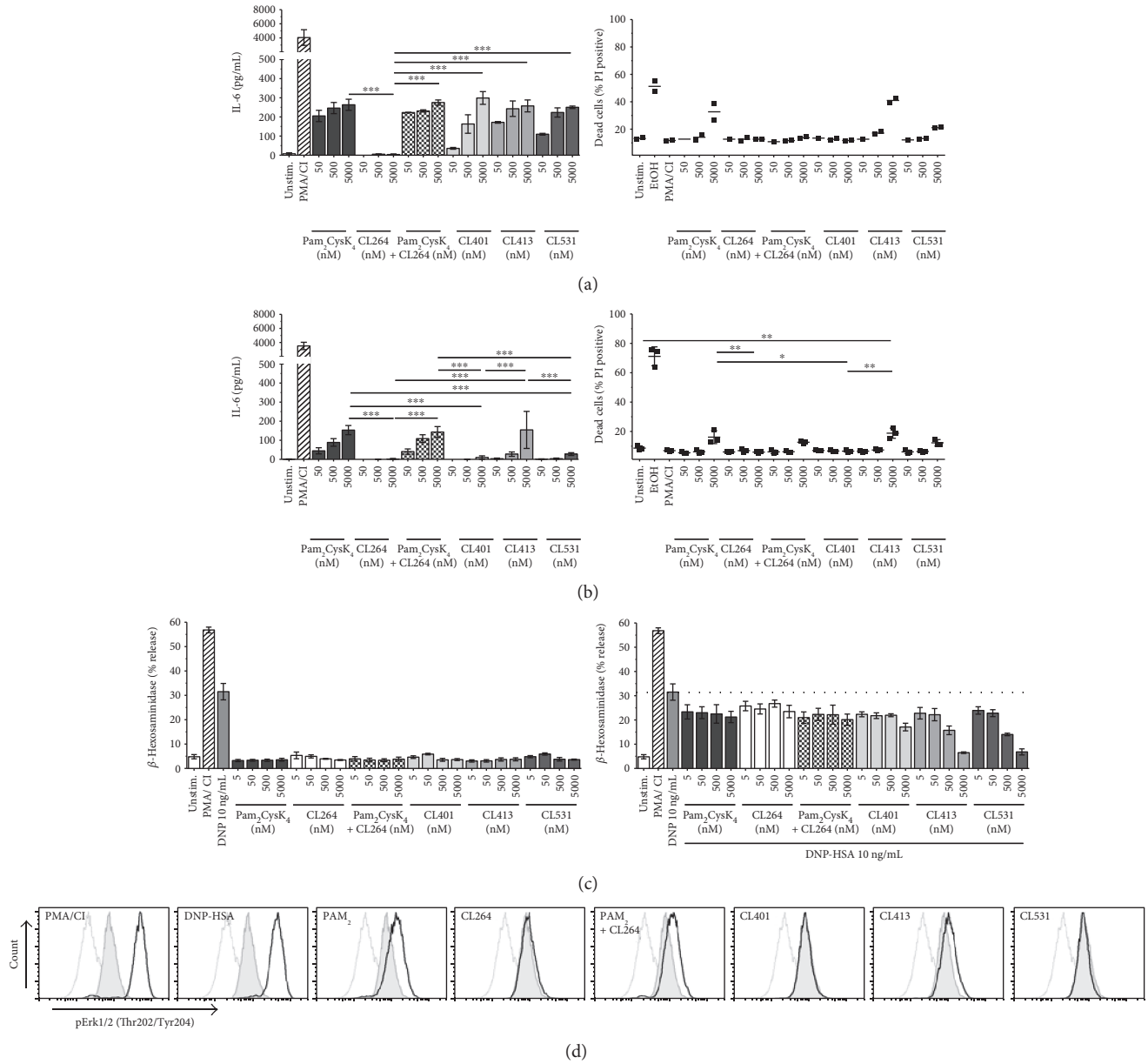

Figure 3: Dual TLR2/7 ligands induce limited mast cell activation directly but suppress IgE-and-antigen-induced mast cell degranulation. IL-6 secretion and cytotoxicity of stimulated BALB/c (a) and C57BL/6 (b) BMCMCs. TLR2/7 ligand-induced degranulation in the presence or absence of DNP-HSA from αDNP-IgE-sensitized C57.1 MCs. Dashed line indicates the level of β-hexosaminidase release induced by stimulation with 10 ng/mL DNP-HSA alone (c). Analysis of phospho-ERK1/2 (Thr202/Tyr204) levels in C57BL/6 BMCMCs stimulated with 5 μM of the different TLR ligands for 5 min (d). Grey: unstained cells; grey tinted: unstimulated; black: stimulated as indicated; Data are representative results of two (d) or mean of three (a, b, c) independent experiments ± SD. $^{*}P < 0.05$; $^{**}P < 0.01$; $^{***}P < 0.001$.

Analysis of DNP-HSA-induced C57.1 mast cell degranulation revealed that, even when applied in high concentrations, all ligands induced very little direct C57.1 degranulation (Figure 3(c)). Notably, when coapplied with DNP-HSA, all dual TLR2/7 ligands dose-dependently suppressed DNP-HSA-induced degranulation. Remarkably, this effect was not observed for Pam_2CysK_4 and CL264 either provided alone or provided as a mixture (Figure 3(c)).

Mechanistically, compared to unstimulated controls, stimulation of BMCMCs with 5 μM Pam_2CysK_4, Pam_2CysK_4 + CL264, or CL413, but not with CL264, CL401, or CL531, resulted in increased levels of ERK1/2 phosphorylation (Figure 3(d)), consistent with the induction of IL-6 secretion from BMCMCs by these ligands (Figure 3(b)). However, no induction of phosphoPLCγ1 was observed upon stimulation with the different ligands (data not shown).

3.3. Dual TLR2/7 Ligands Induce Both TLR2- and TLR7-Mediated Cytokine Secretion in Mice. Next, we evaluated the cytokine response induced by application of the different ligands *in vivo* in an established mouse model of TLR ligand-induced immune activation (Figure 4, [21]).

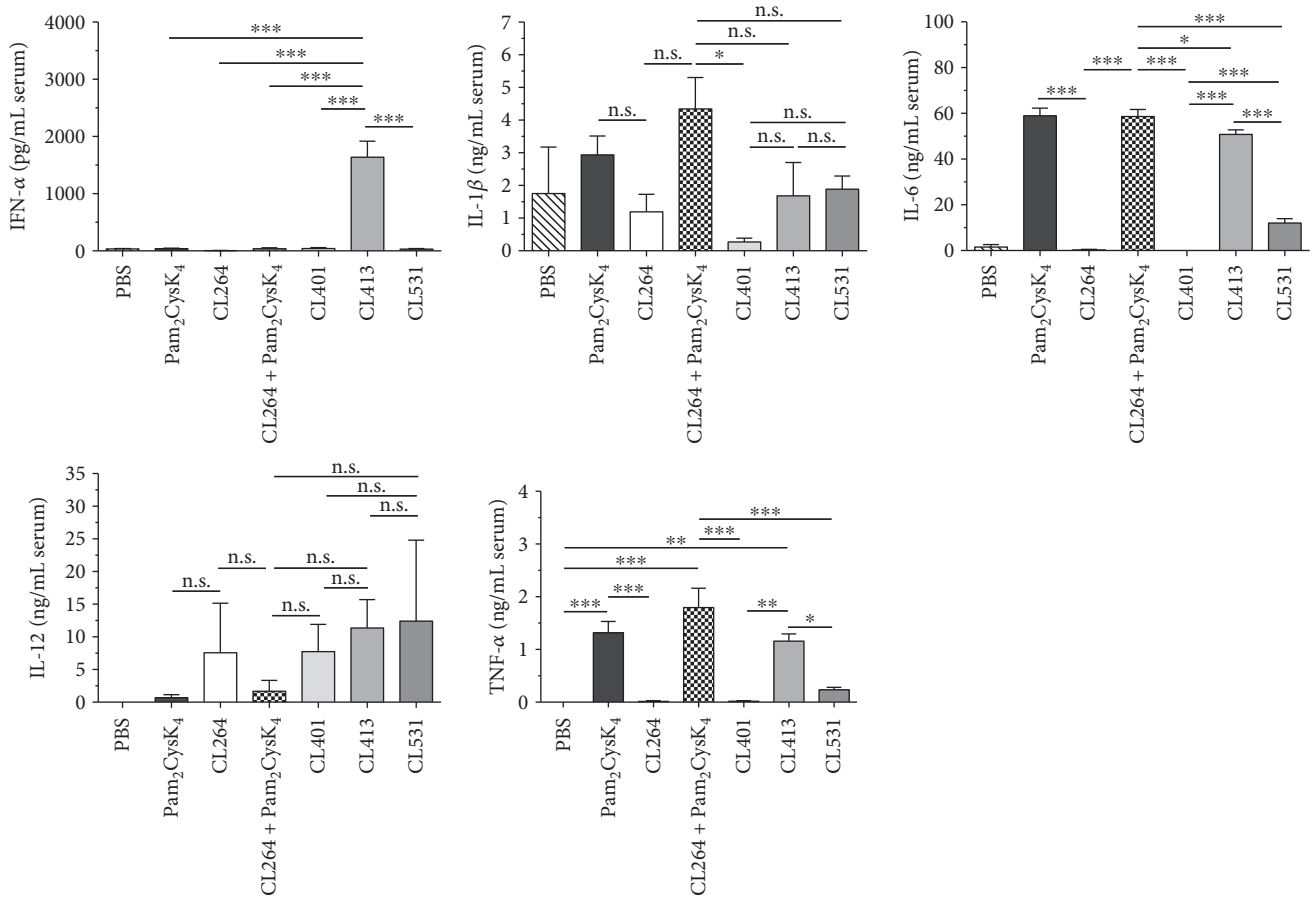

Figure 4: Dual TLR2/7 ligands induce both TLR2- and TLR7-mediated cytokine secretion *in vivo*. Serum cytokine levels 8 h post i.p. application of 0.2 mM of the indicated ligands. Data are mean results of 5 mice per group ± SD. $^{*}P < 0.05$; $^{**}P < 0.01$; $^{***}P < 0.001$.

For this purpose, we measured serum cytokine concentrations 8 h post i.p. application of the different ligands in BALB/c mice. Interestingly, of all TLR ligands tested, only CL413 resulted in a robust, and compared to the other groups, highly significant secretion of IFN-α (Figure 4). Moreover, we found that IL-6 production and TNF-α production were only induced in the presence of Pam_2CysK_4 (either alone or contained within the TLR2/7 ligands CL413 and CL513) but not CL264 (Figure 4). Remarkably, for both cytokines, CL401 did not induce significant secretion of these proinflammatory cytokines. Moreover, IL-1β secretion was only observed in animals injected with either Pam_2CysK_4 or Pam_2CysK_4 + CL264 (Figure 4). Of note, Th1-promoting IL-12 production was observed for ligands containing the TLR7 ligand CL264, either alone or as part of a dual TLR2/7 ligand (CL264, CL401, CL413, and CL531, Figure 4). We found that all dual TLR2/7 ligands induced similar levels of IL-12 production (Figure 4).

3.4. Prophylactic Vaccination with CL531 Suppresses OVA-Specific IgE Production in a Mouse Model of OVA-Induced Intestinal Allergy. Finally, because of the promising results obtained for the immune-activating capacities of CL531, in combination with the lack of ERK1/2 phosphorylation observed in BMCMCs stimulated with CL531, we decided to investigate whether CL531 might suppress allergic sensitization in a prophylactic vaccination approach using an established mouse model of OVA-induced intestinal allergy (Figure 5(a), for more information on the experimental groups see Repository Figure 5) [22].

We found that intranasal coapplication of CL531 and OVA, but not CL531 or OVA alone, resulted in significantly reduced OVA-specific IgE levels after 7 days of challenge with OVA-containing food pellets, compared to vaccination with OVA alone (Figure 5(b)). OVA-specific IgE levels were also lower in the mice vaccinated with CL531 and OVA compared to those vaccinated with PBS, although this difference was not statistically significant ($p = 0.215$). Vaccination with CL531 plus OVA strongly enhanced OVA-specific IgG1 titers compared to nonvaccinated animals (Figure 5(c)). Moreover, no significant differences in OVA-specific IgG1 levels were observed among animals vaccinated with the dual ligand (CL531) alone, CL531 with OVA, or with Pam_2CysK_4 plus OVA. In addition, animals vaccinated with the mixture of CL531 and OVA displayed significantly increased levels of OVA-specific IgG2a antibodies compared to animals vaccinated with PBS or with either OVA alone or CL264 plus OVA (Figure 5(d)). Similar levels of OVA-specific IgG2a antibodies were observed in animals vaccinated with CL531

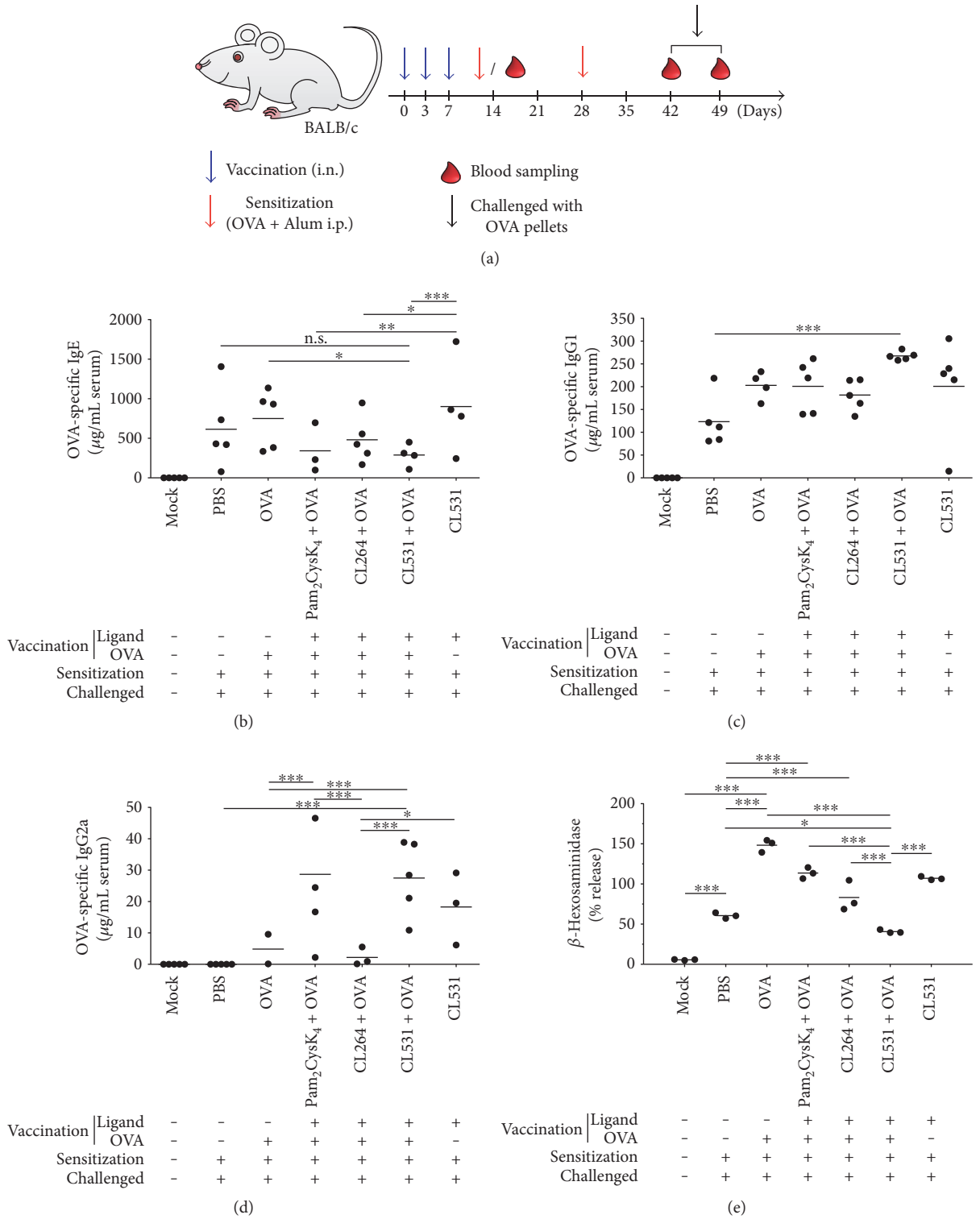

Figure 5: Prophylactic vaccination with CL531 plus OVA suppresses OVA-specific IgE production while inducing OVA-specific IgG production in a mouse model of OVA-induced intestinal allergy. Schematic representation of prophylactic vaccination approach (a). Blue arrows represent intranasal (i.n.) vaccination or mock vaccination (in "Mock" group); red arrows represent intraperitoneal (i.p.) sensitization with 10 μg OVA with 2 mg Alum in 200 μL sterile PBS (or, in "Mock" group, with sterile PBS alone). Blood drops represent blood sampling from the tail after vaccination and sensitization or cardiac puncture after challenged with OVA-containing food pellets. Serum concentration of OVA-specific IgE (b), IgG2a (c), and IgG1 antibodies (d) was measured throughout the vaccination experiment by ELISA. β-Hexosaminidase release from RBL 2H3 cells upon crosslinking with OVA was performed with pooled sera from the final bleeding (e). Results are means ± SD from five mice per group (b, c, d) or means of three technical replicates measured using the same serum pool to sensitize the RBL 2H3 cells (e). $^{*}P < 0.05$; $^{**}P < 0.01$; $^{***}P < 0.001$.

plus OVA, CL531 alone, and Pam_2CysK_4 plus OVA, suggesting that IgG2a production was driven by TLR2-signaling induced by both CL531 and Pam_2CysK_4.

In line with the results obtained for OVA-specific IgE levels, RBL 2H3 cells passively sensitized with pooled serum from animals vaccinated with CL531 plus OVA displayed the lowest levels of antigen- (OVA-) induced β-hexosaminidase release, compared to all other experimental groups (Figure 5(e) and Repository Figure 6). Here, vaccination with CL531 plus OVA significantly reduced mediator release from RBL-2H3 cells compared to PBS-vaccinated and OVA-sensitized animals (PBS group). By contrast, vaccination with OVA alone, significantly increased β-hexosaminidase release compared to nonvaccinated animals (PBS group, Figure 5(e) and Repository Figure 6). Vaccination with CL264 plus OVA or Pam_2CysK_4 plus OVA also resulted in higher levels of β-hexosaminidase release compared to nonvaccinated animals (Figure 5(e) and Repository Figure 6).

4. Discussion

Currently, TLR2 ligands are undergoing clinical testing as adjuvants in vaccines for the treatment of Lyme disease, malaria, HIV, HBV, and HPV, while TLR7 ligands are being tested for their benefits in the treatment of cancer (leukemia, prostate cancer, melanomas, breast cancer, and B cell lymphomas), chronic hepatitis, asthma, and rhinitis [2–4, 23]. TLR2 ligands, like the synthetic Pam_3CysK_4, have repeatedly been shown to induce tolerogenic DC and Tr responses [8, 9, 11], and TLR7 ligands show promising adjuvant capacity but are limited in their usage due to their induction of proinflammatory cytokines and the associated side effects [5, 6]. In contrast, several reports suggest that TLR7 ligands have potential as adjuvants for the treatment of Th2-mediated allergic diseases: in an experimental mouse allergy model, the TLR7 ligand Imiquimod significantly inhibited chronic inflammation, persistent airway hyperreactivity (AHR), and airway remodeling, while reducing serum IgE levels and Th2 cytokines in BAL fluids [24]. In addition, the Imiquimod-derivative resiquimod (R848) was shown to inhibit IgE production and induce IFN-γ secretion *in vivo* [25]. In line with these findings, prophylactic, epicutaneous treatment with R848 and the major birch pollen allergen Bet v 1 inhibited the production of biologically active Bet v 1-specific IgE antibodies, suppressed lung inflammation, and reduced AHR compared to Bet v 1 applied alone [26]. Finally, in a mouse model of established, OVA-induced allergic asthma, therapeutic treatment with R848 reduced allergic features via a Tr-dependent mechanism [27]. However, until now, no data have been available describing the application of the TLR7 activator CL264 as adjuvant for the treatment of allergic diseases.

In light of the studies reviewed above and the results presented in this study, we hypothesize that the dual TLR2/7 ligands CL413 and CL531, but not CL401, hold potential as adjuvants for the treatment of Th2-mediated allergic diseases. Upon stimulation with CL413 and CL531, we observed a strong anti-inflammatory IL-10 secretion from BMmDCs, correlating with a suppression of OVA-induced IL-5 and IL-13 secretion.

Moreover, direct mast cell activation by these TLR2/7 ligands was rather limited and we observed a suppression of DNP-HSA-induced, IgE-and-Ag-specific mast cell degranulation *in vitro* as well as the production of Th1-promoting IL-12 secretion upon *in vivo* application of these TLR2/7 ligands to naïve mice. In the context of allergy treatment, the immune-modulating effects of all three dual TLR2/7 ligands on mast cells are of special interest, since they constitute evidence of potentially important safety features. Moreover, in contrast to CL413, mast cell stimulation with CL401 or CL531 did not result in ERK1/2 phosphorylation, which is known to be associated with mast cell activation.

Interestingly, although structurally very similar (Repository Figure 1), the different dual TLR2/7 ligands displayed clearly distinct immune activation profiles. CL413 and CL531 induced epithelial cell-derived chemoattractant CCL2 secretion and BMmDC-derived IL-10 secretion, suppressed both OVA-induced IL-5 secretion and Ag-specific mast cell degranulation, and induced proinflammatory cytokine secretion *in vivo*. In contrast to this, CL401 induced considerably less IL-10 secretion from BMmDCs, induced IL-17A production in BMmDC:TC cocultures, and failed to induce either C57BL/6 BMCMC IL-6 secretion *in vitro* or IL-6 and TNF-α production *in vivo*. Among these findings, the IL-17A production observed in BMmDC:TC cocultures costimulated with CL401 and OVA is especially important. Indeed, concerns regarding the skewing of T cell responses towards Th17-dominated responses by the TLR2 ligand lipoprotein OspA, and the potential for this to contribute to the development of autoimmune diseases, have stopped the commercialization of a Lyme disease vaccine containing this TLR2 ligand [28].

Of note, among the tested TLR ligands, only *in vivo* application of CL413 resulted in a robust, and compared to the other groups, highly significant secretion of IFN-α (Figure 4). This result suggests that only CL413 may be able to activate plasmacytoid DCs. However, we cannot exclude the possibility that the increased secretion of either IL-6 or IL-10 from Flt-3L cultures upon stimulation with either CL531 or CL413 may in part be mediated by plasmacytoid DCs within these cultures (Repository Figure 3). Here, interestingly, both CL413 and CL531 induced significantly higher IL-6 and tended to induce higher (but not statistically significant) IL-10 secretion than observed for CL401. Since IFN-α is known to induce flu-like symptoms such as fever, fatigue, and joint pain [29], we suggest that the observed immune-activating profile of CL531, combined with a lack of IFN-α induction (as observed for CL531, but not for CL413), is likely to prevent these side effects observed upon *in vivo* application of such adjuvants, particularly CL531.

Indeed, in our own *in vivo* prophylactic treatment experiment with the dual TLR2/7 ligand CL531 *in vivo*, we demonstrated that coapplication of CL531 with OVA as a vaccine, but not vaccination with CL531 or OVA alone, displayed promising immune-modulating effects, suppressing OVA-specific IgE antibody production, in comparison to mice vaccinated with OVA alone while increasing the production of potentially blocking OVA-specific IgG1 and IgG2a

antibodies *in vivo*. In line with these results, sera from animals vaccinated with the mixture of CL531 plus OVA showed the lowest capacity to sensitize RBL-2H3 cells for antigen-dependent degranulation *in vitro*. These results are in agreement with our *in vitro* results, where CL531 or CL413 induced by themselves only limited mast cell activation but suppressed DNP-HSA-induced, IgE-and-Ag-specific mast cell degranulation.

Given the way we tested our serum's ability to passively sensitize RBL-2H3 cells to respond to OVA challenge *in vitro* (which involved washing the cells after incubating them with sera for 1 h), we were more likely to detect the presence of anti-OVA IgE than anti-OVA IgG1 antibodies. In line with this, Segal and coworkers reported that although IgG receptors can be detected on RBL-2H3 cells, their affinity for IgG is much lower than the affinity of IgE for FcεRI [30]. Moreover, IgG aggregates bound to RBL-2H3 cells were shown to neither elicit mediator release by themselves nor modulate IgE-mediated histamine release [30]. However, we cannot exclude the possibility that some of the OVA-specific IgG1 antibodies which were induced might be able to activate mast cells *in vivo* via an IgG1-antigen immune complex-dependent mechanism [31], as OVA-specific IgG1 antibodies were increased in sera of animals vaccinated with CL531 plus OVA (Figure 5).

Notably, clinical trials of allergen-specific immunotherapy in humans however suggest that a successful therapeutic outcome can be achieved in association with the induction of blocking allergen-specific IgG4 antibodies even when allergen-specific IgG1 and IgE levels remain unchanged over long periods of time [32]. The serology of animals vaccinated with CL531 and OVA thus mirrored these results observed in human trials regarding the induction of allergen-specific IgG1 and IgG2a antibodies, while also significantly reducing levels of allergen-specific IgE.

Taken together, our results indicate that *in vivo*, CL531, coadministered with OVA, shows promising immune-modulating effects, suppressing the main features of allergy: allergen-specific IgE production and IgE-dependent mast cell degranulation and mast cell activation, while inducing the production of allergen-specific IgG antibodies. We speculate that these effects may reflect, at least in part, the ability of these dual TLR2/7 ligands to induce IL-10 secretion from BMmDCs.

These results are in line with the recently reported study by Gutjahr et al. who showed that the structurally very similar dual TLR2/7 ligand PamadiFectin (CL307) induced significantly stronger human DC and cytotoxic T cell responses than the nonconjugated TLR2- and TLR-7 ligands, provided either alone or as a mixture [16]. In accordance with our own results, application of CL307 resulted in highly enhanced production of antigen-specific IgG2a antibodies against the coapplied HIV antigen p24 [16].

The observed difference in immune-modulating capacity between the different dual TLR2/7 ligands might be explained by sterical hindrance of ligand binding to TLR2 and TLR7 induced by the conjugation. Furthermore, the lack of the Pam_2CysK_4-associated four lysine residues in CL401 in comparison to unconjugated Pam_2CysK_4 is likely to result in reduced and/or altered TLR2 activation capacity. In line with this hypothesis, when the capacities of the different TLR2 and TLR7 ligands to activate their target receptors were determined using TLR2- or TLR7-transfected HEK293 cells, Pam_2CysK_4 and CL531 were shown to induce identical levels of TLR2 activation, whereas CL413 and CL401 were 10- and 100-fold weaker TLR2 activators, respectively [15]. Correspondingly, TLR7 activation in transgenic HEK293 cells was shown to be identical for CL401, CL413, and CL531, with all dual TLR2/7 ligands being 10-fold weaker TLR7 activators compared to the unconjugated TLR7 ligand CL264 [15].

It is interesting that the immune-modulating effects could not be achieved when using the individual TLR2 and TLR7 ligands alone or as a simple mixture of these ligands. Therefore, we think that the combination of TLR2- and TLR7 ligands into dual TLR2/7 ligands is a promising strategy to leverage the beneficial immune-modulating properties of each of the single ligands while also ensuring the simultaneous costimulation of the target cell with both components in a fixed one-to-one ratio. Moreover, TLR2-mediated uptake of the dual TLR2/7 ligands is likely to facilitate intracellular delivery to TLR7 and therefore enhance immune cell activation and subsequent immune responses. We hypothesize that the 3-dimensional structure of dual TLR2/7 ligands is a key factor for their immunomodulatory effect. Our results suggest that CL413 and CL531, but not CL401, have a structure that allows the interaction between the TLR2-activating Pam_2CysK_4 component of the dual ligand with TLR2 on the cell surface. This interaction likely has two main effects: (1) the induction of immunosuppressive IL-10 secretion by DCs via TLR2 activation in agreement with previous studies [8, 33] and (2) internalization of the dual ligand, facilitating the interaction of the contained TLR7 ligand with TLR7, contributing to the induction of Th1-biassed immune responses by synergic activation of signaling cascades leading to IL-10 gene expression. In line with this hypothesis, we observed that the dual TLR2/7 ligands retained the ability to induce both TLR2- and TLR7-mediated cytokine secretion upon *in vivo* application (Figure 4).

In accord with this speculation, stimulation of DCs with Pam_3CysK_4 chemically conjugated to an OVA-derived $CD8^+$ TC peptide resulted in enhanced uptake and presentation of the OVA-derived $CD8^+$ TC peptide by the stimulated DCs [12].

Considering the overall immune-modulating properties of the different ligands, we think that dual TLR2/7 ligands have the potential to induce Th1-biased immune modulation *in vivo*. Therefore, we suggest that the dual TLR2/7 ligands CL413 (with the caveat of its high IFN-α induction *in vivo*) and especially CL531, due to its reduced ability to activate mast cells *in vitro* and capacity to suppress allergen-specific IgE production *in vivo* (together with a lower capacity than CL413 to induce IFN-α), are promising adjuvant candidates to further improve the treatment of allergic diseases. These findings also suggest that it will be of substantial interest to conduct future studies to elucidate the molecular mechanisms by which these promising adjuvants can modulate immune responses.

Abbreviations

BMmDCs: Bone marrow-derived myeloid dendritic cells
BMpDCs: Bone marrow-derived plasmacytoid dendritic cells
BMCMCs: Bone marrow-derived cultured mast cells
MCs: Mast cells
OVA: Ovalbumin
PAMPs: Pathogen-associated molecular patterns
TCs: T cells
TLR: "Toll-" like receptor
Th: T helper cells
Tr: T regulatory cells.

Conflicts of Interest

The authors declare that there is no conflict of interest regarding the publication of this paper.

Acknowledgments

The authors would like to thank InvivoGen for providing the chemical structure files of the different ligands used to generate Repository Figure 1. This work has been funded by the budget of the Paul-Ehrlich-Institut, Langen, Germany, and funds available of the Galli Lab, Department of Pathology, Stanford University School of Medicine, Stanford, USA (including NIH/NIAMS R01 AR067145 and funds from the Department of Pathology and the Sean N. Parker Center for Allergy and Asthma Research). Adam Flaczyk received funding from the DAAD RISE professional program and an EAACI Medium-Term Research Fellowship. Jonathan Laiño received funding from the DAAD—country-related cooperation program with Argentina—ALEARG fellowship.

References

[1] M. Wills-Karp, J. Santeliz, and C. L. Karp, "The germless theory of allergic disease: revisiting the hygiene hypothesis," *Nature Reviews Immunology*, vol. 1, pp. 69–75, 2001.

[2] D. Toussi and P. Massari, "Immune adjuvant effect of molecularly-defined toll-like receptor ligands," *Vaccine*, vol. 2, pp. 323–353, 2014.

[3] H. J. Schulze, B. Cribier, L. Requena et al., "Imiquimod 5% cream for the treatment of superficial basal cell carcinoma: results from a randomized vehicle-controlled phase III study in Europe," *The British Journal of Dermatology*, vol. 152, pp. 939–947, 2005.

[4] M. Lebwohl, S. Dinehart, D. Whiting et al., "Imiquimod 5% cream for the treatment of actinic keratosis: results from two phase III, randomized, double-blind, parallel group, vehicle-controlled trials," *Journal of the American Academy of Dermatology*, vol. 50, pp. 714–721, 2004.

[5] E. Stockfleth, U. Trefzer, C. Garcia-Bartels, T. Wegner, T. Schmook, and W. Sterry, "The use of toll-like receptor-7 agonist in the treatment of basal cell carcinoma: an overview," *The British Journal of Dermatology*, vol. 149, Supplement 66, pp. 53–56, 2003.

[6] D. Vidal and A. Alomar, "Mode of action and clinical use of imiquimod," *Expert Review of Dermatology*, vol. 3, pp. 151–159, 2008.

[7] T. Lan, E. R. Kandimalla, D. Yu et al., "Stabilized immune modulatory RNA compounds as agonists of Toll-like receptors 7 and 8," *Proceedings of the National Academy of Sciences*, vol. 104, pp. 13750–13755, 2007.

[8] Q. Chen, T. S. Davidson, E. N. Huter, and E. M. Shevach, "Engagement of TLR2 does not reverse the suppressor function of mouse regulatory T cells, but promotes their survival," *The Journal of Immunology*, vol. 183, pp. 4458–4466, 2009.

[9] Y.-G. Tsai, K. D. Yang, D.-M. Niu, J.-W. Chien, and C.-Y. Lin, "TLR2 agonists enhance $CD8^{+}Foxp3^{+}$ regulatory T cells and suppress Th2 immune responses during allergen immunotherapy," *The Journal of Immunology*, vol. 184, pp. 7229–7237, 2010.

[10] P. A. Sieling, W. Chung, B. T. Duong, P. J. Godowski, and R. L. Modlin, "Toll-like receptor 2 ligands as adjuvants for human Th1 responses," *The Journal of Immunology*, vol. 170, pp. 194–200, 2003.

[11] R. W. DePaolo, K. Kamdar, S. Khakpour, Y. Sugiura, W. Wang, and B. Jabri, "A specific role for TLR1 in protective T(H)17 immunity during mucosal infection," *The Journal of Experimental Medicine*, vol. 209, pp. 1437–1444, 2012.

[12] S. Khan, M. S. Bijker, J. J. Weterings et al., "Distinct uptake mechanisms but similar intracellular processing of two different toll-like receptor ligand-peptide conjugates in dendritic cells," *Journal of Biological Chemistry*, vol. 282, pp. 21145–21159, 2007.

[13] T. Imanishi, H. Hara, S. Suzuki, N. Suzuki, S. Akira, and T. Saito, "Cutting edge: TLR2 directly triggers Th1 effector functions," *The Journal of Immunology*, vol. 178, pp. 6715–6719, 2007.

[14] R. C. Taylor, P. Richmond, and J. W. Upham, "Toll-like receptor 2 ligands inhibit TH2 responses to mite allergen," *The Journal of Allergy and Clinical Immunology*, vol. 117, pp. 1148–1154, 2006.

[15] InvivoGen, "Multi-TLR Agonists: Potential for Therapeutic Success - Review," in *InvivoGen Insight*, pp. 1–8, InvivoGen, San Diego, CA, USA, 2013, Spring 2013.

[16] A. Gutjahr, L. Papagno, F. Nicoli et al., "Cutting edge: a dual TLR2 and TLR7 ligand induces highly potent humoral and cell-mediated immune responses," *The Journal of Immunology*, vol. 198, pp. 4205–4209, 2017.

[17] S. Schülke, Z. Waibler, M.-S. Mende et al., "Fusion protein of TLR5-ligand and allergen potentiates activation and IL-10 secretion in murine myeloid DC," *Molecular Immunology*, vol. 48, pp. 341–350, 2010.

[18] Z. Waibler, M. Anzaghe, H. Ludwig et al., "Modified vaccinia virus Ankara induces Toll-like receptor-independent type I interferon responses," *Journal of Virology*, vol. 81, pp. 12102–12110, 2007.

[19] P. N. Hill and F. T. Liu, "A sensitive enzyme-linked immunosorbent assay for the quantitation of antigen-specific murine immunoglobulin E1," *Journal of Immunological Methods*, vol. 45, pp. 51–63, 1981.

[20] A. Hoffmann, A. Jamin, K. Foetisch et al., "Determination of the allergenic activity of birch pollen and apple prick test solutions by measurement of β-hexosaminidase release from RBL-2H3 cells. Comparison with classical methods in allergen standardization," *Allergy*, vol. 54, pp. 446–454, 1999.

[21] S. N. Vogel, D. Johnson, P. Y. Perera et al., "Cutting edge: functional characterization of the effect of the C3H/HeJ defect in mice that lack an Lps^{n} gene: in vivo evidence for a dominant

negative mutation," *The Journal of Immunology*, vol. 162, pp. 5666–5670, 1999.

[22] M. Burggraf, H. Nakajima-Adachi, S. Hachimura et al., "Oral tolerance induction does not resolve gastrointestinal inflammation in a mouse model of food allergy," *Molecular Nutrition & Food Research*, vol. 55, pp. 1475–1483, 2011.

[23] F. Steinhagen, T. Kinjo, C. Bode, and D. M. Klinman, "TLR-based immune adjuvants," *Vaccine*, vol. 29, pp. 3341–3355, 2011.

[24] Q. Du, L.-F. Zhou, Z. Chen, X.-Y. Gu, M. Huang, and K.-S. Yin, "Imiquimod, a Toll-like receptor 7 ligand, inhibits airway remodelling in a murine model of chronic asthma," *Clinical and Experimental Pharmacology and Physiology*, vol. 36, pp. 43–48, 2009.

[25] B. Frotscher, K. Anton, and M. Worm, "Inhibition of IgE production by the imidazoquinoline resiquimod in nonallergic and allergic donors," *The Journal of Investigative Dermatology*, vol. 119, pp. 1059–1064, 2002.

[26] S. Siebeneicher, S. Reuter, M. Krause et al., "Epicutaneous immune modulation with Bet v 1 plus R848 suppresses allergic asthma in a murine model," *Allergy*, vol. 69, pp. 328–337, 2014.

[27] L. P. Van, E. Bardel, S. Gregoire et al., "Treatment with the TLR7 agonist R848 induces regulatory T-cell-mediated suppression of established asthma symptoms," *European Journal of Immunology*, vol. 41, pp. 1992–1999, 2011.

[28] L. E. Nigrovic and K. M. Thompson, "The Lyme vaccine: a cautionary tale," *Epidemiology and Infection*, vol. 135, pp. 1–8, 2007.

[29] G. M. Scott, D. S. Secher, D. Flowers, J. Bate, K. Cantell, and D. A. Tyrrell, "Toxicity of interferon," *British Medical Journal (Clinical Research Ed.)*, vol. 282, pp. 1345–1348, 1981.

[30] D. M. Segal, S. O. Sharrow, J. F. Jones, and R. P. Siraganian, "Fc (IgG) receptors on rat basophilic leukemia cells," *The Journal of Immunology*, vol. 126, pp. 138–145, 1981.

[31] H. Wakayama, Y. Hasegawa, T. Kawabe, H. Saito, H. Kikutani, and K. Shimokata, "IgG-mediated anaphylaxis via Fc γ receptor in CD40-deficient mice," *Clinical and Experimental Immunology*, vol. 114, pp. 154–160, 1998.

[32] H. Fujita, M. B. Soyka, M. Akdis, and C. A. Akdis, "Mechanisms of allergen-specific immunotherapy," *Clinical and Translational Allergy*, vol. 2, p. 2, 2012.

[33] S. Jang, S. Uematsu, S. Akira, and P. Salgame, "IL-6 and IL-10 induction from dendritic cells in response to mycobacterium tuberculosis is predominantly dependent on TLR2-mediated recognition," *The Journal of Immunology*, vol. 173, pp. 3392–3397, 2004.

Hindawi
Journal of Immunology Research
Volume 2017, Article ID 5689709, 17 pages
https://doi.org/10.1155/2017/5689709

Research Article

Immunization with Bivalent Flagellin Protects Mice against Fatal *Pseudomonas aeruginosa* Pneumonia

Bahador Behrouz,[1] Farhad B. Hashemi,[2] Mohammad Javad Fatemi,[3] Sara Naghavi,[4] Gholamreza Irajian,[5] Raheleh Halabian,[1] and Abbas Ali Imani Fooladi[1]

[1]*Applied Microbiology Research Center, Baqiyatallah University of Medical Sciences, Tehran, Iran*
[2]*Department of Microbiology, School of Medicine, Tehran University of Medical Sciences, Tehran, Iran*
[3]*Burn Research Center, Hazrat Fatima Hospital, Iran University of Medical Sciences, Tehran, Iran*
[4]*Department of Bacteriology, Faculty of Medical Sciences, Tarbiat Modares University, Tehran, Iran*
[5]*Department of Microbiology, School of Medicine, Iran University of Medical Sciences, Tehran, Iran*

Correspondence should be addressed to Abbas Ali Imani Fooladi; imanifouladi.a@gmail.com

Received 6 January 2017; Revised 25 August 2017; Accepted 10 September 2017; Published 19 October 2017

Academic Editor: Peirong Jiao

Pseudomonas aeruginosa lung infections present a major challenge to healthcare systems worldwide because they are commonly associated with high morbidity and mortality. Here, we demonstrate the protective efficacy of type a and b flagellins (bivalent flagellin) against acute fatal pneumonia in mice. Mice immunized intranasally with a bivalent flagellin vaccine were challenged by different flagellated strains of *P. aeruginosa* in an acute pneumonia model. Besides the protective effect of the vaccine, we further measured the host innate and cellular immunity responses. The immunized mice in our study were protected against both strains. Remarkably, active immunization with type a or b flagellin significantly improved survival of mice against heterologous strain compared to flagellin a or b antisera. We also showed that after an intranasal challenge by *P. aeruginosa* strain, neutrophils are recruited to the airways of vaccinated mice, and that the bivalent flagellin vaccine was proved to be protective by the generated $CD4^+IL\text{-}17^+$ Th17 cells. In conclusion, bivalent flagellin vaccine can confer protection against different strains of *P. aeruginosa* in an acute pneumonia mouse model by eliciting effective cellular and humoral immune responses, including increased IL-17 production and improved opsonophagocytic killing.

1. Introduction

Pseudomonas aeruginosa pulmonary infection as a life-threatening complication frequently causes bacteremia and sepsis in hospitalized and immunocompromised patients [1, 2]. Moreover, the widespread and empirical use of broad-spectrum antibiotics in critical care units has led to the continuous emergence of multidrug-resistant (MDR) *P. aeruginosa* strains that present a major challenge to clinical therapy and contribute significantly to increased morbidity and mortality [3]. The high mortality and prevalence of infection with MDR *P. aeruginosa* strains accompanied by the paucity of new effective antibiotic classes present unique challenges to clinicians and highlight the necessity for designing new treatment approaches, such as immunotherapy, which targets pathogen-specific virulence factors to reduce pathogenesis without inducing multidrug resistance [4, 5]. Moreover, the complexity of the *P. aeruginosa* genome, which encodes numerous antigens, indicates that immunotherapy using a single antigen will not provide sufficient protection.

To date, most *P. aeruginosa* vaccines focusing on immunization and treatment targeting pseudomonal virulence factors, such as LPS O antigen [6], the outer membrane proteins F and I [7], or the type III secretion system component PcrV [8], have been described in the literature as having conventional protective mechanisms, namely, antibody-mediated opsonophagocytic killing and/or antibody-mediated toxin inhibition. Recently, studies have shown that Th17 cells are critical for providing

protection against *P. aeruginosa* pneumonia via rapid recruitment of neutrophils to the airways in the absence of opsonophagocytic antibody [9, 10]. These findings suggest that an effective vaccine for providing full-fledged protection against various *P. aeruginosa* infections in different tissues can induce multiple cellular and humoral effectors.

Most clinical isolates of *P. aeruginosa* are motile with the aid of a single polar flagellum, which is essential for systemic spread throughout the organs from the initial site of colonization [11]. Flagellin is the primary protein component of the flagella, which is classified into two distinct serotypes a and b [12]. Furthermore, the conserved domains of flagellin are strongly antigenic and serve as a pathogen-associated molecular pattern (PAMP) that induce a strong NFκB-mediated inflammatory response via toll-like receptor 5 (TLR5) signal transduction [13]. Several studies have shown the strong immunogenicity of flagellin initiates a general recruitment of both T and B cells to secondary lymphoid sites, eliciting $TLR5^+$, $CD11c^+$, and T cell-like similar antigen recognition [14, 15]. Due to TLR5 agonist activity of flagellin, they play an important role as potent adjuvants to enhance protective humoral responses [15, 16]. Several *in vivo* studies not only have demonstrated the importance of flagellins as a crucial virulence factor contributing to the pathogenesis of lung infections but also validated them as target antigens for immunization [17–22]. Immunization with type a or b flagellin provided protection against lung infections [23], keratitis [24], urinary tract, and burn wound infections [25]. These studies have confirmed that protection provided by flagellin is highly type specific and the presence of both types of flagellin is crucial. The results of our recent studies [20, 26] demonstrating protection provided by flagellin in *P. aeruginosa* burn infection via induction of IL-17 encouraged us to study active and passive immunization strategies using bivalent flagellin in order to provide full-fledged protection against various *P. aeruginosa* clinical isolates in the acute fatal pneumonia model.

2. Materials and Methods

2.1. Bacterial Strains. P. aeruginosa strains PAK and PAO1 were used for the purification of type a and b flagellin proteins, respectively.

2.2. Animals. Female 6–8-week-old BALB/C mice were purchased from Pasteur Institute (Tehran, Iran). All animal experiments were complied with institutional animal care committee (IACC) guidelines regarding the use of animals in research.

2.3. Preparation of Recombinant Proteins. Recombinant type a and b flagellin proteins were purified from *E. coli* BL21 (DE3) carrying pET-28a vector as previously described [27, 28].

2.4. Immunization of Mice. Mice were immunized intranasally (i.n.) as described previously. Briefly, mice were anesthetized by mixture of ketamine (6.7 mg/ml) and xylazine (1.3 mg/ml) and then immunized by placing 10 μl of mixed flagellins (1 μg of each flagellin), or flagellin a (2 μg), or flagellin b (2 μg), or PBS on each nostril at weekly intervals. In several published *P. aeruginosa* vaccine studies, PBS has been used as a control [9, 29–31]. At day 42, mice were challenged i.n. with 2×10^7 CFU of *P. aeruginosa* strains directly into each nostril, as described previously [23]. In addition, five mice from each group were sacrificed 24 h after infection. Then the lung, liver, blood, and spleen were harvested for bacterial load enumeration. Bronchoalveolar lavage fluid (BALF) was collected 6 and 18 h after infection for quantitation of CFU, neutrophils, and IL-17 cytokine. For passive immunization, mice were injected intraperitonealy (i.p.) with 200 μl of antibodies raised to bivalent flagellin, or flagellin a, or flagellin b 12 h before and after challenge. All mice were closely monitored for one week.

2.5. Enzyme-Linked Immunosorbent Assay (ELISA). To determine the levels of specific antibodies (total IgG, IgG1, and IgG2a) in mouse sera, ELISA was performed with plates coated with a whole live cell of *P. aeruginosa* strains PAK or PAO1 or mixed flagellins as described previously [20]. Briefly, 100 μl of either *P. aeruginosa* strains PAK or PAO1 or mixed flagellins was incubated overnight at 4°C, washed with 0.5% Tween-PBS (T-PBS), and blocked with PBS + 3% bovine serum albumin (Sigma-Aldrich). Indicated dilutions of sera from immunized mice were incubated overnight at 4°C and washed 3x with T-PBS, and 100 μl of 1 : 7000-diluted horseradish peroxidase-conjugated goat anti-mouse (HRP; Sigma-Aldrich) was incubated (1 h, RT). Plates were then washed five times with T-PBS, and of TMB substrate (Sigma-Aldrich) was added (100 μl/well; 30 min. at RT). Concentrations of serum IgG1 and IgG2a subtypes against mixed flagellins were determined as described above, except that we used 100 μl/well of IgG subtype-specific HRP-conjugated secondary anti-mouse IgG1, or IgG2a antibody (Sigma-Aldrich) diluted 1 : 8000 in 0.5% skim milk/T-PBS.

2.6. Cell Proliferation and Cytokine Measurements. For lymphocyte proliferation assays, ELISA plates were seeded with 1×10^5 T cells, 1×10^5 irradiated (1500 rad) splenocytes isolated from naïve mice as antigen-presenting cells (APCs), and 1 μg of flagellin a, or flagellin b as antigen, while other groups contained 1 μg per well anti-CD4, anti-CD8, and rat IgG isotype (all are from BD Biosciences) antibody. The cells were all cultured in RPMI 1640 containing 10% heat-inactivated FBS. At 24 h and 72 h after incubation, T lymphocyte proliferation assay was carried out using 5-bromo-2-deoxyuridine (BrdU; Roche, Germany) according to the manufacturer's protocol. At the same time, IL-17 levels were measured by examining cell-free culture supernatant fluid using specific ELISA assay (R&D Systems).

2.7. Depletion of Immune Effectors. Immune cell subsets were depleted as described [32]. For *in vivo* CD4 or CD8 T cells, T cell depletion, CD4-specific mAb (GK1.5; BD PharMingen), or CD8-specific mAb (53-6.7; BD PharMingen) were administered both intranasally and intraperitoneally (100 μg/dose and 500 μg/dose, resp.) 72 and 24 hours before bacterial challenge. Depletion of the targeted cell types was confirmed by subsequent FACS analysis, which showed >98% depletion

of the respective cell type. Polyclonal antibody to murine IL-17 was produced by immunizing rabbits at multiple intradermal sites with mouse recombinant IL-17 (R&D Systems) mixed with CFA, as previously described [33]. Affinity chromatography (using protein G) was used for the separation of anti-IL-17 IgG from the whole serum, according to the manufacturers' instructions (Thermo Fisher Scientific, USA). This antibody was specific for IL-17, as determined by ELISA, but did not cross-react IL-2, IFN-γ, IL-4, IL-10, IL-5, or IL-13. The control antibody used in these experiments was the IgG fraction from normal rabbit serum purified by protein G affinity chromatography, as described above. IL-17 depletion studies were done using anti-IL-17 IgG (1 mg i.p.) or control IgG for 3 consecutive days before the mice were challenged by *P. aeruginosa* strains as described by Li et al. [34].

2.8. Opsonophagocytic Activity Assay. The assay was performed as described [20, 25]. Briefly, assays were performed in a sterile microcentrifuge tube 100 μl of each component, polymorphonuclear leukocytes (PMNs; 2×10^9 cells), *P. aeruginosa* strains (5×10^7 CFUs), infant rabbit serum, and diluted antibodies. Generally, ≥50% opsonic killing activity of immune serum is considered biologically significant [10].

2.9. Motility Inhibition Assay. Assays were performed as described [20, 25]. Briefly, antibodies were added to motility agar (LB with 0.3% (*w*/*v*) agar) in 24-well plates (Greiner Bio-One, Germany). *P. aeruginosa* strains ($OD_{600} = 0.2$) were added into the central well of each plate and incubated at 37°C. Mean diameters of bacterial colonies with sharp and less distorted rings were measured after incubating for 18 h.

2.10. Statistical Analysis. All statistical analyses were performed using GraphPad Prism 6 (GraphPad Software Inc., USA). Nonparametric data were analyzed by Kruskal-Wallis followed by Dunn's multiple comparison tests. Parametric data were evaluated by ANOVA with Tukey's multiple comparison tests. All results were expressed as the mean ± standard deviation (SD). The log-rank test was used to compare Kaplan-Meier between different treatment mouse groups. P value of <0.05 was considered statistically significant.

3. Result

3.1. Protective Efficacy of Bivalent Flagellin Immunization. To determine the protective efficacy of the bivalent flagellin vaccine against *P. aeruginosa* strains, immunized mice were challenged i.n. with different flagellated strains of *P. aeruginosa*. As shown in Figures 1(a) and 1(b), nasal immunization with bivalent flagellin protected against lethal pneumonia due to PAK (100% survival) and PAO1 (91.66% survival) and survival rates were all significantly higher than those in mice administered with PBS ($P > 0.01$). Flagellin a-immunized mice were significantly protected ($P > 0.05$) from lethality after challenge with homologous strain PAK with a survival rate of 91.66%, compared to 58.33% for heterologous strain PAO1 (Figures 1(c) and 1(d)). Nasal immunization with flagellin b leads to 83.33% protective effect for homologous strain PAO1 compared with 41.66% in the heterologous PAK challenge ($P > 0.05$; Figures 1(e) and 1(f)). However, provided heterologous protection by flagellin a or flagellin b immunization was significantly higher than that of the controls.

Moreover, we evaluated the efficacy of passive immunization with antisera from bivalent flagellin-, or flagellin a-, or flagellin b-, or PBS-immunized mice against *P. aeruginosa* strains. Bivalent flagellin antisera completely protected mice from challenge with PAK (75% survival) and PAO1 (83.33% survival; Figures 1(a) and 1(b)). Transfer of flagellin a antisera exhibited significant protective effect role against homologous strain PAK (83.33% survival, $P < 0.01$) but only has a partial protective role against heterologous strain PAO1 (25% survival, Figures 1(c) and 1(d)). Passive immunization with flagellin b significantly protected immunized mice against homologous strain PAO1 (75% survival, $P < 0.01$) compared with heterologous strain PAK (16.66% survival, Figures 2(e) and 2(f)). However, provided heterologous protection by antisera to flagellin a or flagellin b was significantly higher than that of the controls ($P < 0.05$; Figures 1(c), 1(d), 1(e), and 1(f)).

3.2. Opsonic Killing Activity of Bivalent Flagellin Immune Sera. To test the functional activity of serum antibodies in the protection afforded by the bivalent flagellin vaccine, we evaluated the *in vitro* opsonic killing activity of pooled sera obtained from immunized mice 3 weeks after the third (final) nasal immunization. As shown in Figure 3, bivalent flagellin antisera at a dilution 1 : 10 significantly promoted the phagocytosis of *P. aeruginosa* strains PAK (82.70%) and PAO1 (86.23%) compared with that of serum isolated from control group mice ($P < 0.01$). Flagellin a antiserum in the immune serum showed significantly higher killing ability against homologous strain PAK (78.61%, $P < 0.01$) in comparison with PAO1 strain (33.56%, Figure 3). Sera from flagellin b-immunized mice had significantly killing activity against homologous strain PAO1 (80.59%, $P < 0.01$), comparable to that against heterologous strain PAK (24.27%, Figure 3). However, the opsonic killing activity of flagellin a or flagellin b antisera against the heterologous strain was significantly higher than that of serum from control mice ($P < 0.05$).

3.3. Antimotility Activity of Bivalent Flagellin Immune Sera. We evaluated the functional activity of bivalent flagellin immune sera to inhibit the motility of different flagellated *P. aeruginosa* strains. As shown in Figures 4(a) and 4(b), bivalent flagellin immune sera at a dilution of 1 : 300 or less completely inhibited the motility of *P. aeruginosa* strains compared with the controls ($P < 0.01$). Antisera to flagellin a at dilution of 1 : 300 or less completely inhibited the motility of the homologous strain ($P < 0.01$), but there was some cross-reactivity with the heterologous strain ($P < 0.05$; Figures 4(a) and 4(b)). Antibodies against flagellin b at dilution of 1 : 300 or less inhibited the motility of homologous strain PAO1 more significantly than heterologous strain PAK ($P < 0.05$; Figures 4(a) and 4(b)).

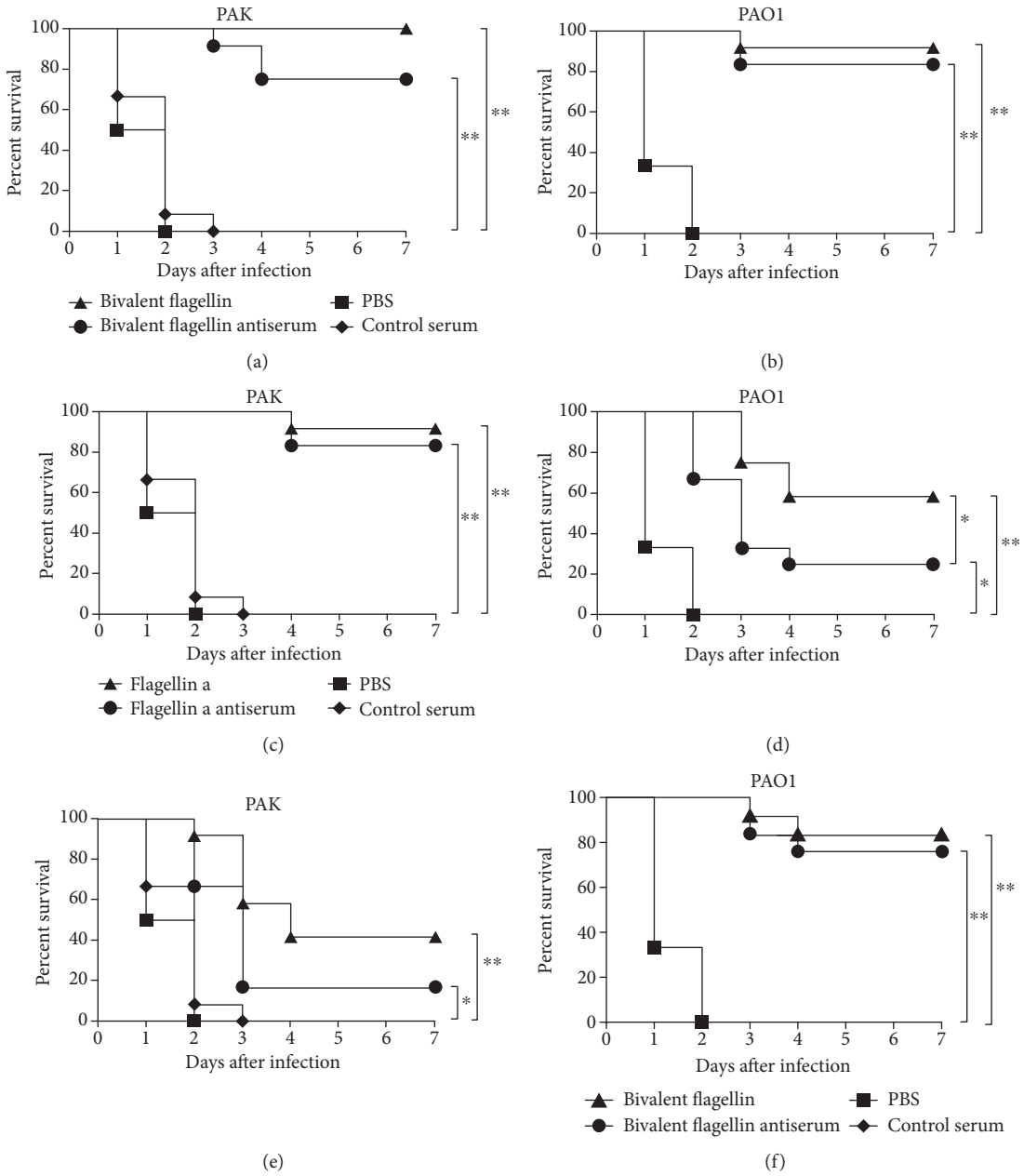

Figure 1: Survival rates of actively and passively immunized BALB/c mice ($n = 12$ mice/group) to infection with *P. aeruginosa* strains. Active and passive immunization against bivalent flagellin (a, b), flagellin a (c, d), and flagellin b (e, f). Kaplan-Meier curves were plotted for mice of the above groups, which were challenged by 2×10^7 CFUs of *P. aeruginosa* strains PAO1 and PAK and monitored the seven day survival rates. $^*P < 0.05$ and $^{**}P < 0.01$.

3.4. Specificity of Antibodies Raised against Bivalent Flagellin. To assess the humoral responses evoked by bivalent flagellin vaccine, we compared serum IgG levels among immunized mice challenged with either the PAK or PAO1 strain. While the prechallenge IgG levels of mice injected with bivalent flagellin against whole live cells of *P. aeruginosa* strains or mixed flagellins were similar, the serum IgG levels significantly increased after infection with PAK or PAO1 strains infection ($P < 0.05$; Figures 5(a), 5(b), and 5(c)). IgG titer in sera from vaccinated mice with type a or b flagellin significantly increased after challenge with the homologous strain compared with that in heterologous strain of *P. aeruginosa* infection ($P < 0.01$; Figures 5(a), 5(b), and 5(c)). Similar results were obtained when IgG1 subtype was examined (Figure 5(d)). Among bivalent flagellin-immunized mice, no significant differences in the titer increases for specific IgG2a subtypes against mixed flagellins were observed in pre- and postchallenge with PAK or PAO1, respectively ($P > 0.05$; Figure 5(e)). IgG2a level in mice immunized with type a or b flagellin was significantly decreased after challenge with the heterologous strain compared with mice challenged with the heterologous strain ($P < 0.05$; Figure 5(e)). The titer of antigen-specific antibodies induced by bivalent flagellin was similar to that induced

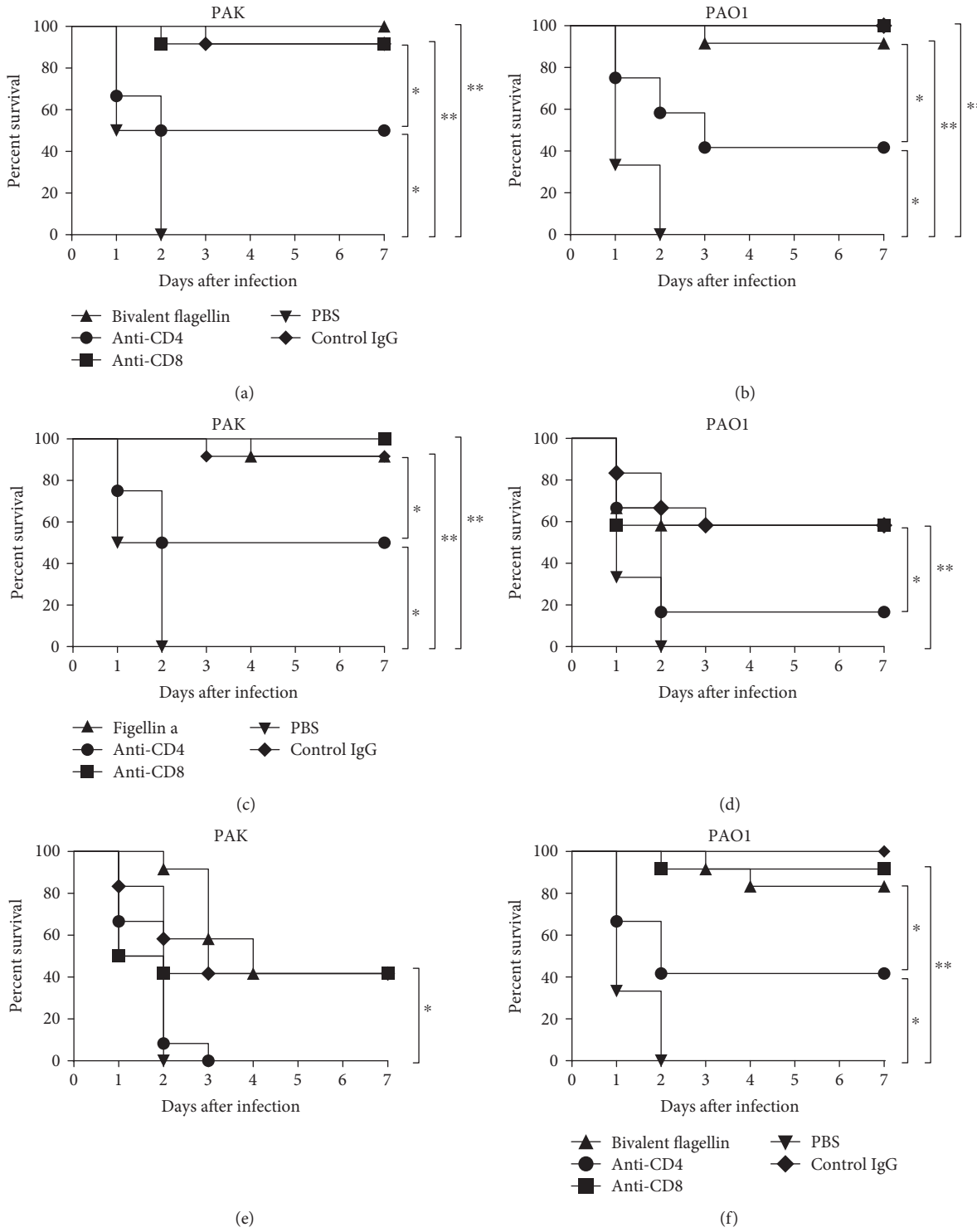

Figure 2: The protective role of $CD4^+$ T lymphocytes in bivalent flagellin vaccine against *P. aeruginosa* strains. Bivalent flagellin- (a, b), flagellin a- (c, d), and flagellin b- (e, f) immunized mice ($n = 12$ mice/group) were treated with either anti-CD8 monoclonal antibody, or anti-CD4 monoclonal antibody, or normal rat IgG and then were challenged with 2×10^7 CFUs of *P. aeruginosa* strains PAO1 and PAK. $^*P < 0.05$ and $^{**}P < 0.01$. NS = nonsignificance.

by flagellin a or b, which indicated that there is no interference among each vaccine component in induction of protective antibodies (data not shown).

3.5. T Cell Responses Induced by Bivalent Flagellin Vaccine. To test whether vaccine candidates could induce lymphocyte proliferation, we analyzed the stimulation index of splenic T

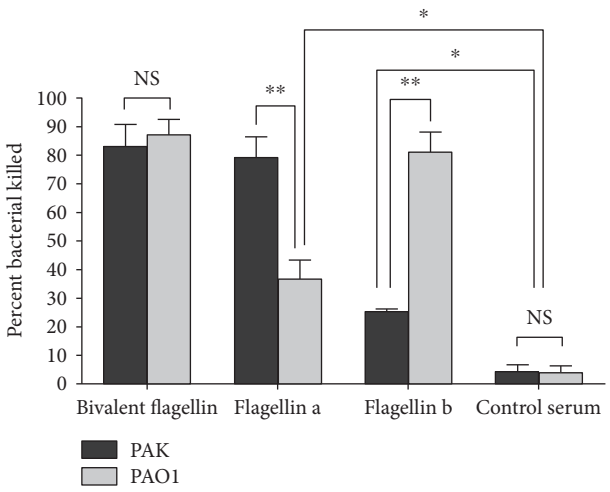

FIGURE 3: The opsonic killing activity of sera from bivalent flagellin-, flagellin a-, and flagellin b-immunized mice 3 weeks after the final immunization. Values presented as the mean of triplicate technical replicates ± SD. $^{*}P < 0.05$ and $^{**}P < 0.01$. NS = nonsignificance.

cells from immunized mice. As shown in Figures 6(a) and 6(b), there was a higher proliferation level of bivalent flagellin immune T cells to either flagellin a or flagellin b at both 24 and 72 h when compared with T lymphocytes isolated from the controls ($P < 0.01$), which means vaccinated T lymphocytes could be stimulated by both types of flagellin without interference. (Figures 6(a) and 6(b); $P < 0.05$). The proliferation rate of flagellin a or b immune T cell cultures stimulated with the homologous antigen at both 24 and 72 h was significantly higher than the cultures stimulated with heterologous antigen (Figures 6(c) and 6(d) and Figures 6(e) and 6(f); $P < 0.01$). Additionally, the proliferation level of flagellin a or b immune T cell cultures stimulated with heterologous antigen was significantly higher than T cells from control mice (Figures 6(c) and 6(d) and Figures 6(e) and 6(f); $P < 0.05$).

In order to further distinguish whether $CD4^+$ T lymphocytes were the immune cells involved in the anti-infection effect by bivalent flagellin vaccine *in vivo*, $CD4^+$ or $CD8^+$ T lymphocytes were depleted independently by corresponding antibodies as described above. We demonstrated that anti-infection activity with the bivalent flagellin immunization relatively abrogate in *in vivo* depletion of $CD4^+$ T lymphocytes. After depletion of $CD4^+$ T lymphocytes in the bivalent flagellin-immunized group, the survival rate decreased to 50% and 41.66% when infected with strain PAK and PAO1, respectively (Figures 2(a) and 2(b)). Also, the survival rate was not decreased compared to the control group when challenged by PAK (Figure 2(a)) and PAO1 (Figure 2(b)), since the killing ability of immune serum against *P. aeruginosa* strains was effective. Depletion of $CD4^+$ T lymphocytes in flagellin a-immunized group decreased the survival rate to 50% and 16.16% when challenged with strain PAK and PAO1, respectively (Figures 2(c) and 2(d)). The survival rate of mice in flagellin b-immunized group after depletion of $CD4^+$ T lymphocytes decreased to 41.66% and 0% when challenged with the strain PAO1 and PAK, respectively (Figures 2(e) and 2(f)). Depletion of $CD8^+$ T lymphocytes showed no effect on the survival rate of immunized mice. Also, the treatment with normal rat IgG showed no effect on the survival rate.

3.6. Th17 Cells and IL-17 Were Activated by Bivalent Flagellin Vaccine. To test whether the bivalent flagellin vaccine could induce IL-17, we evaluated IL-17 production by the $CD4^+$ T cells recovered from immunized mice in the presence of irradiated splenocytes and flagellin a or flagellin b. The levels of IL-17 in the supernatants of the immunized T cells were significantly higher than those of control T cells ($P < 0.05$, Figures 7(a) and 7(b)). The presence of the anti-CD4 monoclonal antibody during coculture returned the IL-17 levels as those of the control T cells, further indicating that $CD4^+$ T cells are the predominant source of IL-17 in this system (Figures 7(a) and 7(b)). The IL-17 levels in the presence of the anti-CD8 monoclonal antibody during coculture had no significant difference between each group (Figures 7(a) and 7(b); $P > 0.05$). IL-17 production by flagellin a- or flagellin b-immunized T cells when stimulated with the homologous antigen was significantly higher than that of T cells stimulated with heterologous antigen ($P < 0.05$; Figures 7(c) and 7(d) and Figures 7(e) and 7(f)). IL-17 production by flagellin a- or flagellin b-immunized T cells when stimulated with heterologous antigen was significantly higher than that of the control T cells ($P < 0.05$; Figures 7(c) and 7(d) and Figures 7(e) and 7(f)). Flagellin a- or flagellin b-immunized T cells when stimulated with homologous or heterologous antigen in the presence of the anti-CD4 monoclonal antibody during coculture returned the IL-17 levels as those of the control T cells. There was no significant difference between the IL-17 levels of flagellin a or flagellin b among cultures treated by either immunized T cells, anti-CD8 monoclonal antibody, or control IgG ($P > 0.05$; Figures 7(c) and 7(d) and Figures 7(e) and 7(f)). T cell proliferation and IL-17 secretion response assays were confirmatory data showing the evidence for a heterologous T cell response among immunized flagellin a or b mice indicating an active clonal expansion and a neutrophil response that lead to higher survival (protective) rates among immunized mice than control mice.

3.7. Bivalent Flagellin Vaccine Decreased P. aeruginosa Strain Burden. In order to evaluate the protective efficacy of bivalent flagellin vaccine, we determined the bacteria number in the lung, liver, blood, and spleen of infected immunized mice. Immunization with bivalent flagellin reduced the PAK and PAO1 strain burden in the lung, liver, blood, and spleen compared with mice injected with PBS ($P < 0.01$; Figures 8(a), 8(b), 8(c), and 8(d)). Immunization with flagellin a significantly decreased homologous strain PAK burden in the main organs and blood compared with the heterologous strain PAO1 burden ($P < 0.05$; Figures 8(a), 8(b), 8(c), and 8(d)). Immunization with flagellin a significantly decreased homologous strain PAO1 burden in the main organs and blood compared with heterologous strain PAK burden ($P < 0.05$; Figures 8(a), 8(b), 8(c), and 8(d)).

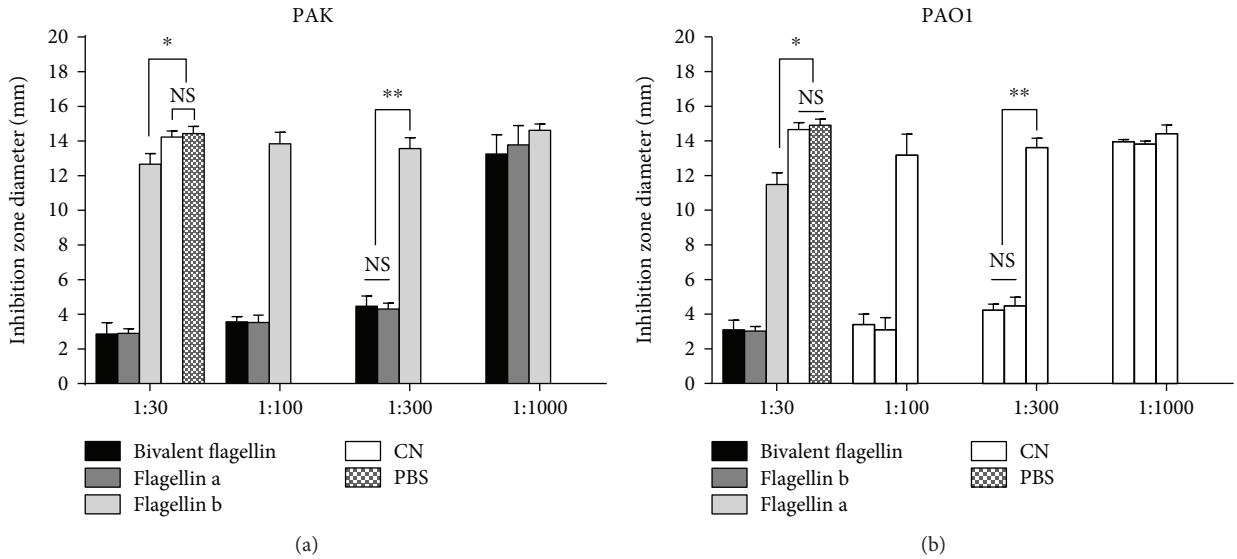

Figure 4: Assessment of motility inhibition of *P. aeruginosa* strains PAK (a) and PAO1 (b) by different dilutions of sera from bivalent flagellin-, flagellin a-, or flagellin b-immunized mice. Motility agar plates are prepared with diluted antibodies in each well prior to stabbing each well with fresh overnight bacterial cultures. The mean diameters of *P. aeruginosa* strains were measured in millimeters (mean + SD). Values presented as mean of triplicate independent experiments ± SD. $^{*}P < 0.05$ and $^{**}P < 0.01$. NS = not significant. CS = control serum.

3.8. Neutrophil Recruitment to the Lungs of Bivalent Flagellin-Immunized Mice. As IL-17 is a critical mediator for neutrophil recruitment to the lung, we evaluated the numbers of neutrophils recruited to the airways in immunized mice. As shown in Figures 9(a), 9(e), and 9(f), in bivalent flagellin-immunized mice, the number of BALF neutrophils and IL-17 levels at 6 h after the challenge were significantly more than those of the controls ($P < 0.05$). At this point in time, the bacteria numbers in the BALF of bivalent flagellin-immunized were significantly lower than those of the controls ($P < 0.05$, Figure 9(c)). IL-17 levels and neutrophil numbers in BALF of the flagellin a- or b-immunized mice obtained 6 h after homologous challenge were significantly higher than those in mice challenged with the heterologous strain ($P < 0.05$; Figures 9(a), 9(e), and 9(f)). In flagellin a- or b-immunized mice, IL-17 levels and neutrophil numbers in BALF obtained 6 h after challenge with the heterologous strain were significantly higher than those in nonimmunized mice ($P < 0.05$; Figures 9(a), 9(e), and 9(f)). At this point in time, the heterologous strain numbers in the BALF of flagellin a- or b-immunized mice were significantly lower than those in mice challenged with the heterologous strain. ($P < 0.05$, Figure 9(c)). At 18 h after bacterial challenge, the number of BALF neutrophils and bacterial CFU in bivalent flagellin-immunized mice was significantly lower than that of the controls ($P < 0.05$; Figures 9(b) and 9(d)). IL-17 levels and neutrophil in BALF of the flagellin a- or b-immunized mice obtained 18 h after homologous challenge were significantly higher than those in mice challenged with the heterologous strain ($P < 0.05$; Figures 9(b), 9(e), and 9(f)). At this point in time, the heterologous strain numbers in the BALF of flagellin a- or b-immunized mice were significantly lower than those in mice challenged with the heterologous strain. ($P < 0.05$, Figure 9(d)).

3.9. Effect of Neutralization of IL-17 on Protective Efficacy of Bivalent Flagellin Vaccine. To further assess the protective role of IL-17 in the bivalent flagellin vaccine efficacy, we investigated the effects of neutralization of IL-17 prior to lung challenge with *P. aeruginosa* strains. As shown in Figures 10(a) and 10(b), mortality in the bivalent flagellin-immunized mice which received anti-IL-17 IgG was significantly higher than that given in the control IgG ($P < 0.05$). In flagellin a-immunized group, the survival rate decreased to 50% and 8.33% after receiving anti-IL-17 IgG when challenged with the strains PAK and PAO1, respectively (Figures 10(c) and 10(d)). In flagellin b-immunized group, the survival rate decreased to 41.66% and 0% after receiving anti-IL-17 IgG when challenged with the strains PAO1 and PAK, respectively (Figures 10(e) and 10(f)).

4. Discussion

Pulmonary infections due to *P. aeruginosa* have emerged as a serious challenge for medical therapy, mainly due to the paucity of new effective antibiotic classes and high morbidity and mortality [35]. This terrible situation has motivated attention in the vaccine, a possible approach to combat *P. aeruginosa*. In addition, the complex pathogenicity of *P. aeruginosa* and the diverse function of its virulence factors represent major obstacles to the development of effective universal vaccines [36]. For full-fledged protection against various *P. aeruginosa* infection, incorporation of innate and adaptive immune system is crucial. In lung tissue, a combination of opsonizing antibodies and inflammatory responses of the innate immune cell is mediated full-fledged protection against *P. aeruginosa* [34]. Thus, antigens in an effective vaccine against *P. aeruginosa* infections should induce both humoral and cellular immune responses. Although several *P. aeruginosa*

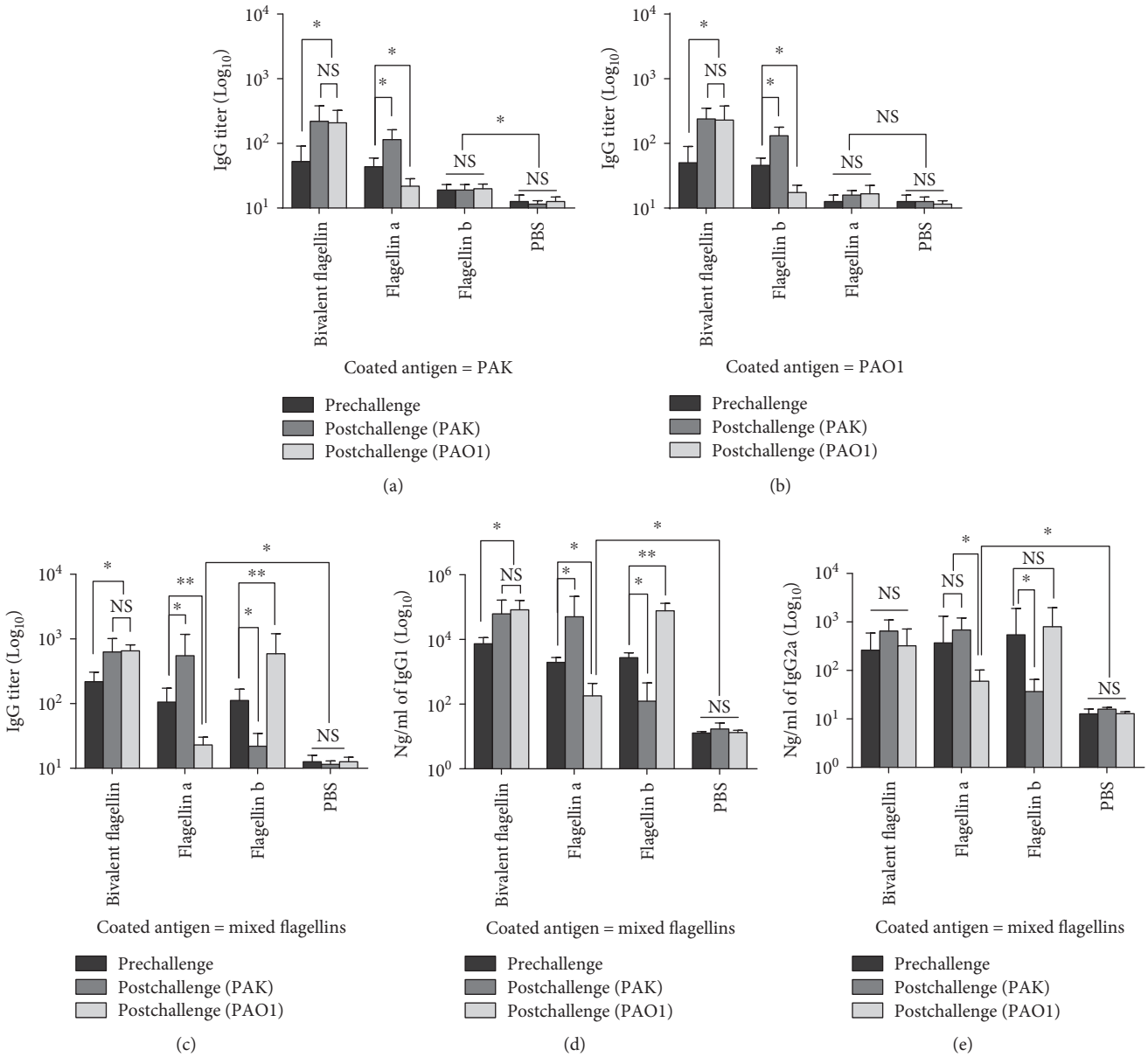

Figure 5: Effects of bivalent flagellin immunization on pre and postchallenge levels of serum total IgG against the whole cell of *P. aeruginosa* PAK (a), PAO1 (b), and mixed flagellins (c). The pre- and postchallenge serum IgG1 (d) and IgG2a (e) titers against mixed flagellins. Values are represented as mean ± SD based on five mice in each group. $^{*}P < 0.05$ and $^{**}P < 0.01$. NS = nonsignificance.

antigens have so far been evaluated as *P. aeruginosa* vaccine candidates, flagellin proteins hold a greatest promise because these *P. aeruginosa* components evoke *in vivo* immune responses which in turn promote opsonophagocytic activity [25]. They are also vital for *P. aeruginosa* survival during infection and are expressed by the majority of clinical *P. aeruginosa* strains [26]. Moreover, flagellin promotes marked increases in T and B lymphocyte recruitment to secondary lymphoid sites, increasing the likelihood of these cells encountering their specific antigen, and can also directly stimulate $CD4^+$ and $CD8^+$ T cells [14, 15].

Here, we have shown that bivalent flagellin vaccine provided significant homologous and heterologous protection against fatal *P. aeruginosa* pneumonia and it was associated with antiopsonophagocytic killing and antimotility activities as well as an effector IL-17 cytokine response. Indeed, the antiopsonophagocytic killing and antimotility activities provided by bivalent flagellin antiserum to blunt the pathogenesis and invasive progression of infection coupled with the effector cytokines of Th17 cells augmented a broader spectrum of protective activity against *P. aeruginosa*-induced fatal pneumonia. Evaluation of various aspects of mouse immune response and protective efficacy of the vaccine in a murine acute pneumonia model indicated robust protection against potentially lethal *P. aeruginosa* infections.

The cytokine secretion of splenic T cells indicated that bivalent flagellin could induce efficient Th17 type cytokines by antigen stimulation in combination with the findings that

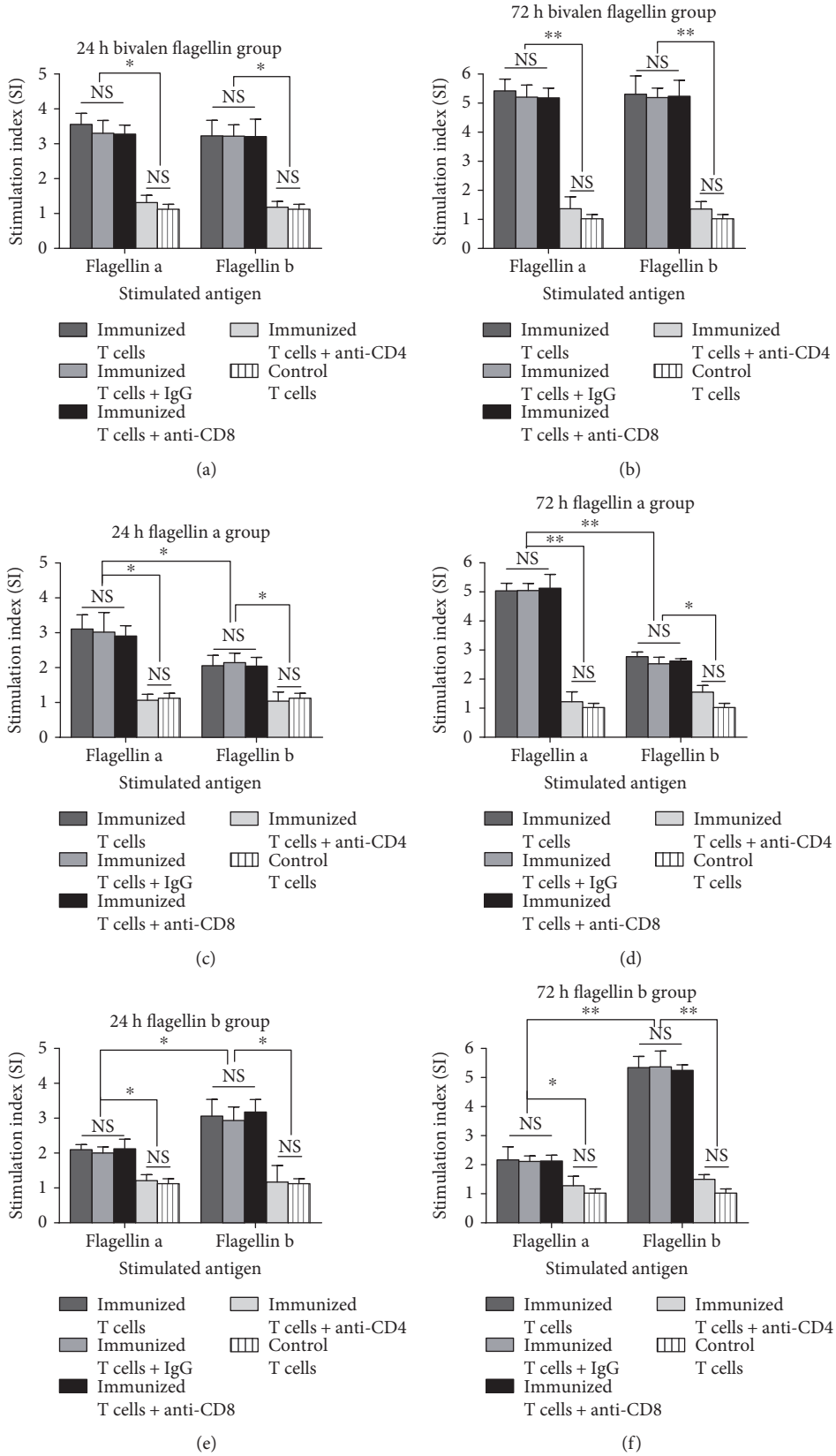

Figure 6: Proliferative assay of immune splenic T cells from bivalent flagellin (a, b), flagellin a (c, d), and flagellin b (e, f) stimulated with antigens *in vitro* for 24 h and 72 h. Values are represented as mean ± SD based on five mice in each group. $^{*}P < 0.05$ and $^{**}P < 0.01$. NS = nonsignificance.

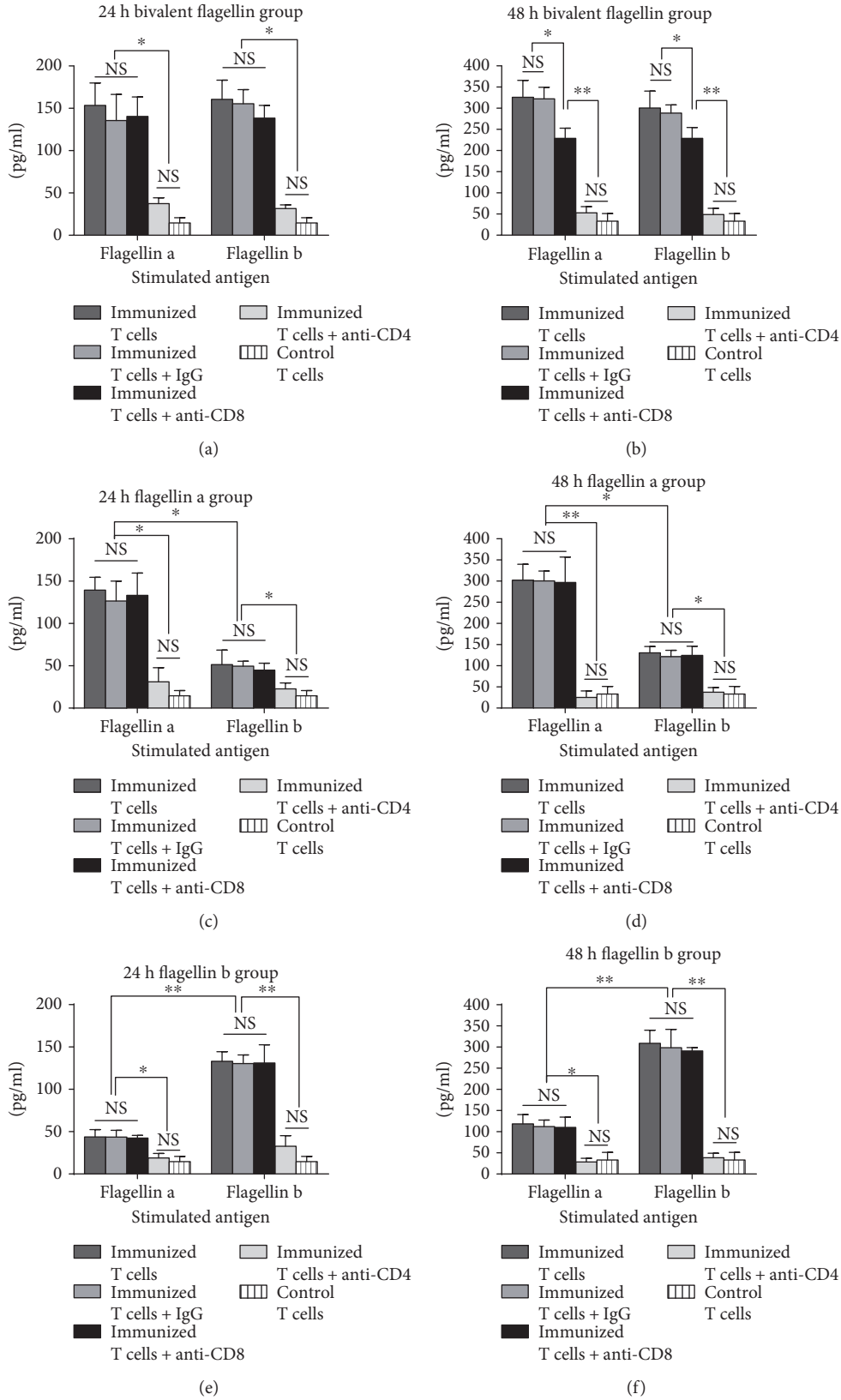

Figure 7: Effects of active immunization with bivalent flagellin on IL-17 production of immune splenic T cells from bivalent flagellin (a, b), flagellin a (c, d), and flagellin b (e, f) at 24 h and 48 h after stimulation with flagellin a or flagellin b. Values represented as mean ± SD based on five mice in each group. $^{*}P < 0.05$ and $^{**}P < 0.01$. NS = nonsignificance.

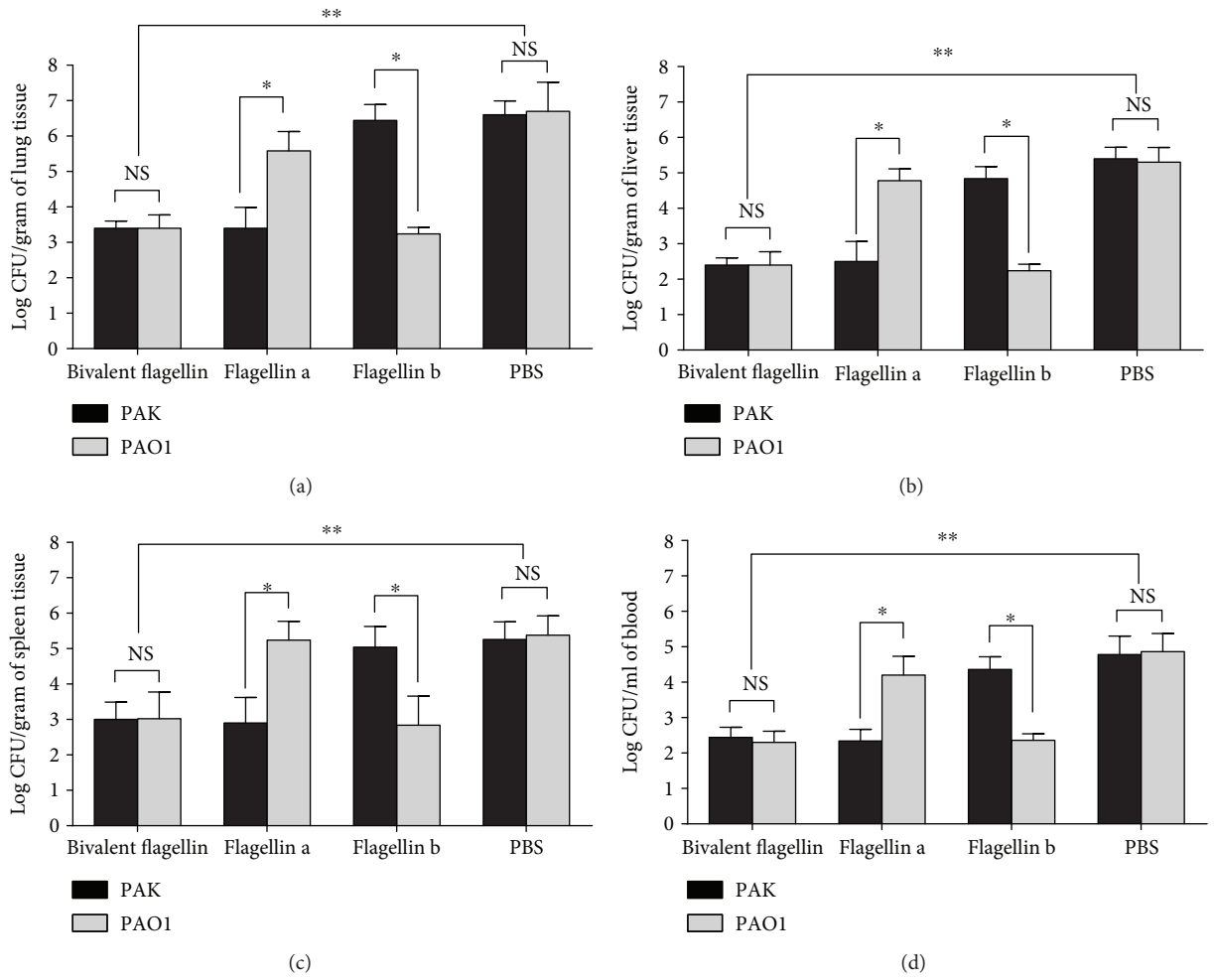

Figure 8: The effect of nasal immunization with bivalent flagellin, flagellin a, and flagellin b on the local and systemic spread of *P. aeruginosa* strains PAK and PAO1. Bacterial load was determined as CFUs (log) in the lung (a), liver (b), spleen (c), and blood (d). Values represented as mean ± SD based on five mice in each group. $^{*}P < 0.05$ and $^{**}P < 0.01$. NS = nonsignificance.

IgG1 and IgG2a subtypes in the serum of immunized mice further confirm that flagellin evokes the development of humoral and cell-mediated immune responses and acquires greater efficacy than monovalent flagellin to provide protection against different flagellated strains of *P. aeruginosa*. These data suggested that collaboration of $CD4^+$ T cells with the capacity to produce IL-17 and opsonic antibodies is required for protective immunity against acute *P. aeruginosa* pneumonia [37, 38]. The protective immune response following *P. aeruginosa* immunization of rats is associated with $CD4^+$ T cell-dependent immunity [39]. *P. aeruginosa* immunization of mice pulsed DCs protecting mice against pulmonary infection, depending on the presence of $CD4^+$ T cells [38].

It must so be mentioned that IL-17 was recently shown to be a critical factor in a vaccine that induced protection to *P. aeruginosa* [10]. IL-17 mainly mediates its immune regulatory function by promoting the production of antimicrobial peptides from lung epithelia or of proinflammatory cytokines and chemokines, which leads to the attraction of neutrophils and macrophages to the lung and the subsequently increased phagocytosis of bacteria and enhanced clearance of infection [9, 10, 40]. Early increased neutrophil number in bivalent flagellin-immunized mouse lung tissue is associated with a rapid reduction of bacterial load in lung tissue as well as in homologous and heterologous protection. Our data suggest that $CD4^+$ T cells may be one of the sources of IL-17 during acute pulmonary *P. aeruginosa* infection and could be a key component of full immunity to lung infection by this pathogen [41, 42]. A recent study has shown that $\gamma\delta$ T cells produced IL-17 in the lungs as early as 2 h after *Bordetella pertussis* infection [43]. The level of IL-17 increased 6 h after infection, demonstrating that acute pulmonary infection with *P. aeruginosa* rapidly induced IL-17 production in the lungs; this IL-17 may be involved in the innate immune response to the infection [44, 45].

Also, T cells from nasally immunized mice with live-attenuated *P. aeruginosa* vaccine show a high IL-17 levels after antigen stimulation and high number of $CD4^+$IL-17^+Th17 cells in the spleen at 6 h after challenge and mediated protective immune responses [34]. Although the focus of studies examining IL-17 production has largely been on $CD4^+\alpha\beta$ T cells, $\gamma\delta$ T cells have also been shown to be a potent source of IL-17 and, in some cases, produce more

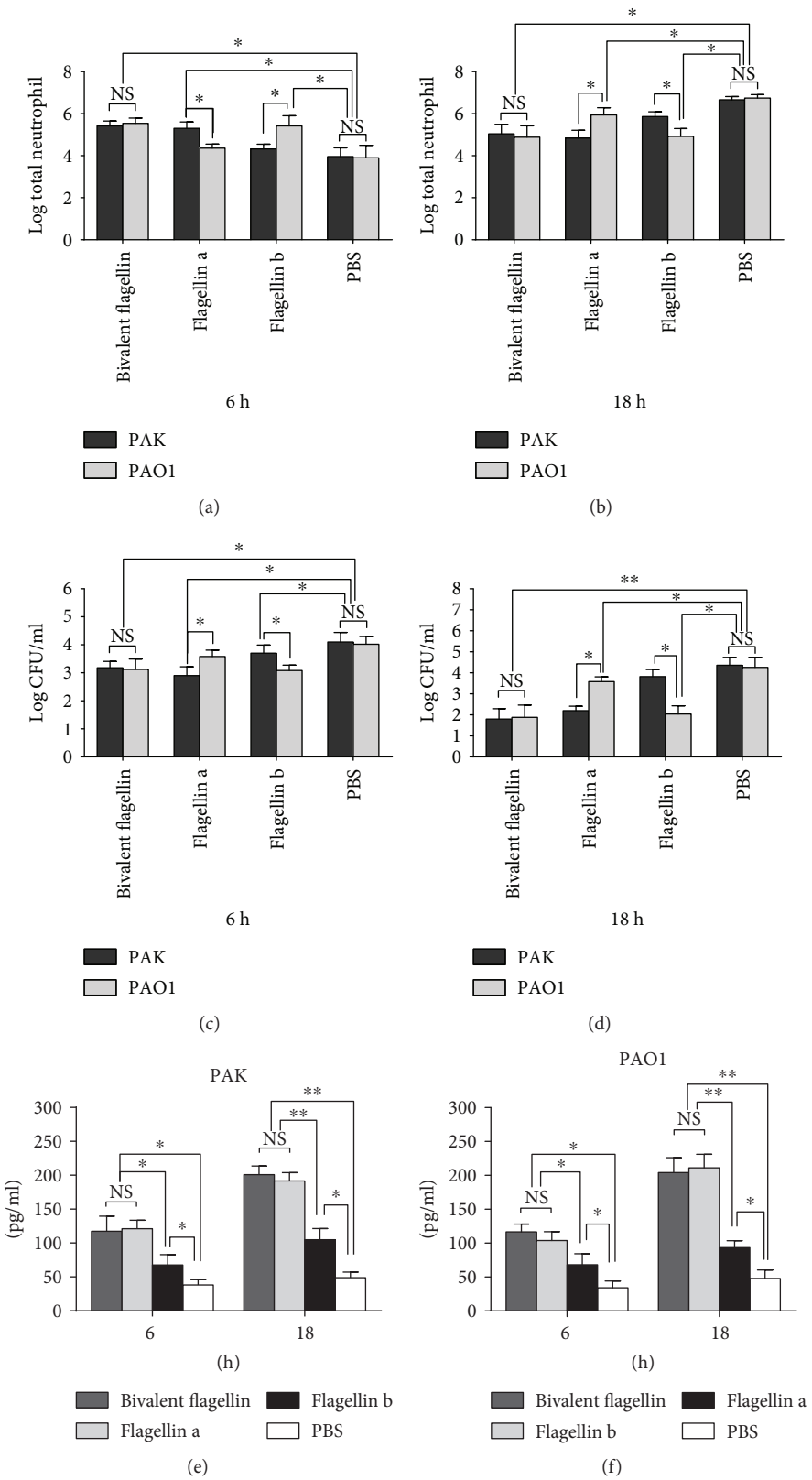

Figure 9: Total BALF neutrophils at 6 h (a) and 18 h (b) after infection of immune and nonimmune mice with *P. aeruginosa* strains PAK and PAO1. The bacterial CFU in BALF at 6 h (a) and 18 h (b) after infection of immune and nonimmune mice with PAK (e) and PAO1 (f). IL-17 level in BALF at 6 h (a) and 18 h (b) after infection of immune and nonimmune mice with PAK (e) and PAO1 (f). Values represented as mean ± SD based on five mice in each group. $^{*}P < 0.05$ and $^{**}P < 0.01$. NS = nonsignificance.

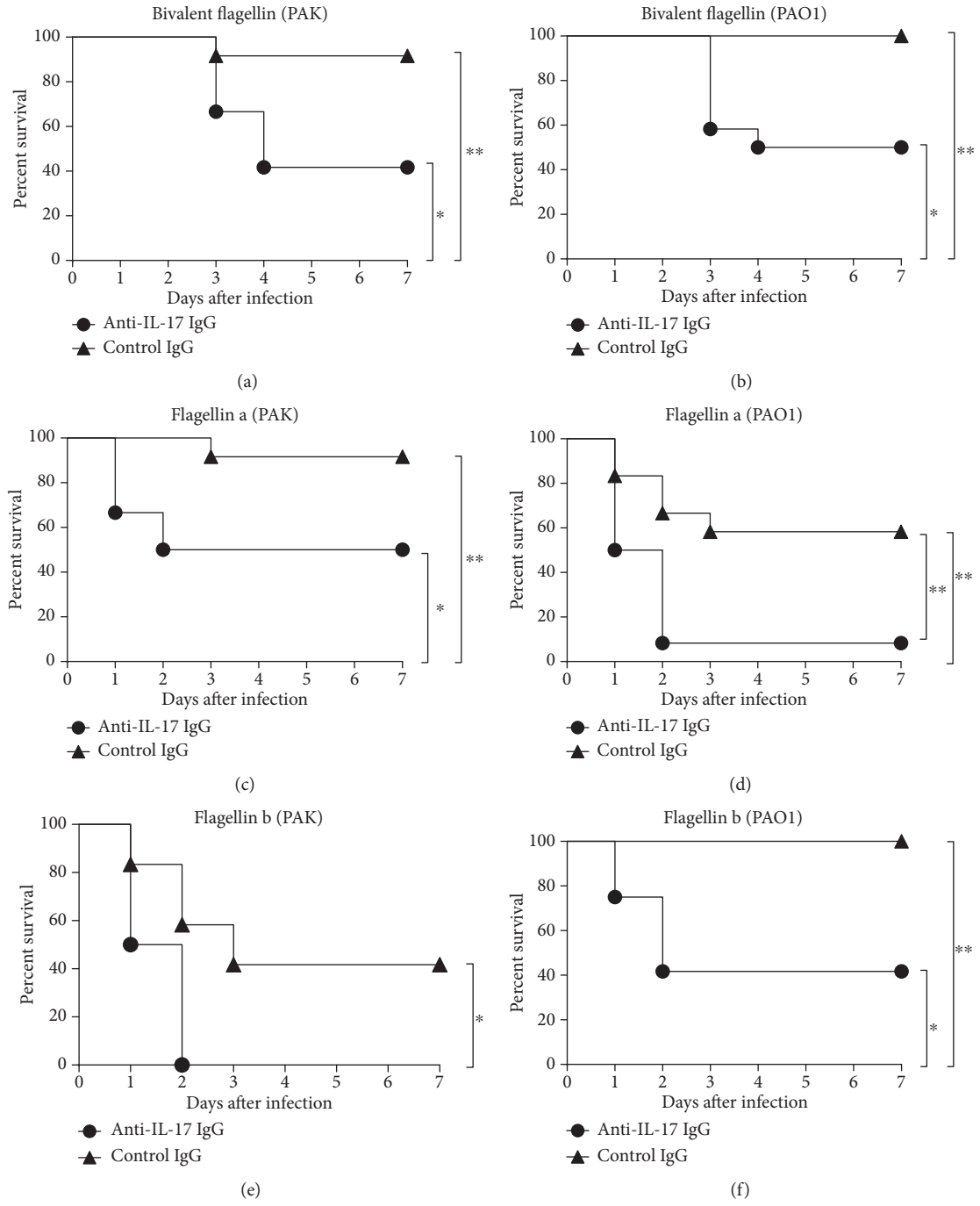

Figure 10: The role of IL-17 in vaccine based protection against *P. aeruginosa* strains. Bivalent flagellin- (a, b), flagellin a- (c, d), and flagellin b- (e, f) immunized mice ($n = 12$ mice/group) were given IL-17 IgG or control IgG for 3 consecutive days prior to challenge with 2×10^7 CFUs of *P. aeruginosa* strains PAO1 and PAK. $^*P < 0.05$ and $^{**}P < 0.01$.

IL-17 than $\alpha\beta$ T cells [46–49]. Interestingly, it has been shown that Th17 cells increase after 8 h of infection with *P. aeruginosa*, and the level of IL-23 also increases in the acute pulmonary *P. aeruginosa* infection [44]. Recent studies suggest that IL-23 promotes the Th17 cell development from effector memory $CD4^+$ cells. The major cell type in the lung responsible for the clearance of *P. aeruginosa* is the neutrophil [9, 50]. Protection achieved in the killed *P. aeruginosa*-immunized animals was associated with $CD4^+IL\text{-}17^+Th17$ and rapid requirement of neutrophil in the lung [51]. The lower bacterial burden in the liver, spleen, and blood showed that the antibodies to bivalent flagellin could systemically disrupt the dissemination of both *P. aeruginosa* stains in the liver and spleen via the blood by inhibition of bacterial motility at the site of infection, which is the principal mechanism of protection in the bloodstream infections following *P. aeruginosa* acute pneumonia model [17, 18, 52]. Although the antibodies against type a or b flagellin completely inhibited

the motility of the homologous strain, they also had slight effects on the heterologous strain. The results of motility inhibition and opsonophagocytic activities indicated that the protective effect of antibodies against either type a or b flagellin is strain specific. Passive transfer of bivalent flagellin antisera protected mice against infection with both flagellated strains of *P. aeruginosa*. The achieved results are also consistent with several investigations that employed a burn wound model to show that passive immunization with antibodies raised to type a or b flagellin protects the infected mice with the homologous strain [53, 54]. The protection provided by antibodies raised against flagellin is highly type specific, and the presence of antibodies to both flagellin types is critical. Thus, antibodies against bivalent flagellin showed a great activity against two different *P. aeruginosa* strains and did not interfere with the individual components for improving the opsonophagocytic killing and immobilizing different flagellated strains of *P. aeruginosa*. Hence, immunotherapy with the antibodies to bivalent flagellin is more successful in providing homologous and heterologous protection than therapy with antibodies raised to each monovalent type a or b flagellin. Also, immunization with our novel bivalent flagellin vaccine does not interfere with the individual components in improving survival or induction of protective antibodies. We acknowledge that our protective efficacy data are contrary to Campodonico et al. [23], who exposed that antibodies against type a or b flagellin had a low protective activity against the homologous strain and no activity against the heterologous strain. It seems feasible that the apparent data discrepancy might be explained by our approach using the full-length type a and b flagellins as the target antigen of the study. In addition, Campodonico et al. separately examined the effects of type a and b flagellins but did not assess bivalent flagellin [23]. Our finding that antibodies against type a or b flagellin show high activity against homologous strains and low activity against a heterologous strain is contrary to a recent report [23], in which it was shown that antitype a flagellin antibodies against homologous *P. aeruginosa* strain have low opsonic killing activity and no killing activity. They also reported that type b flagellin antibodies have no opsonic killing activity against either homologous or heterologous strain [23]. The apparent discrepancy may partially be explained by utilizing a mixture of full-length type a and b flagellins (containing N′ and C′-terminal domains) as immunogen, rather than flagellin subunits, and might account for the protective antibody response observed in our study. It is also worth mentioning that several reports have shown that both N′- and C′-termini of flagellin protein have proinflammatory motifs [55, 56] and both trigger activation of the innate immune response via TLR5 that enhances protective inflammatory response and enhance recruitment of PMNs and facilitate *Pseudomonas* clearance postinfection [57]. Also, previous studies have shown that flagellin mutant bacteria elicited severe mucosal damage by a mechanism that also appears to involve the induction of apoptosis in the epithelial cells via inhibition of NF-κB activation [58, 59]. The TLR5 activation via flagellin may prevent bacteria to evade the host's innate immune responses and alter the level of tissue damage associated with late-stage bacterial infection [60]. After colonization, *P. aeruginosa* downregulates the expression levels of flagella to evade from the TLR5-mediated host's innate immune activation [61]. *H. pylori* may have evolved to express inactive flagellin to prevent activation of the TLR5-mediated host's mucosal immunity, enabling persistent infection in the stomach epithelia [62]. Also, Campodonico et al.'s 2011 report demonstrated that conjugation of polymannuronic acid (PMA) to type a flagellin enhanced its immunogenicity via TLR5, indicating desirable protective antibodies were elicited and conserved mechanism of innate immune resistance to *P. aeruginosa* [63]. These observations have important implications for use of flagellin vaccine rather than flagella against flagellated pathogens. It seems that activation of TLR5 may induce the protective immunity against *P. aeruginosa* and decrease the risk to acquire infections from other flagellated bacteria that activate TLR5 [23, 63]. Lastly, we acknowledge that our findings are contrary to the 2010 report [23], which concluded that flagella are a better candidate to provide protection against infection because they observed that antitype a flagellin and antitype b flagellin antibodies have poor protective activity against homologous or heterologous *P. aeruginosa* strains. Several reports, however, have demonstrated that flagellin-induced antibodies raised against a or b type flagellins have protective activity in various murine infection models [53, 64, 65]. Indeed, one novel feature of our approach is targeting both domains of full-length type a and b flagellins, as target antigen, protective anti-flagellin antibodies, as well as inducing $CD4^+IL\text{-}17^+Th17$ cell response among immunized mice indicating an active clonal expansion and a neutrophil response that leads to higher survival (protective) rates among immunized mice than control mice.

It is also worth indicating that the active immunization with type a or b flagellin provided significantly protected mice against the heterologous strain than passive therapy with antibodies raised to type a or b flagellin. This phenomenon indicated that $CD4^+IL\text{-}17^+Th17$ cell-mediated immune response might be responsible for the anti-infection activity afforded by the bivalent flagellin when antiopsonophagocytic killing and antimotility antibody levels were low. Also, *in vivo* $CD4^+$ T cell depletion during immunization diminished the bivalent flagellin or type a or b flagellin vaccine-based protection against *P. aeruginosa* infection. However, the depletion of CD8 lymphocytes showed no abrogation of the anti-infection activity against the *P. aeruginosa* strains. The result of present study demonstrated the fact that both adaptive ($CD4^+$ T cells and antibodies) and innate (macrophage and neutrophil) effectors are required for protective immunity against *P. aeruginosa* strains. T cell proliferation and IL-17 secretion response assays were confirmatory data showing the evidence for a heterologous T cell response among immunized flagellin a or b mice indicating an active clonal expansion and a neutrophil response that leads to higher survival (protective) rates among immunized mice than control mice. A recent study demonstrated that protection mediated by PopB immunization against *P. aeruginosa* pneumonia is associated with increased IL-17 cytokine whereas antisera to PopB had neither opsonophagocytic nor anticytotoxic activity [9]. An important feature of a desirable vaccine for

P. aeruginosa is the ability to induce IL-17 for rapid recruitment of neutrophils to the site of infection, where they can mediate opsonophagocytic bacterial killing. In a recent research [25], we demonstrated that bivalent flagellin vaccine could confer protection against burn wound infection with different flagellated strains of *P. aeruginosa*, by eliciting an effective humoral immune response, including improved opsonophagocytic killing and an immobilization of the pathogen at the wound site. Following burn injury, the failure of local and systemic cellular immune responses allows pathogenic bacteria to disseminate systemically from the site of infection to the bloodstream and easily escalate into sepsis. Thus, it seems that protective immune response against *P. aeruginosa* burn wound infection is mediated by opsonic antibodies. Hence, flagellin is a unique feature because of its ability to induce both cellular and humoral immune responses, which in turn provides protection against different *P. aeruginosa* infections.

Taken together, these results offer evidence that bivalent flagellin vaccine can confer protection against different flagellated strains of *P. aeruginosa* infection in a burn wound model by eliciting effective cellular and humoral immune responses, including induction of IL-17 and improved opsonophagocytic killing. Thus, reducing the systemic pathogen dissemination caused an increase in the survival of mice infected with *P. aeruginosa*. Moreover, these data further confirmed that targeting both types of flagellin with antibodies resulted in significantly improved efficacy in comparison with each monovalent antigen with the potential of broadening the coverage against *P. aeruginosa* strains which might not express one of the two targets. We maintain optimism that an effective *P. aeruginosa* bivalent flagellin vaccine may eventually be developed and tested in humans toward reducing the morbidity and mortality associated with lung infections caused by *P. aeruginosa*.

Conflicts of Interest

There are no conflicts of interest.

References

[1] P. H. Gilligan, "Infections in patients with cystic fibrosis: diagnostic microbiology update," *Clinics in Laboratory Medicine*, vol. 34, no. 2, pp. 197–217, 2014.

[2] N. Safdar, C. Dezfulian, H. R. Collard, and S. Saint, "Clinical and economic consequences of ventilator-associated pneumonia: a systematic review," *Critical Care Medicine*, vol. 33, no. 10, pp. 2184–2193, 2005.

[3] B. K. Chan, M. Sistrom, J. E. Wertz, K. E. Kortright, D. Narayan, and P. E. Turner, "Phage selection restores antibiotic sensitivity in MDR *Pseudomonas aeruginosa*," *Scientific Reports*, vol. 6, p. 26717, 2016.

[4] M. W. Douglas, K. Mulholland, V. Denyer, and T. Gottlieb, "Multi-drug resistant *Pseudomonas aeruginosa* outbreak in a burns unit—an infection control study," *Burns : Journal of the International Society for Burn Injuries*, vol. 27, no. 2, pp. 131–135, 2001.

[5] M. Mudau, R. Jacobson, N. Minenza et al., "Outbreak of multidrug resistant *Pseudomonas aeruginosa* bloodstream infection in the haematology unit of a South African academic hospital," *PLoS One*, vol. 8, no. 3, article e55985, 2013.

[6] G. B. Pier, "Promises and pitfalls of *Pseudomonas aeruginosa* lipopolysaccharide as a vaccine antigen," *Carbohydrate Research*, vol. 338, no. 23, pp. 2549–2556, 2003.

[7] E. T. Weimer, H. Lu, N. D. Kock, D. J. Wozniak, and S. B. Mizel, "A fusion protein vaccine containing OprF epitope 8, OprI, and type A and B flagellins promotes enhanced clearance of nonmucoid *Pseudomonas aeruginosa*," *Infection and Immunity*, vol. 77, no. 6, pp. 2356–2366, 2009.

[8] T. Sawa, T. L. Yahr, M. Ohara et al., "Active and passive immunization with the Pseudomonas V antigen protects against type III intoxication and lung injury," *Nature Medicine*, vol. 5, no. 4, pp. 392–398, 1999.

[9] W. Wu, J. Huang, B. Duan et al., "Th17-stimulating protein vaccines confer protection against *Pseudomonas aeruginosa* pneumonia," *American Journal of Respiratory and Critical Care Medicine*, vol. 186, no. 5, pp. 420–427, 2012.

[10] G. P. Priebe, R. L. Walsh, T. A. Cederroth et al., "IL-17 is a critical component of vaccine-induced protection against lung infection by lipopolysaccharide-heterologous strains of *Pseudomonas aeruginosa*," *Journal of Immunology*, vol. 181, no. 7, pp. 4965–4975, 2008.

[11] J. Haiko and B. Westerlund-Wikstrom, "The role of the bacterial flagellum in adhesion and virulence," *Biology*, vol. 2, no. 4, pp. 1242–1267, 2013.

[12] H. C. Ramos, M. Rumbo, and J. C. Sirard, "Bacterial flagellins: mediators of pathogenicity and host immune responses in mucosa," *Trends in Microbiology*, vol. 12, no. 11, pp. 509–517, 2004.

[13] F. Hayashi, K. D. Smith, A. Ozinsky et al., "The innate immune response to bacterial flagellin is mediated by Toll-like receptor 5," *Nature*, vol. 410, no. 6832, pp. 1099–1103, 2001.

[14] S. K. Gupta, P. Bajwa, R. Deb, M. M. Chellappa, and S. Dey, "Flagellin a toll-like receptor 5 agonist as an adjuvant in chicken vaccines," *Clinical and Vaccine Immunology : CVI*, vol. 21, no. 3, pp. 261–270, 2014.

[15] S. Delavari, M. Sohrabi, M. S. Ardestani et al., "*Pseudomonas aeruginosa* flagellin as an adjuvant: superiority of a conjugated form of flagellin versus a mixture with a human immunodeficiency virus type 1 vaccine candidate in the induction of immune responses," *Journal of Medical Microbiology*, vol. 64, no. 11, pp. 1361–1368, 2015.

[16] E. T. Weimer, S. E. Ervin, D. J. Wozniak, and S. B. Mizel, "Immunization of young African green monkeys with OprF epitope 8-OprI-type A- and B-flagellin fusion proteins promotes the production of protective antibodies against nonmucoid *Pseudomonasaeruginosa*," *Vaccine*, vol. 27, no. 48, pp. 6762–6769, 2009.

[17] D. Drake and T. C. Montie, "Protection against *Pseudomonas aeruginosa* infection by passive transfer of anti-flagellar serum," *Canadian Journal of Microbiology*, vol. 33, no. 9, pp. 755–763, 1987.

[18] H. Ochi, H. Ohtsuka, S. Yokota et al., "Inhibitory activity on bacterial motility and in vivo protective activity of human monoclonal antibodies against flagella of Pseudomonas aeruginosa," *Infection and Immunity*, vol. 59, no. 2, pp. 550–554, 1991.

[19] M. J. Rosok, M. R. Stebbins, K. Connelly, M. E. Lostrom, and A. W. Siadak, "Generation and characterization of murine antiflagellum monoclonal antibodies that are protective

against lethal challenge with Pseudomonas aeruginosa," *Infection and Immunity*, vol. 58, no. 12, pp. 3819–3828, 1990.

[20] B. Behrouz, M. Mahdavi, N. Amirmozafari et al., "Immunogenicity of *Pseudomonas aeruginosa* recombinant b-type fagellin as a vaccine candidate: protective efficacy in a murine burn wound sepsis model," *Burns : Journal of the International Society for Burn Injuries*, 2016.

[21] H. Ahmadi, B. Behrouz, G. Irajian, N. Amirmozafari, and S. Naghavi, "Bivalent flagellin immunotherapy protects mice against *Pseudomonas aeruginosa* infections in both acute pneumonia and burn wound models," *Biologicals : Journal of the International Association of Biological Standardization*, vol. 46, pp. 29–37, 2017.

[22] M. Saffari, S. Behbood, G. Irajian, A. Khorshidi, R. Moniri, and B. Behrouz, "Antibodies raised against divalent type b flagellin and pilin provide effective immunotherapy against *Pseudomonas aeruginosa* infection of mice with burn wounds," *Biologicals : Journal of the International Association of Biological Standardization*, vol. 45, pp. 20–26, 2017.

[23] V. L. Campodonico, N. J. Llosa, M. Grout, G. Doring, T. Maira-Litran, and G. B. Pier, "Evaluation of flagella and flagellin of *Pseudomonas aeruginosa* as vaccines," *Infection and Immunity*, vol. 78, no. 2, pp. 746–755, 2010.

[24] A. Kumar, L. D. Hazlett, and F. S. Yu, "Flagellin suppresses the inflammatory response and enhances bacterial clearance in a murine model of *Pseudomonas aeruginosa* keratitis," *Infection and Immunity*, vol. 76, no. 1, pp. 89–96, 2008.

[25] P. Laghaei, F. B. Hashemi, G. Irajian, F. Korpi, N. Amirmozafari, and B. Behrouz, "Immunogenicity and protective efficacy of *Pseudomonas aeruginosa* type a and b flagellin vaccines in a burned mouse model," *Molecular Immunology*, vol. 74, pp. 71–81, 2016.

[26] F. Korpi, G. Irajian, M. Mahadavi et al., "Active immunization with recombinant PilA protein protects against Pseudomonas aeruginosa infection in a mouse burn wound model," *Journal of Microbiology and Biotechnology*, 2015.

[27] G. Goudarzi, M. Sattari, M. H. Roudkenar, M. Montajabi-Niyat, A. Zavaran-Hosseini, and K. Mosavi-Hosseini, "Cloning, expression, purification, and characterization of recombinant flagellin isolated from *Pseudomonas aeruginosa*," *Biotechnology Letters*, vol. 31, no. 9, pp. 1353–1360, 2009.

[28] B. Behrouz, N. Amirmozafari, N. Khoramabadi, M. Bahroudi, P. Legaee, and M. Mahdavi, "Cloning, expression, and purification of *Pseudomonas aeruginosa* flagellin, and characterization of the elicited anti-flagellin antibody," *Iranian Red Crescent Medical Journal*, vol. 18, no. 6, article e28271, 2016.

[29] A. DiGiandomenico, J. Rao, K. Harcher et al., "Intranasal immunization with heterologously expressed polysaccharide protects against multiple *Pseudomonas aeruginosa* infections," *Proceedings of the National Academy of Sciences of the United States of America*, vol. 104, no. 11, pp. 4624–4629, 2007.

[30] S. Farajnia, S. N. Peerayeh, A. Tanomand et al., "Protective efficacy of recombinant exotoxin A—flagellin fusion protein against *Pseudomonas aeruginosa* infection," *Canadian Journal of Microbiology*, vol. 61, no. 1, pp. 60–64, 2015.

[31] F. Yang, J. Gu, L. Yang et al., "Protective efficacy of the trivalent *Pseudomonas aeruginosa* vaccine candidate PcrV-OprI-Hcp1 in murine pneumonia and burn models," *Scientific Reports*, vol. 7, no. 1, p. 3957, 2017.

[32] A. Kamei, W. Wu, D. C. Traficante et al., "Collaboration between macrophages and vaccine-induced $CD4^+$ T cells confers protection against lethal *Pseudomonas aeruginosa* pneumonia during neutropenia," *The Journal of Infectious Diseases*, vol. 207, no. 1, pp. 39–49, 2013.

[33] D. R. Chung, D. L. Kasper, R. J. Panzo et al., "$CD4^+$ T cells mediate abscess formation in intra-abdominal sepsis by an IL-17-dependent mechanism," *Journal of Immunology*, vol. 170, no. 4, pp. 1958–1963, 2003.

[34] Y. Li, Z. Wang, X. Liu, J. Tang, B. Peng, and Y. Wei, "X-ray irradiated vaccine confers protection against pneumonia caused by *Pseudomonas aeruginosa*," *Scientific Reports*, vol. 6, p. 18823, 2016.

[35] J. B. Lyczak, C. L. Cannon, and G. B. Pier, "Establishment of *Pseudomonas aeruginosa* infection: lessons from a versatile opportunist," *Microbes and Infection/Institut Pasteur*, vol. 2, no. 9, pp. 1051–1060, 2000.

[36] I. A. Holder, "Pseudomonas immunotherapy: a historical overview," *Vaccine*, vol. 22, no. 7, pp. 831–839, 2004.

[37] L. D. Hazlett, S. A. McClellan, X. L. Rudner, and R. P. Barrett, "The role of Langerhans cells in *Pseudomonas aeruginosa* infection," *Investigative Ophthalmology & Visual Science*, vol. 43, no. 1, pp. 189–197, 2002.

[38] S. Worgall, T. Kikuchi, R. Singh, K. Martushova, L. Lande, and R. G. Crystal, "Protection against pulmonary infection with *Pseudomonas aeruginosa* following immunization with *P. aeruginosa*-pulsed dendritic cells," *Infection and Immunity*, vol. 69, no. 7, pp. 4521–7, 2001.

[39] M. L. Dunkley, R. L. Clancy, and A. W. Cripps, "A role for CD4+ T cells from orally immunized rats in enhanced clearance of Pseudomonas aeruginosa from the lung," *Immunology*, vol. 83, no. 3, pp. 362–369, 1994.

[40] S. Shahrara, S. R. Pickens, A. M. Mandelin 2nd et al., "IL-17-mediated monocyte migration occurs partially through CC chemokine ligand 2/monocyte chemoattractant protein-1 induction," *Journal of Immunology*, vol. 184, no. 8, pp. 4479–4487, 2010.

[41] S. Aggarwal, N. Ghilardi, M. H. Xie, F. J. de Sauvage, and A. L. Gurney, "Interleukin-23 promotes a distinct CD4 T cell activation state characterized by the production of interleukin-17," *The Journal of Biological Chemistry*, vol. 278, no. 3, pp. 1910–1914, 2003.

[42] N. J. Kotloski, D. T. Nardelli, S. H. Peterson et al., "Interleukin-23 is required for development of arthritis in mice vaccinated and challenged with Borrelia species," *Clinical and Vaccine Immunology : CVI*, vol. 15, no. 8, pp. 1199–1207, 2008.

[43] A. Misiak, M. M. Wilk, M. Raverdeau, and K. H. Mills, "IL-17-producing innate and pathogen-specific tissue resident memory $\gamma\delta$ T cells expand in the lungs of *Bordetella pertussis*-infected mice," *Journal of Immunology*, vol. 198, no. 1, pp. 363–374, 2017.

[44] J. Liu, Y. Feng, K. Yang et al., "Early production of IL-17 protects against acute pulmonary *Pseudomonas aeruginosa* infection in mice," *FEMS Immunology and Medical Microbiology*, vol. 61, no. 2, pp. 179–188, 2011.

[45] T. Pan, R. Tan, M. Li et al., "IL17-producing $\gamma\delta$ T cells may enhance humoral immunity during pulmonary *Pseudomonas aeruginosa* infection in mice," *Frontiers in Cellular and Infection Microbiology*, vol. 6, p. 170, 2016.

[46] E. Lockhart, A. M. Green, and J. L. Flynn, "IL-17 production is dominated by $\gamma\delta$ T cells rather than CD4 T cells during mycobacterium tuberculosis infection," *Journal of Immunology*, vol. 177, no. 7, pp. 4662–4669, 2006.

[47] K. Shibata, H. Yamada, H. Hara, K. Kishihara, and Y. Yoshikai, "Resident V$\delta1^+$ $\gamma\delta$ T cells control early infiltration of neutrophils after *Escherichia coli* infection via IL-17 production," *Journal of Immunology*, vol. 178, no. 7, pp. 4466–4472, 2007.

[48] R. K. Braun, C. Ferrick, P. Neubauer et al., "IL-17 producing $\gamma\delta$ T cells are required for a controlled inflammatory response after bleomycin-induced lung injury," *Inflammation*, vol. 31, no. 3, pp. 167–179, 2008.

[49] C. L. Roark, P. L. Simonian, A. P. Fontenot, W. K. Born, and R. L. O'Brien, "$\gamma\delta$ T cells: an important source of IL-17," *Current Opinion in Immunology*, vol. 20, no. 3, pp. 353–357, 2008.

[50] R. T. Sadikot, T. S. Blackwell, J. W. Christman, and A. S. Prince, "Pathogen-host interactions in *Pseudomonas aeruginosa* pneumonia," *American Journal of Respiratory and Critical Care Medicine*, vol. 171, no. 11, pp. 1209–1223, 2005.

[51] A. Buret, M. L. Dunkley, G. Pang, R. L. Clancy, and A. W. Cripps, "Pulmonary immunity to Pseudomonas aeruginosa in intestinally immunized rats roles of alveolar macrophages, tumor necrosis factor alpha, and interleukin-1 alpha," *Infection and Immunity*, vol. 62, no. 12, pp. 5335–5343, 1994.

[52] D. Drake and T. C. Montie, "Flagella, motility and invasive virulence of *Pseudomonas aeruginosa*," *Journal of General Microbiology*, vol. 134, no. 1, pp. 43–52, 1988.

[53] L. F. Neville, Y. Barnea, O. Hammer-Munz et al., "Antibodies raised against N′-terminal Pseudomonas aeruginosa flagellin prevent mortality in lethal murine models of infection," *International Journal of Molecular Medicine*, vol. 16, no. 1, pp. 165–171, 2005.

[54] Y. Barnea, Y. Carmeli, E. Gur et al., "Efficacy of antibodies against the N-terminal of Pseudomonas aeruginosa flagellin for treating infections in a murine burn wound model," *Plastic and Reconstructive Surgery*, vol. 117, no. 7, pp. 2284–2291, 2006.

[55] K. D. Smith, E. Andersen-Nissen, F. Hayashi et al., "Toll-like receptor 5 recognizes a conserved site on flagellin required for protofilament formation and bacterial motility," *Nature Immunology*, vol. 4, no. 12, pp. 1247–1253, 2003.

[56] K. G. Murthy, A. Deb, S. Goonesekera, C. Szabo, and A. L. Salzman, "Identification of conserved domains in *Salmonella muenchen* flagellin that are essential for its ability to activate TLR5 and to induce an inflammatory response *In Vitro*," *The Journal of Biological Chemistry*, vol. 279, no. 7, pp. 5667–5675, 2004.

[57] R. Ramphal, V. Balloy, J. Jyot, A. Verma, M. Si-Tahar, and M. Chignard, "Control of *Pseudomonas aeruginosa* in the lung requires the recognition of either lipopolysaccharide or flagellin," *Journal of Immunology*, vol. 181, no. 1, pp. 586–592, 2008.

[58] M. Vijay-Kumar, H. Wu, R. Jones et al., "Flagellin suppresses epithelial apoptosis and limits disease during enteric infection," *The American Journal of Pathology*, vol. 169, no. 5, pp. 1686–1700, 2006.

[59] A. B. Molofsky, B. G. Byrne, N. N. Whitfield et al., "Cytosolic recognition of flagellin by mouse macrophages restricts *Legionella pneumophila* infection," *The Journal of Experimental Medicine*, vol. 203, no. 4, pp. 1093–1104, 2006.

[60] S. Saha, F. Takeshita, T. Matsuda et al., "Blocking of the TLR5 activation domain hampers protective potential of flagellin DNA vaccine," *Journal of Immunology*, vol. 179, no. 2, pp. 1147–1154, 2007.

[61] T. S. Murray, M. Egan, and B. I. Kazmierczak, "Pseudomonas aeruginosa chronic colonization in cystic fibrosis patients," *Current Opinion in Pediatrics*, vol. 19, no. 1, pp. 83–88, 2007.

[62] E. Andersen-Nissen, K. D. Smith, R. Bonneau, R. K. Strong, and A. Aderem, "A conserved surface on Toll-like receptor 5 recognizes bacterial flagellin," *The Journal of Experimental Medicine*, vol. 204, no. 2, pp. 393–403, 2007.

[63] V. L. Campodonico, N. J. Llosa, L. V. Bentancor, T. Maira-Litran, and G. B. Pier, "Efficacy of a conjugate vaccine containing polymannuronic acid and flagellin against experimental *Pseudomonas aeruginosa* lung infection in mice," *Infection and Immunity*, vol. 79, no. 8, pp. 3455–3464, 2011.

[64] N. Sabharwal, S. Chhibber, and K. Harjai, "New possibility for providing protection against urinary tract infection caused by *Pseudomonas aeruginosa* by non-adjuvanted flagellin 'b' induced immunity," *Immunology Letters*, vol. 162, no. 2, Part B, pp. 229–238, 2014.

[65] N. Sabharwal, S. Chhibber, and K. Harjai, "Divalent flagellin immunotherapy provides homologous and heterologous protection in experimental urinary tract infections in mice," *International Journal of Medical Microbiology : IJMM*, vol. 306, no. 1, pp. 29–37, 2016.

Hindawi
Journal of Immunology Research
Volume 2017, Article ID 3736201, 6 pages
https://doi.org/10.1155/2017/3736201

Review Article

Safety of Human Papillomavirus 9-Valent Vaccine: A Meta-Analysis of Randomized Trials

Ana Paula Ferreira Costa,[1] Ricardo Ney Oliveira Cobucci,[2] Janine Medeiros da Silva,[3] Paulo Henrique da Costa Lima,[3] Paulo César Giraldo,[4] and Ana Katherine Gonçalves[1,3]

[1]*Postgraduate Program in Health Sciences, Federal University of Rio Grande do Norte, Natal, RN, Brazil*
[2]*Department of Gynecology and Obstetrics, University Potiguar (UnP), Natal, RN, Brazil*
[3]*Department of Gynecology and Obstetrics, Federal University of Rio Grande do Norte (UFRN), Natal, RN, Brazil*
[4]*Department of Gynecology and Obstetrics, State University of Campinas (UNICAMP), Campinas, SP, Brazil*

Correspondence should be addressed to Ricardo Ney Oliveira Cobucci; rncobucci@hotmail.com

Received 24 February 2017; Revised 9 May 2017; Accepted 4 June 2017; Published 24 July 2017

Academic Editor: Angelika Riemer

Vaccination against human papillomavirus (HPV) has been progressively implemented in most developed countries for approximately 10 years. In order to increase the protection of the vaccines, a 9-valent vaccine (HPV9) was developed, which provides protection against nine types of the virus. Studies evaluating its safety are rare. Thus, we performed a meta-analysis of three clinical trials assessing adverse effects on women randomly vaccinated with HPV9 or tetravalent vaccine (HPV4), with the objective of analyzing whether the HPV9 is as safe as HPV4. An electronic data search was performed through the PubMed, Embase, Scopus, Web of Science, and SciELO databases. The studies selected 27,465 women who received one of the two vaccines. Pain (OR 1.72; 95% CI 1.62–1.82) and erythema (OR 1.29; 95% CI 1.21–1.36) occurred significantly more in the HPV9 group. However, there was no significant difference between the groups for the following adverse effects: headache (OR 1.07; 95% CI 0.99–1.15), dizziness (OR 1.09; 95% CI 0.93–1.27), and fatigue (OR 1.09; 95% CI 0.91–1.30), and the occurrence of serious events related to vaccination was similarly rare among those vaccinated. Therefore, our findings demonstrate that HPV9 in female patients is as safe as the tetravalent vaccine.

1. Introduction

The human papillomavirus (HPV) can cause cervical premalignant and malignant lesions [1, 2] as well as genital warts [3, 4]. Vaccines directed against the most relevant HPV types have collaborated to prevent virus-related diseases [5]. Three effective vaccines are approved by the Food and Drug Administration (FDA): the bivalent vaccine (HPV2), which protects against HPV types 16 and 18; the tetravalent vaccine (HPV4), which protects against types 16, 18, 6, and 11; the 9-valent vaccine (HPV9), which protects against types 6, 11, 16, 18, 31, 33, 45, 52, and 58 [6, 7].

The effects of HPV vaccination programs on population health have already been observed in the form of reduced incidences of HPV infections, genital warts, and HPV-attributed precancerous lesions. However, it is too early to study the effects of vaccination on cervical cancer rates, as it takes decades for HPV infection to progress to cervical cancer [8].

Since the vaccination programs started, several safety and efficacy surveillance protocols for the vaccines have been implemented [9]. Some are passive, such as the Vaccine Adverse Event Reporting System (VAERS) in the United States, which showed that the postvaccination adverse event rates with the HPV4 were not higher than

the historical rates of other vaccines [10]. Others use more active surveillance such as the multicenter study in seven health care organizations in the United States, on women between 9 and 26 years, who received 600,558 doses of HPV4; the purpose of which was to monitor certain adverse events, such as Guillain-Barre Syndrome, cerebrovascular accident, venous thromboembolism, appendicitis, convulsions, syncope, allergic reactions, and anaphylaxis. No meaningful increase was found in the risk of predetermined objectives [11].

The fact that HPV vaccination showed positive outcomes in several countries has contributed to the development of HPV9 to increase protection against five more strains (i.e., HPV types 31, 33, 45, 52, and 58), making it nine HPV strains. Such a vaccine has the potential to offer protection against approximately 90% of cervical cancers, an increase from the 70% offered by the HPV4. HPV9 is similar in composition to the tetravalent vaccine, using virus-like particles to elicit immune responses [8].

Recipients of the 9-valent vaccine were slightly more likely to experience adverse events than recipients of the tetravalent vaccine were, possibly owing to the higher amounts of virus-like particles and adjuvants in the HPV9 [8]. This meta-analysis aims to assess whether HPV9 is as safe as HPV4 in the female population.

2. Materials and Methods

2.1. Study Design. This meta-analysis follows the Preferred Reporting Items for Systematic Reviews and Meta-Analyses (PRISMA) guidelines [12].

Two researchers (APFC and JMS) performed the selection of the studies of interest. Subsequently, data were extracted by three other researchers (APFC, AKS, and RNC) according to the data extraction protocol. They evaluated the studies found based on the following inclusion criteria: (1) randomized controlled trial- (RCT-) type studies that evaluated the side effects of HPV4, Gardasil, and HPV9 (Gardasil9); (2) experiments involving women; (3) studies evaluating the safety, immunogenicity, and efficacy parameters of the vaccines; and (4) studies that presented similar vaccination protocols. The exclusion criteria were as follows: (1) studies involving men, (2) pregnant women, (3) women who were vaccinated only with 9-valent vaccine, and (4) observational studies. All discrepancies between these three reviewers were resolved by the consensus of all authors.

2.2. Search Strategy. The research was performed by a wide and comprehensive search of literature from databases (PubMed, Embase, Web of Science, Scopus, and SciELO) until December 2016. The following descriptors were used: (HPV OR Human papillomavirus) AND (vaccines OR vaccination) OR (tetravalent HPV vaccine) OR (9-valent vaccine) AND (side effects) OR (adverse events) AND (randomized controlled trial) OR (double blind method) OR (clinical trial). No language restrictions were applied. The flowchart of this study is shown in Figure 1.

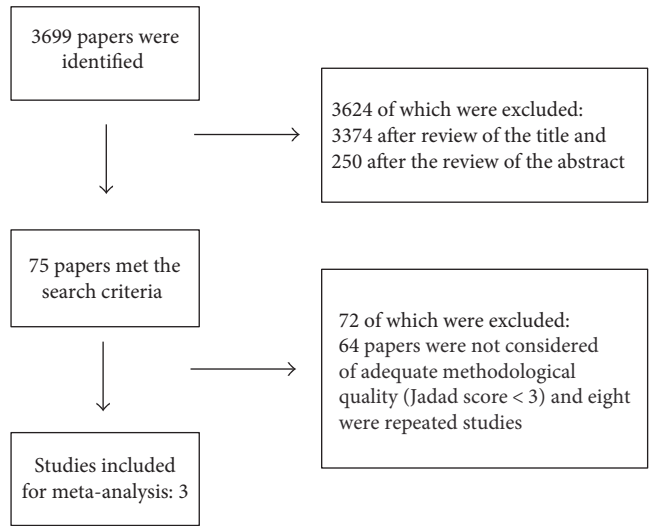

Figure 1: Flow diagram of the selection process of studies.

2.3. Data Analysis. Data were entered in the Review Manager software (RevMan 5.2), which allows the user to enter protocols as well as complete reviews, including text, features of studies, comparison tables, and study data, as well as to perform meta-analysis of the entered data.

To evaluate the safety and efficacy between the 9-valent and tetravalent vaccines, dichotomous data were extracted from each study and were inserted into a 2×2 contingency table, with subsequent individual determination of odds ratio (OR), to obtain a summarized overall estimate. Fixed-effects or random-effects models were chosen depending on whether there was an absence or presence of heterogeneity between studies. Heterogeneity was assessed by the I2 statistic. Statistical heterogeneity between studies was assessed by the I2 statistic (<25%, no heterogeneity; 25%–50%, moderate heterogeneity; and >50%, strong heterogeneity). When a significant heterogeneity existed across the included studies ($I2 > 50\%$), a random-effects model was used for the analysis; otherwise, the fixed-effects model was used [13, 14]. In addition, we use the Egger funnel plot to assess possible publication bias [13].

A Jadad score, which was based on the following three subscales: randomization (2–0), blind (2–0), and withdrawals and dropouts (1–0), assessed the study quality. For every answer of yes, unclear, or not, the values of 2 to 0 points were assigned, respectively. In our analysis, we judged that the studies evaluated that had a score ≥ 3 would be considered high quality. The level of evidence of each study (Table 1) was defined according to the definitions of the Oxford Centre for Evidence-Based Medicine [15].

We chose to use the fixed-effects model during statistical analysis, because this model is applied when there is little variability between the results of studies [16]. To determine OR, we used a confidence interval

Table 1: Description of the characteristics of included studies.

Author, year	Country	Design of study	Jadad	Follow-up	Age range (y)	Sample size
Joura et al., 2015	Asia-Pacific, Europe, Latin America, and North America	RCT	5	7 months	16–26	14,215
Vesikari et al., 2015	Belgium, Denmark, Finland, Italy, Spain, and Sweden	RCT	5	7 months	9–15	600
Moreira et al., 2016	Africa, Asia-Pacific, Europe, Latin America, and North America	RCT	5	7 months	9–26	12,650

RCT: randomized controlled trial.

(CI) of 95% with values of $P < 0.05$ considered statistically significant.

3. Results

Three studies were included for meta-analysis involving 27,465 women who received the HPV9 or HPV4 [6, 17, 18] (Table 1).

Rates of systemic events such as headaches (OR 1.07; 95% CI 0.99–1.15), dizziness (OR 1.09; 95% CI 0.93–1.27), and fatigue (OR 1.09; 95% CI 0.91–1.30) were similar between 9-valent and tetravalent vaccine groups (Figure 2). However, women vaccinated with HPV9 presented more fever (OR 1.18; 95% CI 1.03–1.36), pruritus (OR 1.44; 95% CI 1.26–1.15), and gastrointestinal (GI) symptoms: diarrhea, nausea, and vomiting (OR 1.24; 95% CI 1.09–1.45) (Figure 2).

Injection site-related adverse effects like pain (OR 1.72; 95% CI 1.62–1.82) and erythema (OR 1.29; 95% CI 1.21–1.36) occurred significantly more in the HPV9 group (Figure 3).

Out of more than 27,000 vaccine recipients, a total of 29 and 23 recipients from the HPV9 and HPV4 groups, respectively, experienced a serious vaccine-related adverse event. A total of 6 deaths were recorded from each group but none was judged to be vaccine related.

4. Discussion

In clinical trials and meta-analysis, the tetravalent HPV vaccine was found to be safe and efficacious [8, 9]. A recent observational study with human papillomavirus 9-valent vaccine shows that administration of the HPV9 was generally well tolerated. A lower proportion of girls (81.9%) and boys (72.8%) compared to that of young women (85.4%) reported injection-site adverse effects; most of which were mild to moderate in intensity [19].

In this meta-analysis, occurrence of adverse effects was reported in all RCTs [6, 17, 18]. The most reported side effects (SE) were injection-site reactions; most of these SE were mild or moderate in intensity. The most common among subjects who received the HPV9 vaccine when compared with HPV4 subjects were pain and erythema, seen in approximately 80% and 22%, respectively. Headache, fever, pruritus, and GI symptoms were the most common vaccine-related systemic SE of all participants; however, just fever, pruritus, and GI symptoms were significantly more reported in women vaccinated with HPV9. The 9-valent vaccine recipients were slightly more likely to experience these adverse events than tetravalent vaccine recipients were, and this possibly occurs due to the higher amounts of virus-like particles and adjuvants in the 9-valent vaccine, as well as serotypes [8].

Nowadays, in the scientific literature, only observational studies on the adverse effects of the 9-valent vaccine, without comparison with the side effects of the tetravalent vaccine, were found. Thus, this innovative study was compiled in a meta-analysis of randomized clinical trials, involving only women aged 9–26 years, vaccinated by HPV9 or by the tetravalent vaccine, by comparing adverse effects between the two groups.

Serious vaccine-related adverse events and deaths were not common, and there was no significant difference in both groups in our analysis. Furthermore, no vaccine-related deaths were reported. Some observational studies also found similarly low levels of vaccine-related severe adverse events and no vaccine-related deaths [19–22].

This meta-analysis was conducted using only the RCT, thus greatly reducing the possibility of bias. Since the authors of the different trials used the same vaccination protocols, confounding bias was therefore minimized. Publication bias is not believed to have occurred as shown by the funnel plots. However, the fact that Joura et al.'s study selected only women between 16 and 26 years old establishes a bias and prevents our results from being considered in the female population aged between 11 and 15 years, which is included in the current vaccination recommendations for both vaccines [6].

The results of our study should be interpreted with some caution because it has limitations. First, the work has been conducted using three RCTs only, and the selected studies investigated just women with different age ranges and had different sample sizes. The short follow-up period of the selected studies is also responsible for other potential weaknesses of the data.

5. Conclusions

Despite the limitations discussed above, the results of our meta-analysis show that the 9-valent vaccine in female patients is as safe as the tetravalent vaccine. However, firm

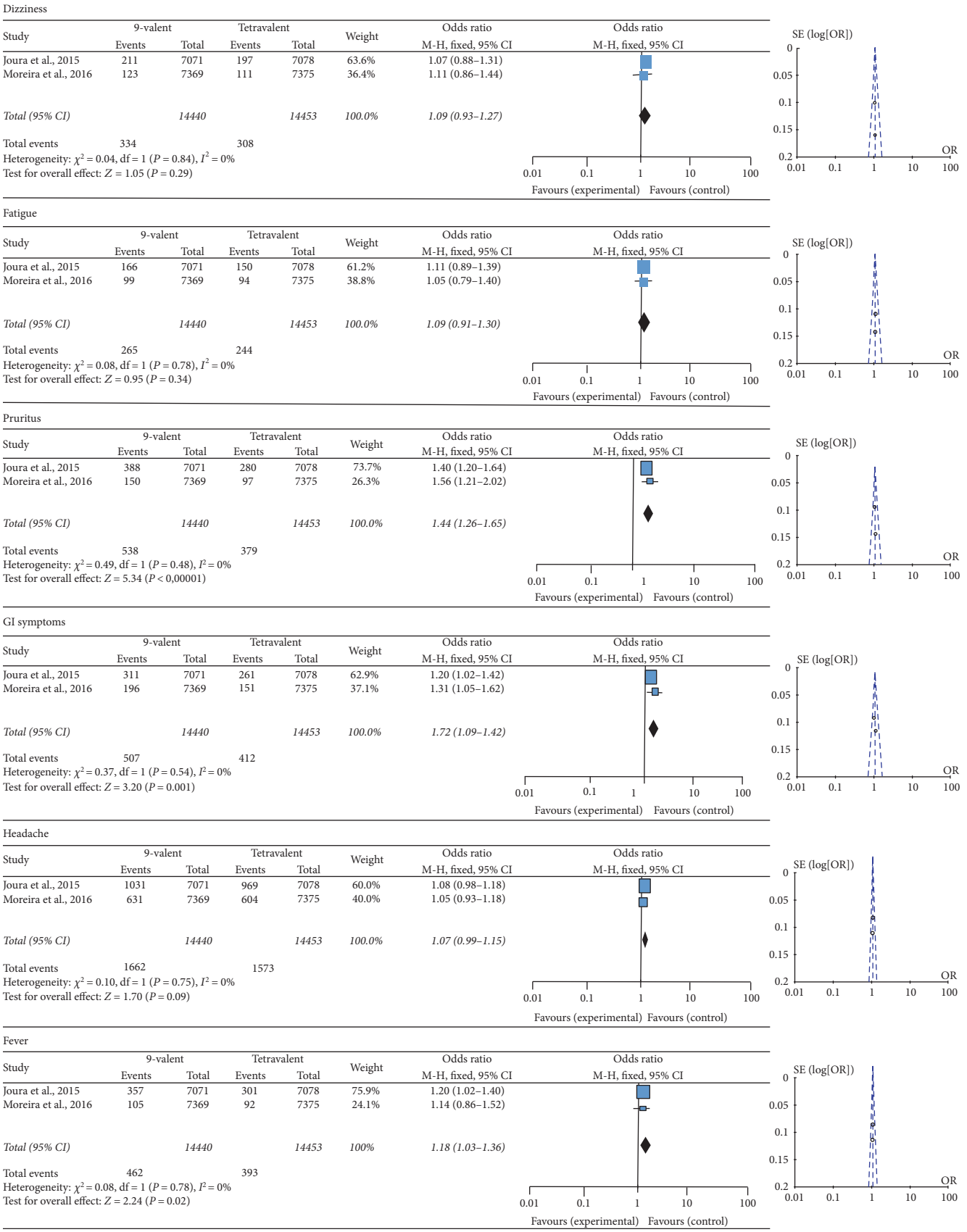

Figure 2: Forest and funnel plots of systemic adverse effects.

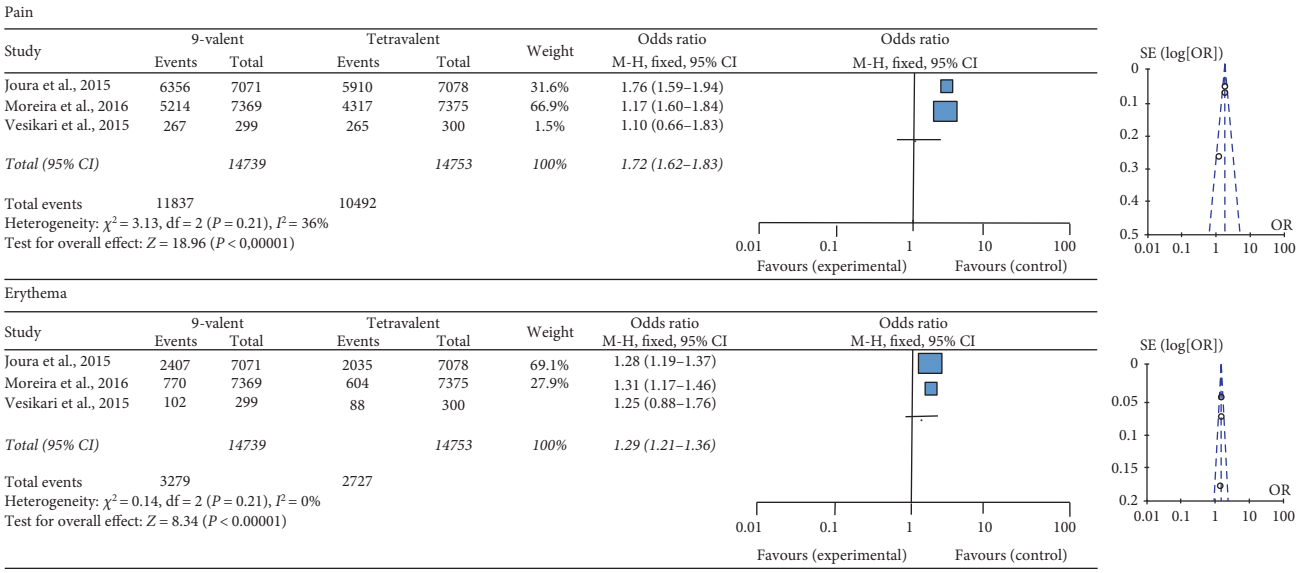

Figure 3: Forest and funnel plots of injection site-related adverse effects.

results to generalize our findings among specific populations, such as men, are precluded by the small number of enrolled studies involving only women. Thus, future research in the field becomes necessary.

Disclosure

This research did not receive any specific grant from funding agencies in the public, commercial, or not-for-profit sectors.

Conflicts of Interest

The authors declare no potential conflicts of interest.

References

[1] J. M. Walboomers, M. V. Jacobs, M. M. Manos et al., "Human papillomavirus is a necessary cause of invasive cervical cancer worldwide," *The Journal of Pathology*, vol. 189, pp. 12–19, 1999.

[2] S. Sanjose, W. G. Quint, L. Alemany et al., "Human papillomavirus genotype attribution in invasive cervical cancer: a retrospective cross-sectional worldwide study," *The Lancet Oncology*, vol. 11, pp. 1048–1056, 2010.

[3] S. K. Kjaer, T. N. Tran, P. Sparen et al., "The burden of genital warts: a study of nearly 70,000 women from the general female population in the 4 Nordic countries," *The Journal of Infectious Diseases*, vol. 196, pp. 1447–1454, 2007.

[4] S. M. Garland, M. Steben, H. L. Sings et al., "Natural history of genital warts: analysis of the placebo arm of 2 randomized phase III trials of a quadrivalent human papillomavirus (types 6, 11, 16, and 18) vaccine," *The Journal of Infectious Diseases*, vol. 199, pp. 805–814, 2009.

[5] N. D. Christensen, "Emerging human papillomavirus vaccines," *Expert Opinion on Emerging Drugs*, vol. 10, pp. 5–19, 2005.

[6] E. A. Joura, A. R. Giuliano, O. E. Iversen et al., "A 9-valent HPV vaccine against infection and intraepithelial neoplasia in women," *The New England Journal of Medicine*, vol. 372, pp. 711–723, 2015.

[7] J. Luna, M. Plata, M. Gonzalez et al., "Long-term follow-up observation of the safety, immunogenicity, and effectiveness of Gardasil™ in adult women," *PLoS One*, vol. 8, no. 12, article e83431, 2013.

[8] D. Y. Yang, "Update on the new 9-valent vaccine for human papillomavirus prevention," *Canadian Family Physician*, vol. 62, pp. 399–402, 2016.

[9] A. K. Gonçalves, R. N. Cobucci, H. M. Rodrigues, A. G. de Melo, and P. C. Giraldo, "Safety, tolerability and side effects of human papillomavirus vaccines: a systematic quantitative review," *The Brazilian Journal of Infectious Diseases*, vol. 18, no. 6, pp. 651–659, 2014.

[10] B. A. Slade, L. Leidel, C. Vellozzi et al., "Postlicensure safety surveillance for quadrivalent human papillomavirus recombinant vaccine," *JAMA*, vol. 302, no. 7, pp. 750–757, 2009.

[11] J. Gee, A. Naleway, I. Shui et al., "Monitoring the safety of quadrivalent human papillomavirus vaccine: findings from the Vaccine Safety Datalink," *Vaccine*, vol. 29, pp. 8279–8284, 2011.

[12] D. Moher, A. Liberati, J. Tetzlaff, D. G. Altman, and The PRISMA Group, "Preferred reporting items for systematic reviews and meta-analyses: the PRISMA statement," *PLoS Medicine*, vol. 6, no. 7, article e1000097, 2009.

[13] J. P. Higgins, S. G. Thompson, J. J. Deeks, and D. G. Altman, "Measuring inconsistency in meta-analyses," *BMJ*, vol. 327, pp. 557–560, 2003.

[14] R. DerSimonian and N. Laird, "Meta-analysis in clinical trials," *Controlled Clinical Trials*, vol. 7, pp. 177–188, 1986.

[15] A. R. Jadad, R. A. Moore, D. Caroll et al., "Assessing the quality of reports of randomized clinical trials: is blinding necessary?" *Controlled Clinical Trials*, vol. 17, pp. 1–12, 1996.

[16] R. J. Harris, M. J. Bradburn, J. J. Deeks, R. M. Harbord, D. G. Altman, and J. A. C. Sterne, "Metan: fixed- and random-effects meta-analysis," *The Stata Journal*, vol. 8, pp. 3–28, 2008.

[17] T. Vesikari, N. Brodszki, P. Van Damme et al., "A randomized, double-blind, phase III study of the immunogenicity and

safety of a 9-valent human papillomavirus L1 virus-like particle vaccine (V503) versus Gardasil® in 9-15-year-old girls," *The Pediatric Infectious Disease Journal*, vol. 34, no. 9, pp. 992–998, 2015.

[18] E. D. Moreira Jr., S. L. Block, D. Ferris et al., "Safety profile of the 9-valent HPV vaccine: a combined analysis of 7 phase III clinical trials," *Pediatrics*, vol. 138, no. 2, 2016.

[19] P. Van Damme, S. E. Olsson, S. Block et al., "Immunogenicity and safety of a 9-valent HPV vaccine," *Pediatrics*, vol. 136, no. 1, pp. e28–e39, 2015.

[20] A. Schilling, M. M. Parra, M. Gutierrez et al., "Coadministration of a 9-valent human papillomavirus vaccine with meningococcal and Tdap vaccines," *Pediatrics*, vol. 136, no. 3, pp. e563–e572, 2015.

[21] X. Castellsagué, A. R. Giuliano, S. Goldstone et al., "Immunogenicity and safety of the 9-valent HPV vaccine in men," *Vaccine*, vol. 33, no. 48, pp. 6892–6901, 2015.

[22] S. Iwata, S. Murata, S. R. Han, A. Wakana, M. Sawata, and Y. Tanaka, "Safety and immunogenicity study of a 9-valent human papillomavirus vaccine administered to 9-to-15 year-old Japanese girls," *Japanese Journal of Infectious Diseases*, 2016.

Hindawi
Journal of Immunology Research
Volume 2017, Article ID 7573154, 13 pages
https://doi.org/10.1155/2017/7573154

Research Article

Adoptive Cell Therapy of Induced Regulatory T Cells Expanded by Tolerogenic Dendritic Cells on Murine Autoimmune Arthritis

Jie Yang,[1] Lidong Liu,[1] Yiming Yang,[1] Ning Kong,[2] Xueyu Jiang,[1] Juan Sun,[1] and Rufeng Xie[1]

[1]*Blood Engineering Laboratory, Shanghai Blood Center, Shanghai 200051, China*
[2]*Division of Rheumatology, Huashan Hospital, Fudan University, Shanghai 200040, China*

Correspondence should be addressed to Jie Yang; allareblue@gmail.com

Received 15 January 2017; Revised 1 April 2017; Accepted 27 April 2017; Published 18 June 2017

Academic Editor: Carol Leung

Objective. Tolerogenic dendritic cells (tDCs) can expand TGF-β-induced regulatory T cells (iTregs); however, the therapeutic utility of these expanded iTregs in autoimmune diseases remains unknown. We sought to determine the properties of iTregs expanded by mature tolerogenic dendritic cells ($iTreg_{mtDC}$) in vitro and explore their potential to ameliorate collagen-induced arthritis (CIA) in a mouse model. *Methods.* After induction by TGF-β and expansion by mature tDCs (mtDCs), the phenotype and proliferation of $iTreg_{mtDC}$ were assessed by flow cytometry. The ability of iTregs and $iTreg_{mtDC}$ to inhibit $CD4^+$ T cell proliferation and suppress Th17 cell differentiation was compared. Following adoptive transfer of iTregs and $iTreg_{mtDC}$ to mice with CIA, the clinical and histopathologic scores, serum levels of IFN-γ, TNF-α, IL-17, IL-6, IL-10, TGF-β and anti-CII antibodies, and the distribution of the $CD4^+$ Th subset were assessed. *Results.* Compared with iTregs, $iTreg_{mtDC}$ expressed higher levels of Foxp3 and suppressed $CD4^+$ T cell proliferation and Th17 cell differentiation to a greater extent. In vivo, $iTreg_{mtDC}$ reduced the severity and progression of CIA more significantly than iTregs, which was associated with a modulated inflammatory cytokine profile, reduced anti-CII IgG levels, and polarized Treg/Th17 balance. *Conclusion.* This study highlights the potential therapeutic utility of $iTreg_{mtDC}$ in autoimmune arthritis and should facilitate the future design of iTreg immunotherapeutic strategies.

1. Introduction

Rheumatoid arthritis (RA) is an autoimmune disease causing chronic inflammation of the synovial joints. The inflammatory processes occurring in RA result in hyperplasia of the synovial membrane and infiltration of monocytes, macrophages, T and B cells, mast cells, and dendritic cells (DCs) [1]. Pharmacological therapies for RA include analgesics and anti-inflammatory steroids, which halt the progression of RA but do not cure it. Currently, a curative treatment has yet to be found. Therefore, the development of novel antirheumatic therapies that specifically target aberrant immune processes, dampen inflammation, and promote tolerance is needed.

Recently, cellular therapy for autoimmune diseases has attracted much attention, and as the master regulators of all immune responses, regulatory T cells (Tregs) are the most promising candidates for cell therapy. Natural Tregs (nTregs) are primarily derived from the thymus, and induced Tregs (iTregs) are differentiated from $CD4^+$ $CD25^-$ $Foxp3^-$ T cells in the periphery or in vitro, both of which maintain immunological tolerance and may prevent a variety of autoimmune rheumatic diseases [2, 3]. According to previous reports, iTregs induced by TGF-β in vitro, but not nTregs, retain Foxp3 expression and immunosuppressive activity in the inflammatory microenvironment [4]. In addition, iTregs have been shown to suppress bone erosion and other clinical measures of disease progression in the well-established collagen-induced arthritis (CIA) mouse model of human RA [5, 6], suggesting that iTregs may be therapeutically beneficial for RA [7].

However, culturing iTregs for a period of 5 days has been reported to result in high levels of cell death (detected using propidium iodide staining) [8]. As shown in the study by Kong et al., 3×10^6 iTregs per mouse (20 ± 2 g/mouse) were required to significantly inhibit established CIA [9]. The numbers of iTregs induced by TGF-β alone during conventional iTreg culture are not sufficient to satisfy therapeutic

demands. Furthermore, after induction by TGF-β, only approximately 60% of $CD4^+$ T cells express Foxp3 [8, 9], a percentage that is too low to meet the clinical requirements for relevant cell purity, although the remaining $CD4^+$ $Foxp3^-$ cells did not appear to have any pathogenic effects [10].

Fortunately, tolerogenic dendritic cells (tDCs), which typically present low levels of self-peptide-MHC complexes (signal 1) coupled with limited cell surface expression of costimulatory molecules (signal 2) and secretion of proinflammatory cytokines (signal 3), have been reported to potentially induce tolerance [11]. As the most potent antigen-presenting cells (APCs), DCs are regarded as key instigators or regulators of innate and adaptive immunity. Conventional DCs have the unique ability to activate or promote immune responses depending on their maturation status, whereas tDCs have the ability to induce activated T cell energy and apoptosis and generate/expand nTregs or iTregs in vivo or in vitro. Thus, tDCs are likely to act as both stimulators and inducers to further increase cell numbers and enhance Foxp3 expression in a mixed iTreg population [12].

In this study, we established a new polyclonal expansion method for the generation of iTregs. This method represents the first strategy for generating tDCs induced by IL-10/TGF-β in the Treg-induction/expansion system. Mature tDCs (mtDCs), which retained the tolerogenic functions of tDCs and had a stronger expansive ability than tDCs, were employed as the stimulator/inducer. We used mtDCs to successfully expand iTregs, while retaining their regulatory phenotype and potent suppressor functions. These mtDC-expanded iTregs ($iTreg_{mtDC}$) were associated with a significant reduction in cytokine and CII-directed antibody secretion, polarization of the Treg/Th17 balance, and more effective inhibition of CIA than iTregs. Our findings suggest the potential use of $iTreg_{mtDC}$ as a therapy for autoimmune arthritis.

2. Materials and Methods

2.1. Mice. Wild-type male DBA/1J (D1) mice (8 weeks old) were obtained from the Shanghai Laboratory Animal Center of the Chinese Academy of Science (SLACCAS, China). All mice were housed in a pathogen-free environment.

2.2. Ethics Statement. This study was conducted in strict accordance with the recommendations in the guidelines of the Institutional Animal Care and Use Committee of the Chinese Association for Laboratory Animal Sciences. The protocol was approved by the Committee on the Ethics of Animal Experiments of the Shanghai Blood Center (permit number: SBC-IRB-2013-07). All surgery was performed under diethyl ether anesthesia, and all efforts were made to minimize suffering.

2.3. Induction and Evaluation of CIA. CIA was induced in D1 mice via a subcutaneous injection of bovine type II collagen (CII, Chondrex, Redmond, WA, USA) emulsified with an equal volume of complete Freund's adjuvant (Difco, Detroit, MI, USA) on day 0. On day 21, mice received the next injection of 50 μg of CII in incomplete Freund's adjuvant (Difco). The onset of CIA was confirmed on day 25. From day 21 to day 49 after the first immunization, mice were scored every two days for clinical evidence of arthritis of the limb joints by a macroscopic examination. Limb joint arthritis was scored using an established scoring system [13] as follows: no detectable arthritis, 0; erythema and mild swelling, 1; mild erythema and mild swelling involving the entire paw, 2; severe swelling and redness from the ankle to digits, 3; and maximal swelling and redness or obvious joint destruction associated with visible joint deformity or ankylosis, 4. The clinical scores for each mouse are presented as the sum of the scores for the four limbs, and the maximum score for each mouse was sixteen. Two independent observers without knowledge of the experimental protocol performed the scoring. During the 49-day observation period, the arthritis scores increased quickly and constantly and CIA developed in up to 90% of mice.

2.4. Preparation of DCs. DCs were prepared as described [13]. In brief, D1-derived bone marrow (BM) cells were collected and, after red cell lysis, seeded at a density of 5×10^5 cells/ml in RPMI 1640 medium supplemented with 10% fetal bovine serum (Invitrogen). On day 0, murine GM-CSF (20 ng/ml, PeproTech) was added to the cultures, following which the cultures were pulsed with fresh medium, GM-CSF, murine IL-10 (15 ng/ml, PeproTech), and human TGF-β1 (15 ng/ml, PeproTech) on days 4 and 7. After 10 days in culture, nonadherent cells were collected and $CD11c^+$ cells were sorted as the tDCs. mtDCs were harvested after stimulation with 100 ng/ml lipopolysaccharide (LPS, Sigma-Aldrich) during the final 48 h of culture. Immature DCs (iDCs) were propagated in the presence of GM-CSF alone under the same conditions, and mature DCs (mDCs) were generated following exposure to LPS for 48 h.

All types of DCs were stained with anti-mouse CD11c-APC, CD86-FITC, CD80-PE, and IA-IE-PE mAbs (BD Biosciences Pharmingen) for phenotypic analysis by flow cytometry. Cytokine expression was determined using real-time quantitative PCR. Primer sequences (in the 5′ to 3′ orientation) were IL-12 p40, GGAAGCACGGCAGCAGAA TA and AACTTGAGGGAGAAGTAGGAATGG; TGF-β, TTGCTTCAGCTCCACAGAGA and TGGTTGTAGAGGG CAAGGAC; IL-10, CCAAGCCTTATCGGAAATGA and T TTTCACAGGGGAGAAATCG; and β-actin, ATCCGTAA AGACCTCTATGC and ACACAGAGTACTTGCGCTCA. PCR results were normalized to the expression of the housekeeping gene β-actin [14]. Data shown are a representative of six independent experiments.

2.5. Ex Vivo Generation of $iTreg_{mtDC}$. iTregs were derived from $CD4^+$ $CD25^-$ T cells that were purified from the splenocytes of D1 mice using a $CD4^+$ $CD25^+$ regulatory T cell isolation kit (Miltenyi Biotec, Germany) and stimulated with an anti-CD3/CD28 mAb (50 ng/ml, PeproTech) in the presence of TGF-β1 (5 ng/ml, PeproTech) and IL-2 (100 ng/ml, PeproTech) for 5 days [8]. Then, $iTreg_{mtDC}$ or $iTreg_{mDC}$ were generated by expanding iTregs for 4 days using mtDCs or mDCs at a 5 : 1 ratio (5 T cells : 1 DC). The different types of iTregs were collected, counted, incubated with anti-mouse

CD4-FITC and CD25-PE-Cy5 mAbs, fixed, permeabilized, and stained with antimouse Foxp3-PE or isotype control mAbs (BD Biosciences Pharmingen). Then, the coexpression of CD25 and Foxp3 was determined by flow cytometry.

2.6. Proliferation Assay. In the classical polyclonal proliferation assay, responder cells were $CD4^+$ T cells, which were isolated from splenocytes of D1 mice using a $CD4^+$ T Cell Isolation Kit (Miltenyi Biotec, Germany). The $CD4^+$ T cells were labeled with carboxyfluorescein succinimidyl ester (CFSE; Invitrogen, Germany) and stimulated with anti-CD3/28 mAbs (50 ng/ml, PeproTech). Then, different ratios of iTregs, $iTreg_{mDC}$, or $iTreg_{mtDC}$ (as suppressor cells) were added to the responder cultures. Four days later, the cells were harvested and analyzed by flow cytometry.

In addition, $CD4^+$ T cells were isolated from splenocytes of mice with CIA (on day 25 after the primary immunization) and used in the antigen-specific $CD4^+$ T cell proliferation assay. Mature DCs were induced as described above and loaded with CII, as stimulator APCs. CFSE-labeled responding $CD4^+$ T cells were activated following coculture with CII-loaded mDCs. Then, different ratios of iTregs, $iTreg_{mDC}$, or $iTreg_{mtDC}$ (as suppressor cells) were added to the responder cultures. Four days later, the cells were harvested and analyzed using flow cytometry.

2.7. Evaluation of CIA after $iTreg_{mtDC}$ Treatment. At the onset of CIA, 1×10^6 iTregs, $iTreg_{mDC}$, or $iTreg_{mtDC}$ were adoptively transferred into CIA-recipient mice ($n = 10$ per group) via the tail vein. Control mice were treated with PBS alone. Mice were scored using an established scoring system from days 21 to 49 after the primary immunization [13].

2.8. Histology. The hind paws of iTreg-treated, $iTreg_{mtDC}$-treated, and CIA mice were collected on day 49 after the primary immunization, and the tissues were stained with hematoxylin and eosin (H&E) and Safranin O. Two independent observers who were blinded to the experimental groups examined the paw sections using a four-point scale: normal, 0; inflammatory infiltrates and synovial hyperplasia, 1; pannus formation and cartilage erosion, 2; and import cartilage erosion and bone destruction, 3. This global histological score reflected both synovitis (synovial proliferation and inflammatory cell infiltration) and joint destruction (bone and cartilage thickness, irregularity, and the presence of erosions) [13].

2.9. Analysis of Serum Anti-CII Antibody and Cytokine Levels Using CBA and ELISA. Sera were obtained from iTreg-treated, $iTreg_{mtDC}$-treated, and CIA mice 49 days after the primary immunization and stored at −80°C. The serum levels of IFN-γ, TNF-α, IL-17, IL-6, and IL-10 were determined using a mouse CBA Kit (BD Biosciences Pharmingen) and analyzed by flow cytometry. The concentration of TGF-β was assessed using the mouse TGF-β Platinum ELISA kit (eBioscience), and the concentrations of anti-CII antibodies were measured using a standard sandwich ELISA (Chondrex, Redmond, WA, USA) according to the manufacturer's instructions. Five samples from each group were analyzed.

2.10. Analysis of Treg/Th17 Subsets in Mice with CIA. T cells were isolated from the spleen and inguinal lymph nodes of the iTreg-treated, $iTreg_{mtDC}$-treated, and CIA mice on day 49 after the primary immunization. These cells were incubated with an anti-mouse CD4-FITC mAb, fixed, permeabilized, stained with anti-mouse FoxP3-PE, IL-17-PE, or isotype control mAbs (BD Biosciences Pharmingen), and then assessed by flow cytometry.

2.11. Th17 Cell Differentiation. Naive $CD4^+$ T cells were sorted from the splenic cells of mice with CIA, stained with CFSE as described above, and stimulated with an anti-CD3/CD28 mAb (50 ng/ml, PeproTech), IL-1β (10 ng/ml, PeproTech), IL-6 (25 ng/ml, PeproTech), and TGF-β1 (1 ng/ml, PeproTech). Then, iTregs, $iTreg_{mDC}$, or $iTreg_{mtDC}$ were added to the culture at a 1 : 1 ratio. After 4 days of coculture, the cells were harvested, incubated with an anti-mouse CD4-APC mAb, fixed, permeabilized, and stained with an anti-IL-17A-PE mAb (BD Biosciences Pharmingen). The production of IL-17A in the cell culture supernatant was measured using the mouse cytokine cytometric bead array (CBA, BD Biosciences Pharmingen) according to the manufacturer's instructions.

2.12. Statistical Analyses. Results were analyzed using GraphPad Prism 5.0 software (GraphPad Software, San Diego, CA, USA), and data are expressed as means ± standard errors of the means (SEM). Student's *t*-test was used to assess statistically significant differences between two paired groups, and an alpha value of $P < 0.05$ was considered statistically significant.

3. Results

3.1. BM-Derived DCs Induced by IL-10 and TGF-β1 Maintain the Tolerogenic Surface Phenotype and Express Substantial Levels of "Immunosuppressive" Cytokines. According to previous reports, tDCs derived from mouse BM are induced to differentiate with GM-CSF, IL-10, and TGF-β1, which does not affect DC development from replicating BM progenitors [15]. In the present study, a large proportion of induced BM cells were positive for CD11c (>80%), indicating that these cells exhibited a DC phenotype. MHC molecules (IA-IE) and costimulatory molecules (CD86 and CD80) were expressed at low levels on tDCs. Following stimulation with LPS for 48 h, the mean fluorescence intensity (MFI) of each of these molecules was consistently lower on the mature tDCs (mtDCs) than on the mature DCs (mDCs) (Figure 1(a)). Thus, tDCs were comparatively resistant to maturation in response to LPS stimulation and retained the tolerogenic surface phenotype. Additionally, cytokine production by DCs was assessed using real-time PCR. The tDCs displayed higher levels of "immunosuppressive" cytokines, such as IL-10 and TGF-β, than iDCs. These cytokines were still expressed at high levels after tDCs were stimulated with LPS, although the expression of the TGF-β mRNA in mtDCs was lower than, but not significantly different from, that in tDCs. However, IL-12 p40 production by tDCs was negligible, even upon stimulation with LPS (Figure 1(b)). There

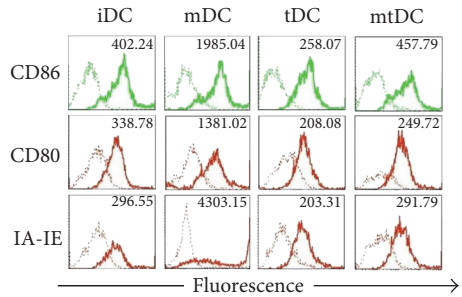

The mean fluorescence intensity

	iDC	mDC	tDC	mtDC
CD86	336.79 ± 82.55	2474.36 ± 613.39	246.01 ± 134.23	362.88 ± 86.93 **
CD80	340.81 ± 72.05	1445.34 ± 86.32	214.98 ± 55.72	277.09 ± 43.73 **
IA-IE	365.05 ± 96.83	3736.40 ± 910.87	245.79 ± 55.99	336.89 ± 52.27 **

(a)

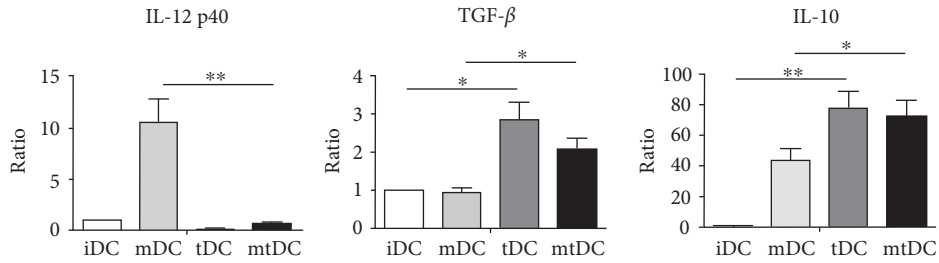

(b)

Figure 1: Characteristic profile of tolerogenic DCs derived from D1 mice.iDCs, mDCs, tDCs, and mtDCs were induced to differentiate in vitro, as described in the Materials and Methods, after which $CD11c^+$ cells were harvested. (a) These four types of DC were stained with CD86, CD80, IA-IE (thick lines), or isotype-matched mAbs (thin lines), and the expression of these markers was analyzed by FACS using flow cytometry. The frequency of positively stained cells and MFI of a representative of 10 independent experiments are shown in the FACS profile. The mean fluorescence intensity is reported as the mean ± SEM ($n = 10$). $^{**}P < 0.01$ for the comparison of mDCs with mtDCs using unpaired t-tests. (b) IL-12 p40, IL-10, and TGF-β expression in DCs was determined by real-time PCR. All results were normalized to the expression of the housekeeping gene β-actin and are expressed as the means ± SEM of six independent experiments. $^{*}P < 0.05$ and $^{**}P < 0.01$ for the comparisons of the indicated groups using the unpaired t-test.

was no significant difference on induction efficiency and cell yields between iDCs, mDCs, tDCs, and mtDCs, though the frequency of $CD11c^+$ cells were increased after LPS stimulation.

Based on these data, tDCs induced by GM-CSF, IL-10, and TGF-β1 maintained a tolerogenic surface phenotype, even after LPS stimulation, and expressed substantial levels of "immunosuppressive" cytokines.

3.2. iTregs Generated after mtDC-Mediated Expansion Retain Foxp3 Expression and Potently Suppress Polyclonal $CD4^+$ T Cell Proliferation In Vitro. Our iTreg culture strategy consisted of two expansion cycles: (1) the induction of iTregs and (2) the expansion of iTregs by mtDCs (Figure 2(a)). First, $CD4^+$ $CD25^-$ T cells that were purified from splenocytes of D1 mice were stimulated with an anti-CD3/CD28 mAb (50 ng/ml, PeproTech) in the presence of TGF-β1. After 5 days, these cells, "iTregs," were harvested. Then, iTregs were cocultured with mtDCs at a 5 : 1 ratio. After 4 days, the cells, termed "$iTreg_{mtDC}$," were collected, and a significant increase in the total cell number was observed. According to the FACS results, the intracellular expression of Foxp3 in $iTreg_{mtDC}$ was markedly higher (82.0 ± 3.6%) than that in iTregs (54.9 ± 2.5%). Using our new culture method, we obtained $3.52–4.3 \times 10^6$ $Foxp3^+$ cells from the 2×10^6 $CD4^+$ $CD25^-$ T cells that were originally plated and included approximately 0.02×10^6 $Foxp3^+$ cells (Figure 2(b)). In other words, the $Foxp3^+$ cells had expanded approximately 150-fold compared with original cells. However, the $iTreg_{mDC}$, which were expanded by mDCs, appeared to expand more rapidly but generated a lower percentage of cells that expressed Foxp3 (37.4 ± 4.1%) than the $iTreg_{mtDC}$.

iTregs exhibit immunosuppressive activity. Therefore, the classical polyclonal effector T cell proliferation assay was used as a functional readout to show the inhibitory capacity of iTregs expanded by mtDCs. In this assay, $CD4^+$ T cells (responders) were isolated from splenocytes of D1 mice and stimulated with anti-CD3/28 mAbs. As shown in Figure 2(c), the responder cells underwent vigorous proliferation in the absence of suppressors, generating large numbers of dividing T cells in culture. However, this vigorous proliferation was suppressed by the presence of iTregs, $iTreg_{mtDC}$, or $iTreg_{mDC}$ (suppressors). Significantly, $iTreg_{mtDC}$ inhibited $CD4^+$ T cell proliferation more effectively than iTregs or $iTreg_{mDC}$ at all the tested suppressor-to-responder (S : R) cell ratios. Even the lowest dose of $iTreg_{mtDC}$ (an S : R ratio of 1 : 8) resulted in the effective inhibition of $CD4^+$ T cell expansion, whereas both iTregs and $iTreg_{mDC}$ showed weaker suppression at the same S : R ratio.

Based on these results, iTregs were expanded by mtDCs and maintained the stronger regulatory phenotype and more effective inhibitory potency.

3.3. In CIA Mice, $iTreg_{mtDC}$ Exhibited More Potent Antiarthritic Activity than iTregs. As shown in previous studies, iTregs exert protective effects on established arthritis

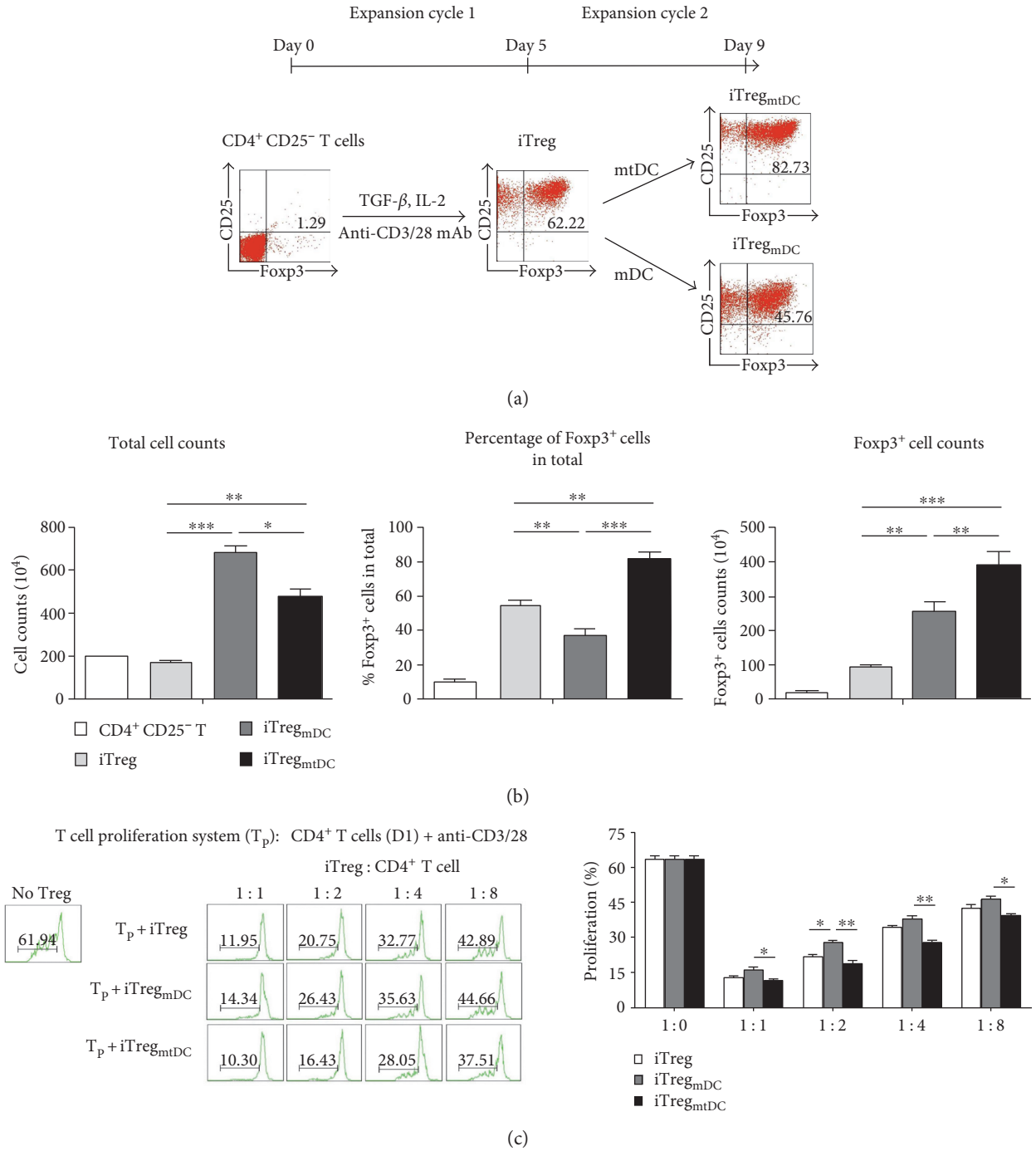

Figure 2: iTregs expanded in vitro by mtDCs retained Foxp3 expression and efficiently inhibited $CD4^+$ T cell proliferation. (a) Schematic overview of the induction/expansion strategy for iTregs. The two expansion cycles were established as described in the Materials and Methods. The differentiation of iTregs was first induced with an anti-CD3/CD28 mAb, TGF-β, and IL-2 for 5 days in vitro. Then, $iTreg_{mtDC}$ or $iTreg_{mDC}$ were generated by expanding iTregs for 4 days using mtDCs or mDCs, respectively. The expression of the transcription factor Foxp3 and CD25 in cells was determined in each cycle using flow cytometry. Data are representative of three independent experiments. (b) Expansion of different types of iTregs was determined by counting the cells, and Foxp3 expression levels were determined by flow cytometry. All data are presented as means ± SEM ($n = 5$), and $^*P < 0.05$, $^{**}P < 0.01$, and $^{***}P < 0.001$ for the comparisons of the indicated groups using the unpaired t-test. (c) The ability of iTregs to inhibit the proliferation of $CD4^+$ T cells was assessed using the proliferation assay. In this assay, $CD4^+$ T cells (responders) were isolated from splenocytes of D1 mice, stained with CFSE, and stimulated with an anti-CD3/CD28 mAb and IL-2. Then, different ratios of iTregs, $iTreg_{mDC}$, or $iTreg_{mtDC}$ (suppressor cells) were added to the responder cultures. Four days later, the cells were harvested and analyzed by flow cytometry. Progressive dilution of CFSE in responder cells was used as a readout of proliferation in the presence or absence of different types of iTregs. The results are presented as means ± SEM ($n = 3$). $^*P < 0.05$ and $^{**}P < 0.01$ compared with the indicated groups using the unpaired t-test.

[4, 9]; therefore, we determined the capacity of $iTreg_{mtDC}$ to improve established CIA. Mice with CIA were injected with the same dose (1×10^6 cells/animal) of either iTregs, $iTreg_{mDC}$, or $iTreg_{mtDC}$, and then, the arthritic index and histopathology were examined to assess the antiarthritic activities of these three types of iTregs.

According to the arthritic scores, all types of iTregs markedly decreased the incidence of CIA and reduced the severity of arthritis compared with that of the untreated control group. More importantly, the injection of $iTreg_{mtDC}$ almost completely inhibited the progression of arthritis during the first 10 days, and subsequently, the arthritic severity never reached the level observed in the CIA control group. When compared with the therapeutic effects of iTregs and $iTreg_{mDC}$ at any time point, treatment with the same doses of $iTreg_{mtDC}$ inhibited the development of CIA to a greater extent, which was substantiated by both the clinical scores and the incidence of arthritis (Figures 3(a) and 3(b)). During the 4-week observation period, $iTreg_{mtDC}$-treated mice had the mildest arthritic symptoms and the lowest arthritis scores compared with those mice treated with iTregs or $iTreg_{mDC}$.

Next, histopathological specimens of the joints of mice with CIA treated with $iTreg_{mtDC}$ showed the least significant cartilage destruction and least inflammatory cell infiltration compared with those of control CIA mice, although the iTreg or $iTreg_{mDC}$ treatment also reduced the joint damage and inflammation to some extent (Figure 3(c)). The results of the histological examinations were consistent with the resulting clinical scores (Figure 3(d)).

Thus, these in vivo observations confirmed that treatment of CIA mice with $iTreg_{mtDC}$ inhibits the progression of CIA more effectively than the iTreg or $iTreg_{mDC}$ treatment.

3.4. $iTreg_{mtDC}$-Mediated Inhibition of CIA Was Associated with Modulated Cytokine and Anti-CII Antibody Secretion and the Polarization of the Treg/Th17 Balance. The amelioration of CIA in mice following the iTreg treatment has been attributed to the immune-modulating properties of iTregs [4]. Therefore, we sought to characterize the mechanism by which $iTreg_{mtDC}$ modulates the disease.

First, the secretion of IFN-γ, TNF-α, IL-17, IL-6, IL-10, and TGF-β in the sera of CIA mice treated with various iTregs was analyzed on day 49 after the first immunization. The production of IFN-γ and IL-10 significantly increased in $iTreg_{mtDC}$-treated mice compared with those productions in iTreg- or $iTreg_{mDC}$-treated mice. In addition, the levels of TNF, IL-17, and IL-6 were significantly reduced and TGF-β was markedly elevated in iTreg-treated, $iTreg_{mDC}$-treated, or $iTreg_{mtDC}$-treated mice compared with CIA mice, though there were no significant differences on the levels of those cytokines between the groups treated with different iTregs (Figure 4(a)). Clearly, the attenuation of CIA in mice following adoptive transfer of iTregs was a consequence of their immune modulatory effect on the secretion of various cytokines, and $iTreg_{mtDC}$ showed the strongest modulating effect.

Additionally, the importance of antibodies in the development of CIA pathology is also well described [16]. The serum levels of total anti-CII-specific immunoglobulin (anti-CII IgG) in $iTreg_{mtDC}$-treated mice were significantly lower than the levels observed in mice with CIA on day 49 following the first immunization, whereas treatment with either iTregs or $iTreg_{mDC}$ failed to obviously reduce anti-CII IgG levels. And there was no significant difference on the levels of anti-CII IgG between $iTreg_{mtDC}$-treated mice and iTregs- or $iTreg_{mDC}$-treated mice (Figure 4(b)). Thus, $iTreg_{mtDC}$ inhibited anti-CII-specific antibody responses more powerfully than iTregs or $iTreg_{mDC}$, which contributed to the suppression of the development of CIA.

Furthermore, the Treg/Th17 ratio is considered an important indicator of the severity of CIA. Thus, we determined the percentages of Th17 ($CD4^+$ $IL\text{-}17^+$) and Treg ($CD4^+$ $Foxp3^+$) cells among $CD4^+$ T cells isolated from the spleen or inguinal lymph nodes of CIA mice that were treated with various iTregs on day 49 after the first immunization. As shown in Figure 4(c), the Foxp3 : IL-17 ratio increased due to an increase in the frequency of Treg cells and a decrease in the frequency of Th17 cells following all types of iTreg treatment. Obviously, the highest Foxp3 : IL-17 ratio was detected in $iTreg_{mtDC}$-treated mice compared with that in either iTreg- or $iTreg_{mDC}$-treated mice. Thus, $iTreg_{mtDC}$ exerted the most significant modulatory effects on the polarization of the Treg/Th17 balance in vivo.

Taken together, compared to iTregs and $iTreg_{mDC}$, the adoptive transfer of $iTreg_{mtDC}$ exerted the most obvious suppression of cytokine secretion, reduction of CII-directed antibodies, and the most significant polarization of the Treg/Th17 balance.

3.5. $iTreg_{mtDC}$ Inhibit the Antigen-Specific Proliferation of CIA-$CD4^+$ T Cells and Suppress Th17 Cell Differentiation In Vitro More Effectively than iTregs. We utilized an in vitro antigen-specific proliferation assay to simulate the in vivo response as a functional readout and to demonstrate the ability of $iTreg_{mtDC}$ to suppress the antigen-specific proliferation of CIA-$CD4^+$ T cells. In this assay, $CD4^+$ T cells (responders) were isolated from splenocytes of CIA mice and stimulated with CII-loaded mDCs (stimulators). As shown in Figure 5(a), a large number of CIA-$CD4^+$ T cells underwent antigen-specific amplification after expansion by CII-loaded mDCs. However, no matter if iTregs, $iTreg_{mtDC}$, or $iTreg_{mDC}$ (suppressors) were added to the proliferation assay, this strong proliferation was obviously inhibited. At all tested S : R ratios, $iTreg_{mtDC}$ inhibited antigen-specific $CD4^+$ T cell expansion more effectively than iTregs. Notably, a significant difference between the abilities of $iTreg_{mtDC}$ and $iTreg_{mDC}$ to inhibit the antigen-specific $CD4^+$ T cell expansion was only observed when they were added at a low dose (at an S : R ratio of 1 : 8); iTregs showed weaker suppression at the same S : R ratio.

Given the close relationship between Tregs and Th17 cells [17] and our observations that the adoptive transfer of iTregs decreased the number of Th17 cells and subsequent polarization of the Treg/Th17 balance in the CIA mice, we next investigated whether $iTreg_{mtDC}$ could maintain suppression of Th17 differentiation in vitro, which simulated the in vivo response. In the Th17 induction system, Th17 cells were differentiated from CIA-$CD4^+$ T cells by stimulation

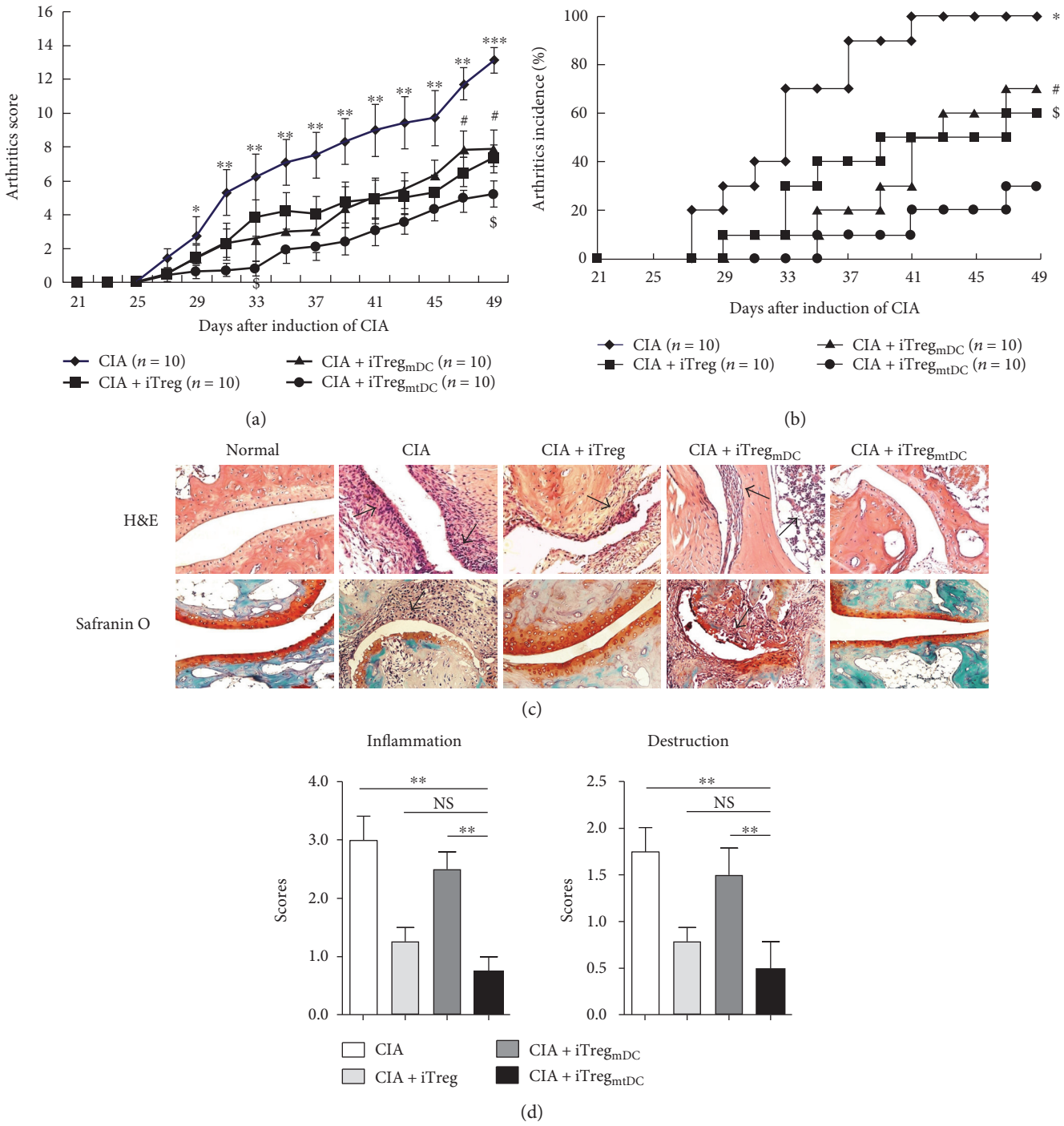

FIGURE 3: $iTreg_{mtDC}$ exhibited a more potent antiarthritic activity in CIA mice than iTregs. Following the onset of experimentally induced CIA (on day 25 after the primary immunization), recipient mice received adoptively transferred iTregs, $iTreg_{mDC}$, or $iTreg_{mtDC}$ (1×10^6 cells/animal). Mice were scored for clinical signs of arthritis in the limb joints by macroscopic examination three times per week. Limb joint arthritis was assessed using an established scoring system. The mice were sacrificed on the 49th day after the first immunization with CII. (a) Arthritic scores and incidence for each group following the adoptive transfer of different types of iTregs ($n = 10$) during the observation period are shown. $^{*}P < 0.05$, $^{**}P < 0.01$, and $^{***}P < 0.001$ for the comparison of the CIA group and the CIA + $iTreg_{mtDC}$ group; $^{\#}P < 0.05$ for the comparison of the CIA + iTreg group and the CIA + $iTreg_{mtDC}$ group; and $^{\$}P < 0.05$ for the comparison of the CIA + $iTreg_{mDC}$ group and the CIA + $iTreg_{mtDC}$ group using the unpaired t-test. (b) Hind paw specimens were collected from recipient mice treated with different types of iTregs on the 49th day after the first immunization with CII and were stained with H&E (top, synovial joint inflammation) and Safranin O (bottom, cartilage erosion). All specimens were shown at ×200. (c) Histopathological scores for inflammation and destruction in each group are expressed as the means ± SEM of four individual experiments. $^{**}P < 0.01$ for the comparisons of the indicated groups using the unpaired t-test.

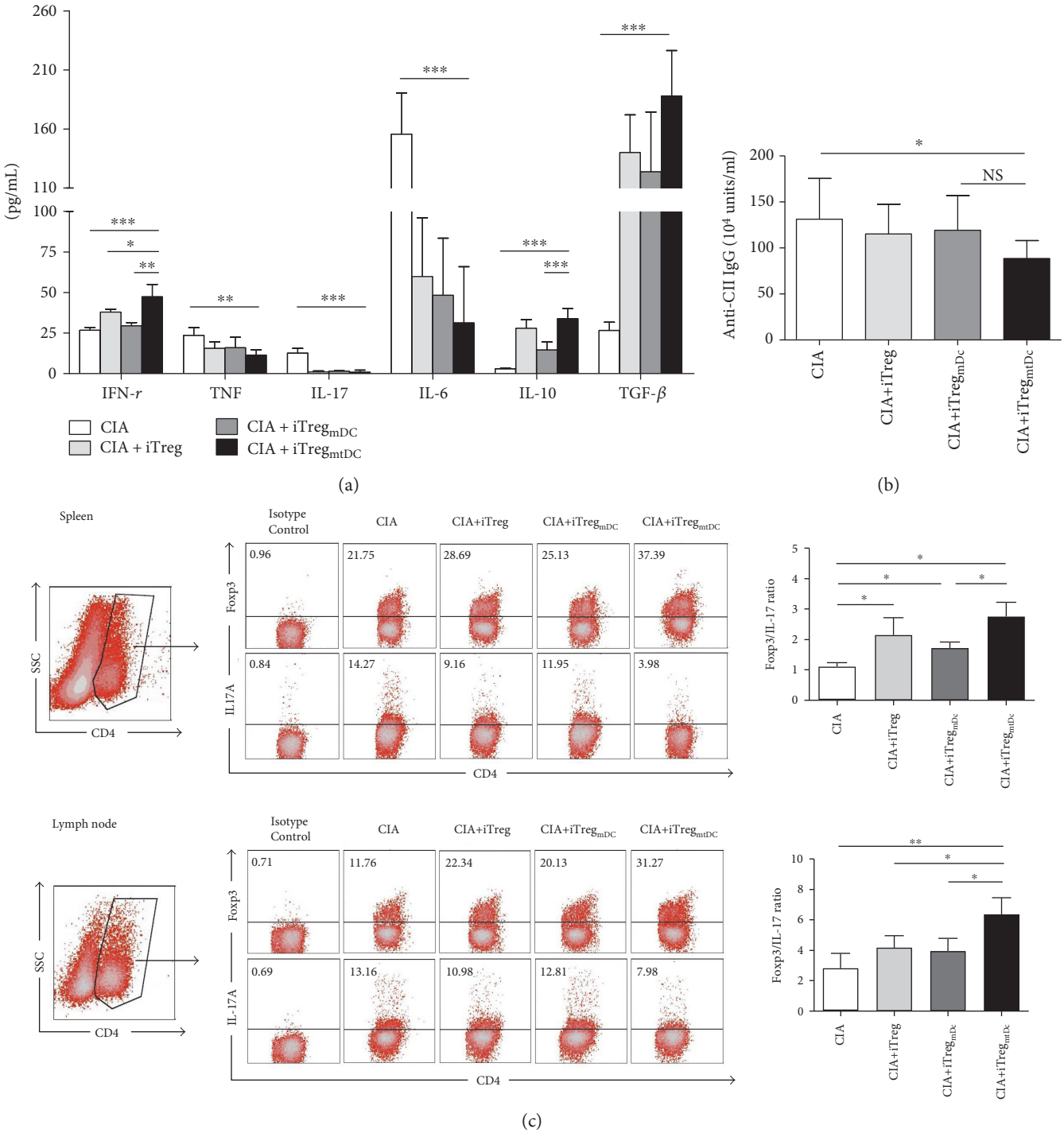

Figure 4: In the CIA mouse model, iTreg$_{mtDC}$ modulated the secretion of cytokines and anti-CII antibodies and polarized the Treg/Th17 balance. Recipient mice that received adoptively transferred iTregs, iTreg$_{mDC}$, or iTreg$_{mtDC}$ were sacrificed on the 49th day after the first immunization with CII, and serum was collected from each group of mice. (a) Serum levels of IFN-γ, TNF-α, IL-17, IL-6, and IL-10 were measured using CBA assays, and TGF-β secretion was measured using an ELISA. Data are reported as means ± SEM ($n = 5$). $^{*}P < 0.05$, $^{**}P < 0.01$, and $^{***}P < 0.001$ for the comparisons of the indicated groups using the unpaired t-test. (b) Serum levels of total CII-specific immunoglobulin were determined using an ELISA. The results from five independent replicate experiments were pooled. Data are reported as means ± SEM ($n = 5$). $^{*}P < 0.05$ and $^{**}P < 0.01$ for the comparisons of the indicated groups using the unpaired t-test. (c) CD4^{+} T cells from the spleen and inguinal lymph nodes of CIA mice treated with or without different types of iTregs were collected, permeabilized, and stained with an anti-Foxp3 mAb and an anti-IL-17 mAb to detect intracellular expression. FACS flow cytometry was used to measure the percentage of positively stained cells, and the ratios of Treg/Th17 cells are expressed as the means ± SEM of five independent experiments. $^{*}P < 0.05$ and $^{**}P < 0.01$ for the comparisons of the indicated groups using the unpaired t-test.

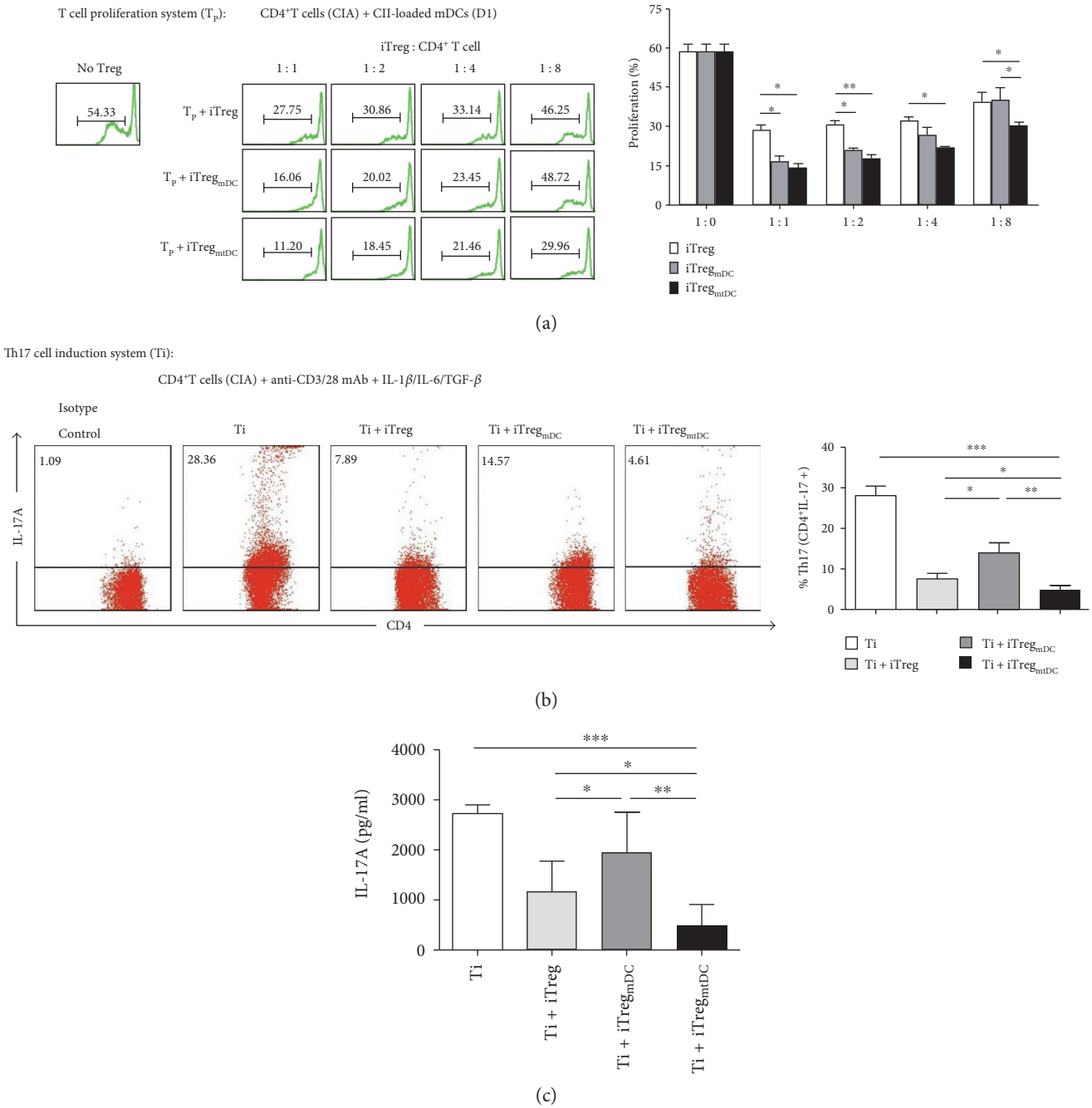

Figure 5: $iTreg_{mtDC}$ exerted a more potent immunosuppressive effect on antigen-specific $CD4^+$ T cell proliferation and suppressed Th17 cell differentiation more effectively. (a) The ability of $iTreg_{mtDC}$ to inhibit the proliferation of antigen-specific $CD4^+$ T cells was assessed using the proliferation assay. In this assay, $CD4^+$ T cells (responders) were isolated from splenocytes of CIA mice (on day 25 after the primary immunization), stained with CFSE, and stimulated with CII-loaded mDCs (stimulators) derived from the BM of normal D1 mice. Then, different ratios of iTregs, $iTreg_{mDC}$, or $iTreg_{mtDC}$ (suppressor cells) were added to the responder cultures. Four days later, the cells were harvested and analyzed by flow cytometry. The results are shown as means ± SEM ($n = 3$). $^*P < 0.05$ and $^{**}P < 0.01$ for the comparisons of the indicated groups using the unpaired t-test. (b) The suppression of Th17 cell differentiation by coculture with $iTreg_{mtDC}$ was assessed using the standard Th17 cell differentiation system. As described in the Materials and Methods, naive $CD4^+$ T cells were isolated from the splenocytes of CIA mice, stained with CFSE, and stimulated with an anti-CD3/CD28 mAb, IL-1β, IL-6, and TGF-β1. Then, a 1 : 1 ratio of iTregs, $iTreg_{mDC}$, or $iTreg_{mtDC}$ was added to this differentiation system. After 4 days of cocultivation, the percentages of $CFSE^+$ $CD4^+$ IL-$17A^+$ cells in the different groups were determined by flow cytometry as the percentage of induced Th17 cells. Data are reported as means ± SEM ($n = 3$), and $^*P < 0.05$, $^{**}P < 0.01$, and $^{***}P < 0.001$ represent the comparisons of the indicated groups using unpaired t-test. (c) After 4 days of cocultivation, supernatants were collected from the groups mentioned in (b). The concentration of soluble IL-17A in the coculture supernatant was determined using CBA. Data are reported as means ± SEM ($n = 3$), and $^*P < 0.05$, $^{**}P < 0.01$, and $^{***}P < 0.001$ represent the comparisons of the indicated groups using the unpaired t-test.

with IL-6, IL-1β, and TGF-β for 4 days. The 1 : 1 ratio of $iTreg_{mtDC}$ to CIA-$CD4^+$ T cells markedly reduced the fraction of cells that expressed intracellular IL-17A from $28.12 \pm 4.79\%$ to $4.83 \pm 1.53\%$. The addition of the same ratio of iTregs and $iTreg_{mDC}$ to $CD4^+$ T cells achieved a weaker suppression of intracellular IL-17A expression (Figure 5(b)). Meanwhile, the level of soluble IL-17A, the key cytokine which Th17 secreted, detected in the supernatant also decreased significantly upon the addition of $iTreg_{mtDC}$ (Figure 5(c)).

Based on these results, $iTreg_{mtDC}$ were the most effective at inhibiting antigen-specific CIA-$CD4^+$ T cell proliferation, suppressed Th17 cell differentiation to a greater extent and decreased the secretion of IL-17 in vitro compared with iTregs or $iTreg_{mDC}$, providing strong evidence that adoptive transfer of $iTreg_{mtDC}$ reflected more potent antiarthritic activity in the CIA mice.

4. Discussion

$CD4^+$ $CD25^+$ $Foxp3^+$ regulatory T cells play a crucial role in maintaining immune tolerance. As shown in multiple studies, nTregs prevent the appearance and development of autoimmune diseases in many animal models [18, 19]. However, nTregs are unable to treat established autoimmune diseases because of their instability in an inflammatory milieu [20–22]. In addition, the widespread use of nTreg-based therapy is hindered by the low frequency and lack of reliable surface markers for purification [23, 24]. In 2002, Zheng et al. were the first to report that TGF-β induces the differentiation of $CD4^+$ $CD25^-$ cells into $CD4^+$ $CD25^+$ Tregs (iTregs) in vitro [25]. Over the past decade, a number of studies on iTregs and their relationship to the regulation of immunity and the outcomes of autoimmune diseases have shown that adoptive transfer of $Foxp3^+$ iTregs ameliorates autoimmune disease in mouse models of lupus, gastritis, diabetes, and RA [4, 26–28], although the capacity to apply this therapy in the clinic remains controversial [29, 30]. In this study, we established a new method for the polyclonal expansion of iTregs using mtDCs and assessed the suppressive capacity of $iTreg_{mtDC}$ in vitro and in CIA mice. According to our results, $iTreg_{mtDC}$ corrected defects in the number and function of iTregs in vivo and in vitro and thus possessed the potential to be a powerful tool in the treatment of autoimmune diseases.

In the classical iTreg culture method, iTreg differentiation is induced by an anti-CD3/CD28 antibody and TGF-β. This method produces few cells due to a high cell death rate, and the number of cells obtained is not sufficient to meet therapeutic demands. We modified the iTreg-induction/culture protocol to produce more cells and to promote the clinical application of iTreg-based therapy. In the conventional polyclonal expansion method, an anti-CD3/28 antibody or mature DCs are used as stimulators, and the addition of high doses of anti-CD3/28 antibody led to severe cell apoptosis caused by excessive activation, as the anti-CD3/28 antibody preferentially amplified $CD4^+$ effector cells and not iTregs. Mature DCs had a similar effect. Fortunately, semimature DCs [31] or DCs with a tolerogenic phenotype [32], such as the low expression of MHC or/and costimulatory molecules, had the ability to expand or generate Tregs de novo and promote the apoptotic death of effector T cells in some studies. Tolerogenic DCs were the optimal candidate to amplify the $Foxp3^+$ iTregs, particularly in a mixed population of cells.

DCs have the unique ability to activate or suppress immune responses depending on their maturation status, phenotype, and tissue of origin. Due to their inherent plasticity, DCs are regarded as key instigators or regulators of innate and adaptive immunity. It is commonly held that conventional DCs have the unique ability to activate or suppress immune responses depending on their maturation status, whereas tolerogenic DCs exhibit the distinct functional properties in promoting tolerance. tDCs describe a broad range of immunoregulatory DCs that are usually immature [33], exhibit a plasmacytoid morphology [34], or are alternatively activated [15]. And on the basis of traditional definition, Jiang et al. [35] further hierarchically arranged two classes of maturation programs for DCs. They found that DCs matured by E-cadherin contained the phenotypic hallmarks of conventional mature DCs but without the secretion of inflammatory cytokines. And these E-cadherin-matured DCs could induce peripheral T cell tolerance in vivo and protect against EAE. Thus, alterations in adhesion could be seen as producing "phenotypically mature" immunogenic DCs, whereas microbial stimuli yield "functionally mature" immunogenic DCs under conditions of inflammation. Also, Vander Lugt et al. [36] provided a gene regulatory framework and indicated that the presence of DCs in peripheral tissues appeared phenotypically mature and had a critical role in peripheral tolerance, which illuminated the molecular underpinnings of DC maturation and function. Meanwhile, Guilliams et al. [37] provided a universal toolbox for the automated identification of DCs using unsupervised analysis of flow cytometry, paving the way toward the faithful identification of DC subsets to grasp the fascinating functional heterogeneity of DCs.

In this study, DCs exposed to IL-10 and TGF-β were resistant to maturation in response to LPS stimulation. The MFI of IA-IE, CD80, and CD86 expression on mtDCs was lower than the MFI on mDCs. Moreover, mtDCs secreted higher levels of IL-10 and TGF-β than mDCs, whereas IL-12 p40 production by mtDCs was negligible. Considering the limited cell expansion capability of tDCs, mtDCs matured by LPS were employed in this new method. mtDCs also displayed the tolerogenic surface phenotype and secreted a large number of "immunosuppressive" cytokines, whose tolerogenic characteristics were not significantly different from those of tDCs. More importantly, mtDCs effectively expand T cells, but tDCs always show a poor capacity to activate T cells. Due to their stable tolerogenic functions and improved ability to expand iTregs, mtDCs were employed as the best stimulator/inducer in this study. As a positive control, conventional mDCs were also added to expand iTregs in parallel experiments. As expected, fewer cells expanded by mDCs ($iTreg_{mDC}$) expressed Foxp3 ($37.4 \pm 4.1\%$) than cells before amplification. Interestingly, these $iTreg_{mDC}$ suppressed effector $CD4^+$ T proliferation to a greater extent than iTregs in vitro, possibly because iTregs have enhanced

functional activities after activation. Similarly, activated nTregs exert a stronger suppressive effect than silent nTregs [20]. This reason may be why $iTreg_{mtDC}$, which are activated further by mtDCs, exerted more potent inhibitory effects than iTregs induced by TGF-β alone.

Noticeably, although more than 80% of the cells were $Foxp3^+$ after the combined induction/expansion with TGF-β and mtDCs, approximately 10% $CD4^+$ $Foxp3^-$ cells and less than 5% $CD11c^+$ mtDCs were observed. So $iTreg_{mtDC}$ were the mixture of $CD4^+$ $Foxp3^+$ cells, $CD4^+$ $Foxp3^-$ cells, and mtDCs. Lan et al. compared the suppressive effects of a mixed population of iTregs and $Foxp3^+$ iTregs and showed that these activated $CD4^+$ $Foxp3^-$ cells did not develop the ability to exert pathogenic effects after TGF-β treatment [10]. Thus, the purified $Foxp3^+$ Treg population may not need to be sorted. Meanwhile, established murine arthritis is significantly inhibited by a tDC infusion [38, 39]. As shown in our previous study, mtDCs exerted suppressive effects in vitro and on the CIA mouse model after IL-10 and TGF-β polarization [13]. In this study, we did not isolate $iTreg_{mtDC}$ from mtDCs; therefore, we cannot exclude the possibility that the very limited number of mtDCs infused with $iTreg_{mtDC}$ may have contributed to the suppression of CIA.

Multiple mechanisms are involved in the inhibitory activities of iTregs in vivo. Our study has confirmed that different types of iTregs suppressed CIA in mice through similar mechanisms, including modulation of cytokine secretion, prolonged inhibition of anti-CII IgG antibodies, and polarization of the Treg/Th17 balance. Following treatment with $iTreg_{mtDC}$, the serum levels of TNF-α, IL-17, and IL-6 were significantly reduced, whereas the levels of IFN-γ, IL-10, and TGF-β were markedly elevated in mice with CIA compared with the levels in mice treated with iTreg or $iTreg_{mDC}$. In addition, $iTreg_{mtDC}$ inhibit anti-CII-specific antibody responses more powerfully than iTregs or $iTreg_{mDC}$, which contribute to the suppression of the development of CIA. Interestingly, the levels of IFN-γ, which is mainly produced by NK cells and Th1 cells and induces inflammation, were increased after the adoptive transfer of iTregs. In fact, an increasing number of studies have recently confirmed that IFN-γ acts as a disease-limiting factor in CIA and not a pathogenic factor [40, 41], though several studies have recently revealed a role for IFN-α in the pathogenesis of a subset of RA patients [42]. The protective mechanism of IFN-γ is to inhibit the differentiation of monocytes/macrophages into osteoclasts and suppress IL-1β-mediated MMP1 and MMP3 production by synovial fibroblasts in antigen-induced arthritis, thereby limiting cartilage degradation. More importantly, IFN-γ facilitates the development of Tregs from precursor T cells and increases their suppressive effects on CIA. Conversely, IFN-γ inhibits Th17 cell development and suppresses their effector functions. Therefore, the high level of IFN-γ may reduce inflammation and osteoclast differentiation in CIA mice. Additionally, another therapeutic benefit of iTregs is attributed to the fact that they express low levels of the IL-6 receptor and subsequent STAT-3 phosphorylation [43], express high levels of the Bcl-2 gene, and resist apoptosis [25], and, most importantly, iTregs shift the Treg/Th17 balance to a Treg-predominant phenotype [9]. Thus, a tolerant state was established following the iTreg treatment in vivo, which promoted Treg cell differentiation and proliferation while limiting the differentiation of Th17 cells in vivo. As expected, compared with iTregs or $iTreg_{mDC}$, $iTreg_{mtDC}$ showed more significant polarization of the Treg/Th17 balance in the CIA mice. Based on our in vitro experiments, $iTreg_{mtDC}$ were the most effective cell type at reducing IL-17A secretion from $CD4^+$ T cells and suppressing Th17 cell differentiation. Meanwhile, $iTreg_{mtDC}$ more effectively inhibited antigen-specific $CD4^+$ T cell expansion than iTregs at all tested S : R ratios, whereas a significant difference in the inhibition of antigen-specific $CD4^+$ T cell expansion between $iTreg_{mtDC}$ and $iTreg_{mDC}$ was only observed at a low S : R ratio (1 : 8). Thus, $iTreg_{mtDC}$ promoted a more potent tolerogenic microenvironment, a feature that was evidenced by the effectively reduced presentation of CIA symptoms and inhibition of CIA progression. Because $iTreg_{mtDC}$ had the strongest antiarthritic effects, we were able to adoptively transfer low doses of $iTreg_{mtDC}$ (1×10^6 cells/CIA mouse) compared with the higher doses of iTregs ($\geq 3 \times 10^6$ cells/CIA mouse) required to achieve the same inhibition of established arthritis. Therefore, under the same culture condition, $iTreg_{mtDC}$ meet the requirements for clinical application more readily than other iTregs, in terms of both the $Foxp3^+$ cell purity and the number of cells produced.

In general, antigen-specific iTregs are believed to have a stronger suppressive ability than nonspecific iTregs [9]. However, in autoimmune diseases, such as RA and lupus, the specific antigens responsible for the disease processes remain undefined. Polyclonal $iTreg_{mtDC}$ suppressed T cell proliferation and CIA, suggesting that manipulation of polyclonal $iTreg_{mtDC}$ may represent a therapeutic tool with which to combat autoimmune diseases in which specific antigens have not been defined. Moreover, once the specific pathogenic antigens of RA are identified, mtDCs, potent APCs, could acquire and present specific antigens to iTregs, subsequently activating and propagating the antigen-specific iTregs. Thus, we believe that the involvement of mtDCs in the iTreg culture system will greatly improve future iTreg-induction/expansion methods.

In summary, we established a new iTreg polyclonal expansion method. Using this method, iTregs were efficiently expanded by tolerogenic DCs ex vivo to reach clinically relevant cell numbers while retaining and even strengthening their regulatory phenotypes and potent suppressor functions. In our study, these $iTreg_{mtDC}$ prevented established CIA by modulating cytokine secretion, anti-CII antibodies, and the polarization of the Treg/Th17 balance. Based on these results, we confidently postulate that human mtDCs are a suitable stimulator to expand human Tregs to achieve clinically relevant cell numbers and enhance their inhibitory activity in vitro and in vivo, although some differences have been observed between human Tregs and mouse Tregs. Moreover, mtDCs are also potent APCs. mtDCs could acquire/present specific antigens to Tregs and then activate/propagate the antigen-specific Tregs, which are thought to have a stronger suppressive ability and better therapeutic effects than nonspecific iTregs. Thus, we have sufficient reasons to

believe that the use of mtDCs in the iTreg culture system may contribute to improve future Treg-induction/expansion methods, establish a large-scale in vitro cell culture system for clinical applications, and enhance the therapeutic effects and extensive use of Treg-based cell therapy in the forthcoming decade.

Conflicts of Interest

The authors declare no financial interest or commercial conflict of interest.

Authors' Contributions

Jie Yang and Lidong Liu contributed equally to this work.

Acknowledgments

This work was supported by grants from Shanghai Public Health Construction Projects Foundation (15GWZK0501), Shanghai Natural Science Foundation (13ZR1452100, 15ZR1438300), the Foundation of Shanghai Municipal Commission of Health and Family Planning (201440439, 201640096, 20154Y0192, and 20154Y0079), and China National Natural Science Foundation (81302571). The authors also thank the Department of Animal Science in Shanghai Jiao Tong University School of Medicine for laboratory animal husbandry.

References

[1] V. Lutzky, S. Hannawi, and R. Thomas, "Cells of the synovium in rheumatoid arthritis. Dendritic cells," *Arthritis Research Theraphy*, vol. 9, p. 219, 2007.

[2] M. Miyara, Y. Ito, and S. Sakaguchi, "TREG-cell therapies for autoimmune rheumatic diseases," *Nature Reviews. Rheumatology*, vol. 10, pp. 543–551, 2014.

[3] J. A. Bluestone, E. Trotta, and D. Xu, "The therapeutic potential of regulatory T cells for the treatment of autoimmune disease," *Expert Opinion on Therapeutic Targets*, vol. 19, pp. 1091–1103, 2015.

[4] N. Kong, Q. Lan, M. Chen et al., "Induced T regulatory cells suppress osteoclastogenesis and bone erosion in collagen-induced arthritis better than natural T regulatory cells," *Annals of the Rheumatic Diseases*, vol. 71, pp. 1567–1572, 2012.

[5] L. Bevaart, M. J. Vervoordeldonk, and P. P. Tak, "Evaluation of therapeutic targets in animal models of arthritis: how does it relate to rheumatoid arthritis?" *Arthritis and Rheumatism*, vol. 62, pp. 2192–2205, 2010.

[6] D. D. Brand, K. A. Latham, and E. F. Rosloniec, "Collagen-induced arthritis," *Nature Protocols*, vol. 2, pp. 1269–1275, 2007.

[7] X. Zhou, N. Kong, H. Zou et al., "Therapeutic potential of TGF-beta-induced CD4(+) Foxp3(+) regulatory T cells in autoimmune diseases," *Autoimmunity*, vol. 44, pp. 43–50, 2011.

[8] M. C. Fantini, S. Dominitzki, A. Rizzo, M. F. Neurath, and C. Becker, "In vitro generation of CD4+ CD25+ regulatory cells from murine naive T cells," *Nature Protocols*, vol. 2, pp. 1789–1794, 2007.

[9] N. Kong, Q. Lan, M. Chen et al., "Antigen-specific transforming growth factor beta-induced Treg cells, but not natural Treg cells, ameliorate autoimmune arthritis in mice by shifting the Th17/Treg cell balance from Th17 predominance to Treg cell predominance," *Arthritis and Rheumatism*, vol. 64, pp. 2548–2558, 2012.

[10] Q. Lan, X. Zhou, H. Fan et al., "Polyclonal CD4+Foxp3+ Treg cells induce TGF-beta-dependent tolerogenic dendritic cells that suppress the murine lupus-like syndrome," *Journal of Molecular Cell Biology*, vol. 4, pp. 409–419, 2012.

[11] S. Manicassamy and B. Pulendran, "Dendritic cell control of tolerogenic responses," *Immunological Reviews*, vol. 241, pp. 206–227, 2011.

[12] R. A. Maldonado and U. H. von Andrian, "How tolerogenic dendritic cells induce regulatory T cells," *Adv Immuno*, vol. 108, pp. 111–165, 2011.

[13] J. Yang, Y. Yang, Y. Ren, R. Xie, H. Zou, and H. Fan, "A mouse model of adoptive immunotherapeutic targeting of autoimmune arthritis using allo-tolerogenic dendritic cells," *PloS One*, vol. 8, no. article e77729, 2013.

[14] M. W. Pfaffl, "A new mathematical model for relative quantification in real-time RT–PCR," *Nucleic Acids Research*, vol. 29, no. article e45, 2001.

[15] Y. Y. Lan, Z. Wang, G. Raimondi et al., ""Alternatively activated" dendritic cells preferentially secrete IL-10, expand Foxp3+ CD4+ T cells, and induce long-term organ allograft survival in combination with CTLA4-Ig," *Journal of Immunology*, vol. 177, pp. 5868–5877, 2006.

[16] C. Penaranda and J. A. Bluestone, "Is antigen specificity of autoreactive T cells the key to islet entry?" *Immunity*, vol. 31, pp. 534–536, 2009.

[17] S. G. Zheng, "Regulatory T cells vs Th17: differentiation of Th17 versus Treg, are the mutually exclusive?" *Am J Clin Exp Immunol*, vol. 2, pp. 94–106, 2013.

[18] K. Wing and S. Sakaguchi, "Regulatory T cells exert checks and balances on self tolerance and autoimmunity," *Nature Immunology*, vol. 11, pp. 7–13, 2010.

[19] M. G. Roncarolo and M. Battaglia, "Regulatory T-cell immunotherapy for tolerance to self antigens and alloantigens in humans," *Nature Reviews. Immunology*, vol. 7, pp. 585–598, 2007.

[20] R. Y. Lan, A. A. Ansari, Z. X. Lian, and M. E. Gershwin, "Regulatory T cells: development, function and role in autoimmunity," *Autoimmunity Reviews*, vol. 4, pp. 351–363, 2005.

[21] X. Zhou, N. Kong, J. Wang et al., "Cutting edge: all-trans retinoic acid sustains the stability and function of natural regulatory T cells in an inflammatory milieu," *Journal of Immunology*, vol. 185, pp. 2675–2679, 2010.

[22] E. N. Huter, G. H. Stummvoll, R. J. DiPaolo, D. D. Glass, and E. M. Shevach, "Cutting edge: antigen-specific TGF beta-induced regulatory T cells suppress Th17-mediated autoimmune disease," *Journal of Immunology*, vol. 181, pp. 8209–8213, 2008.

[23] J. Yang, H. Fan, J. Hao et al., "Amelioration of acute graft-versus-host disease by adoptive transfer of ex vivo expanded human cord blood CD4+ CD25+ forkhead box protein 3+ regulatory T cells is associated with the polarization of Treg/Th17 balance in a mouse model," *Transfusion*, vol. 52, pp. 1333–1347, 2012.

[24] K. L. Hippen, S. C. Merkel, D. K. Schirm et al., "Generation and large-scale expansion of human inducible regulatory T

cells that suppress graft-versus-host disease," *American Journal of Transplantation*, vol. 11, pp. 1148–1157, 2011.

[25] S. G. Zheng, J. D. Gray, K. Ohtsuka, S. Yamagiwa, and D. A. Horwitz, "Generation ex vivo of TGF-beta-producing regulatory T cells from CD4+CD25- precursors," *Journal of Immunology*, vol. 169, pp. 4183–4189, 2002.

[26] S. G. Zheng, J. H. Wang, M. N. Koss, F. Quismorio Jr, J. D. Gray, and D. A. Horwitz, "CD4+ and CD8+ regulatory T cells generated ex vivo with IL-2 and TGF-beta suppress a stimulatory graft-versus-host disease with a lupus-like syndrome," *Journal of Immunology*, vol. 172, pp. 1531–1539, 2004.

[27] M. C. Fantini, C. Becker, I. Tubbe et al., "Transforming growth factor beta induced FoxP3+ regulatory T cells suppress Th1 mediated experimental colitis," *Gut*, vol. 55, pp. 671–680, 2006.

[28] E. Godebu, D. Summers-Torres, M. M. Lin, B. J. Baaten, and L. M. Bradley, "Polyclonal adaptive regulatory CD4 cells that can reverse type I diabetes become oligoclonal long-term protective memory cells," *Journal of Immunology*, vol. 181, pp. 1798–1805, 2008.

[29] J. Andersson, D. Q. Tran, M. Pesu et al., "CD4+ FoxP3+ regulatory T cells confer infectious tolerance in a TGF-beta-dependent manner," *The Journal of Experimental Medicine*, vol. 205, pp. 1975–1981, 2008.

[30] S. Floess, J. Freyer, C. Siewert et al., "Epigenetic control of the foxp3 locus in regulatory T cells," *PLoS Biology*, vol. 5, no. - article e38, 2007.

[31] D. S. Lim, M. S. Kang, J. A. Jeong, and Y. S. Bae, "Semi-mature DC are immunogenic and not tolerogenic when inoculated at a high dose in collagen-induced arthritis mice," *European Journal of Immunology*, vol. 39, pp. 1334–1343, 2009.

[32] J. Yang, Y. Yang, H. Fan, and H. Zou, "Tolerogenic splenic IDO (+) dendritic cells from the mice treated with induced-Treg cells suppress collagen-induced arthritis," *Journal of Immunology Research*, vol. 2014, Article ID 831054, 2014.

[33] B. M. Fu, X. S. He, S. Yu et al., "A tolerogenic semimature dendritic cells induce effector T-cell hyporesponsiveness by activation of antigen-specific CD4+ CD25+ T regulatory cells that promotes skin allograft survival in mice," *Cellular Immunology*, vol. 261, pp. 69–76, 2010.

[34] M. Gilliet and Y. J. Liu, "Human plasmacytoid-derived dendritic cells and the induction of T-regulatory cells," *Human Immunology*, vol. 63, pp. 1149–1155, 2002.

[35] A. Jiang, O. Bloom, S. Ono et al., "Disruption of E-cadherin-mediated adhesion induces a functionally distinct pathway of dendritic cell maturation," *Immunity*, vol. 27, pp. 610–624, 2007.

[36] B. Vander Lugt, J. Riddell, A. A. Khan et al., "Transcriptional determinants of tolerogenic and immunogenic states during dendritic cellmaturation," *The Journal of Cell Biology*, vol. 216, pp. 779–792, 2017.

[37] M. Guilliams, C. A. Dutertre, C. L. Scott et al., "Unsupervised high-dimensional analysis aligns dendritic cells across tissues and species," *Immunity*, vol. 45, pp. 669–684, 2016.

[38] H. J. Ko, M. L. Cho, S. Y. Lee et al., "CTLA4-Ig modifies dendritic cells from mice with collagen-induced arthritis to increase the CD4+CD25+Foxp3+ regulatory T cell population," *Journal of Autoimmunity*, vol. 34, pp. 111–120, 2010.

[39] M. S. Ahmed and Y. S. Bae, "Dendritic cell-based immunotherapy for rheumatoid arthritis: from bench to bedside," *Immune Netw*, vol. 16, pp. 44–51, 2016.

[40] S. H. Venkatesha, S. Dudics, B. Acharya, and K. D. Moudgil, "Cytokine-modulating strategies and newer cytokine targets for arthritis therapy," *International Journal of Molecular Sciences*, vol. 16, pp. 887–906, 2014.

[41] E. Schurgers, A. Billiau, and P. Matthys, "Collagen-induced arthritis as an animal model for rheumatoid arthritis: focus on interferon-γ," *Journal of Interferon & Cytokine Research*, vol. 31, pp. 917–926, 2011.

[42] J. Rodríguez-Carrio, P. López, and A. Suárez, "Type I IFNs as biomarkers in rheumatoid arthritis: towards disease profiling and personalized medicine," *Clinical Science (London, England)*, vol. 128, pp. 449–464, 2015.

[43] S. G. Zheng, J. Wang, and D. A. Horwitz, "Cutting edge: Foxp3+CD4+CD25+ regulatory T cells induced by IL-2 and TGF-beta are resistant to Th17 conversion by IL-6," *Journal of Immunology*, vol. 180, pp. 7112–7116, 2008.